UNIVERSITEIT VAN PRETORIA
UNIVERSITY OF PRETORIA
YUNIBESITHI YA PRETORIA

THE MODIFICATION OF WAXY OIL FOR PREPARING A POTENTIAL FEEDSTOCK FOR NEEDLE COKE PRODUCTION

by

John Graham Clark

A thesis submitted in partial fulfilment of the requirements for the degree

Philosophiae Doctor in Chemical Engineering

in the

Institute of Applied Materials
Department of Chemical Engineering
Faculty of Engineering, the Built Environment and Information Technology

University of Pretoria
Pretoria

July 2011

Promoter: Professor Brian Rand

DECLARATION

I declare that this dissertation is my own unaided work. It is being submitted for the Degree of Philosophiae Doctor at the University of Pretoria, Pretoria. It has not been submitted before for any degree or examination to any other University

……

(Signature of Candidate)

On this 18th day of October 2011

DEDICATION

This doctoral thesis is dedicated to my mother

Catherine Janet Clark

ABSTRACT

This research study determines the potential to increase substantially the anisotropy of a coke from an aliphatic Waxy Oil produced by Sasol Synfuels at Secunda, South Africa. Experimental modifications included filtration, distillation and thermal treatment, followed by distillation with the aim of producing a carbonised product similar to needle coke. The substantial concentration of an iron oxide catalyst (up to 2%) in Waxy Oil is increased by an order of magnitude upon carbonisation and calcination due to low coke yield and reactivity factors. The catalyst also promotes oxidative polymerisation of the residue, acts as a barrier to mesophase formation and promotes multi-phase graphitisation. Filtration of Waxy Oil using a 0.5 µm sintered metal filter reduces the ash content to 0.006% and increases the anisotropy of the carbonised product to 54% flow domains compared with 22% for the carbonised product of virgin Waxy Oil. Thermal treatment followed by distillation of Waxy Oil reduces the effect of organic reactivity promoters (mainly multi-alkylated aliphatics/aromatics and oxygenates), while increasing the concentration of thermally stable (C_{18} to C_{30}) normal alkanes to 85% compared with 38% in the filtered Waxy Oil. Compared with the filtered Waxy Oil, thermally stabilised Waxy Oil reduces the amount of the pre-carbonisation residue (from 98.7 to 43.0%), while "static" carbonisation thereof increases the green coke yield (from 19.8 to 36.3%) and increases the anisotropicity (from 54 to 100% flow domains). The carbonisation mechanism of filtered and thermally treated Waxy Oil involves initial cracking of high molecular weight normal alkanes (C_{18} to C_{30}), thus concentrating the molecular weight of normal alkanes (C_{18} to C_{22}). This is followed by a slow cyclisation step involving both self condensation and cyclo addition reactions to form two- to six-ring cyclo-alkanes or hydro-aromatics. The hydro-aromatics are dehydrogenated rapidly to form methyl and di-methyl three- to six-ring substituted aromatics. Further thermal degradation dealkylates these molecules to form stable four- to six-ring "pre-mesogens". The mesospheres are nucleated from the isotropic matrix and grow to more than 0.050 mm in diameter, with a volume of 2.61×10^{-3} mm^3. Subsequent coalescence of the mesospheres produces mesospheres with diameters of over 0.200 mm and volumes of 41.82×10^{-3} mm^3. The resultant microstructure of the solid carbon is composed of flow domains more than 400 µm in length. Although needle cokes have historically been produced from aromatic residues, this research is the first to show that a coke with a similar microstructure can be produced from a totally aliphatic residue. The research thus provides potential for the development of a needle coke from a totally unique Waxy Oil residue with negligible sulphur (< 0.008%) and nitrogen (< 0.09%) contents. This is the first academic study of the chemistry of Waxy Oil.

Keywords: Waxy Oil, Anisotropic, Thermal treatment, Needle coke, Mesophase

ACKNOWLEDGEMENTS

It is with great humility that I wish to acknowledge and thank the people who aided in my doctoral studies.

This work is based on research supported by the South African Research Chairs Initiative of the Department of Science and Technology and the National Research Foundation, whose support is gratefully acknowledged.

I would like to express my thanks and appreciation to my supervisor, Professor Brian Rand (University of Pretoria), who constantly checked my work and gave his expert opinion as to ideas which could be tested. Brian, your valuable input as my supervisor will never be forgotten.

I would also like to thank Sasol Synfuels Marketing for financial support of my studies, especially Dr Flip Hayes who acted as my industrial supervisor. Flip's knowledge of both the technical and marketing aspects of the coking industry proved invaluable in the creation of this thesis.

I would also like to thank the personnel at INCAR in Spain where I did a great deal of the research for this thesis. Your friendly and helpful attitude contributed greatly towards the original knowledge gained during this project. I would especially like to thank Drs Rosa Mendez, Ricardo Santamaria, Alba Centeno Perez and Clara Blanco. I truly appreciate the assistance of Antonio José Martin Fernandez and Daniel Barreda Garcia.

I would further like to acknowledge and thank people who throughout my career in the delayed coking industry I consider to have been my mentors. In this list I include Messrs Piet Ligthelm, Gregor van Deventer, Jo Spieth and Quentin Beukes, and Drs Flip Hayes and John Chang.

I would like to thank my family for their interest in and support of my doctoral studies. I would especially like to thank my wife Karen for her continuous encouragement and for checking my thesis for errors, but mostly for the time over weekends and at night when I got time to study. In this respect I would also like to thank my daughter Megan for the time I had to study instead of playing in the garden with her.

I would like extend my appreciation to Dr Ricardo Santa-Maria and Mr Deon van der Westhuizen for proofreading my thesis.

Further, I would like to acknowledge the support and kindness of my friends at Pizza Viali, especially Marco, Louis, Gavin, David, Brian, Raymond, Deon, Linda, Nikita, Barry, Vincenzo, Nicky and Michael.

While it would be almost impossible to name everybody who in some way contributed towards this thesis, I would also like to thank the following people:

- Professor Walter Focke (University of Pretoria)
- Drs Wilhelm Frohs and Thomas Mueller (SGL Carbon Ltd, Germany)
- Mr David Grace (SLFC)

- Dr Jaco van der Walt (NECSA)
- Mr Etienne Schuin (Sasol Technology – Research and Development)
- Mr Ben Ashton (Sasol Technology – Research and Development)
- Dr Esna du Plessis (Sasol Technology – Research and Development)
- Messrs Johann Snyman and Ewie Du Plooy (Synfuels laboratories)
- Messrs Siyanda Lubhelwana and Werner Barnard (Sasol Technology – Research and Development)
- Mrs Vivien du Cann
- Mr Johan Joubert (Sasol Technology – Research and Development)
- Mr Allen Hall (University of Pretoria)
- Mrs Beverlie Davies (for editing the thesis)

TABLE OF CONTENTS

LIST OF FIGURES

LIST OF TABLES

LIST OF ABBREVIATIONS AND SYMBOLS

Symbol	Description
amu	atomic mass units
µm	microns or x 10^{-6} metres
Å	Angstrom or x 10^{-10} metres
CCR	Conradson Carbon Residue
cSt	Centistokes
CTE	Coefficient of Thermal Expansion
CTP	Coal-Tar Pitch
DTA	Differential Thermal Analysis
DTG	Differential Thermal Gravimetry
EAF	Electric Arc Furnace
ETP	Ethylene Tar Pitch
FCC	Fluidised Catalytic Cracker
FCCDO	Fluidised Catalytic Cracker Decant Oil
FDMS	Field Desorption Mass Spectroscopy
FTIR	Fourier Transform Infra-Red
GC-AED	Gas Chromatography–Atomic Energy Detection
GCMS	Gas Chromatography Mass Spectroscopy
HDDC	Hydrogen Donor Diluent Cracking
He (density)	Real density
HGI	Hardgrove Grindability Index
HI	Heptane Insolubles
HPLC	High Performance Liquid Chromatography
I_{ar}	Aromaticity Index (FTIR)
IBP	Initial Boiling Point
LDMS	Laser Desorption Mass Spectroscopy
LSVR	Low-Sulphur Vacuum Residue
MIQ	Mass Insoluble in Quinoline
MIT	Mass Insoluble in Toluene
NMP	N-methyl-2-pyrrolidone
NMR	Nuclear Magnetic Resonance
OTI	Optical Texture Index
PAH	Polycyclic Aromatic Hydrocarbons
PDA	Photodiode Array
PSD	Particle Size Distribution
QI	Quinoline Insolubles
SDO	Synthol Decant Oil
SEM	Scanning Electron Microscopy
SRC	Solvent Refined Coal
TGA	Thermogravimetric Analysis
TI	Toluene Insolubles
VBD	Vibrated Bulk Density
VCM	Volatile Carbon Matter
VR	Vacuum Residue
XRD	X-Ray Diffraction
XRF	X-Ray Fluorescence

1 INTRODUCTION

1.1 Background to the investigation

Heavy petroleum residues originating from crude oil and coal tar are processed by delayed coking to produce lighter petrol, diesel intermediates, hydrocarbon gases and a solid carbonaceous product called "green coke". Delayed coking involves a multitude of chemical reactions, including cracking and polycondensation of Polycyclic Aromatic Hydrocarbons (PAH) to form green coke between 450 and 500 °C. Green coke is calcined at approximately 1 350 °C to form calcined coke which is sold into a variety of industrial markets.

Needle coke in particular is differentiated (from other calcined cokes) by its highly ordered microstructure and its visual resemblance to a collection of vertically aligned needles. Needle cokes are industrially used as carbonaceous filler for the production of graphite electrodes in the steel smelting industry.

The demand for and value of synthetic delayed coke is driven by the market requirement for carbon intermediates in the energy, foundry, steel and aluminium industries. Of the 91 million tons (mt) of delayed coke produced globally per annum, 68 mt is sold as cheap fuel-grade green coke and 23 mt is calcined, producing 18 mt of calcined coke. Of the 18 mt, 14 mt is used as anode coke (for aluminium smelters), 3 mt is used as carbon raisers (in foundries) and only 1 mt meets the stringent quality specifications to be utilised as **needle coke** for the production of graphite electrodes in the steel smelting industry (Driscoll, 2007).

Compared with other commodity delayed (calcined) cokes produced for the aluminium, recarburiser or foundry industries, the comparative value of needle coke is differentiated by the following considerations:

- Needle coke has the highest comparative market value per metric ton and is in the shortest supply (Driscoll, 2007).
- There are only a limited variety of petroleum and coal-tar pitch residues which, based on their molecular and chemical composition, are suited for the production of needle coke (Driscoll, 2007).
- Needle coke precursors attract the greatest process cost prior to delayed coking (Mochida *et al.*, 1990).
- Needle coke is in certain cases (depending on the international crude oil price) more valuable than the hydrocarbon distillates (petrol and diesel) produced during delayed coking.
- The generally accepted philosophy of delayed coking is to maximise the production of petrol and diesel intermediates. However, needle coke production requires the operation of the delayed coker in the "carbon"[1] mode, given the quality requirements and value of the calcined coke.

[1] It is the author's experience that the operation of commercial delayed cokers is either in the "carbon" or "white product" mode. White products are defined as the hydrocarbon distillates produced during delayed coking. They include petrol intermediates, diesel intermediates and heavy recycle oil. Hydrocarbon gases are not included in this definition, although they are produced in the process.

- Electrodes produced from needle coke are required to withstand temperatures in excess of 3 000 °C (Frohs *et al.*, 2007). By contrast, anodes produced from sponge cokes[2] in the aluminium industry operate at only 960 °C (Hulse *et al.*, 2000).
- Needle coke has the most stringent specifications in respect of sulphur, nitrogen, ash content and especially the Coefficient of Thermal Expansion (CTE) (Frohs *et al.*, 2007).
- Needle coke has attracted the greatest amount of funding for academic research.

It thus stands to reason that the identification of a potentially new feedstock which could produce needle coke with appropriate characteristics would attract research interest. Accordingly, the current research has been conducted to study Sasol Synfuels Waxy Oil and determine its potential for the production of highly anisotropic needle-like coke.

The aliphatic composition of Waxy Oil is in stark contrast to the preferred aromatic composition of needle coke precursors (Mochida *et al.*, 1990). As discussed in this study, the industrial and academic focus on aromatic residues has historically been justified by availability and the natural predisposition thereof for intrinsic molecular self-assembly during carbonisation, producing anisotropic or highly ordered carbon. Thus the diminutive academic drive to develop needle cokes from aliphatic residues cannot necessarily be ascribed to technical incapacity, but rather to lack of industrial necessity.

However, as viable reserves of needle coke precursors diminish due to availability, environmental legislation and quality deterioration, the nature of research has evolved to maximise the viable lifespan of these residues by developing ever-more-costly and technically advanced interventions to maintain coke specifications (Mochida *et al.*, 1989). The philosophy of knowledge advancement to address ever-worsening quality symptoms is finite and may in future increasingly require reconsideration.

Waxy Oil is a heavy aliphatic by-product produced by the gas phase reaction of carbon monoxide and hydrogen over an iron-based catalyst. It is produced on a commercial scale at Sasol's Coal-to-Liquid refinery at Secunda, South Africa. Waxy Oil is currently utilised to produce calcined coke and serves as a recarburiser, although high catalyst contents frequently diminish the market value. Waxy Oil produces a calcined coke with negligible sulphur and nitrogen content; this was the overriding consideration when choosing this feed for the study.

1.2 Feedstock quality

Precursors for needle coke production have historically been limited to available residues whose aromatic molecular composition naturally predisposes them to form highly anisotropic carbon during carbonisation. However, further requirements of the feedstock include:

- Low ash content (Mochida *et al.*, 1987) and (Martinez-Escandell *et al.*, 1999)
- Low Quinoline Insoluble (QI) content (Crelling, 2008)
- Low asphaltene content (Seshardi *et al.*, 1982)
- Reduced content of stable nitrogen or sulphur heterocyclics (Weinberg *et al.*, 1988)
- Low oxygenate content (Marsh *et al.*,1973) and (Sima *et al.*, 2003)

[2] While there are many ways of defining types of coke, it is common practice to assign a descriptive name, e.g. needle and sponge cokes.

- Low air and carboxy reactivity of the coke during calcination (Hippo and Walker, 1975) and (Walker *et al.*, 1983)

Feedstocks historically utilised for needle coke production include Coal-Tar Pitch (CTP), Fluidised Catalytic Cracker Decant Oil (FCCDO), petroleum vacuum residues and ethylene tar. Theoretically, it should be possible to convert any heavy carbonaceous residue into needle coke given the appropriate pre-carbonisation modifications (Mochida *et al.*, 2000).

In evaluating the characteristics of Waxy Oil for the production of needle coke, it may be compared against known commercial needle coke precursors to determine the degree of modification that may be required. Waxy Oil exhibits a comparative dissimilarity to the abovementioned feedstocks and the generally accepted quality requirements listed above. This provides a natural template against which a problem statement may be defined.

1.3 Problem statement

The aim of the study is to identify the characteristics of Waxy Oil that retard the formation of anisotropic coke and remediate them prior to carbonisation. These characteristics may include the molecular composition (e.g. the presence of oxygenates, multi-alkylated alkanes) but the overriding concern is the lack of aromaticity. Another source of concern is the presence of substantial iron oxide catalyst. These areas of concern form the basis of the problem statement as detailed below:

- The iron oxide catalyst content of Waxy Oil is particularly erratic. This increases the ash content which ranges from 0.05–2.0% in Waxy Oil and, due to the low yield, may increase to between 5–20% in the calcined coke. This is far in excess of the required ash content for needle coke, which is 0.20% (Frohs *et al.*, 2007). The iron oxide induces further detrimental effects on coke characteristics, including rapid oxidative polymerisation (Wang *et al.*, 2001), leading to an isotropic microstructure and an increased CTE. It is also capable of modifying the mechanism of graphitisation as it induces catalytic graphitisation (Wang *et al.*, 2001).
- The porosity of Waxy Oil “green coke” increases the surface area available for oxidative carbon consumption during calcination (which is normally carried out in oxidising conditions), further compounding carbon loss which, by default, increases the relative ash content and enhances greenhouse gas emissions.
- Compared with the carbonisation cycle of aromatic residues, the aliphatic nature of Waxy Oil requires an extra aromatisation step prior to the formation of pre-mesogens (Domine *et al.*, 2002).
- Although Waxy Oil is composed predominantly of alkanes, the potential for the formation of oxygenated hydrocarbons is enhanced as one of the co-reactants in the Fischer-Tropsch process is carbon monoxide. While the effect of oxygenated alkanes is unknown, oxygenated aromatics are known to increase the reaction rate, forming mosaic cokes, as previously described by Sima *et al.* (2004)
- Furthermore, there is a potential for the presence of iso-alkanes. Aliphatic side chains on aromatic molecules are known to form radicals and increase the rate of reaction, forming mosaic microstructures, as previously determined by Obara *et al.* (1981)
- However, of all the potential reactivity promoters, the lack of Waxy Oil aromaticity is the greatest potential concern. Although there is abundant literature promoting the importance of aromaticity in determining the anisotropicity of coke, the molecular

range of certain needle coke precursors, e.g. coal-tar pitch, is vast (200–2 000 amu). By contrast, both Wang and Eser (2007) and Lewis (1987) denote the importance of three- to six-ring aromatic precursors for the production of anisotropic microstructures. So, in the author's opinion, the question of total aromaticity vs. the type of aromaticity remains unanswered.

- Waxy Oil is a synthetic product and vastly different from favoured feeds for needle coke production, including petroleum decant oils (originating from crude oil) and coal-tar residues (originating from blast furnaces). Thus, comparing the carbonisation chemistry of Waxy Oil with the bulk of available published academic literature requires caution.

1.4 Scope of the investigation

The development of a commercially acceptable needle coke from an unknown residue such as Waxy Oil is a multi-disciplined process. A simplified list of basic phases[3] is given below.

- Evaluating the molecular chemistry of the residue
- Evaluating the carbonisation chemistry of the residue
- Modification of the molecular composition to enhance coke anisotropy
- Pilot plant production of delayed coke
- Production of trial coke on a commercial scale

It is for the most part unnecessary to conduct extensive academic investigations into known needle coke precursors as they are limited to coal tar or petroleum residues which have historically been the subject of numerous academic research projects and published articles.

It would be myopic to expect success based on immediate pilot plant experimentation while negating the value of a prior understanding of Waxy Oil chemistry and its carbonisation mechanism.

As the chemistry of Waxy Oil has not previously been studied, the scope of this research encompasses identifying Waxy Oil characteristics that are detrimental to the production of anisotropic carbon and then identifying modifications to promote anisotropy, as well as a reasonable description of the reaction mechanism. It is only with this knowledge that future larger-scale investigations may prove worthwhile. Thus, the scope of work in this study does not include pilot plant delayed coking.

The thesis is divided into chapters and a brief description of each is given below.

Introductory chapters

Chapter 1. Introduction

This chapter serves as a general introduction to needle coke and compares Waxy Oil with other needle coke precursors. This information is then used to define the problem statement, objectives and scope of work.

[3] The list of basic phases for this development is by no means definitive. It is given for descriptive purposes only to identify phases that are evaluated by the current scope of investigation.

Chapter 2. The needle coke value chain

This chapter provides a basic overview of needle coke production from feedstock selection to the use of electrodes in an arc furnace. The aim of the chapter is to lay a foundation in needle coke chemistry for readers who may not previously have been exposed to this science. It is the author's opinion that a basic chemistry approach, including aspects of commercial production, enhances the understanding of the review of previous academic research discussed in the next chapter.

Chapter 3. The Waxy Oil value chain

Given the unique characteristics of Waxy Oil, this chapter provides a brief description of its origin through to the production of calcined coke. It also provides a "specification sheet" approach to Waxy Oil and calcined coke. The chemistry of Waxy Oil is not discussed in any detail as it has not been the subject of academic research prior to this study.

Chapter 4. Review of previous work

This chapter examines previously published academic research within the field of needle coke chemistry and the relevance thereof to Waxy Oil as a precursor for highly anisotropic coke. As Waxy Oil is vastly different from any known needle coke precursors, direct comparisons are not possible. However, the literature study serves to identify experimental interventions that may aid the formation of coke anisotropy.

Main Chapters[4]

Chapter 5. Experimental

This chapter describes the experimental procedures and analytical techniques used to examine the chemistry of Waxy Oil and Waxy Oil coke. The results of the laboratory research are reported in Chapters 6 to 9.

Chapter 6. The influence of catalyst concentration on the characteristics of commercial Waxy Oil coke

This chapter examines the effect of increasing the concentration of iron oxide catalyst on the chemical and physical properties of Waxy Oil green coke, as well as thermally treated variants. The effect of iron oxide on the characteristics of Waxy Oil coke is one of the major factors contributing to its ineligibility as a needle coke. The technical viability of particle graphitisation as a potential process for reducing the catalyst content of Waxy Oil coke and the effects on the chemical, physical and crystal characteristics of the graphite produced are discussed.

Chapter 7. Waxy oil modification

[4] At the end of each of the main chapters, both conclusions and recommendations based on the knowledge gained in that chapter are presented. These are used to determine the optimal set of experimental conditions for the following chapters. Thus the thesis attempts to present a "golden line" leading up to the production of needle coke from Waxy Oil.

This chapter discusses various experimental procedures utilised to reduce the catalyst concentration and modify the organic molecular composition of Waxy Oil. These interventions include filtration, distillation and thermal treatment. The molecular composition of these modified Waxy Oils is compared with heavy residue characteristics known to promote coke anisotropy. This chapter also discusses the modified Waxy Oil samples produced for "static" carbonisation.

Chapter 8. "Static" carbonisation of modified Waxy Oils

This chapter evaluates the potential of "static" carbonisation of modified Waxy Oils to provide a semi-quantitative procedure for determining the quality of green coke produced, based mainly on a microstructural analysis through the longitudinal plane of the coke.

Chapter 9. The carbonisation mechanism of Waxy Oil

This chapter examines the carbonisation mechanism of filtered and thermally treated Waxy Oil. In comparison with highly aromatic feedstock, the mechanism of Waxy Oil carbonisation is complex in that it includes an aromatisation step.

Concluding chapters

Chapter 10. Conclusions

Chapter 11. Contribution to original knowledge

Chapter 12. References and bibliography

1.5 Objectives of the investigation

The main objectives of the investigation are broadly divided into creating an understanding of the effects of (i) catalyst concentration and (ii) the organic molecular composition of Waxy Oil on the structural characteristics and properties of coke. The objectives may be further be subdivided as follows.

- An initial objective of this study is to determine how **increasing catalyst concentration** influences the characteristics of Waxy Oil green coke with reference to the carbon macrostructure, microstructure, crystal development, real density and air/carboxy reactivity.

- **Graphitisation as a process to remove catalyst from green coke** – It is the objective of this part of the research to establish whether graphitisation is a viable solution to reducing the catalyst content.

- **Modification of Waxy Oil prior to carbonisation** – It is the primary objective of this part of the research to reduce the catalyst concentration (as determined by the ash content) of Waxy Oil to needle coke precursor specifications. Furthermore, the characteristics of filtered and virgin Waxy Oil are compared.

- Based on the fulfilment of the primary objective, the secondary objective is to create an understanding of the **organic molecular composition** of filtered Waxy Oil and to identify reactivity promoters that, during carbonisation, may have a detrimental effect on the anisotropy of the carbonised product.

- Based on the fulfilment of the secondary objective of the research, the tertiary objective is to determine the effect of distillation and thermal treatment of filtered Waxy Oil on the **molecular chemistry** thereof. Furthermore, the objective is to provide an explanation of how these interventions lower the carbonisation rate.

- **"Static" carbonisation of modified Waxy Oils** – The objective of this part of the research is show how "static" carbonisation in test tubes can be used to determine the difference in the quality of coke based on modified Waxy Oils.

- **The carbonisation mechanism of Waxy Oil** – The objective of this part of the research is to provide a reasonable explanation for the variance between the carbonisation mechanism of filtered Waxy Oil and the modified Waxy Oil that produced the greatest degree of anisotropy in the coke.

2 INTRODUCTION TO NEEDLE COKE

In this chapter, two main focus areas relating to needle coke are discussed, namely:

- The value chain of graphite electrode production
- The chemistry of needle coke formation from heavy residues

2.1 The industrial value chain of graphite electrode production

2.1.1 Feedstock selection

Feedstocks used for the production of needle coke include:

- Petroleum Fluidised Catalytic Cracker Decant Oils (FCCDO)
- Petroleum Low-Sulphur Vacuum Residues (LSVR) or Vacuum Residues (VR)
- Coal-Tar Pitches (CTP)
- Ethylene Tar Pitches (ETP)
- Solvent Refined Coals (SRC)[5]

2.1.1.1 Fluidised Catalytic Cracker Decant Oil (FCCDO)

Petroleum FCCDO is a heavy residue formed by catalytic cracking of either VR, atmospheric residues or a blend of both. The primary function of the catalytic cracking reaction is the production of naphtha: the greater the severity of the reaction, the more aromatic the FCCDO. Less severe cracking conditions produce a greater abundance of long alkyl side chains bound to parent aromatic molecules of which the FCCDO is predominantly composed. The catalyst is a powdered alumino-silicate which contributes to the ash content (to varying degrees, based on the efficacy of removal within the decanter or upstream removal processes) and may have a detrimental effect on the coke quality. Cokes with high catalyst contents may also form lower density graphites due to the sublimation of metals during graphitisation, forming voids within the graphite electrode.

Chemically, FCCDO is generally characterised by high concentrations of Polycyclic Aromatic Hydrocarbons (PAH) of >70%, (Mochida *et al.*, 1987), with a negligible concentration of reactive asphaltenes. These precursor characteristics aid in the formation of anisotropic needle coke with a lower CTE (compared with VR or LSVR). FCCDO has even been known to produce cokes with negative CTEs (Mochida *et al.*, 1987) in the longitudinal direction.

2.1.1.2 Low-Sulphur Vacuum Residues (LSVR) and Vacuum Residues (VR)

Petroleum Vacuum Residues (VR) are produced as the residue product of vacuum distillation of atmospheric residue. Compared with other feedstocks, they are usually composed of higher

[5] There is no evidence in the literature cited that the production of needle coke from SRC is conducted on a commercial scale. The literature (Hoover, 1988) refers only to laboratory investigations.

asphaltene concentrations and sulphur contents. They are further characterised by a high concentration of aliphatic molecules and a lower concentration of aromatics compared with their more stabilised downstream counterpart, FCCDO (Mochida *et al.*, 1987).

While they are known to produce inferior needle cokes (CTE typically 5.0–8.0 x 10^{-7}.°C^{-1}), they are, in comparison with the other commercial precursors, relatively abundant. The LSVR may be used in a blend with a more aromatic decant oil to increase the quality of the resultant needle coke, with specific reference to the sulphur content. The ash content of LSVR or VR feedstocks is totally dependent on mineral matter originating from crude oil and the efficacy of upstream desalination.

2.1.1.3 Coal-Tar Pitch (CTP)

Coal tar is a heavy by-product of coke oven furnaces used to produce metallurgical coke for the blast furnace and other applications. The properties of coal-tar pitch are very much determined by conditions in the furnace. Low-rank coals processed at lower temperatures may yield pitches with a large number of alkyl functions bound to the aromatic ring, higher oxygen contents and higher reactivity rates during carbonisation, leading to less appropriate coke for electrodes. By contrast, pitches produced at excessive temperatures may produce highly stable aromatic molecules which produce less gas during carbonisation, thus affecting pore morphology.

Coal-tar pitches are characterised by comparatively high densities (approximately 1.18 g.cm^{-3}), higher nitrogen (1.5–1.70%) and lower sulphur (0.50%) contents in comparison with petroleum residues. The oxygen content may vary according to furnace conditions but is typically in the 1.0–2.0% range. Carbon aromaticity is high (93–96%) and the average molecular weight is in the 200–2 000 amu (atomic mass unit) range.

There are two main challenges faced in the production of needle coke from coal-tar pitch. The pitches usually require removal of primary quinoline insolubles (QI), which is solid carbonaceous matter carried over from the coke oven. QI is known to impede mesophase development which is essential in controlling the coke morphology, by presenting a three-dimensional inert obstruction to parallel alignment of mesogenic molecules, thus producing a coke with a higher CTE. Various methods for QI removal are utilised, including filtration, centrifugation and aliphatic/aromatic solvent precipitation.

The other challenge is the stability of nitrogen heterocyclics and their subsequent inclusion in the coke matrix. During graphitisation (of the electrode), nitrogen is released (1 600–1 800 °C) which leads to puffing of the electrode. Inhibitors utilised to suppress puffing include iron (III) sulphate, boron compounds and sodium salts.

From a market perspective coal tar is used as both binder and impregnation pitch as it is the only residue historically deemed to have the correct specifications.[6] It is also less favoured for cracking owing to its aromatic stability compared with that of petroleum residues. Furthermore, the exclusive use of coal tar and the size of the binder market presents competition to its use as a needle coke feedstock.

[6] Heavy petroleum residues, for example, have been used as extenders in the binder pitch market. However, their comparative volume is low.

2.1.1.4 Ethylene Tar Pitch (ETP)

Ethylene tar is the residue product from the production of ethylene (via steam cracking) and is characterised by high reactivity rates during the onset of carbonisation, limiting the extent of mesophase formation by prematurely increasing the viscosity of the developing mesophase and leading to less anisotropic carbon. Ethylene tar precursors may be upgraded when used in blends with more aromatic feedstock, e.g. FCCDO.

2.1.1.5 Solvent Refined Coal (SRC)

It is not certain whether needle coke is commercially produced from SRC; however, it has been the subject of substantial research. It is usually considered an inappropriate feedstock due to the high process cost associated with solvent recovery. While SRC typically has high oxygen (3.0%) and nitrogen (2.2%) contents, it requires hydrogenation to promote formation of a needle coke as it is relatively hydrogen-deficient. Needle cokes produced from SRC are typically in the premium and regular grades (CTE of 5.0–8.0 x 10^{-7}.°C^{-1}) as previously described by Hoover *et al.* (1988).

2.1.2 Delayed coking

The quality characteristics of needle coke are determined by its microstructure, which in turn is controlled by mesophase development of the precursor during carbonisation. While this research relates to specific facets of needle coke mesophase chemistry, for readers not familiar with this science a general description may be found in the literature cited (Marsh *et al.*, 1997; Clark, 2008; Mochida *et al.*, 1994).

Delayed coking is the onset of molecular transition from a complex mixture of aromatic molecules to the production of a solid carbon. All the processes, including delayed coking, calcining and graphitisation, only provide a source of thermal energy. Thus, the chemical composition of the molecules in needle coke precursors determines the characteristics of the eventual graphite electrode. All needle coke feedstocks (or for that matter any delayed coker feedstock) may be described as having a specific “predisposition” towards the formation of a certain green coke microstructure.

An empirical diagram of a delayed coker is shown in Figure 2-1, but note that the design of commercial delayed cokers may vary according to volumes of feedstock processed.

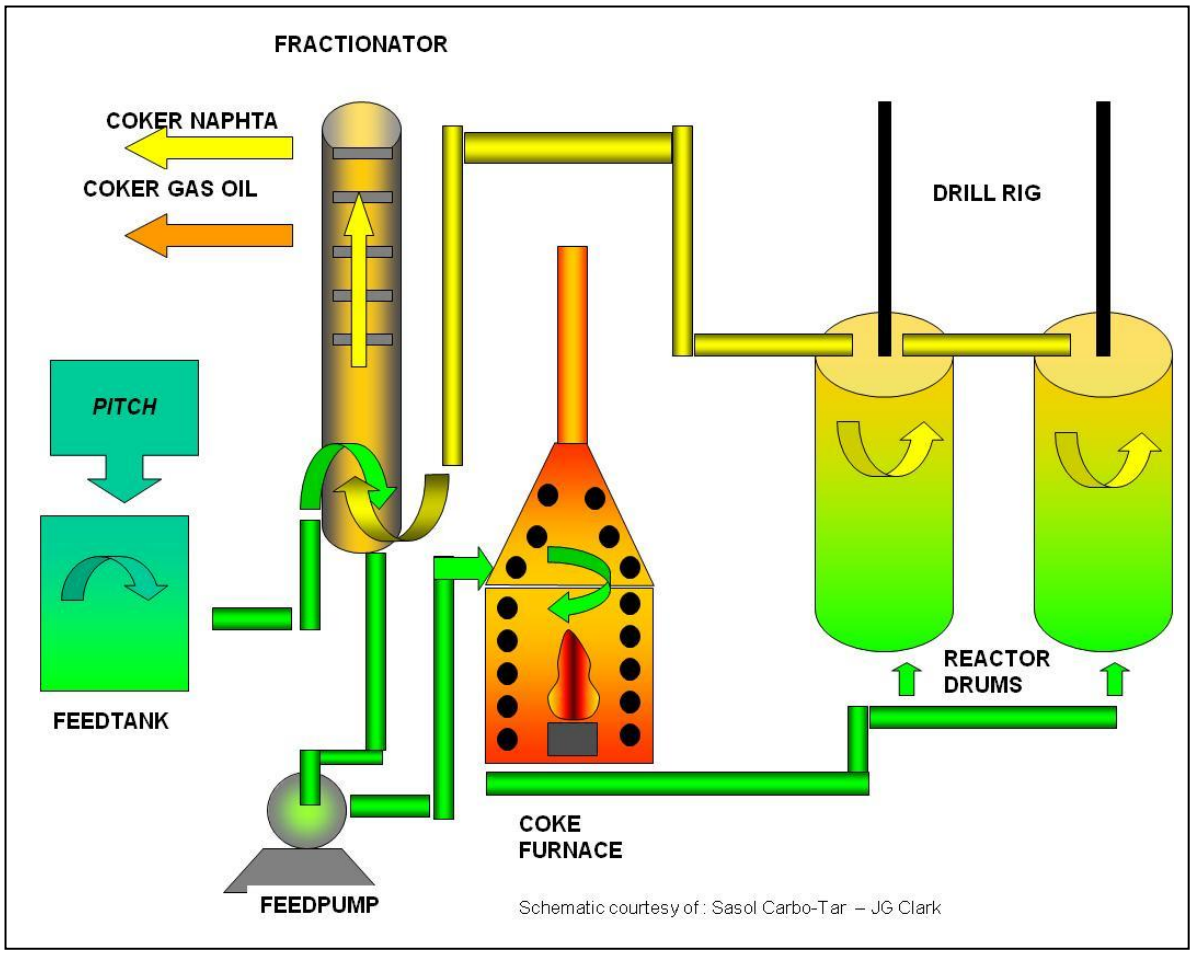

Figure 2-1 Diagram of a delayed coker (Clark, 2008)

Feedstock is stored in heated tanks and pumped via a series of pipes through two or more pre-heaters into the fractionator. The feed is pumped through gas-fired heater tubes and into the reactor drum. In the drum both exothermic cracking and dealkylation reactions provide vapours which are removed at the top of the drum and condensed in the fractionator. These vapours form hydrocarbon gases, naphtha (petrol intermediate) and coker gas oil (diesel intermediate). Naphtha and coker gas oil require hydrogenation prior to utilisation as petrol and diesel blend components, as delayed coking is a dehydrogenative process. The heavier molecules, which are not removed at the top of the drum, undergo polycondensation reactions. The coke forms from the bottom of the drum towards the top in a vertical direction.

Within the reactor several progressive phases of the carbonisation cycle are present: at the bottom is green coke, on top of this is the developing mesophase (a liquid crystalline state) and above this is virgin feedstock. The level of the coke in the reactor increases to approximately 70% of the drum's volume. On the completion of a cycle, feed is switched to another drum to prevent carryover of solid carbonaceous solids to the fractionator and risk of damage to the fractionator plates. The drum is then steamed and water is injected to cool the coke and remove some of the volatile organic matter. Although the diameter of various drums may vary, the coke is usually cut with a water jet using a two-stage process. The first stage cuts a "pilot hole" down the centre of the drum, followed by removal of the rest of the coke usually using a process called "undercutting", which cracks the coke rather than pulverising it, in order to minimise the production of fine carbon.

The velocity of gases through the delayed coker drum is dependent on both the volume of cracked gases from the feedstock and other non-oxidising gases injected, e.g. steam. Steam has two main functions: to increase the velocity of the feed through the heater tubes to prevent coke laydown; and to strip lighter organic volatiles from green coke in the reactor drum. As a consequence, the increased flow of gases through the drum has a substantial effect on the coke microstructure and pore morphology by affecting the alignment of mesophase domains.

During delayed coking, the top layers exercise pressure on the coke towards the bottom of the reactor. Because of thermal distribution within the drum, the coke in the bottom of the drum is usually denser due to constant pitch intrusion. Higher CTE coke at the bottom of the drum may also be affected by the precipitation of asphaltenes during carbonisation, producing fine isotropic, high CTE shot coke. Shot coke at the bottom of a drum may present a further safety concern as the coke forms in the shape of balls which may vary in size from a couple of millimetres to over 0,5 m in diameter.

Typical drum cycle times may last between 18 and 24 h, depending on the viscosity and green coke yield from the fresh feed. Each feedstock will have an optimum temperature for carbonisation, the more stable feeds requiring greater activation energy. However, delayed coking temperatures usually range between 460 and 500 °C. While it is optimum to operate the delayed coker at the minimum temperature for a specific feed, cognisance needs to be taken of the Volatile Carbon Matter (VCM) of the green coke. If the reaction temperature is too low, the VCM will increase to levels at which the green coke may become uncalcinable (due to instability in the calciner). Another reason for controlling the VCM of the green coke to between 7 and 10% is that during calcination the VCM is combusted, causing porosity which decreases the bulk density of the calcined coke and may increase the binder pitch demand during electrode forming.

Pressure over the delayed coking system serves to increase the yield by retaining vapours in the drum. All delayed cokers producing needle coke are operated to maximise coke yield and thus the pressure remains constantly high (approximately 500 kPa). Decreasing the system pressure can lead to green coke yield losses, while increasing the pressure too much may retard the release of vapours and affect the pore morphology of the coke.

The drum vapour of heavier molecular weight is called the “recycle oil”. As the name implies, it is recycled to the fresh feed stream, given its propensity to increase the green coke yield of the virgin feedstock.

The control of carbonisation **temperature** and **pressure** is critical for producing coke with a low CTE. As each of the feedstocks has a different molecular composition, their specific optimum kinetics for carbonisation differs.

2.1.3 Calcination

Calcination is the process of VCM reduction and graphene layer densification between temperatures of 600 °C and approximately 1 350 °C. A diagram of a typical kiln calciner is shown in Figure 2-2.

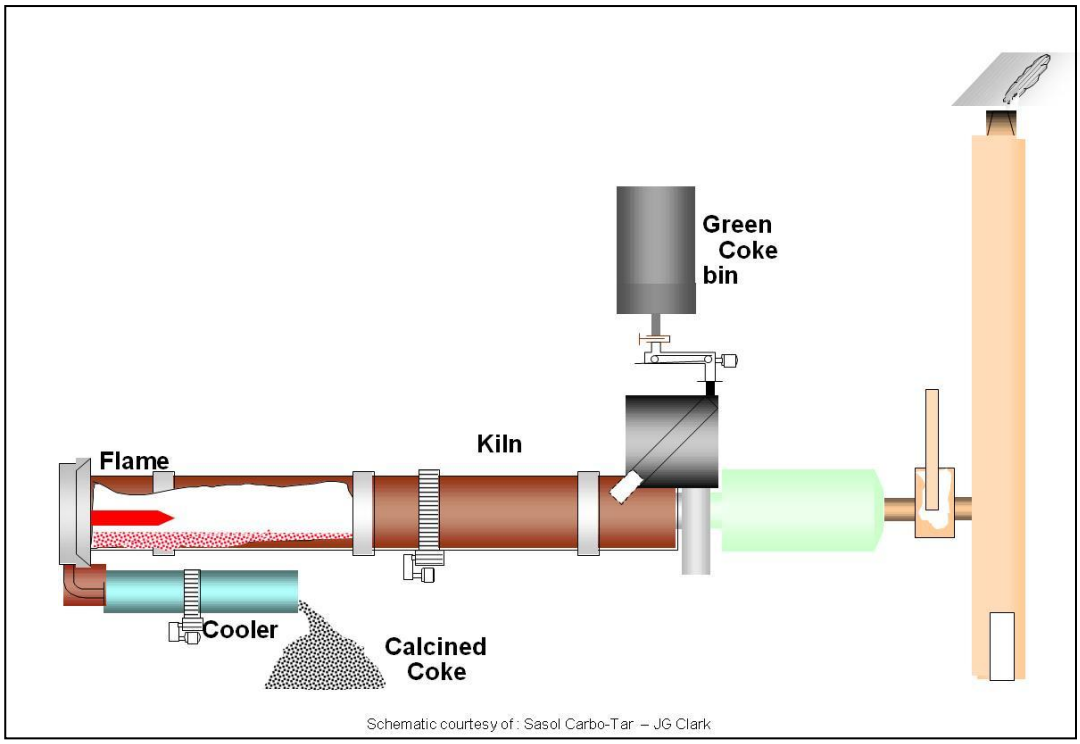

Figure 2-2 Diagram of a counter-current calciner (Clark, 2008)

Coke enters the kiln at 600 °C and is immediately dehydrated. At 700–800 °C dehydrogenation occurs. The temperature and atmosphere within the rotary kiln have a distinct effect on the properties of the calcined coke. Densification of the graphene planes occurs in the 1 100–1 400 °C range and is especially significant for the production of needle coke due to crystallite development.

Upon exiting the kiln at 1 400 °C, the coke enters a cooler where rapid shrinkage occurs, yielding cracks and determining the friability of the coke. While the coke is at 1 400 °C, the temperature is not high enough to affect the release of stable heteroatoms. Rapid cooling may induce microcracks either parallel or perpendicular to the flow domain of the coke, which provide a pathway for the escape of the gases released in the early stages of electrode graphitisation, thereby decreasing the puffing phenomenon.

2.1.4 Electrode production

The production of electrodes is a closely controlled process. While exact formulations and process conditions are closely guarded intellectual capital, it is possible to present the general flow scheme of electrode production, shown in Figure 2-3.

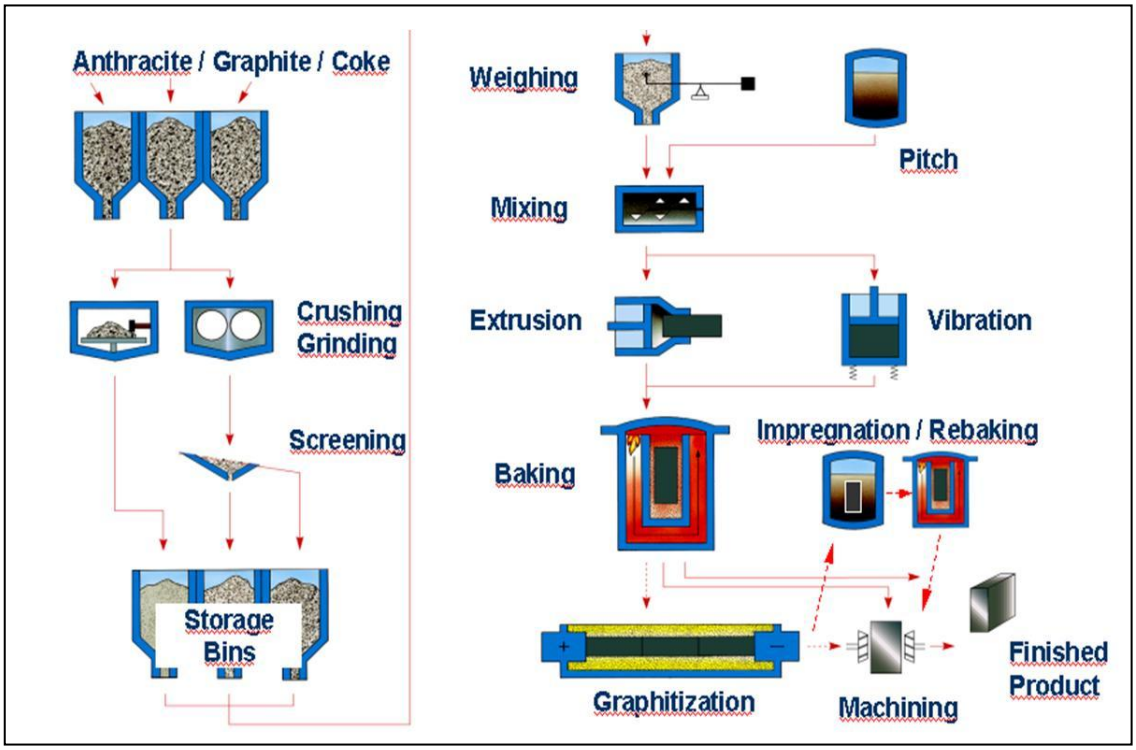

Figure 2-3 Diagram showing the manufacturing process for graphite electrodes (Frohs *et al.*, 2007)

After crushing, needle coke is classified according to particle size and separated into bins. The "dry recipe" is then formulated according to a predetermined programme. The larger the diameter of an electrode, the higher the thermal stress it will need to withstand (without significant expansion or cracking), both during graphitisation and within an Electric Arc Furnace (EAF). The "ceramic toughening" principle to hinder crack propagation on bigger particles has led to the formulation of larger electrodes with larger coke particles (up to 20 mm). This has had a knock-on effect on the producers of calcined coke to reduce the friability thereof.

Binder pitch is mixed with the dry recipe at a temperature of 160–180 °C, which is 50–65 °C above the softening point of the pitch. The amount of pitch used is specific to the recipe and the macroporosity of the coke.

Forming of a green electrode is conducted by extruding the paste through a die with a specific diameter, producing a green electrode. The electrode is cut to size (in length) and usually rolled into a water bath to cool the pitch matrix down, allowing the green electrode to maintain the integrity of its shape.

Green electrodes are placed in metal cylinders and baked (in a vertical position) for a number of days at a slow temperature gradient, eventually reaching 900–1 000 °C. During the baking process the binder pitch is carbonised, providing a solid infusible carbon cylinder with the filler coke. The slow temperature gradient is particularly important in controlling the dimensions and possible shrinkage of the electrode as a result of pitch pyrolysis. Binder pitch dosage is equally important: if the mix is too wet, deformation during baking may occur and if the mix is too dry, the baked electrode will have a lower mechanical strength and bulk density.

Impregnation of baked electrodes is conducted to increase the bulk density and ultimately the mechanical strength. Baked electrodes are placed in an autoclave in the vertical position. The hood is closed and a vacuum drawn on the system. Impregnation pitch is introduced to the system covering the electrodes under a pressure of up to 10 atmospheres. The softening point of impregnation pitch (approximately 95 °C) is lower than that of binder pitches (approximately 115 °C) and contains a substantially lower percentage of primary QI. The combination of the lower softening point, negligible primary QI and pressure allows penetration of the inner macropores of the electrode. After impregnation, excess pitch is drained and the electrode is re-baked. This process may be repeated until the required bulk density is reached.

The purpose of graphitisation is to transform the filler needle coke and carbonised pitch into graphite. The process heats electrodes to approximately 2 900–3 000 °C, at a predetermined heating gradient, and keeps it at that temperature, allowing it to cool afterwards.

2.2 The chemistry of needle coke formation

In this section the chemistry of needle coke formation is discussed with sequential reference to feedstock composition, mesophase formation, microstructure and characteristics of needle coke.

2.2.1 Composition of needle coke feedstock

The molecular composition of needle coke feedstock has by far the greatest influence on the coke's performance as a filler material in an electrode. Furthermore, feedstock aromaticity is a leading indicator in predicting the anisotropy of needle coke produced.

However, the mere determination of total aromaticity either using ^{1}H (Stecker, 1984) or ^{13}C (Seshardi *et al.*, 1982) Nuclear Magnetic Resonance (NMR) or Fourier Transform Infra-Red (FTIR) spectroscopy to determine the Aromatic Index (Sima *et al.*, 2003) does not solely produce an adequate explanation as the type of aromaticity is equally important.

Needle coke feedstocks are heterogeneous systems composed of (in some cases) many thousands of different aromatic molecules (Domine *et al.*, 2002) and may, as in the case of coal-tar pitch, be composed of a wide molecular weight distribution – between 200 and 2000 amu as determined by Gullien *et al.* (1998), which means that compounds from 2-25-ring aromatics may be present. Secondly, the presence of asphaltenes (large molecular weight aromatics, highly contaminated by heteroatoms and minerals) as determined by Dickakian (1984) increases the thermal reactivity of the heavy residue, thus prematurely increasing the viscosity and having a dominating effect on the microstructure of the coke.

As determined by Gullien *et al.* (1998), coal-tar pitch is also composed largely of three- to six-ring aromatic compounds. Comparatively, petroleum decant oil is composed largely of alkylated three- to six-ring aromatic compounds (Wang & Eser, 2007). Both the abovementioned authors determined this range of aromatics to be the preferred molecular weight precursors for the production of highly anisotropic needle coke. These aromatic compounds are referred to as "pre-mesogens" meaning, those Polycyclic Aromatic Hydrocarbons (PAH) from which the mesophase is generated. A compilation of typical gas chromatography-amenable PAH compounds present in needle coke feedstocks is shown in Figure 2-4.

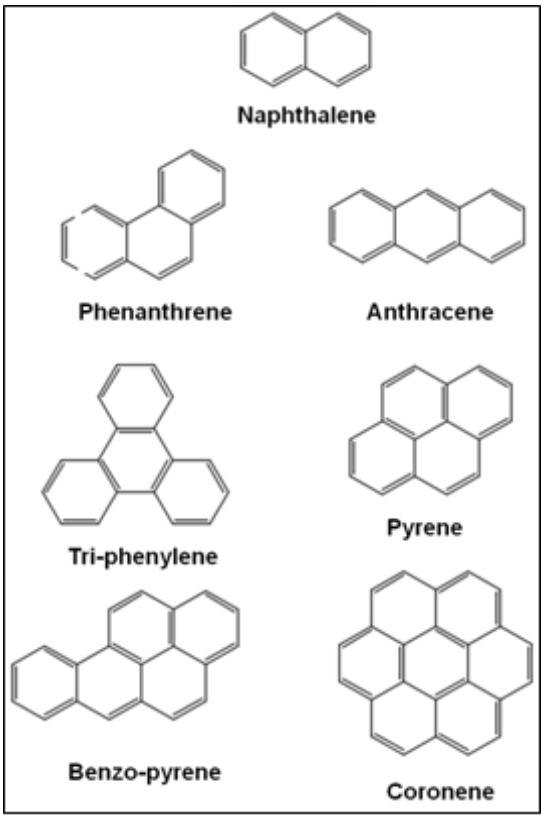

Figure 2-4 Typical aromatic pre-mesogens in needle coke feedstock

2.2.2 Mesophase formation

Mesophase is the intermediate liquid crystal phase formed by polycondensation of PAHs before solidification to form coke as defined by Mochida *et al.* (1994). Mesophase grows from an isotropic phase in the form of small spheres as seen in Figure 2-5.

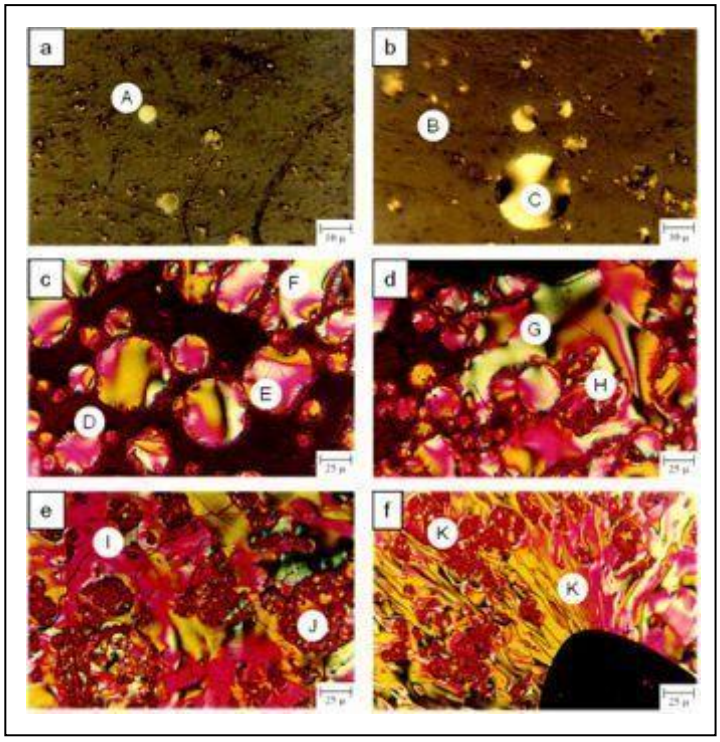

Figure 2-5 Mesophase development and the influence of primary Quinoline Insolubles (QI) (Crelling, 2008)

Incipient mesospheres grow by incorporating mesogens from the isotropic matrix, as seen in Figure 2-5 (Positions A, B and C). The spheres coalesce to form larger spheres (shown in Positions D and E), eventually forming semi-coke (as seen by Position F). The degree to which the spheres grow and coalesce while maintaining maximum fluidity is defined as the "extent" of mesophase formation. This defines the morphology of the microstructure as seen in Positions G, H, I, J and K.

The extent of mesophase formation is not dependent solely on the type of aromaticity, but may also be affected by other feedstock compositional factors, including:

- The oxygen, nitrogen and sulphur content of the feedstock (Sima *et al.*, 2003)
- The asphaltene content of the feedstock (Dickakian, 1984)
- Alkyl side chains bound to the parent aromatic compounds, e.g. in VR (Mochida *et al.*, 1989) or ethylene tars (Mochida *et al.* 1989)
- The mineral concentration in the feedstock either chemically modifying mesophase development (e.g. iron oxide as described by Wang *et al.*, 2001) or providing an inert barrier to mesophase development (e.g. silica gel as described by Obara *et al.*, 1985)
- QI, which are small solid particles of carbon especially predominant in coal-tar feedstock due to the temperature of formation (approximately 1 100 °C). QI is pushed towards the edge of the developing spheres (as shown in Positions E and H) and may prevent further coalescence, thus producing mosaic coke

2.2.3 Coke microstructure

Any one or a combination of the factors listed above will affect the kinetics (or the rate) at which heavy residues are transformed into coke. If the mesophase "cures" too quickly, its viscosity will prevent further coalescence of mesogenic spheres. By so doing coalescence is retarded and this gives rise to the family of microstructures known as "mosaics", which include:

- Fine mosaic
- Medium mosaic
- Coarse mosaic

These appear as a "collection of balls" of varying sizes. This type of material is **isotropic** (on a micro/milli-dimensional scale) as seen in Figure 2-6, but within the "balls" on a smaller dimensional scale there are anisotropic regions.

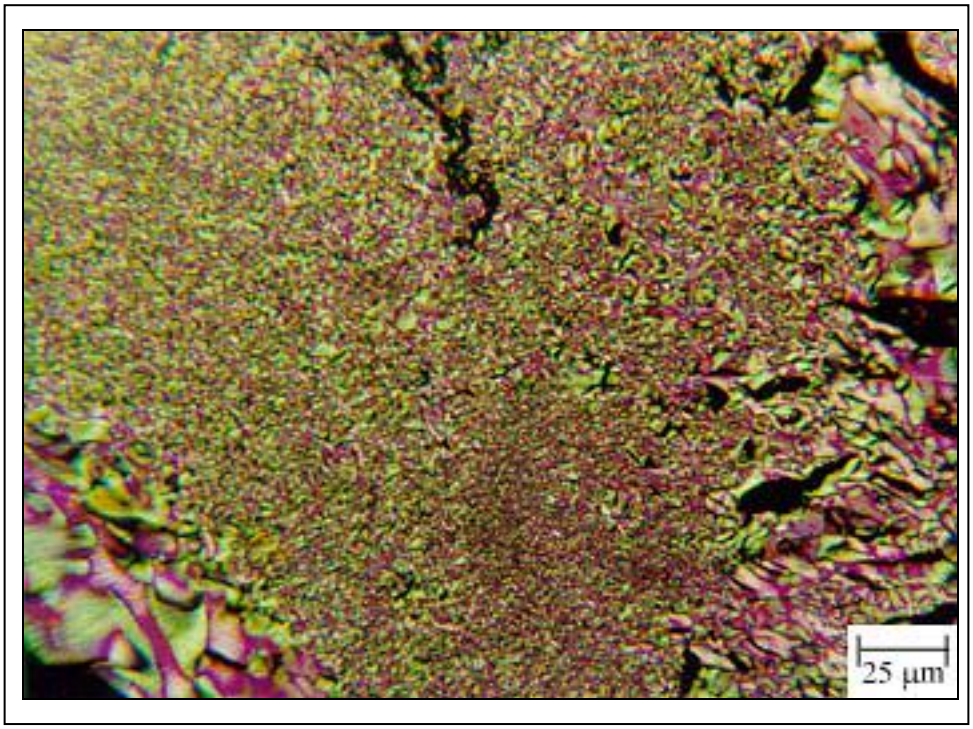

Figure 2-6 Micrograph of an isotropic coke showing fine mosaic structures (Crelling, 2008)

If the mesophase kinetics allows unhindered coalescence of spheres, microstructures resembling flow domains are produced. **Flow** patterns include:

- Coarse
- Granular
- Laminar

These thus appear as a collection of elongated domains and are common in higher order sponge and needle cokes. These cokes are typically referred to as **anisotropic** (with order) as shown in Figure 2-7. Needle coke microstructure is typically composed of these flow domains.

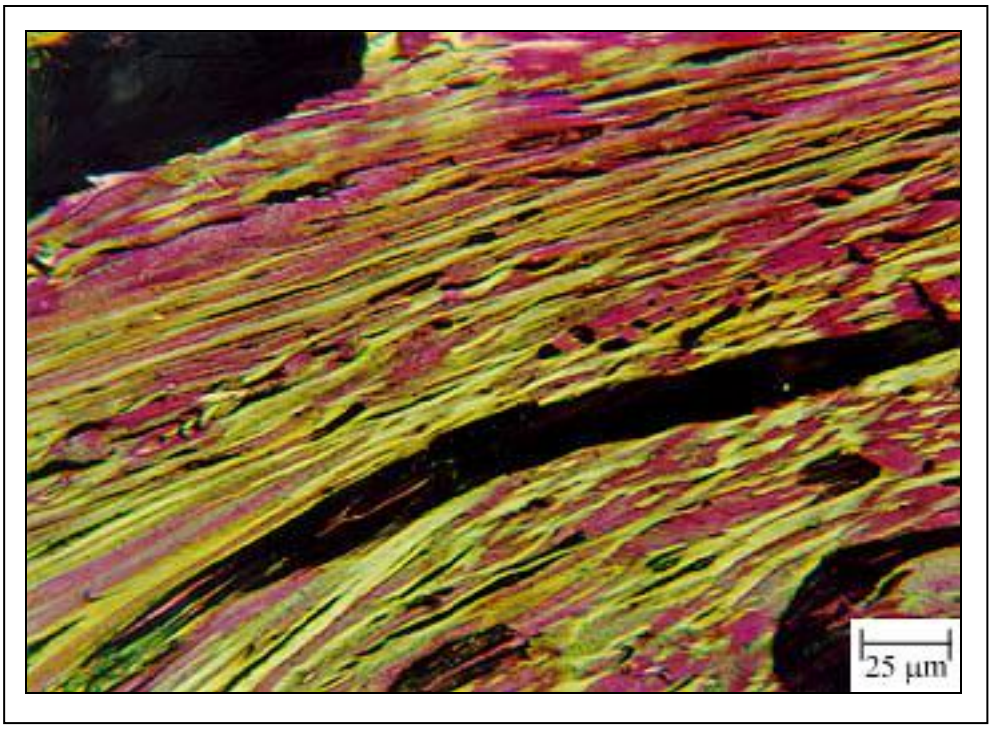

Figure 2-7 Micrograph of anisotropic coke showing flow domain microstructures (Crelling, 2008)

Historically, one of the most reliable methods for evaluating the microstructure of cokes is the Optical Texture Index (OTI). The procedure entails setting the carbon in an epoxy resin mould and then polishing the flat surface of a piece of carbon with fine alumina powder. The polished surface of the carbon is then examined under a light microscope at low magnification within a drop of oil. Under magnification the carbon reveals "shapes or structures" which are point-counted to determine an "index value" and reveal the relative anisotropy/isotropy of the material on a milliscale. The OTI reference table is given in Table 2-1. The higher the OTI factor, the more ordered or anisotropic the coke, as discussed by Marsh *et al.* (1997).

Table 2-1 Optical Texture Index (OTI) (Marsh *et al.*, 1997)

Category	Description	OTI Factor
Fine mosaics	Small circular < 0.8 µm in diameter	0
Medium mosaics	Circular > 0.8 µm < 2.0 µm in diameter	1
Course mosaics	Large circular > 2.0 µm < 10 µm in diameter	3
Granular flow	> 2.0 µm in length and > 1 µm in width	7
Course flow	> 10.0 µm in length and > 2 µm in width	20
Lamellar flow	> 20.0 µm in length and > 10 µm in width	30

The relative degree of anisotropy within a carbon matrix has significant effects on the in situ performance of the carbon filler within the graphite electrode, including the Coefficient of Thermal Expansion (CTE) discussed later in this chapter.

2.2.4 Microstructure of needle coke

A montage of needle coke micrographs is shown in Figure 2-8.

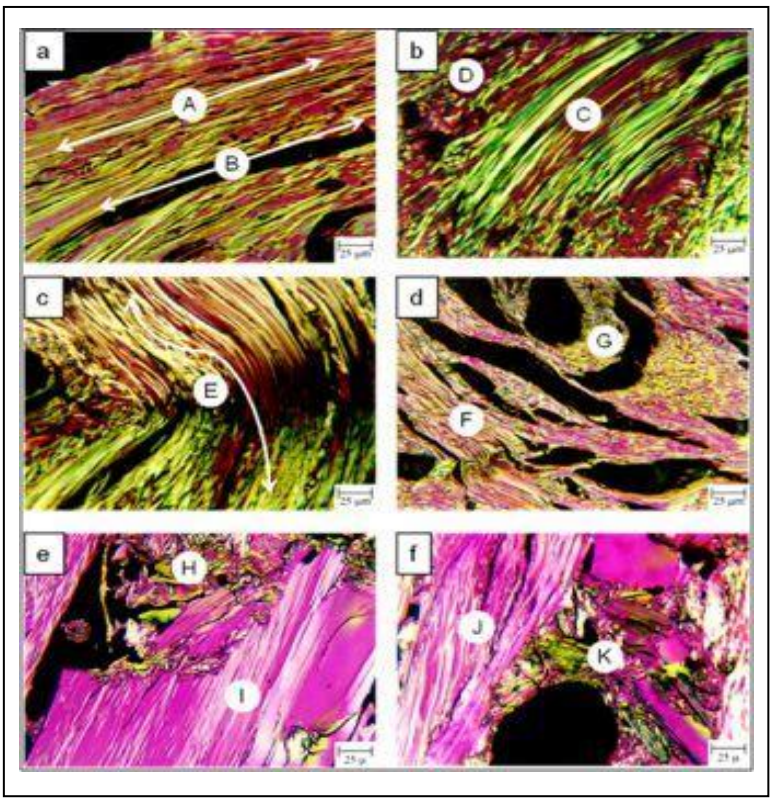

Table 2-8 Montage of needle coke microstructures (a–d) and needle coke in an electrode (e–f) (Crelling, 2008)

Needle coke has a microstructural morphology dominated by long thin flow domains of indeterminable length as shown in Position A. This morphology is largely the result of the hydrocarbon gases produced during cracking escaping in a vertical direction, as seen from the parallel long thin pores formed (Position B), as previously determined by Mochida *et al.* (1998 and 1999).

Depending on the composition of the feedstock, the morphology of needle coke may contain a mixture of flow domains (Position C) and domains of a shorter length yet wider breadth (Position D). The morphology of the flow domains is determined by the path of the escaping gases and may appear straight (as previously shown by Position A) or curved (Position E). Feedstocks producing inferior needle cokes, e.g. ethylene tar (Mochida *et al.*, 1990a), often have lower coke yields and a mixture of coke microstructures as seen from the flow domains (Position F) and medium to coarse mosaics (Position G). Lower green coke yields are often characterised by the production of highly porous morphologies, as described by Mochida *et al.* (1987) and shown in Figure 2-8d.

Figure 2-5 (e–f) shows needle cokes (Positions I and J) as filler material in an electrode. The filler particles are bound by carbonised binder pitch (Positions H and K). The carbonised binder forms a coke with a microstructure that is less anisotropic than the filler material.

The morphology of needle coke is entirely dependent on the angle from which it is viewed as shown in Figure 2-9.

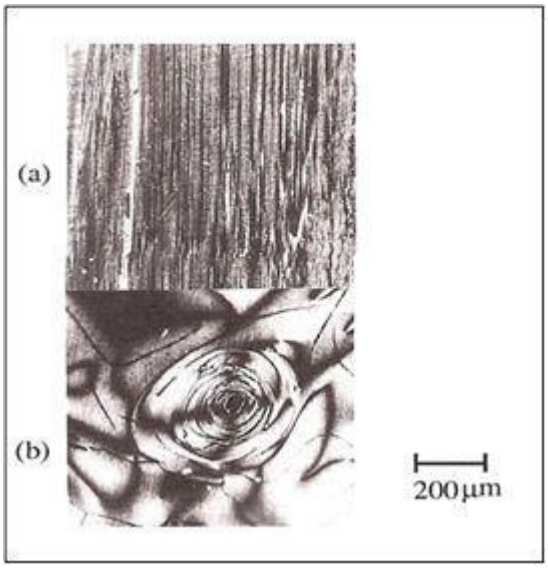

Figure 2-9 Scanning electron micrograph of perpendicular sections of needle coke, (a) in the longitudinal section and (b) in the transverse section (Mochida *et al.*, 1994)

When viewed along the longitudinal a-axis (Figure 2-9a), the microstructure appears entirely composed of long thin flow domains. However, when viewed in the transverse c-axis (Figure 2-6b), the microstructure appears as concentric rings surrounding a central pore. This difference in the microstructure is further explained by examining a three-dimensional diagram of needle coke structure as shown in Figure 2-10.

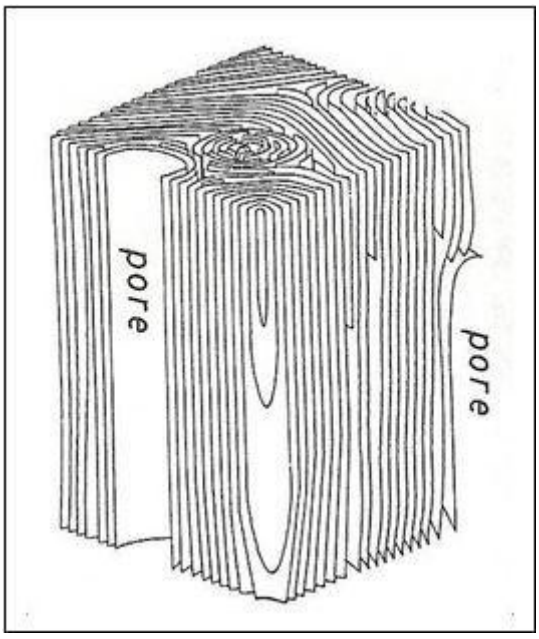

Figure 2-10 Diagram of the structure model of needle coke (Mochida *et al.*, 1994)

Examination of the longitudinal axis of needle coke shows that both pores and cracks run parallel to this axis, providing evidence that gas evolution in the final stages of mesophase solidification determines the uni-axial arrangement of the coke microstructure.

Crystal development is dependent on the graphitisability of the green coke microstructure, which is determined by the mesophase formation, as previously described by Murthy *et al.* (2001).

2.2.5 Needle coke crystallography

Graphitisation depends on the efficacy of thermal energy to produce slight incremental adjustments to the alignment of the graphene planes (Mochida *et al.*, 1994). The mobility of aromatic molecular planes is fixed when the coalesced mesophase solidifies to form the green coke and thus it is impossible to produce a more highly aligned structure from an isotropic coke by increasing the temperature alone.

As optical microscopy is able to show the basic alignment of planes at various heat treatment temperatures on a micron-scale, X-Ray Diffraction (XRD) is able to follow the growth of crystals on a nanoscale (Murthy *et al.*, 2001). The effect of graphitisation on CTE is more easily understood using XRD, which is able to provide finite values (L_a, L_c, d_{002}) rather than relying on point counting of aligned planes using Scanning Electron Microscopy (SEM) or optical microscopy, which provides qualitative aspects of the nano/milli-structure. The effect of increasing the temperature on the XRD indices of a petroleum coke is shown in Table 2-2.

Table 2-2 Crystalline development as a function of heat treatment temperature for an anisotropic petroleum coke (modified from Inagaki, 2000)

Heat treatment temperature (°C)	d_{002} (Å)	L_C (Å)	L_a (Å)
2 300	3.369	440	310
2 400	3.363	490	310
2 500	3.359	550	330
2 600	3.358	560	350
2 700	3.357	610	360
2 800	3.352	670	420

As the heat treatment temperature increases, the interlayer spacing (d_{002}) between the graphene sheets decreases while the height (Lc) and the width of the crystal increase. The anisotropy of the microstructure is fundamental in allowing these modifications of the crystal structure with increasing temperature.

2.2.6 The Coefficient of Thermal Expansion (CTE) of needle coke

The CTE of needle coke is one of the most important, yet most commonly misunderstood, characteristics of needle coke. The CTE is dependent on the orientation of the pores and cracks within a specific particle of coke. It cannot be measured directly but is inferred from

the CTE value of a synthetic electrode manufactured with the coke in question as a filler. The effect of carbonisation temperature on the CTE of test rods produced from coke carbonised at various temperatures is shown in Figure 2-12.

.

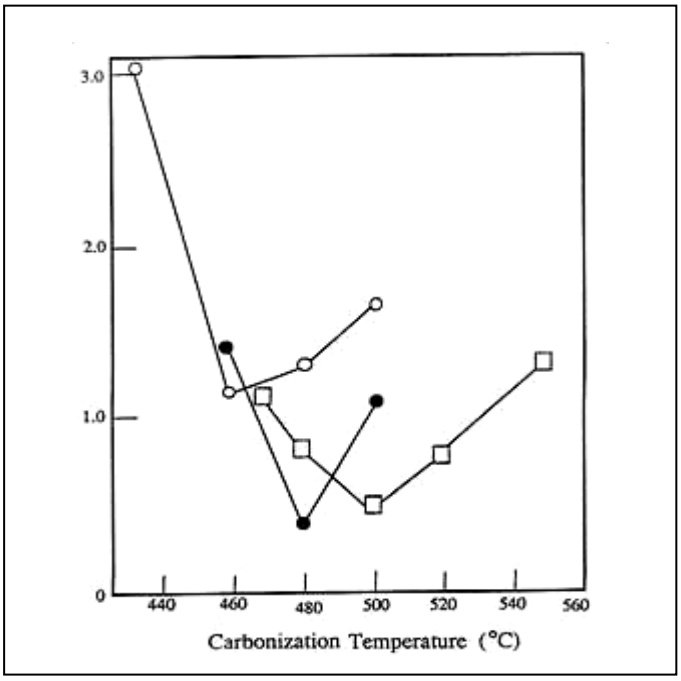

Figure 2-11 CTE values of test electrode rods produced from cokes formed at various temperatures, at a pressure of 16 kg.cm^{-2} from feedstocks. ○ LSVR; ● FCCDO; □ Coal-tar pitch (QI free) (Mochida *et al.*, 1994). The Y-scale is the Coefficient of Thermal Expansion and is measured in units of mm/mm x 10^{-6}.°C^{-1}

The CTE of particulate needle coke or a graphite electrode has the effect of increasing thermal stress on the expansion thereof in both the *a*- and *c*-axes (Mochida *et al.*, 1994). The CTE of a graphite electrode along the direction transverse to the extrusion axis is of importance owing to the extremely high temperatures (approximately 3 000 °C) it has to withstand without cracking.

Figure 2-11 shows that the optimum carbonisation temperatures for producing the lowest CTE coke for various needle coke precursors is different. LSVR and ethylene tar are reactive and thus necessitate carbonisation at lower temperatures (Mochida *et al.*, 1989 and 1990b). However, heavy residues that have undergone some sort of catalyst cracking, e.g. FCCDO (Mochida *et al.*, 1989) or heat treatment during their formation, e.g. coal-tar pitch (Mochida *et al.*, 2000), are less reactive and thus are carbonised at higher temperatures. The optimum temperature for carbonisation is modified when mixtures of residues with higher reactivity residues (e.g. vacuum residues) and residues with lower reactivity (e.g. FCCDO) are mixed to reduce the CTE of the coke, as described by Mochida *et al.* (1989).

At temperatures either below or above the optimum, the CTE of the coke increases. At higher carbonisation temperatures, mesophase development is comparatively rapid. This has the following consequences:

- Gases are evolved before they may have an effect on the pore aspect ratio of the coke (during solidification of the mesophase).
- Due to limited growth of isochromatic areas, their distribution may appear random.
- Microstructures form elongated mosaics rather than domains or flow domains.
- The rapid viscosity increase of the mesophase does not allow optimum growth of mesophase spheres within the liquid crystalline state.
- The lower anisotropy of the coke increases the CTE.

However, the converse is also true: carbonisation at temperatures below the optimum has the following consequences:

- The carbonisation reaction is slow and takes longer.
- Gas evolution is slow and may not provide sufficient gas evolved during the solidification stage of the bulk mesophase, thus affecting the aspect ratio of pore morphology.
- The green cokes produced may contain a substantial VCM content. On calcination these pockets of VCM will carbonise immediately and form areas of high-CTE mosaics.
- Unless the pressure is high enough, co-carbonisation of feedstock with differing optimum carbonisation temperatures may limit the interaction of their kinetics or produce two different types of coke in the same drum.

As indicated by Figure 2-13, CTE measurement along the longitudinal axis (or **a-axis**) yields lower CTE values than along the transverse axis (**c-axis**). Measurement of the CTE on a piece of coke is inaccurate due to porosity variation between pieces (even from the same carbonisation). The coke is thus mixed with binder pitch to produce a graphitised rod, which removes much of the inaccuracies.

However, different graphite producers and researchers are known to vary the temperature range over which the CTE is measured and thus these values are not always comparable. Examples thereof given in the literature include:

- Ambient to 400 °C (Keshun *et al.*, 1985)
- Ambient to 500 °C (Mochida *et al.*, 1989)
- Ambient to 100 °C (Mochida *et al.*, 1987)

The same characteristic may apply to the fracture mechanics of a graphite electrode in an EAF. If the electrical conductivity of a graphite electrode is not high enough, thermal stress in the electrode will translate into mechanical stress. In most instances crack propagation will progress along the longitudinal direction in which the resistance is the lowest.

2.2.7 Puffing

Puffing may be defined as the irreversible expansion of an electrode during graphitisation. It is caused by the release of bound heteroatoms from the carbon matrix between 1 600 and 2 300 °C, as described by Kawano *et al.* (1999a). The nature of the heteroatoms released is dependent on the origin of the needle coke precursor. Petroleum-based needle cokes tend to release higher concentrations of sulphur, as described by Orac *et al*. (1992), while coal-based

needle cokes tend to release higher concentrations of nitrogen, as described by Kawano *et al*. (1999b and 2000).

Graphitisation increases the crystal height **(c-axis)** and width **(a-axis)**. This densification decreases the space between the graphene layers (***d-spacing***). Needle coke expands during graphitisation up to 1 500 °C and then from 1 500 to 1 600 °C the coke shrinks. This is followed by rapid expansion from 1 600 to 2 300 °C (dynamic puffing) and then at 2 500 °C secondary puffing occurs (Mochida *et al.*, 1994). The gases released during dynamic puffing include N_2, CS_2, H_2S and COS, depending on the type of needle coke, as described by Mochida *et al.* (1994).

The initial puffing phase occurs between 1 500 and 1 800 °C as released gases cause a volumetric expansion of the coke on a linear curve as a result of pressure on the coke microstructure due to blocking of pathways. According to Mochida *et al.* (1994), from 1 700 to 1 800 °C, the d-spacing increases slightly due to the release of these heteroatoms. The extent of puffing in an electrode is also dependent on the ability of the released gases to escape through the carbonised binder matrix. Figure 2-13 shows the expansion and shrinkage curves of needle coke heat-treated to 2 500 °C. The coke shrinks on a linear curve on cooling.

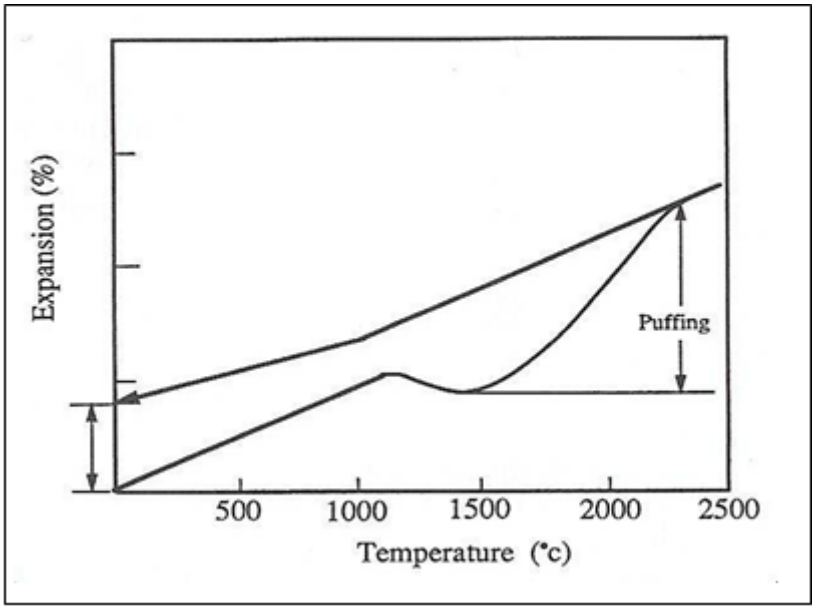

Figure 2-12 Profile of expansion and shrinkage curves of an electrode showing the effect of puffing (Mochida *et al.*, 1994)

The volumetric expansion of a coke particle is not equal in all directions due to the preferred orientation of microstructural flow domains and pore morphology as shown in Figure 2-14.

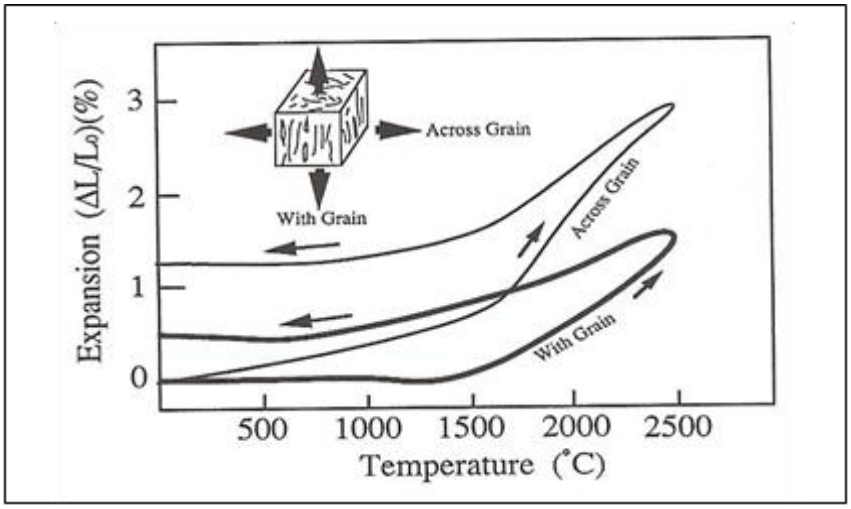

Figure 2-13 Diagram showing the influence of measuring direction on the extent of puffing (Mochida *et al.*, 1994)

The alignment of the pores in the longitudinal (with grain) direction provides a pathway for the release of gases during puffing and thus the pressure increase is less, decreasing the expansion. The opposite is true for expansion in the transverse (across grain) direction as the pathway for released gases is impeded to a greater extent by the carbon structure, causing a pressure build-up and greater expansion. The same theory holds if the expansion (in both directions) were to be measured on an electrode during graphitisation, principally due to the alignment of the coke particles in the longitudinal direction (Mochida *et al.*, 1994).

Traditional methods employed to control puffing include the use of a puffing inhibitor, as previously described by Orac *et al.* (1992) and Kawano *et al.* (1999b). Inhibitors form a chemical bond with heteroatoms and serve to control the rate at which heteroatoms are released from the coke matrix, thus reducing pressure on the inner walls of the electrode. The mineral content within needle coke may be bound in a number of ways, but under the inert conditions of graphitisation normally reduces to the metallic state and sublimates, leaving voids in the crystal structure, thus decreasing the bulk density and the mechanical strength of the electrode, while increasing the electrical resistivity.

2.2.8 Needle coke specifications

A summary of typical super-premium needle coke specifications is shown in Table 2-3. Needle cokes may be broadly classified into three grades which vary in the stringent quality specifications and have a considerable influence on the price. Table 2-3, however, considers only the specifications attributed to the highest grade, namely super-premium grade needle coke.

Table 2-3 Typical super-premium grade needle coke analyses[7] (Frohs *et al.*, 2007)

Analysis	Units	Typical range
CTE	$X10^{-7}$. $°C^{-1}$	3–4
Real density	$g.cm^{-3}$	2.140–2.145
Sulphur	%	0.4–0.5
Nitrogen	%	0.2–0.3
Hydrogen,	%	0.035–0.045
Vibrated Bulk Density (VBD)	$g.cm^{-3}$	080–0.82
Ash	%	0.1-0.2

Needle cokes possess a low CTE, high electrical conductivity, high real and bulk density, low heteroatom content and low ash content (Mochida *et al.*, 1994). It is the compound effect of these needle coke characteristics that determines the in situ performance of a graphite electrode in an EAF.

2.2 Concluding remarks – Introduction to needle coke

A basic understanding of needle coke science is important when discussing the results of this research project. In this chapter a sequential description has been provided, but it is by no means definitive.

The Waxy Oil value chain is discussed in Chapter 3 from production of Waxy Oil to calcined coke

[7] All analyses of needle coke are conducted on the particles, except the CTE which is conducted on a test rod produced by mixing needle coke with binder pitch, extruding, baking and graphitising. Particle CTE is variable due to differences in porosity between the particles.

3 THE WAXY OIL VALUE CHAIN

3.1 The production of Waxy Oil calcined coke from Synthol Decant Oil (SDO)

3.1.1 SDO de-ashing

A simplified process flow diagram showing catalyst removal from SDO is shown in Figure 3-1.

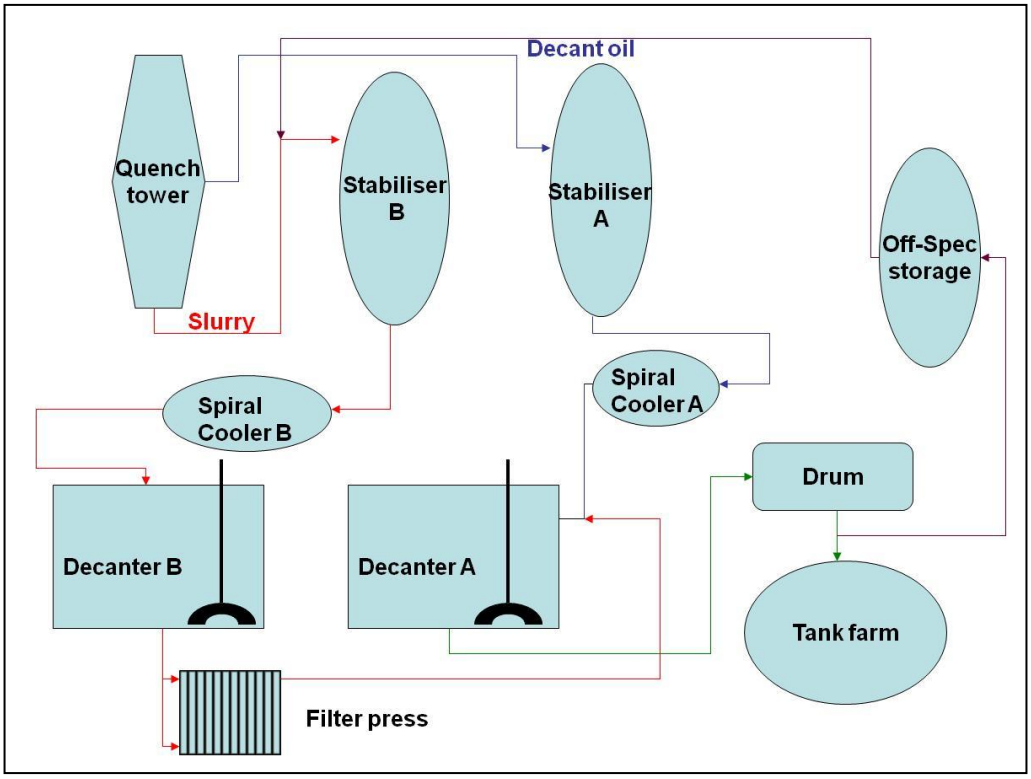

Figure 3-1 Simplified process flow diagram of the Synthol Decant Oil (SDO) filtration plant

Vapours from the Synthol reaction are cooled in a quench tower. Two streams, namely decant oil and the slurry oil, are drawn from the quench tower in different places.

The slurry oil is initially processed in a stabiliser to reduce the pressure. From the stabiliser, slurry oil is cooled in a spiral cooler to 80 °C. The slurry oil then enters a decanter and is processed through a filter press, which consists of 36 sections of cloth screen connected in series. The filtered slurry oil then flows into the stream of lighter decant oil distillate originating from the quench tower. The combined stream is processed by a second decanter and then flows into a “slop” drum to promote catalyst settling. The filtered and decanted product is then pumped to the tank farm, based on appropriate specifications relating to the concentration of solids in the SDO.

3.1.2 Delayed coking of Waxy Oil

The processes for distillation of SDO, as well as the delayed coking and calcination of Waxy Oil, are similar to those used in many delayed cokers worldwide. A simplified process flow diagram is shown in Figure 3-2.

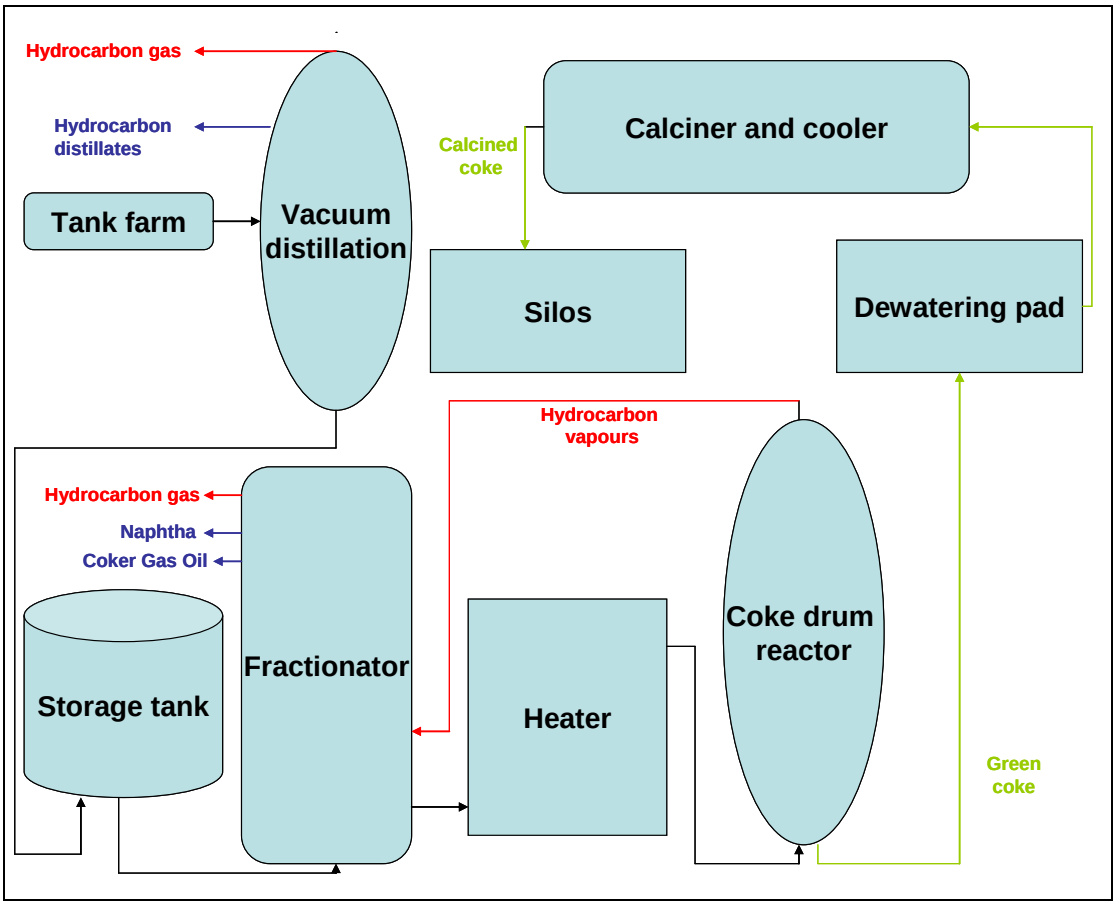

Figure 3-2 Simplified process flow diagram of SDO distillation, delayed coking of Waxy Oil and calcining of Waxy Oil green coke

The SDO is distilled in a vacuum flash column and the heavy residue (Waxy Oil) residue is pumped to the storage tanks on the delayed coker plant. Waxy Oil is processed by the delayed coker and calcined according to prescribed conditions.

3.1.3 Waxy Oil delayed coker feed

Feedstock consistency is integral in determining the variation in the characteristics of calcined Waxy Oil coke. By way of example, the variation in the ash and carbonaceous solids content of Waxy Oil is shown in Figure 3-3. The viscosity variation of Waxy Oil is shown in Figure 3-4. The data were compiled from 550 datum points, each representing a daily average.

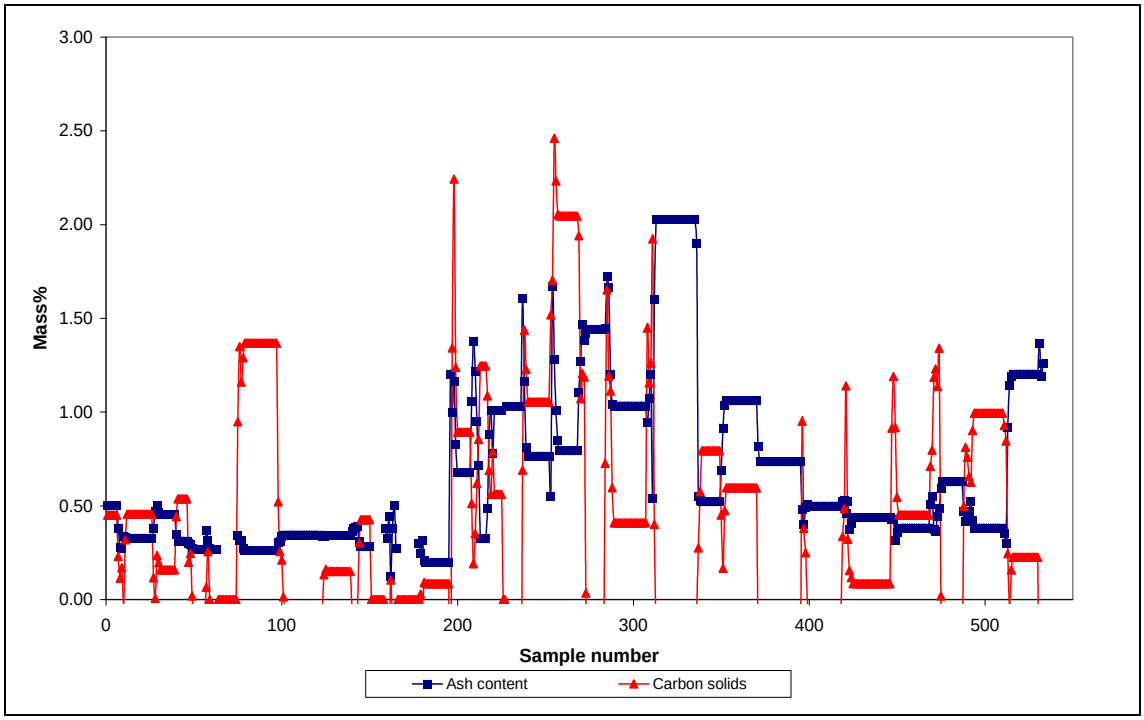

Figure 3-3 Ash content and carbon solids content of Waxy Oil feed to the delayed coker

As shown in Figure 3-3, the ash content of Waxy Oil varies between 0 and 2.00%. As Waxy Oil has an approximate calcined coke yield of 11%, the ash content by far exceeds the requirement for the recarburiser market (less than 0.2% in the Waxy Oil feed) or the needle coke market (less than 0.02% in the Waxy Oil feed). The carbon solids content (as determined by subtracting the ash content from the Mass Insoluble in Quinoline – MIQ – of Waxy Oil) is on average below 1.0%.

There are three specific reasons for the high ash content of the Waxy Oil calcined coke. These are:

- Process interruption of the gunk plant resulting in catalyst breakthrough and high-ash Waxy Oil feed to the delayed coker (shown in Figure 3-3)
- The low viscosity of Waxy Oil feed to the delayed coker (shown in Figure 3-4) and the reactive aliphatic molecular composition
- The lower calcination yield due to increased macroporosity and the catalytic effect of iron and calcium on air and carboxy reactivity

The green coke yield of approximately 18% from Waxy Oil is caused primarily by the lighter composition of the molecules, which results in the lower viscosity (12–22 Cst @ 100 °C) as shown in Figure 3-4. The lower green coke yield further exacerbates the effect of an ash concentration increase.

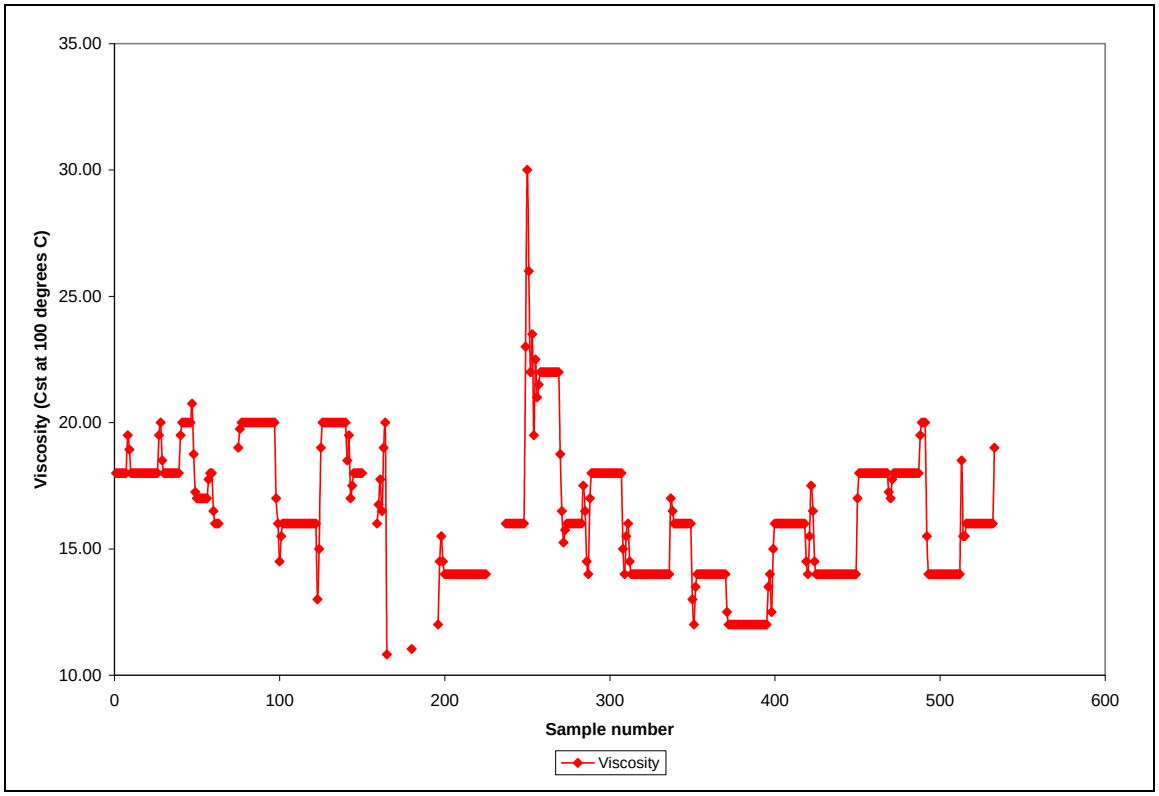

Figure 3-4 Viscosity of Waxy Oil feed to the delayed coker

The typical compositional characteristics of Waxy Oil delayed coker feedstock are shown in Table 3-1.

Table 3-1 Typical compositional characteristics and properties of Waxy Oil delayed coker feedstock

Analysis	Units	Waxy Oil
Carbon	Mass %	85.1
Hydrogen	Mass %	13.2
Sulphur	Mass %	<0.001
Nitrogen	Mass %	<0.0001
Ash content	Mass %	0.25-2.00
MIQ or QI	Mass %	3.2[2]
MIT or TI*	Mass %	3.4[2]
MIH or HI**	Mass %	3.7[2]
Conradson Carbon Residue (CCR)	Mass %	10.7[2]
Viscosity (@ 100 °C)	cSt***	22[1]
Distillation: Initial Boiling Point (IBP)	°C	179
5%	°C	311
10%	°C	371
20%	°C	438
30%	°C	465

1 Viscosity is highly variable (4-25 Cst)
2 Dependant on ash content variation
* TI = Toluene Insolubles
** HI = Heptane Insolubles
*** cSt = Centistokes

Waxy Oil is composed of long-chain aliphatics (whether alkylated or not) and thus the H/C ratio is high. It is the heavy residue product of a catalysed gas-phase reaction at 300 °C and thus the carbonaceous MIT and MIQ content is low. This is especially true for the asphaltene content which is low due to the lack of heavy macromolecular aromatics. Waxy Oil, being the product of a flash distillation, has a comparatively low Initial Boiling Point (IBP) (approximately 179 °C) and requires a substantial temperature increase to yield 5% distillation product (approximately 311 °C). The viscosity of the Waxy Oil is determined primarily by the specification for the diesel intermediates from the distillation of SDO, especially the Ramsbottom carbon content. Thus, the compositional characteristics of the heavy residue are not determined by the requirements of the delayed coker.

3.1.4 Waxy Oil calcined coke

The compositional variation of Waxy Oil calcined coke is shown in Table 3-2.

Table 3-2 Typical compositional variation of Waxy Oil calcined coke

Analysis	Units	Waxy Oil calcined coke
Fixed carbon	Mass%	87–99
Hydrogen[1]	Mass%	0.200
Sulphur	Mass%	0.064
Nitrogen	Mass%	0.003
CO_2 reactivity[1]	Mass %. 100 min^{-1}	67–91
Air reactivity[1]	Mass%	> 1.2
Real density (He)	$g.cm^{-3}$	2.08–2.17
Ash content	Mass%	1-13
Vibrated Bulk Density (VBD)[1]	$g.cm^{-3}$	≈ 0.56

1 Analyses not conducted on a routine basis

The major influence on the compositional variation of the Waxy Oil calcined coke is the ash content, which typically ranges between 1 and 13% with a reciprocal influence on the fixed carbon content. Both the nitrogen and sulphur contents are comparatively low. The carboxy and air reactivities are comparatively high given the macro-porosity of the coke and the presence of both iron and calcium catalysts. The influence of the catalyst concentration on the ash content of Waxy Oil calcined coke is shown in Figure 3-5.

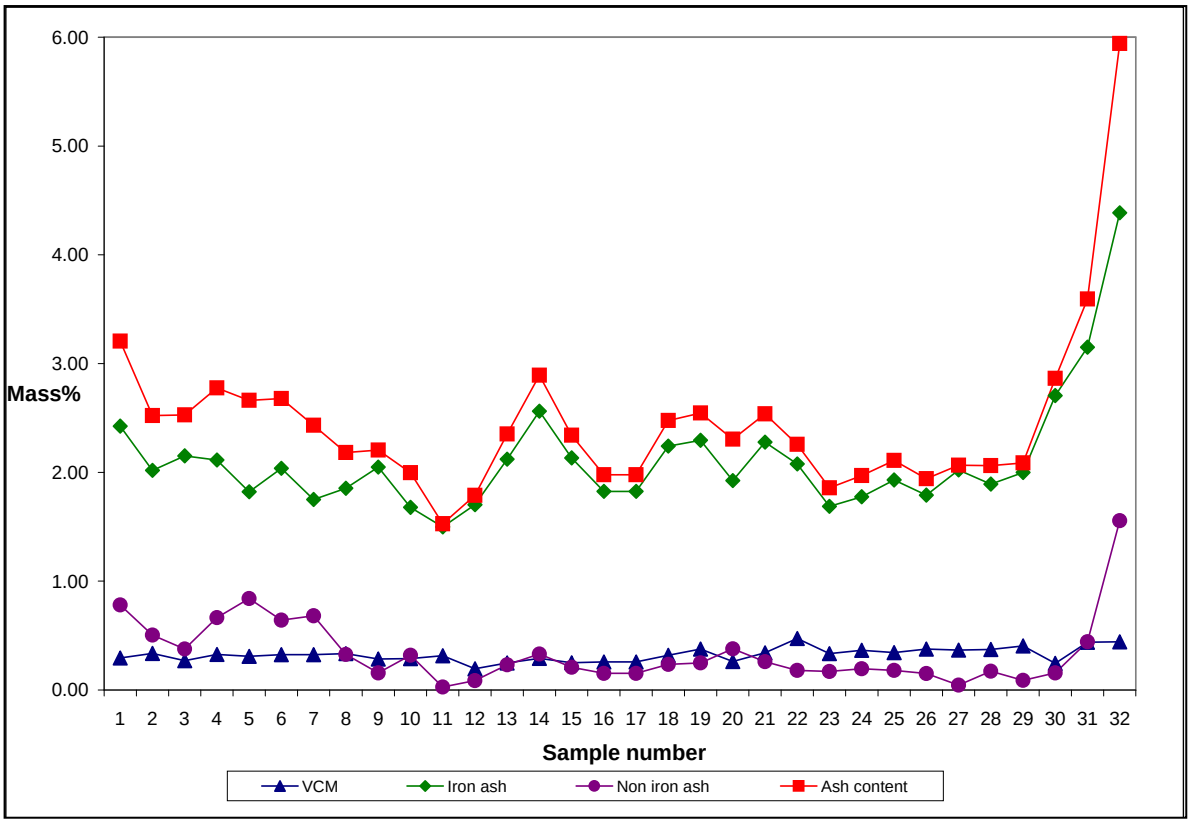

Figure 3-5 Total ash content (comprising non-iron ash and iron ash) and Volatile Carbon Matter (VCM) of Waxy Oil calcined coke

The iron ash component of the total ash content is approximately 90–95%. The non-iron ash content is substantially lower and is composed of contributions from both silicon and calcium.

3.2 Concluding remarks – The Waxy Oil value chain

Analysis of the Waxy Oil production process and compositional characteristics of the feedstock and calcined coke form a template on which the carbonisation chemistry is determined in later chapters. The two predominant detrimental factors in considering Waxy Oil as a needle coke precursor are the catalyst content and the lack of aromaticity.

While catalyst removal would appear a natural process step, it is the author's opinion that a determination of the effect thereof on the characteristics of Waxy Oil coke is necessary as an initial investigation. This is especially true given that the catalyst is iron oxide, which is known to both retard the extent of mesophase formation and promote multi-phase graphitisation, as demonstrated by Wang *et al.* (2001). These effects are further discussed in Chapter 6. The efficacy of graphitisation to sublimate iron from Waxy Oil coke is also discussed in Chapter 6.

However, catalyst removal from heavy residues is not unique to Waxy Oil and thus is more of a general requirement. The "art" will reside in the ability to modify the organic molecular composition of Waxy Oil in such a way as to effect a change in the kinetics of the carbonisation cycle.

If the effects of other reactivity promoters (e.g. hydroxyl substituents) are for the moment discounted, the given the fact that the literature provides convincing arguments to indicate that increasing the aliphatic nature of heavy residues is correlated with the production of isotropic carbon (Martinez-Escandell *et al.*, 1999), it may well be argued that the probability of producing highly anisotropic carbon from Waxy Oil is indeed remote. However, the author asserts that the aliphatic nature of previously studied residues may well differ substantially from that of Waxy Oil, with specific reference to its unique origin. Thus it would be myopic to merely discount Waxy Oil without evaluating its molecular composition and carbonisation chemistry. Waxy Oil modification, subsequent carbonisation and determination of the reaction mechanism are discussed in Chapters 7 to 9.

A comparison of Waxy Oil characteristics with research results provided in the cited academic literature is discussed in Chapter 4.

4 REVIEW OF PREVIOUS WORK

4.1 Introduction

The science of needle coke has been the subject of academic research for many years. Most of the literature cited emphasises the dependence of needle coke characteristics on pre-carbonisation feedstock variables, which in turn are governed largely by their origin and upstream processing, whether the coke is based on crude oil or coal.

This chapter compares what is known about Waxy Oil chemistry at the onset of this study against relevant knowledge described in the published literature. The structure of the chapter includes a short paragraph at the beginning of each section relevant to Waxy Oil (*provided in italics*), followed by a comparison with the literature.

4.2 The chemistry of needle coke precursors

4.2.1 The influence of feedstock aromaticity on needle coke quality

The molecular composition of Waxy Oil is not well understood. However, it is thought to be composed predominantly of normal and multi-alkylated alkanes of varying chain length. This is in stark contrast to the dependence of needle coke on the aromaticity of the carbonisation precursor as described below.

Wang and Eser (2007) used High-Pressure Liquid Chromatography (HPLC) with Photodiode Array (PDA) coupled with Laser Desorption Mass Spectroscopy (LDMS) to determine some of the molecules present in FCCDO, a known precursor for needle coke production. The major compounds present were three- to six-ring PAHs, inclusive of phenanthrene, pyrene, chrysene, perylene, benzopyrene and benzoperylene or multi-alkylated homologues thereof.

Mochida *et al.* (1987) showed the influence of aromaticity on the concentration of microstructural flow domains and the CTE of coke using carbonisation in a tube bomb; FCCDO with 71% aromatic content produced the highest concentration of microstructural flow domains and the lowest CTE in the coke. Comparatively, the same research evaluated two LSVRs, comprising lower aromatic contents (44 and 52% respectively), which produced cokes with more randomly orientated domains (than flow domains) and a higher CTE. The most isotropic of the cokes (displaying fine isotropic microstructural mosaics) was produced from Gilsonite composed almost entirely of reactive asphaltenes. The CTE of the Gilsonite coke was approximately an order of magnitude higher than that of the FCCDO calcined coke.

Although Martinez-Escandell *et al.* (1999) provide a convincing argument as to the effect of aromaticity in reducing the reactivity of petroleum residues during carbonisation, the relationship is not absolute and requires qualification. By way of example, Gilsonite composed almost entirely of aromatic asphaltenes is very reactive, forming highly isotropic coke as described above. The influence of asphaltenes is discussed in more detail in Section 4.5.

Eser and Jenkins (1989) used Fourier Transform Infra Red (FTIR) spectroscopy to determine the degree of aromaticity of various heavy residues and further correlate them with the CTE of the resultant cokes. They also determined that the presence of reactive asphaltenes (producing fine mosaics) had a dominating effect on the optical texture of the coke microstructure. Seshardi *et al.* (1982) used ^{13}C Nuclear Magnetic Resonance (NMR) to determine the carbon aromaticity of various needle coke precursors and showed that an increase in the percentage of ^{13}C aromatic carbons promoted the formation of more anisotropic coke with a reduced CTE. Other studies have also established a similar relationship between increased hydrogen aromaticity and a decrease in the CTE of resultant cokes (Eser & Jenkins, 1989; Mochida *et al.*, 1977; Eser & Hou, 1996). Studies using high-resolution ^{1}H NMR demonstrate the ability to predict the CTE of cokes based on the hydrogen aromaticity (denoted as "bay" protons) of the precursor (Stecker, 1984). The importance of bay protons or hydrogen donors is to cap radical intermediates produced during the onset of carbonisation, preventing extensive premature cross-linking and increasing the duration of the mesophase in a liquid crystalline state. This allows the growth of mesogen spheres and eventual coalescence of the mesophase as determined by Eser and Jenkins (1989).

Mochida *et al.* (2000) state that optimal precursors for the production of anisotropic mesophase include naphthalene and methylnaphthalene. These molecules are particularly suitable as they comprise two-ring aromatics and utilise the alkyl function to create bridges with other aromatics during polycondensation. An added advantage of these molecules is the relative abundance of hydrogen donors (hydrogen bound directly to the aromatic ring structure) (Mochida *et al.*, 2000; Lutz & Wilson, 1986; Eser and Jenkins, 1989).

Given the complexity of both coal tars and decant oils, Lewis (1987) studied the mesophase reaction of some of the most basic of aromatic building blocks, namely naphthalene or dimethyl naphthalene, in order to elucidate a reaction mechanism. This research showed that aromatic polycondensation was integral in the carbonisation process, forming dimers of single aromatic molecules during the onset of carbonisation. Dimethyl naphthalene was found to carbonise at a faster rate than naphthalene due to the activating effect of methyl groups, as explained below.

The initiation step in the carbonisation of alkyl aromatics is thought to be governed by free radical chemistry, involving the abstraction of aromatic hydrogen or the cleavage of the C-H bond on the methyl side chain (Wang & Eser, 2007). These initial reactions include the formation of aryl-aryl bonds, as in the case of naphthalene polymerisation, or methyl-aryl bonds, as in the case of methyl naphthalene carbonisation (Lewis, 1987; Mochida *et al.*, 2000). Further polycondensation and hydrogen loss create the first precursors of the graphene sheet, which is the basic two-dimensional unit of the graphitic crystal structure. Further development of the mesophase has been described by Mochida *et al.* (1977) as the growth and coalescence of spheres composed of these planar aromatic molecules (6-15 Å) with molecular weights in the range of 400 to 3 000 atomic mass units (amu).

The higher thermal stability of aromatic residues compared with aliphatic residues and the propensity thereof to produce anisotropic coke has been previously established by several authors, including Rodriguez-Reinoso *et al.* (2001), Torregrosa-Rodriguez *et al.* (2000) and Martinez-Escandell *et al.* (1999) who studied the carbonisation chemistry of various petroleum residues. These residues varied from a totally aliphatic soft wax to a mostly aromatic FCCDO.

4.2.2 The influence of aromatic hydrogen on mesophase development

Based on the aliphatic nature of Waxy Oil, the absence of aromatic protons is by default a "fait accompli". However, by their very nature aliphatic heavy residues have relatively high hydrogen-to-carbon ratios. The production of coke from aliphatic Waxy Oil will naturally include an aromatisation step prior to mesophase formation. The duration of mesophase fluidity will thus depend on the "reservoir" of stable hydro-aromatic bay protons produced.

Although the role of carbon aromaticity in the development of the mesophase has already been established, the substantial contribution of aromatic hydrogen as a rate-determining factor is integral to the development of the mesophase. Obara *et al.* (1981) described the role of hydrogen-transfer reactions in "extending the temperature zone of maximum fluidity" while stabilising radicals produced during carbonisation. Indeed, Diez *et al.* (1999) further argue that the increased mobility of the pitch system during mesophase development allows aromatic sheets to stack parallel to each other, increasing the anisotropy of the resultant coke

The study of these hydrogen-transfer reactions has been based on the role of aromatic molecules in acting both as hydrogen donors and hydrogen acceptors. Various authors have described these transfer reactions using model compounds, including 9, 10-dihydroanthracene/1, 2, 3, 4-tetrahydroanthracene as the hydrogen donor and anthracene as the acceptor molecule in various precursors – coal-tar pitch (Machnikowski *et al.*, 2001; (Yokono & Marsh, 1979), hydrogenated ethylene tar pitch (Obara *et al.*, 1981) and petroleum pitch (Diez *et al.*, 1999; Yokono *et al.*, 1980).

Mochida *et al.* (2000) used a pure compound, namely tetrahydroquinoline, to show how it reduced the rate at which the carbonisation reaction proceeds and allowed a greater extent of mesophase development. Pure low-order polycyclic aromatics, inclusive of naphthalene, tetralin or anthracene, may be used as a source of aromatic hydrogen (Lutz & Wilson, 1986; Legin-Kohler *et al.*, 1999); however, they are prohibitively expensive on a commercial scale. McConaghy *et al.* (1979) showed how aromatic distillate fractions of either coal tar or petroleum decant oils added to petroleum vacuum residuum (which would usually produce a sponge coke: CTE 20.0 x 10^{-7}.°C^{-1}) using a process called Hydrogen Donor Diluent Cracking (HDDC) produced a premium needle coke with a reduced CTE of 5.0 x10^{-7}.°C^{-1}.

Hishiyama *et al.* (1983) demonstrated that the temperature at which hydrogenation is conducted can similarly affect the microstructure and graphitisability of the coke. Thermal treatment of ethylene pitch at 400 °C, as opposed to lower temperatures (200–300 °C), was shown to promote the development of flow textures, which formed cokes with mosaic microstructures. The significance is the ability of a precursor to allow these hydrogen-transfer reactions during the formation of pre-mesogens and prior to mesophase development.

4.3 The influence of heteroatoms on needle coke quality

Heteroatoms present in needle coke feedstock originating from either crude oil or coal tar play a vital role in the carbonisation process and may influence the texture of the resultant coke.

Waxy Oil differs from either coal-tar or petroleum residues in that it is synthetically produced from a gas-phase reaction, and thus the typical nitrogen content (0.009%) and sulphur content (0.08%) of Waxy Oil calcined coke is comparatively minimal. It is this fact that makes Waxy Oil a potentially attractive residue as a needle coke precursor. Inasmuch as Waxy Oil is devoid of stable nitrogen and sulphur heterocyclics, it is important to define the action of these heteroatoms in better known needle coke precursors to establish the comparative value. While the predominance of oxygen-containing organics in Waxy Oil is not known (at least at the onset of the project), the fact that carbon monoxide is one of the co reactants in the process would indicate the possibility of their presence.

Whereas Lewis (1987) is of the opinion that the optimum aromatic precursor molecule for the production of a highly anisotropic needle coke is naphthalene or methyl naphthalene, based on carbon and hydrogen alone, in reality this feed would be prohibitively expensive and there would not be enough to sustain the demand for needle coke. The two major sources of needle coke precursors are petroleum products originating from crude oil (which by virtue of their origin contain a substantial concentration of stable sulphur heterocyclics) and coal-tar products (which by virtue of their origin contain a substantial concentration of stable nitrogen heterocyclics), as described by Weinberg *et al.* (1988). The inevitable presence of these heteroatoms in these available precursors has attracted substantial research interest with respect to their effect on both the mesophase formation and puffing.

The oxygen content of most delayed coker feedstocks, and certainly those deemed suitable for the production of needle coke, is comparatively low (below 1%) due to loss of the hydroxyl function during production. Both Clark *et al.* (2002) and Wolters & Van der Walt (2007) studied the effect of heavy residues formed by the low-temperature gasification of coal on mesophase formation, in which the oxygen content was substantially higher (5%), dominated by hydroxyl functions.

Studies to determine the effect of heteroatoms on mesophase formation are broadly characterised into two groups:

- Heteroatoms bound as heterocyclics (e.g. furans, thiophenes and pyridines)
- Heteroatoms bound as functionalities to a parent aromatic (e.g. hydroxyls, thiols and amides)

4.3.1 The influence of sulphur on needle coke quality

Mizuntani *et al.* (2007) conducted research into the cracking reaction on petroleum Fluid Catalytic Cracker (FCC) feed and gasoline products using both Field Desorption Mass Spectroscopy (FDMS) and Gas Chromatography-Atomic Energy Detection (GC-AED). The predominant sulphur species found were polycyclic thiophenes, benzothiophenes with alkyl functions up to C_4 and dibenzothiophenes with alkyl side functions up to C_8 in the heavier FCC feed. Using sulphur-selective ligand exchange chromatography, Ma *et al.* (1997) concluded that the major non-polar species present in petroleum vacuum residue were alkyl benzothiophenes, benzonaphtha thiophenes and phenanthrothiophenes.

Sulphur may also present as less-stable side functions bound to the parent aromatic. These sulphydral groups, due to their valency differing from that of carbon, react during the onset of carbonisation with aromatic carbon of the same or neighbouring molecules, disturbing the

planar geometry and resulting in three-dimensional faults in the graphitic structure, as determined by Weinberg *et al.* (1988).

Hossain and Podder (1989) carbonised elemental sulphur with model anthracene and phenanthrene to show the cross-linking effect of sulphur functionalities using Differential Thermal Analysis (DTA). The mesophase microstructures of the sulphur anthracene/phenanthrene compounds were found to be disrupted and disordered, showing mosaic domains as compared with those of the model compounds alone whose mesophase structures appeared to have coarse flow domains.

Furthermore, Marsh *et al.* (1973) reported that carbonisation of model sulphur-containing organic compounds (dibenzothiophene and thianthrene) produced only isotropic carbon. However, the literature is not in complete agreement with respect to the role of sulphur in disrupting mesophase formation. Studies conducted on Khafti asphalt by Oi and Oinishi (1978) determined that sulphur-containing organics have no effect on mesophase development due to these molecules having a similar nature to those in the Khafti asphalt. However, this research has further shown the catalytic effect of vanadium in the presence of sulphur to promote the formation of β-resins, known as the "building blocks" of the developmental mesophase, as suggested by Lewis (1987). The same author also suggests that non-polar heterocycles containing sulphur may readily be incorporated into the macromolecular matrix during mesophase development and thus become stabilised with no substantial reduction in the sulphur content below 1 100 °C.

Didchenko and Lewis (1992) indicated the maximum sulphur concentration for needle coke feedstock to be 1%, producing a calcined premium-grade needle coke with a maximum sulphur content of 0.8%. The same authors emphasise the need to direct hydro-desulphurisation reactions towards the heavier sulphur-containing molecules as the lighter sulphur-containing molecules are vaporised during the delayed coking process.

Given the comparatively low levels of sulphur in Waxy Oil, desulphurisation processes are only of passing interest. Worldwide crude oil resources are known to be getting heavier and more sour (higher concentrations of sulphur), according to the work of Nylen *et al.* (2004). Hydro-desulphurisation reactions using catalysts based on oxides of cobalt and molybdenum supported on an alumina substrate have been utilised to decrease the sulphur content of decant oil (2.35%) to between 0.79 and 1.27%, as described by Didchenko and Lewis (1992).

4.3.2 The influence of nitrogen on needle coke quality

Studies evaluating the role of nitrogen-containing heterocycles on the extent of mesophase formation have for the most part been conducted on either model compounds or coal-tar needle coke feedstock.

While the list is by no means definitive, Murti *et al.* (2005) report pyridines, anilines, quinolines, indoles and carbozoles to be the dominant species.

Marsh *et al.* (1973) showed how the carbonisation of model nitrogen-containing polyaromatic hydrocarbons (carbazole) produced isotropic mosaics, while phenazine produced anisotropic mosaics. The addition of carbozole to model anthracene was found to impede the development of the mesophase. However, as with studies of the carbonisation reactions of

aromatic compounds containing sulphur and oxygen bound as a side chain, Weinberg *et al.* (1988) showed nitrogen in the form of amide groups to be disruptive to mesophase formation.

4.3.3 The influence of oxygen on needle coke quality

Studies pertaining to the effect of oxygen-containing aromatics with hydroxyl/aldehyde side chains have historically been of lesser significance given that the temperatures under which coal-tar and FCCDO residues are produced largely eliminate these functionalities.

However, studies conducted to identify the nature of oxygen-containing aromatics (Murti *et al.*, 2005; Weinberg *et al.*, 1988; Marsh *et al.*, 1973) have identified the presence of furans and coumarin. Oxygen bound as side chain functionality to aromatic molecules has been identified as phenolics, hydroxyl naphthalenes, phthalic anhydrides, various derivatives of anthraqinone and carboxylic acids associated with two- to four-ring aromatics, e.g. napthoic acid.

Both Weinberg *et al.* (1988) and Marsh *et al.* (1973) reported carbonisation of aromatics with bound hydroxyl functions to produce isotropic microstructures. This characteristic has been explained by the ability of a hydroxyl function (for instance) to form ether linkages during the initial phase of carbonisation, resulting in intermediates that are not planar and cannot be incorporated into the ordered graphene structure. The effect is to increase the viscosity of the developing mesophase prematurely, thereby decreasing molecular mobility.

Wolters and Van der Walt (2005) showed that carbonisation of low-temperature coal gasification pitch, which has a comparatively high concentration of phenolics, produced coke with a mixture of fine and medium isotropic mosaics. Using the same feedstock containing up to 5% oxygen, Clark *et al.* (2001) showed on a commercial scale that adding a lesser percentage of FCCDO to this feed increased the anisotropicity of the coke. Further work by the same authors demonstrated the ability to determine microstructural variations along the height of a commercial delayed coker drum (Clark *et al.*, 2002).

4.4 Interventions to control puffing of needle coke

Research to control the puffing reaction during the graphitisation of needle cokes may broadly, irrespective of the precursor, be classified into three main categories:

- Choosing a feed with a low heteroatom content, specifically those bound as heterocyclics
- Removing heterocycles from the feedstock, referring to various hydro-desulphurisation/hydro-denitrification reactions (depending on the origin of the needle coke precursor)
- Treating the symptom, referring to the control of the puffing reaction aided by the addition of inhibitors that control the release of heteroatom gases

The least costly option would involve the identification of needle coke precursors with reduced concentrations of stabilised heterocycles; however, this is not always an option due to limited availability. Furthermore, the quality of a needle coke precursor is not determined solely by either nitrogen or sulphur content, but depends on a range of feedstock characteristics as discussed earlier.

Academic research into controlling the puffing reaction during graphitisation with the aid of additives mainly concentrates on either sulphur puffing (as is the case with petroleum needle cokes) or nitrogen puffing (as is the case with coal-tar pitches). A detailed description of the puffing reaction has been given in Chapter 2, but this section concentrates on inhibitors that are used to control puffing during graphitisation.

With respect to the graphitisation of petroleum cokes, the addition of iron oxide (2% by weight) to calcined coke is the preferred remedy for suppressing puffing in calcined cokes containing more than 0.3% sulphur, based on work conducted by Orac *et al.* (1992). This research also proposes the use of sodium carbonate (either in the form of a fine powder or as an aqueous slurry) as a puffing inhibitor. Sodium carbonate is sprayed onto the calcined coke within the cooler section after the calciner. Sodium is able to penetrate the matrix of the coke particle (via porosity) and inhibit the puffing reaction from "within", reacting with sulphur and stabilising it during graphitisation (especially in the 1 600–1 800 °C range). Orac *et al.* (1992) showed how the addition of 1% sodium carbonate to calcined coke under prescribed conditions was effective in reducing the puffing rate from 62 (with no additive) to 0 (with additive).

Kawano *et al.* (1999b) used boric acid (0.9%) to suppress puffing of petroleum-derived needle cokes from 1.5 to 0.8%. The same authors (Kawano *et al.*, 1999a) showed that the addition of boric acid, followed by heat treatment to 400, 600 and 950 °C, was effective in reducing puffing by 22, 40 and 41% respectively, using the untreated petroleum needle coke as a reference.

Hsu (1982) showed that the addition of iron oxide to decant oil (prior to carbonisation) was effective in reducing coke puffing. However, Wang *et al.* (2001) also showed that the addition of iron oxide to petroleum residues (prior to delayed coking) inhibited mesophase development by increasing the rate of oxidative polymerisation.

4.5 The influence of asphaltenes on needle coke quality

As shown in Chapter 3, Waxy Oil is composed of a negligible percentage of asphaltenes. There are two probable reasons for this. Firstly, during the Fischer-Tropsch reaction, the maximum temperature is 320-350 °C which, secondly, produces long-chain aliphatics not possessing the activity for aromatisation. While asphaltenes are thus important in relation to Waxy Oil (by their absence), this study also identifies molecular groupings that act as reactivity promoters, of which asphaltenes are one. Another reason for describing the contribution of asphaltenes during carbonisation is their tendency to precipitate prematurely out of solution, forming mosaic microstructures and shot coke at the bottom of the coke section. The current study uses much the same methodology to determine the effect of Waxy Oil modification on the microstructure, using "static" carbonisation (discussed in Chapter 8).

Dickakian (1984) described asphaltenes as a group of reactive heavy molecular weight aromatic molecules containing between 3 and 4% heteroatoms, which are soluble in quinoline and therefore cannot be described as solids. Asphaltenes are further characterised by their solubility in paraffinic solvents but insolubility in toluene. Although asphaltenes are highly aromatic (which has previously been described as beneficial in terms of the

anisotropicity), they are large non-planar molecules with high reactivity. Seshardi *et al.* (1982) therefore argue that they are detrimental to the anisotropy of the coke.

Although most polynuclear aromatics absorb ultraviolet light in the region between 280-400 nanometres (nm), asphaltenes have been detected at specific wavelengths of 292, 324 and 340 nm in accordance with ASTM method D2008 (Sien & McGinley, 1983).

Seshardi *et al.* (1982) conducted quantitative ^{13}C NMR to show that the asphaltene fraction of decant oil and pyrolysis tar had a higher average molecular weight than the parent residue. The asphaltene fraction had an average molecular weight of 515 amu vs. 331 amu for the parent decant oil. The average molecular weight of the pyrolysis tar asphaltene fraction (984 amu) was also shown to be substantially higher than that of the parent pyrolysis oil (300 amu).

The effect of asphaltenes on mesophase development has been evaluated previously by several authors and the findings are summarised below.

- They show higher reactivity and the ability to increase the rate of carbonisation (Eser and Jenkins, 1989; Mochida *et al.*, 1989).
- They tend to form isotropic mosaics within the coke structure leading to higher CTE cokes (Eser and Jenkins, 1989; Mochida *et al.*, 1989; Mochida *et al.*, 1987; (Eser *et al.*, 1989).
- They have a "dominating" influence on the microstructure morphology of a coke (Mochida *et al.*, 1987; Mochida *et al.*, 1989).
- They tend to precipitate out of the developing mesophase and settle at the bottom of a coke drum, producing a highly isotropic dense region of coke, commonly referred to as "shot" coke (Mochida *et al.*, 1989)

Eser *et al.* (1989) thermally treated petroleum vacuum residues containing asphaltenes at sub-carbonisation temperatures (350–400 °C) to increase the concentration of aromatic hydrogen, lower the reactivity and promote self-condensation of reactive asphaltic molecules. Compared with the reference coke (produced from the untreated vacuum residues), the cokes produced showed a greater degree of anisotropy (as determined by an increase in flow domains) and a greater graphitisability (as determined by lower d_{002} values and higher L_c values).

Several other processes have been described to reduce the reactivity of asphaltenes, including:

- Hydrogenation followed by catalytic cracking (Murukami *et al.*, 1989)
- Solvent separation using heptane (Dickakian, 1984)
- Hydro-treating followed by asphaltene extraction with pentane (Goyal *et al.*, 1994)
- Solvent extraction of asphaltenes with light naphtha or C_4 to C_6 paraffinic solvents (Bonilla & Elliot, 1987).

4.6 The influence of mineral matter on needle coke quality

The potential impact of mineral matter on the carbonisation of Waxy Oil is of importance as the concentration of the catalyst (iron oxide) therein is variable and may increase to

approximately 2%. Given the low yields during delayed coking and calcination this percentage may then convert to 10% in the calcined coke. The presence of iron contaminates in petroleum residues is limited for two reasons. Firstly, they are not naturally abundant in petroleum residues (compared with vanadium or nickel) and cracking catalysts have historically been based on alumino-silicate powders. However, based on the literature discussed below, iron oxide affects many reactive mechanisms: it may inhibit mesophase development, promote oxidative polymerisation, increase the carboxy or air reactivity of calcined cokes and substantially modify the graphitisation mechanism. Thus this study describes in detail the potential detrimental effect of the iron oxide catalyst on the carbonisation, calcination and graphitisation of Waxy Oil.

4.6.1 The effect of mineral matter on mesophase development

Mineral matter in needle coke feedstock may originate either from the source itself (e.g. coal or crude oil) or from catalysts used in upstream pre-carbonisation processes.

Obara *et al.* (1985) investigated the effect of silica gel (< 45 µm) addition to FDDCO in reducing the size of the microstructural domains of the coke and reducing the amount of transferable hydrogen during carbonisation. This work is supported by that of Wang *et al.* (2001) who determined the effect of iron oxide as catalysing oxidative polymerisation, so producing fine mosaic microstructures. This research used the addition of iron oxide powder (0.1–1.0 µm) to improve the yield of the QI insoluble fraction during carbonisation. However, microstructural evidence showed the formation of anisotropic flow domains (without the iron oxide additive), the development of coarse mosaic texture with the addition of 6% iron oxide and the development of fine mosaics with the addition of 17 and 25% iron oxide respectively. Iron oxide not only presents an inert barrier to parallel stacking, but also promotes chemical oxidative polymerisation, leading to cross-linking, premature viscosity increase during mesophase development and the formation of mosaic microstructures. The severity of oxidative polymerisation is highly dependent on the concentration and particle size distribution of the catalyst, according to the research of Obara *et al.* (1985) and Wang *et al.* (2001).

Sakanishi *et al.* (2002) showed that many metals extracted from coals may bind in the form of silicates, oxides, carbonates, sulphides, sulphates and phosphates. However, the addition of various organo-metallic compounds to PVC pitch was shown to have a varied effect on mesophase formation, attributed more to the type of metal rather than the concentration thereof. Both vanadium acetylacetonate and nickelocene were further found to have a catalytic effect by increasing the thermal decomposition of sulphur heterocyclics (Oi & Onishi, 1978).

Boudou *et al.* (1998) noticed similar effects on the microstructure when iron chloride was added to a coal-tar pitch. The iron chloride converts to iron oxide, which increases the rate of carbonisation, promoting the formation of mosaic microstructures. However, Song *et al.* (2003) argue that the inclusion of iron as an organo-metallic in the form of ferrocene decreases the interlayer spacing of the crystal. In a study aimed at increasing the rate at which carbons react during gasification, Marsh *et al.* (1984) showed how both metal (Li, Na, K, Rb and Cs) hydroxides and carbonates promoted the formation of isotropic carbon when co carbonised with Ashland A240 pitch.

However, some metal oxides have much the opposite effect during carbonisation. Ramos-Fernandez *et al.* (2007) showed that both oxides and carbides of titanium enhanced mesophase development by a process thought to be concerned with facilitating hydrogen transfer and increasing the liquidity range of the pitch system during carbonisation.

4.6.2 The effect of iron oxide on the carboxy and air reactivity of calcined coke

One of the factors contributing to the low yield of Waxy Oil calcined coke is thought to be the ability of iron to catalyse both air and carboxy reactivity during calcination. Quite apart from the loss of solid carbon, there is a substantial and unnecessary increase of the ash content and the carbon footprint of the calcination process.

Mineral catalysts for air reactivity have historically been linked to vanadium, nickel and sodium (Hume *et al.*, 1993), specifically in petroleum cokes where the heavy metals (vanadium and nickel) originate as metal porphyrinic complexes associated with the asphaltenes of crude oil, according to Ali and Abbas (2006). The catalytic activity of sodium is often more enhanced due to its ability to intercalate between carbon lamellae and thus become better dispersed, but this activity is reduced in high-sulphur petroleum cokes (Hume *et al.*, 1993). Patrick and Shaw (1972) showed that sodium increases air reactivity, increases meso/microporosity and reduces the ignition temperature of coke. However, the vanadium, nickel and sodium content of Waxy Oil calcined coke is low.

The carboxy reactivity of the Waxy Oil calcined cokes is far in excess of the normal specification for petroleum calcined cokes (10–15%) in the aluminium industry, as reported by Hume *et al.* (1993). In an extract from Hume's PhD thesis, Hume *et al.* (1993) showed that the catalytic effect of increased sodium and calcium contents of calcined petroleum cokes was to increase substantially the carboxy reactivity. Indeed, the catalytic effect of calcium on the carboxy reactivity of petroleum cokes, coals and chars has been established previously by several authors, namely Walker *et al.* (1993), Hippo and Walker (1975) and Lang and Neavel (1982).

Jenkins *et al.* (1973) showed iron oxide (α-Fe_2O_3) to be a poor catalyst for air and carboxy reactivity. However, within calcined coke, iron oxide is reduced predominantly to iron, which was shown by both Hippo and Walker (1975) and Walker *et al.* (1983) to promote both reactivities. At this point it is necessary to mention that both air and carboxy reactivities are of more importance to the aluminium industry and given the relatively low concentration of iron compared with other metals in delayed cokes, its effect has not been widely studied. Another factor is that no petroleum cokes for either the aluminium or electrode industries have catalyst contents as high as Waxy Oil calcined coke.

4.6.3 Iron oxide as a driving force for multi-phase graphitisation

Iron oxide is listed as one of the 31 minerals that promote multi-phase graphitisation during thermal treatment of green coke. The unusually high concentration of iron oxide in Waxy Oil increases the potential for it to affect the graphitisation mechanism of coke during thermal treatment. The predominant graphitisation mechanism during thermal treatment of needle cokes depends on the anisotropy of the carbon microstructure. Any departure from this mechanism may well provide disingenuous results when trying to compare the

crystallographic indices of Waxy Oil coke with those of other needle cokes. This characteristic is investigated in Chapter 6.

While the addition of chromium, manganese, molybdenum, vanadium and iron oxides has been shown to reduce the temperature at which graphitisation is initiated (increasing the L_c and reducing the d_{002}), this form of catalytic graphitisation is on a localised scale of approximately 1 µm, as reported by Mochida *et al.* (1980). Thus the influence of iron in promoting catalytic graphitisation will depend both on its particle size distribution and on the concentration, as reported by Wang *et al.* (2001).

4.6.4 Methods for removing mineral matter from heavy residues

Apart from the effects of iron oxide on numerous characteristics of Waxy Oil green and calcined coke, the most apparent effect is simply an increase in the ash content. If Waxy Oil coke is used as a recarburiser, the high ash content is less of a problem as the iron reports to the iron melt. However, in producing a highly anisotropic carbon from Waxy Oil for use in the manufacture of carbon artefacts (e.g. needle coke for electrodes), the catalyst would have to be removed either prior to or after delayed coking. This study concentrates on the removal of iron oxide from Waxy Oil using filtration.

Eguchi *et al.* (1997) reduced the mineral content of petroleum decant oils (prior to delayed coking) using filtration, centrifugation, electrostatic aggregation and a combination of these methods. Although the effect of minerals on the formation of isotropic mosaics and the trend towards a higher CTE has been established, this research determined the effect of reducing the alumino-silicate concentration in petroleum decant oil directly on the CTE of the coke produced. The research showed that reducing the mineral content of the petroleum decant oil from 0.0240 to 0.002% reduced the CTE from 6.7 to 4.9 x 10^{-7}.°C^{-1}. In all three of the abovementioned mineral reduction interventions, lowering the viscosity of the feed either by increasing the temperature or by the addition of naphtha was beneficial.

4.7 Molecular modification of needle coke precursors

Molecular modification of Waxy Oil will be beneficial only once the catalyst has been removed. As little is known about Waxy Oil molecular chemistry, its characterisation will be necessary to identify potential reactivity promoters before embarking on modification processes. This study uses distillation and thermal treatment to effect molecular modification. However, it concentrates on molecular modification to increase the anisotropy of the coke.

As the molecular make-up of feedstock determines the quality of the needle coke, modification the make-up will change the reaction kinetics of carbonisation and the microstructure of the coke.

Interventions to optimise the chemical nature of needle coke precursors and thus of coke qualities include:

- Co-carbonisation of feedstock
- Thermal treatment
- Hydrogenation/cracking
- Distillation

4.7.1 Co-carbonisation of feedstock

The co-carbonisation of heavy residues has historically proved a cheap alternative to pre-carbonisation modification processes and thus needs to be discussed in this chapter. It is unlikely that co-carbonisation of Waxy Oil with another heavy residue would be viable for two reasons. The reason for choosing Waxy Oil as a feed for this study was its comparatively negligible sulphur and nitrogen content. Co-carbonisation with another heavy residue (e.g. a petroleum FCCDO), even in small percentages, would substantially increase the sulphur or nitrogen content (given the low coking yield of Waxy Oil) and thus destroy market attractiveness. The other possible reason is that the aliphatic nature of Waxy Oil may present challenges when it is co-carbonised with an aromatic residue due to separation and independent carbonisation of the residues.

As delayed coking of many petroleum vacuum residues produces sponge coke, FCCDO may be added to modify its composition and thus upgrade the feed for the production of needle coke. Using a step increase in the concentration of FCCDO in a blend with a petroleum vacuum residue, Mochida *et al.* (1989) established that the aromaticity of the blend increased in direct proportion to the concentration of FCCDO, the asphaltene content decreased and carbonisation produced coke with an increased percentage of flow domains. The coke produced from the vacuum residue alone yielded a CTE of 13.0 x 10^{-7}.°C^{-1}, while when 30, 50 and 70% FCCDO were added, the CTE of the coke reduced proportionately to 3.9, 2.3 and 1.0 x 10^{-7}.°C^{-1} respectively.

Similar studies investigating the effect of step increases in the addition of FCCDO to ethylene tar were reported by Dickinson and Moore (1988) who showed that it was possible to reduce the CTE of the coke formed from 100% ethylene tar (CTE 9.4 x 10^{-7}.°C^{-1}) using an addition of 75% FCCDO, to 4.7 x 10^{-7}.°C^{-1}.

The purpose of co-carbonisation is to maximise the beneficial attributes of the feedstocks during carbonisation while providing a buffer for detrimental characteristics. A case in point is the co-carbonisation of FCCDO with gasification coal-tar pitch as determined by Clark *et al.* (2001) and in later research by the same authors (Clark *et al*., 2002). This research describes the interaction of the beneficial attributes of FCCDO (lower nitrogen content, higher aromaticity) with those of gasification coal-tar pitch (lower sulphur content, lower metals content, higher density) to form a hybrid coke used in the production of small-diameter electrodes.

4.7.2 Molecular modification of heavy residues

It is incumbent on any process evaluated that its three main objectives are met, namely increasing the coke anisotropy, reducing the pre-carbonisation residue volume and increasing the coke yield. However, in this study the anisotropy of the coke is of the greatest importance. It may well be argued that comparing the low-temperature pyrolysis of Waxy Oil against the cited literature on the basis of aromatic residues would be superfluous. However, the aim of any thermal treatment is to induce thermal stability and thus it is the author's opinion that many parallels may be drawn with the reduction of reactivity promoters.

The use of **catalytic cracking** reactions to produce a highly aromatic needle coke precursor and lighter distillates from petroleum gas oil has been studied by many researchers, including

Lionetti and Schrader (1983) and Beuther *et al.* (1979). Hydrogenation followed by cracking reactions has also been shown to reduce the amount of pre-asphaltenes (the TI soluble component of asphaltenes) and by so doing reduce their reactivity by introducing aromatic hydrogen (Murukami *et al.*, 1989).

Thermal treatment of needle coke precursors prior to carbonisation is a method of stabilising reactive species at sub-carbonisation temperatures. Thermal treatment typically increases the Beta resin (QI - TI) fraction of isotropic pitch prior to mesophase formation. This "stabilisation" of the reaction rate allows the growth of smaller polyaromatics. Eser *et al.* (1989) conducted research to show how thermal treatment of vacuum residue stabilised reactive asphaltenes, increasing the anisotropicity of the coke, decreasing the interlayer spacing and increasing the L_c of the graphite produced.

Dickakian (1985) showed that apart from stabilising the reactivity of the asphaltenes, thermal treatment of petroleum pitch increased the TI content from 1 to over 30%, while at the same time increasing the carbon aromaticity from 55 to over 80%. An increase in the concentration of two six-ring aromatic compounds or dimers thereof was also noticed. Blanco *et al.* (2000a) thermally treated coal-tar pitches at 430 °C for 2 to 4 h to increase the softening point and carbon yield. This was accompanied by a similar increase in the TI content and degree of graphitisation as determined by the interlayer spacing (d_{002}) and crystallite height (L_c). Similar results were obtained by the same researchers (Blanco *et al.*, 2000b), comparing thermally treated (430 °C for 2 to 4 h) coal-tar pitches with air-blown (275 °C for 10–30 h) coal-tar pitches. The air-blown pitches developed isotropic microstructures (caused by oxidative cross-linking), while the thermally treated pitches developed a higher degree of structural ordering with respect to mesophase development.

Perez *et al.* (2002) evaluated the difference between thermally treated and distilled petroleum pitches and determined that thermally treated pitches transformed a substantial amount of the aryl- and alkyl-substituted aromatics into planar aromatic cata-condensed aromatic compounds. The thermally treated pitches enhanced mesophase development compared with the mesophase from distilled petroleum pitches.

4.8 Concluding remarks – Review of previous work

It is clear that the characteristics of Waxy Oil differ substantially from the general characteristics of known needle coke precursors, especially in terms of aromaticity, alkyl side functionalities, the potential of oxygenate functionalities and the presence of iron oxide. All of these differences culminate in an increase in the carbonisation rate and thus a decrease in the extent of mesophase formation. Thus it is evident that substantial pre-carbonisation modification will be required to decrease the thermal reactivity of Waxy Oil

Although the carbonisation chemistry is not known at this stage of the project, it will be determined by its origin and pre-carbonisation processes. A description of the experimental procedures used in the current research is given in Chapter 5.

5 EXPERIMENTAL[8]

5.1 Experimental procedures for Chapter 6

5.1.1 Waxy Oil green coke

Four samples of high-ash Waxy Oil green coke were obtained from the Sasol Synfuels delayed coker at Secunda. The samples were dried and sieved to obtain a particle size fraction of 10–60 mm. This size fraction was crushed to obtain smaller size fractions for analysis, calcination and graphitisation.

5.1.2 Standard analyses

The methods used to characterise the Waxy Oil green coke are shown in Table 5-1.

Table 5-1 Standard test methods used to characterise Waxy Oil green/calcined coke[9]

Analysis	Units	Test method
Ash content	**Mass %**	ASTM D-4422-89
Volatile Carbon Matter (VCM)	**Mass %**	BS-1016 Part 4
Carbon	**Mass %**	LECO CHN Analyzer
Hydrogen	**Mass %**	LECO CHN Analyzer
Nitrogen	**Mass %**	LECO CHN Analyzer
Sulphur	**Mass %**	ASTM D-4239-94
Hardgrove Grindability Index (HGI)		ASTM D-409/D-5003
CO_2 reactivity	**Mass %. 100 min^{-1}**	Alusuisse C110
Vibrated Bulk Density (VBD)	**g.cm^{-3}**	ASTM D-4992-092
Density (-75 µm; helium)	**g.cm^{-3}**	ASTM D-5018-89
Metals	**Mass %**	UOP 927-92

5.1.3 Thermogravimetric Analysis (TGA)

TGA and DTG curves of the Waxy Oil green coke and pre-graphite[10] samples (-150 µm) were obtained using a Mettler TGA1/DSC1 thermogravimetric instrument.

The following programme was used:

- Equilibrate at 30 °C for 3 min under nitrogen flow of 150 ml.min^{-1}
- 30 °C to 110 °C, rate 50 °C.min^{-1}, under nitrogen flow of 150 ml.min^{-1}
- 110 °C for 3 min under nitrogen flow of 150 ml.min^{-1}
- 110 °C to 900 °C, rate 50 °C.min^{-1}, under nitrogen flow of 150 ml.min^{-1}
- 900 °C for 7 min under nitrogen flow of 150 ml.min^{-1}
- 900 °C for 20 min under air flow of 150 ml.min^{-1}

[8] Unless otherwise stated, all the experimental procedures and analyses were conducted by the author.
[9] Standard ASTM analyses were conducted by the Sasol Synfuels quality laboratory.
[10] "Pre-graphite" is the term used in this thesis to describe Waxy Oil green coke heat treated to 2 000 °C in an inert atmosphere.

5.1.4 Optical microscopy

Samples of the green and calcined cokes (+20 mm) were mounted in epoxy resin and polished using ISO 7404-2 (1985) as a guideline. The samples were examined under oil immersion using a Leica DM4500P petrographic polarised light microscope.

Optical microscopy was conducted under Bright field conditions. As the simplest of all microscopy techniques, the contrast is caused by the absorbance of white light in accordance with the density of the various parts of the coke sample. The micrographs were conducted using oil immersion with a 50x objective (thus making the magnification 500x) taking into account the 10x magnification of the ocular lens without an optical polarizer. Thus the catalyst appears as a dark brown colour and the carbon microstructure as a light brown colour. As pores absorb all the white light they appear as a black colour. The scale used for the micrographs is 20 microns.

5.1.5 Calcination

5.1.5.1 Calcination process

Waxy Oil green coke (2–10 mm; approximately 350 g) was calcined in a muffle oven with a nitrogen flux using the flowing temperature programme:

- Ambient (25 °C) to 1 000 °C at approximately 5 °C.min^{-1}; duration 200 min
- 1 000 °C to 1 400 °C at approximately 2 °C.min^{-1}; duration 200 min
- Temperature maintained at 1 400 °C for 80 min
- Cooling to ambient room temperature overnight under nitrogen flux
- The sample was weighed to determine the yield.

5.1.5.2 Standard analyses

The standard analyses are shown in Table 5-1.

5.1.5.3 X-ray Diffraction (XRD)

X-ray powder diffraction data were collected using a Phillips X-pert Pro multi-purpose diffractometer equipped with the X'Celerator detector. The data were acquired at a scanning speed of 0.014 °2θ/s with a step size of 0.017 °2θ and line broadening was conducted. Samples were irradiated with iron-filtered cobalt (Co) K_α X-rays emitted from a sealed tube source. Crystalline phases present in the sample were identified by searching the powder diffraction file database (PDF-4+ 2008) using the X'Pert HighScore Plus Version 2.2d PAN analytical software. The phase's line broadening (from which the L_c values were determined) were obtained by deconvoluting the phase's line broadening from instrumental line broadening – the so-called "fundamental parameters approach" in the software Topas 4.2 in a process of Rietveld refinement. The instrument broadening is determined by measuring a powder diffractogram of a crystalline standard, lanthanium hexaboride (LaB_6).

The powder samples were packed using the back-loading technique to minimise preferred orientation. Each sample was packed and analysed three times to determine the standard deviation.

5.1.5.4 Raman spectroscopy

Samples were placed on a microscope slide and measured using the inVia Raman system, utilising the 514.5 nm line of a 5.3 mW (at the sample) Ar-ion ion laser beam that was focused with a Leica microscope using a x 20 long focus objective. Data were obtained for the region 200–4000 cm^{-1} for 60 s, scanned five times using a laser power of 100% with a 75% defocused beam. Four to five separate spectra were obtained for each sample and then averaged to obtain the final spectrum used for analysis. Wire Version 2, Service Pack 8 software was used for data capturing and instrument control. The Raman band of pure Si was measured before data accumulation commenced for calibration purposes. Normalisation and band deconvolution were done using OPUS software, Version 6, using the Levenberg-Marquardt algorithm. Deconvoluted band shapes were described using pseudo-Voigt functions.

5.1.5.5 Scanning Electron Microscopy (SEM)

Coke samples were stabilised in epoxy resin and polished using ISO 7404-2 (1985) as a guideline. The samples were immersed in ethanol and dried in an oven (at 60 °C). Gold plating was conducted on an Emitech K550X instrument. The SEM photo was obtained on a JEOL JSM-840 Scanning Electron Microscope.

5.1.6 Pre-graphitisation

5.1.6.1 Pre-graphitisation process[11]

The four high-ash Waxy Oil green cokes were pre-graphitised by the author at the National Energy Corporation of South Africa (NECSA). A medium-frequency induction furnace was used to pre-graphitise the samples. The green coke (approximately 17 g; -2.0 mm) was placed in a cylindrical graphite crucible with a graphite lid. The crucible was wrapped with an inner layer of graphite wool insulator and an outer layer of alumina wool. The insulated sample was wedged in between the copper coil. The reactor was closed and a vacuum pump evacuated the reactor to -0.8 bar. The reactor was then connected to an argon line and the pressure kept constant at -0.6 bar.

The power was set at 6 kW for 5 min up to a temperature of 1 500 °C. It was then increased to 17 kW to attain a maximum temperature (measured with a pyrometer) of approximately 2 000 °C, which was maintained for 5 min. The reactor was cooled for an hour and the sample of pre-graphite was weighed to determine the yield.

5.1.6.2 Standard analyses

The test method used to determine the density of the pre-graphite (-75 µm) is shown in Table 5-1. A particle size of -75 µm was chosen to exclude the greater part of the internal

[11] The term “pre-graphitisation” is used in this thesis to describe thermal treatment of Waxy Oil green coke to a temperature of 2 000 °C.

porosity of the virgin sample. At -75 µm the catalyst still reports to this fraction, making the effect on its density easier to determine.

5.1.7 Graphitisation

High-ash Waxy Oil green coke was obtained from the commercial delayed coker at Secunda, South Africa. The green coke was dried and separated into size fractions. The size fractions were recombined to produce a composite sample (2 200 g) for graphitisation. The weights of the size fractions in the composite sample are shown below.

- 0–1 mm (400 g or 18.2%)
- 1–2 mm (400 g or 18.2%)
- 2–4 mm (400 g or 18.2%)
- 4–8 mm (400 g or 18.2%)
- > 8 mm (600g or 27.2%)

The size fractions of green coke were analysed for VCM, ash, metals and real density according to the ASTM standards shown in Table 5-1.

The graphitisation reaction was conducted by the author at Jeenel Technology Services (Pty) Ltd, Boksburg, South Africa. The sample was placed in a graphite crucible, insulated with alumina and graphite wool. The outer lid and the support of the medium-frequency induction furnace were constructed from concrete. Further insulation was provided by zirconium sand. The furnace was equipped with two outlets. The system was continually purged with argon gas.

The medium-frequency induction furnace was heated to approximately 3 000 °C over a period of 120 min. The furnace was held at a temperature of 3 000 °C for 90 min. The system was cooled overnight under an argon flux.

5.1.8 Standard analyses

After cooling, the graphite was removed and sieved into size fractions and the weight percentage of each fraction was recorded. The size fractions were analysed according to the ASTM standards shown in Table 5-1.

5.2 Experimental procedures for Chapter 7

5.2.1 Removal of solids from Waxy Oil

A 40 ℓ sample of Waxy Oil was obtained from the Sasol Synfuels delayed coker. Filtration experiments were conducted by the author on the premises of Solid Liquid Filtration Consultants (SLFC) in Randburg, South Africa. Samples of Waxy Oil (approximately 100 ml) were heated to 90–95 °C prior to filtration. The filtration apparatus is composed of a loading cell (height 6 cm; diameter 7 cm) equipped with a steam jacket on the perimeter. The lid of the cell was connected to a nitrogen pressure line. The base of the cell tapered into a funnel. Sintered metal filters (7 cm in diameter) were obtained from the Mott Corporation. The experiments used filters with apertures of 2.0, 1.0 and 0.5 µm. A diagram of the experimental set-up for the filtration apparatus is shown in Figure 5.1.

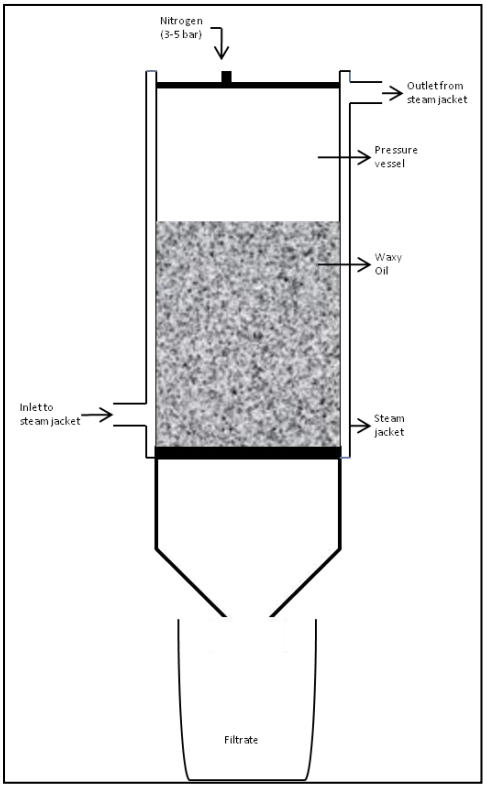

Figure 5-1 Filtration apparatus for Waxy Oil

The filter was loaded at the base of the cell and the sample (100 ml) added. The lid was fitted and a nitrogen pressure of 3–5 bar was applied. The filtrate eluted according to the micron size of the filter disc, the time being measured in minutes. The filtrate was collected in a Pyrex beaker and standard analyses were conducted at the Sasol Synfuels Process Laboratory at Secunda, South Africa. The filtration was repeated many times to obtain the amount of filtered Waxy Oil required for the modification trials. The standard test methods used to determine the characteristics of the Waxy Oil are shown in Table 5-2.

Table 5-2 Test methods used to determine the quality of Waxy Oil

Analysis	Units	Method
Matter Insoluble in Quinoline (MIQ)	**Mass%**	SABS 538/539
Ash content	**Mass%**	ASTM D-2415
Metals content	**Mass%**	UOP 927-92

5.2.2 Waxy Oil distillation[12]

Filtered Waxy Oil (as described in Section 5.1.1) was vacuum distilled to increase the viscosity and remove lighter hydrocarbons. Approximately 250 g of Waxy Oil was placed in a 500 ml round-bottomed flask. The distillation equipment was standard, consisting of a condenser and a receiving glass phial for distillates (submerged in ice water). The vacuum

[12] The research for Chapter 8 (Sections 8.2.2.1 to 8.5) and Chapter 9 was conducted by the author at the Instituto Nacional del Carbón (INCAR) in Oviedo, Spain, under the supervision of Dr Ricardo Santamaria.

used was – 0.9 kPa. Two distillations were conducted to residue temperatures of 340 and 380 °C respectively. After distillation, the residue and distillate were weighed to determine the yields.

A photo of the vacuum distillation equipment is shown in Figure 5-2.

Figure 5-2 Photo of vacuum distillation equipment

Analysis of the distillates and residues is described in Section 5.2.4.

5.2.3 Waxy Oil thermal treatment

Waxy Oil (approximately 20 g) was placed in glass test tubes. The test tubes were placed in a reactor and the lid was closed with bolts. The reactor was connected to a distillate receiver. A photo of the thermal treatment apparatus is shown in Figure 5-3.

Figure 5-3 Photo of thermal treatment apparatus

Table 5-3 lists the experimental conditions for the thermal treatments.

Table 5-3 Experimental conditions for the thermal treatments

Experiment number	Temperature (°C)	Time [1] (h)	Pressure (bar)
D1	400	2	5
D2	430	2	5
D3	410	2	5
D4	420	2	5
E1a	410	2	1 h at 5 bar; 1 h at 1 bar
E2	410	2	1 h at 5 bar; 1 h at 0 bar
E1b	none	none	E1a N_2 strip to max 325 °C

[1]Duration of thermal treatment at maximum heat treatment temperature

5.2.4 Analysis of modified Waxy Oils

5.2.4.1 Fourier Transform Infra-Red spectroscopy (FTIR)

FTIR was conducted on modified Waxy Oil residues using a Nicolet 8700 DTGS with a Thermo-scientific accessory. Data were collected from 4000–400 cm^{-1}. The data were used to calculate the Aromaticity Index (I_{ar}).

5.2.4.2 ^{1}H Nuclear Magnetic Resonance spectroscopy (NMR)

Samples were characterised by liquid-state NMR ^{1}H spectroscopy. $CDCl_3$ was used as solvent and tetramethylsilane (TMS) as the chemical shift reference. Each sample was taken into solution in a proportion of 20 wt% and placed in a 5 mm NMR tube. A 400 MHz AMX Bruker NMR spectrometer was used.

5.2.4.3 Thermogravimetric Analysis

Thermogravimetric analysis (TGA/DTG) of modified Waxy Oil residues was conducted in triplicate using a STD2960 Simultaneous DSC-TGA (the sample boat was made of steel) under the following conditions:

- 0–1 000 °C (10 °C.min^{-1})
- 30–50 mg sample
- 100 ml N_2.min^{-1}

5.2.4.4 Procedure for Gas Chromatography Mass Spectrometry (GCMS)

Both Waxy Oil residues and distillates were refluxed in toluene (1:3 ratio) and sieved. The GCMS analysis of the distillates and residues was conducted on an Agilent-7890A gas chromatograph equipped with an Agilent-MS 5975 mass spectrometer. The samples of the Waxy oil were further diluted to allow for the appropriate elution of heavy alkanes which without dilution may have show overlapping peaks on the GCMS trace. Qualitative analysis of independent peaks was very useful when determining the “shift” therein according to modification procedures.

The conditions for the GCMS analysis are shown in Table 5-4.

Table 5-4 Conditions for the GCMS of Waxy Oil distillates and residues

Description	Units
Stationary phase	HP-5MS (5% phenol-methylpolysilane)
Column length	30 m
Inner diameter of column	0.25 mm
Density of the stationary phase	0.25 m
Flow of the carrier gas	1.2 $ml.min^{-1}$
Injection conditions (ratio)	1:100
Injection temperature	300 ºC
Temperature line of transfer	320 ºC
Temperature of the oven	50 to 280 ºC
Temperature programme	10 min at 50 ºC; 4 $ºC.min^{-1}$ until 280 ºC
Molecular weight range	50 to 400 uma

5.3 Experimental procedures for Chapter 8

5.3.1 "Static" carbonisation of modified Waxy Oils

Modified and virgin Waxy Oil samples as described in Chapter 8 (approximately 50 g) were carbonised in Pyrex glass test tubes within a stainless steel reactor (described in Section 5.1.3). A thermocouple was placed in the Waxy Oil to monitor the temperature. The pressure utilised was five bar for the complete reaction duration. The samples were carbonised utilising the following conditions:

- Heating rate: 3.0 $°C.min^{-1}$
- Final carbonisation temperature: 480 °C for 120 min
- De-coking[13] temperature: 500 °C for 30 min

The green coke samples were removed in the glass test tube from the reactor after overnight cooling. The green coke and distillates in the test tube/distillate vessel were weighed to determine the respective yields. The green coke was removed from the glass tube by cracking it lightly. The "tube" of green coke was cut down the longitudinal plane for further testing

[13] Decoking is a procedure conducted after carbonisation in which the temperature is increased by approximately 20 °C to drive off excess volatile carbon matter and make separation of the test tube and coke easier.

(especially referring to optical microscopy thereof). Green coke analyses were conducted according to procedures shown in Section 5.1.3.

5.3.2 Calcination

Green cokes A and B (approximately 10 g) were calcined in a Xerion tube furnace using the following conditions:

- Heating rate 20 °C.min^{-1}
- Maximum temperature: 1 300 °C for 2 h
- Argon flow: 150 ml.min^{-1}
- Overnight cooling

Calcined coke analyses were conducted according to procedures shown in Section 5.1.5.

5.3.3 Green and calcined coke characterisation

5.3.3.1 Macrostructure

Photos of the green and calcined coke macrostructure were taken along a longitudinal section of the whole green coke sample. The photos were taken using a KL 1500 LCD light source and an Olympus S2 camera.

5.3.3.2 Optical microscopy

Optical microscopy on the green and calcined cokes was conducted in the same manner. Longitudinal sections of the whole piece of coke were cut and mounted in epoxy resin using a Buehler mounting press (150 °C; 29 MPa; 15 min).

The mounted samples were polished using a series of friction media detailed below:

- Grit 120 for 1 minute
- Grit 1200 for 2 min
- Grit 2500 for 2 min
- Alumina powder solution (-0.3 µm) for 2 min
- Alumina powder solution (-0.05 µm) for 2 min

Optical microscopy was conducted on polished samples using a Zeiss Axioplan microscope with a Liera DC100 monitor. Micrographs were taken from the bottom to the top of the green coke particle using a computerised automatic step counter every 14 µm along the length in polarised light and representative micrographs taken with a 10x to x50x objective lens. The percentage of mosaic and flow domains was calculated compared for each micrograph. Micrographs were taken down the length of the coke section and flow domains were the dominant microstructure towards the top of the coke section. Thus, the percentage of micrographs where flow domains were the dominant microstructure compared with mosaics (at the bottom of the coke section) could be calculated to produce a microstructural height profile of the coke section.

Polarised light microscopy was used to determine the difference in the texture of the coke samples. This was conducted using a polarizer between the light source and the mirror. A half wave retarder was additionally used placed between the analyser and the mirror. Polarised light microscopy observes the interference colours due to the variance in the orientation of the graphitic lamellae. Examples of light in the visible spectrum being established due to interference include:

- Purple when the light is reflected perpendicular to the graphite lamellae
- Yellow when the light is reflected to the right of the graphitic lamellae
- Blue when the light is reflected to the left of the graphitic lamellae

Other colours of the visible spectrum may be observed depending on the orientation of the graphitic lamellae for example red. The catalyst is seen as a white colour.
Isotropic cokes appear as small circular areas with the same red colour while anisotropic carbons for example needle coke show oriented flow domains across the micrograph
During polarized microscopy three objective lenses were utilized as described below:

- 10x objective (or 100x magnification) in air using a scale of 100 microns
- 20x objective (or 200x magnification) in air using a scale of 50 microns
- 50x objective (or 500x magnification) using oil immersion and a scale of 20 microns.

In terms of the repeatability and representative nature of the micrographs the longitudinal section of the coke was observed in the middle and to either side thereof to determine an average micro texture.

5.3.3.3 Carboxy (carbon dioxide) and oxidative consumption of carbon

A longitudinal section of calcined coke was ground and sieved to –200 µm. The carboxy reactivity was conducted in the TGA under the following conditions:

- 40–1 000 °C
- Heating rate: 10 °C.min^{-1}
- Nitrogen flow: 150 ml.min^{-1}
- Carbon dioxide flow: 150 ml.min^{-1}, or air flow: 150 ml.min^{-1}
- Isothermal condition for 2 h at 1 000 °C

5.3.3.4 Raman spectroscopy

Raman spectra were obtained in a high-resolution Raman microscope Jobin Yvon Horiba. Extended scans from 500–3500 cm^{-1} were performed to obtain the first- and second-order region of the Raman spectrum of the materials, with typical exposure times of 5 s. Measurements were made on the different parts of the samples embedded in resin, ground with different SiC grades and subsequently polished to 0.05 µm with alumina. A microscope was used to focus the excitation laser beam (green line of an argon laser $\lambda = 532$ nm) on the sample. The band intensity, position and width were determined using a mixed Gaussian-Lorentzian curve-fitting procedure. The degree of disorder was estimated from the relationship I_D/I_T, where I_D corresponds to the intensity of the D band (1350 cm^{-1}) and I_T corresponds to the total intensity of all first-order region bands (D, G, D´ at 1350, 1580 and 1620 cm^{-1} respectively).

5.3.3.5 Scanning Electron Microscopy (SEM)

SEM was performed in a Zeiss DSM 942 microscope, equipped with conventional SE (secondary electrons), solid state (two sectors) and polar BSE (backscattered electrons) signals. Chemical analyses were performed by X-ray energy dispersive analyser coupled to the SEM detector. The polished surfaces of the coke were coated with gold prior to the SEM.

5.4 Experimental procedures for Chapter 9

5.4.1 Filtration and thermal treatment

Virgin Waxy Oil was heated to approximately 100 °C and filtered through a 1 µm plate. The filtrate was thermally treated in a 1 ℓ reactor with connection to a distillate vessel at 410 °C, 5 bar for 2 h. The residue was vacuum distilled to remove lighter cracked molecules at 420 °C with a negative vacuum of 0.9 kPa.

5.4.2 Low-temperature carbonisation

The residue of vacuum distillation was thermally treated in test tubes (in a 1 ℓ reactor connected to a distillate vessel) using approximately 50 g of feed. The carbonisation was conducted at different times, namely 10, 20, 40, 60 and 120 min at 450 °C at a pressure of 5 bar. The test tubes were removed after cooling and weighed to determine the yield.

5.4.3 Thermogravimetric Analysis (TGA) and Differential Thermal Gravimetry (DTG)

Samples of the residue were obtained from the various test tubes and crushed. The TGA/DTG was conducted on representative samples in accordance with the procedure reported in Section 5.2.4.3.

5.4.4 Fourier Transform Infra-Red (FTIR) Spectroscopy

The Aromatic Index (I_{ar}) of the residue was determined using the procedure described in Section 5.2.4.1

5.4.5 Procedure for Gas Chromatography Mass Spectrometry (GCMS)

GCMS was conducted according to the procedure described in Section 5.2.4.4, except for the fact that NMP was used as the solvent and not toluene.

5.5 Concluding remarks – Experimental

The results of the experimental procedures listed above are reported and discussed in Chapters 6 to 9.

6 INFLUENCE OF CATALYST CONCENTRATION ON THE CHARACTERISTICS OF WAXY OIL COKE[14,15]

6.1 Introduction

This chapter examines the effect of iron oxide content (as determined by the ash content) on the physical/chemical characteristics of commercial Waxy Oil green coke and thermally treated variants thereof. Green cokes were thermally treated to 1 400 °C (termed "calcined coke") and 2 000 °C (termed "pre-graphite"[16]). Green coke was further thermally treated to 3 000 °C to determine the percentage reduction in the ash and iron content of Waxy Oil graphite.

The ash content of Waxy Oil calcined coke (as reported in this chapter) is at least an order of magnitude higher than that of the needle coke specification. However, as no scientific evaluation of Waxy Oil coke has previously been conducted, determination of the ash content is a prerequisite since it provides a template against which the effect of interventions (detailed in later chapters) may be compared.

Four commercial Waxy Oil green coke samples with increasing ash contents were obtained. The sample numbers and ash contents of the green coke are shown below.

- Sample 1: Ash content (1.84%)
- Sample 2: Ash content (4.22%)
- Sample 3: Ash content (7.47%)
- Sample 4: Ash content (11.19%

6.2 Macrostructure of needle coke

The ability to show preferred orientation on a macro (visual) scale is characteristic of needle cokes as shown in Figure 6-1.

[14] The research described in this chapter was presented at Carbon 2010, "From Nano to Macro" the Annual World Conference on Carbon, Clemson University, South Carolina, USA, 11–16 July 2010 (JG Clark, B Rand, MP Hayes, W Barnard, S Lubhelwana).

[15] The research described in this chapter was presented at the 15th Coal Science and Technology Conference Indaba 2010, "Clean Coal, Clean Energy", 17–18 November 2010 (JG Clark, B Rand, MP Hayes, W Barnard, S Lubhelwana).

[16] The term "pre-graphite" is used to describe Waxy Oil coke thermally treated at 2 000 °C. It is distinguished from the term "calcined coke"(treated at 1 400 °C) and "graphite" (thermally treated at 3 000°C, as reported in Chapter 7).

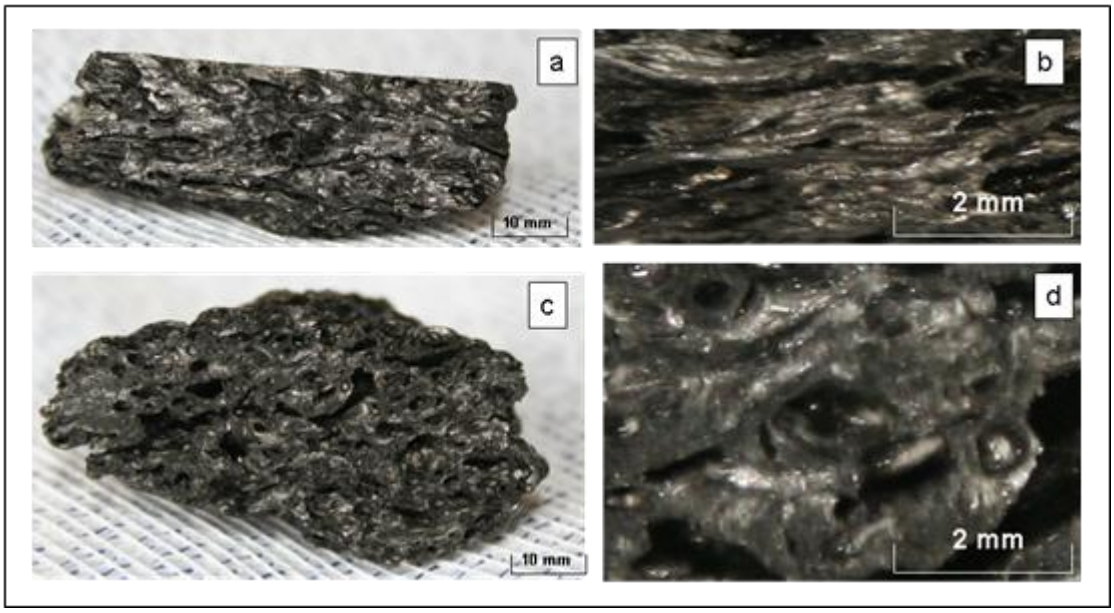

Figure 6-1 Photos of commercial needle coke in the longitudinal direction (a and b) and in the transverse direction (c and d)

Visual examination of needle coke shows flow domains and parallel pore morphology (Figure 6-1a), which become even more evident at a slightly higher magnification (Figure 6-1b). However, the converse is evident in the transverse orientation. The visual cross-section of needle coke (Figure 6-1c) does not show preferred orientation. Under slightly higher magnification (Figure 6-1d), the concentric pattern of carbon planes around a central pore is evident. The photos in Figure 6-1 serve as a template against which the macrostructure of the four Waxy Oil cokes may be compared, as discussed below.

6.3 Macrostructure of Waxy Oil green coke

A piece of high-ash green coke (approximately 70 mm in diameter) from each of Samples 1 to 4 was cut in three separate orthogonal planes in order to represent randomly ascribed X, Y and Z planes. Photos were taken of each of these planes (Figures 6-2 to 6-5).

Figure 6-2 Photos (a–c) of Waxy Oil green coke (Sample 1; 1.841% ash) on an X-, Y- and Z-axis

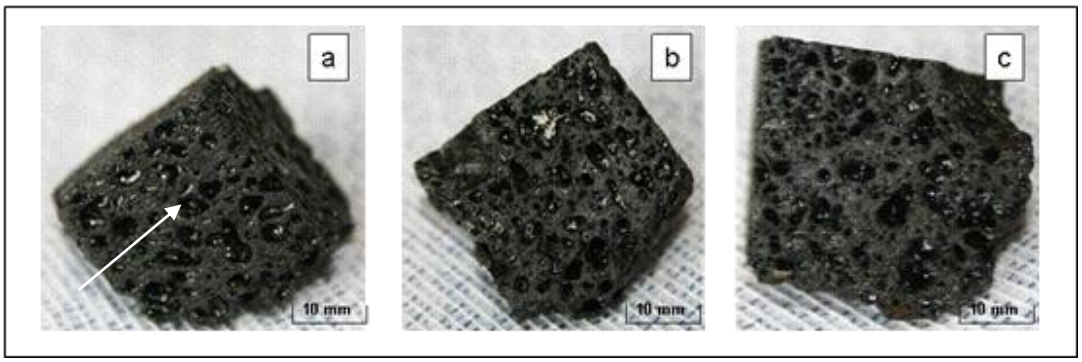

Figure 6-3 Photos (a–c) of Waxy Oil green coke (Sample 2; 4.223% ash) on an X-, Y- and Z-axis

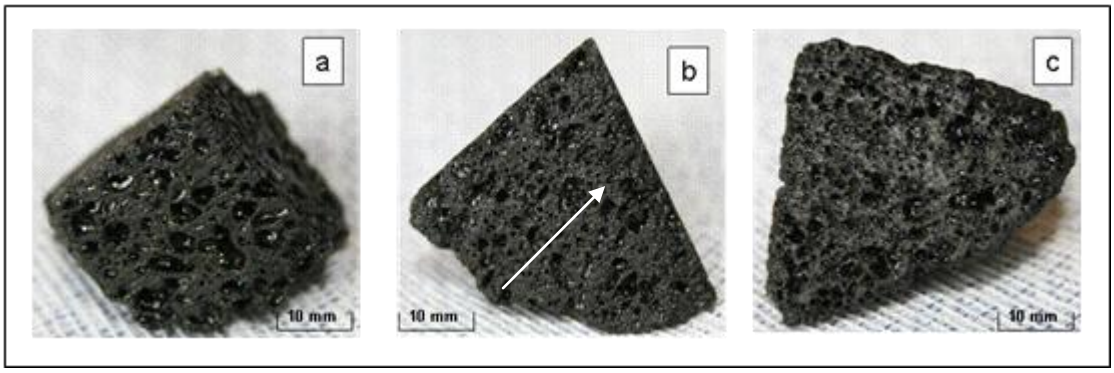

Figure 6-4 Photos (a–c) of Waxy Oil green coke (Sample 3; 7.471% ash) on an X-, Y- and Z-axis

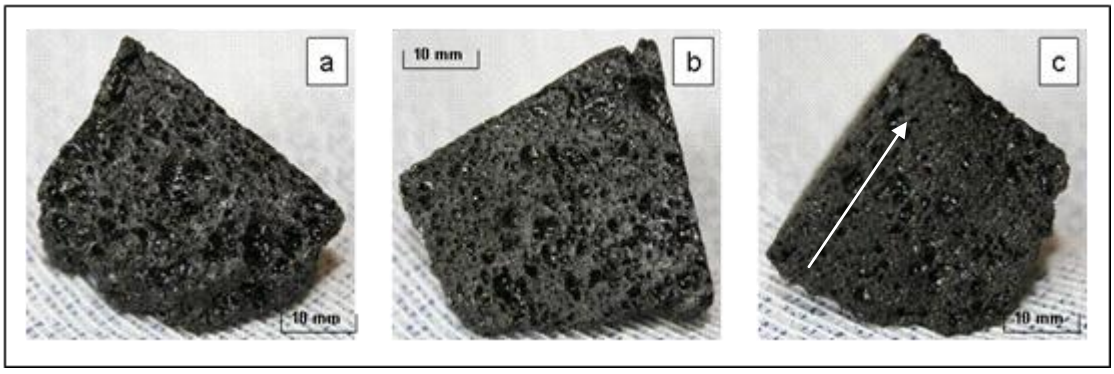

Figure 6-5 Photos (a–c) of Waxy Oil green coke (Sample 4; 11.186% ash) on an X-, Y- and Z-axis

The four high-ash Waxy Oil green cokes exhibit the macro-appearance of a sponge coke (in terms of macropore morphology), and the preferred macro-orientation of the carbon domains is not immediately distinguishable. However, there are slight indications of preferred orientation on one of the planes as indicated by the arrow in Figures 6-2a, 6-3a, 6-4b and 6-5c. There is no visual effect of the increasing ash content on the macrostructure of the four Waxy Oil cokes. The indication of preferred orientation of the Waxy Oil green coke carbon planes is, however, not supported by the parallel orientation of pores as is typical of needle coke (Figure 6-1). Waxy Oil green cokes appear highly porous (in comparison with the needle coke shown in Figure 6-1) due to the low green coke yield (18% from the fresh Waxy Oil feed to the delayed coker).

6.4 Chemical analysis of Waxy Oil green cokes

Analysis of the four Waxy Oil green coke samples is shown in Table 6-1.

Table 6-1 Analysis of Waxy Oil green cokes

	Units	Sample 1	Sample 2	Sample 3	Sample 4
Carbon	**Mass%**	90.200	90.800	89.200	85.600
Hydrogen	**Mass%**	3.680	3.680	3.520	3.630
Nitrogen	**Mass%**	0.050	0.030	0.083	0.020
Sulphur	**Mass%**	0.005	0.004	0.006	0.007
Ash content	**Mass%**	1.84	4.22	7.47	11.19
Volatiles (VCM)	**Mass%**	8.11	8.69	8.97	11.65
Fixed carbon[1]	**Mass%**	90.05	87.09	83.56	77.17
Inherent moisture	**Mass%**	0.20	0.19	0.19	0.23
Real density (-75 µm; helium)	**$g.cm^{-3}$**	1.3879	1.4237	1.456	1.4792

1) Fixed carbon = 100% - (ash + VCM)

The ash contents of the Waxy Oil green cokes increase from Sample 1 to Sample 4 (from 1.84 to 11.19%), with a reciprocal decrease in the fixed carbon content (from 90.05 to 77.17%) due to the increasing catalyst content. The high ash content of Samples 1 to 4 deems these green cokes commercially inappropriate for calcining (in respect of current recarburiser specifications). The VCM of Samples 1 to 3 (from 8.11 to 8.97%) is within the expected commercial range (6–9%), while that of Sample 4 (11.65%) is slightly higher. There is no correlation between the ash and the Volatile contents.

Both the nitrogen content (0.030–0.083%) and sulphur content (0.004–0.007%) of Samples 1 to 4 are comparatively lower than those of most green cokes produced either from petroleum crude oil or coal-tar origins.

The real density of the coke samples is determined by a -75 µm PSD (particle size distribution), thus negating much of the variability associated with particle size and macroporosity. As shown in Table 6-1, there appears to be a correlation between an increase in the real density (1.3879 to 1.4792 $g.m^{-3}$) from Sample 1 to Sample 4 and in the ash content (1.84 to 11.18%) respectively. Plotting a linear regression of the relationship between the real density against the ash content indicates a good linear correlation ($R^2 = 0.9655$). This is to be expected since the inorganic impurities have a higher density than the carbon.

6.4.1 Thermogravimetric Analysis (TGA) of Waxy Oil green cokes

TGA of Samples 1 to 4 was conducted to investigate devolatlisation (in an inert nitrogen atmosphere) and immediately thereafter to determine the oxidative consumption of Waxy Oil coke.

The TGA is shown in Table 6-2 and represented in graphical format in Figure 6-6. The derivative (DTG) of the mass loss rate is shown in Figure 6-7. It should be noted that the ash content shown in Tables 6-1 and 6-2 will differ given the substantial variation of the sample

size. The ash content in Table 6-1 is more representative as it is conducted in-line with an ASTM standard as prescribed in Chapter 5.

Table 6-2 Thermo Gravimetric analysis (TGA) of Waxy Oil green cokes

	Units	TGA (dry base)		
		VCM	Fixed carbon	Ash
Sample 1	**Mass%**	10.6	88.1	1.3
Sample 2	**Mass%**	10.1	87.0	2.9
Sample 3	**Mass%**	9.9	84.8	5.3
Sample 4	**Mass%**	12.9	78.0	9.1

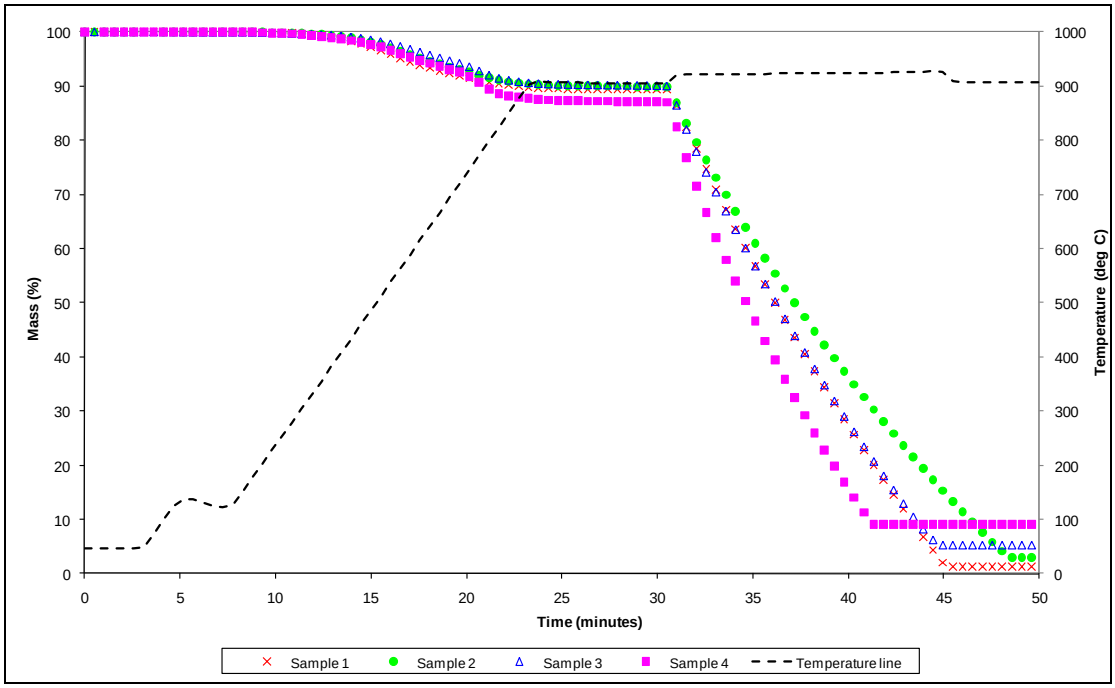

Figure 6-6 Thermogravimetric Analysis (TGA –multiple run average) of Waxy Oil green cokes

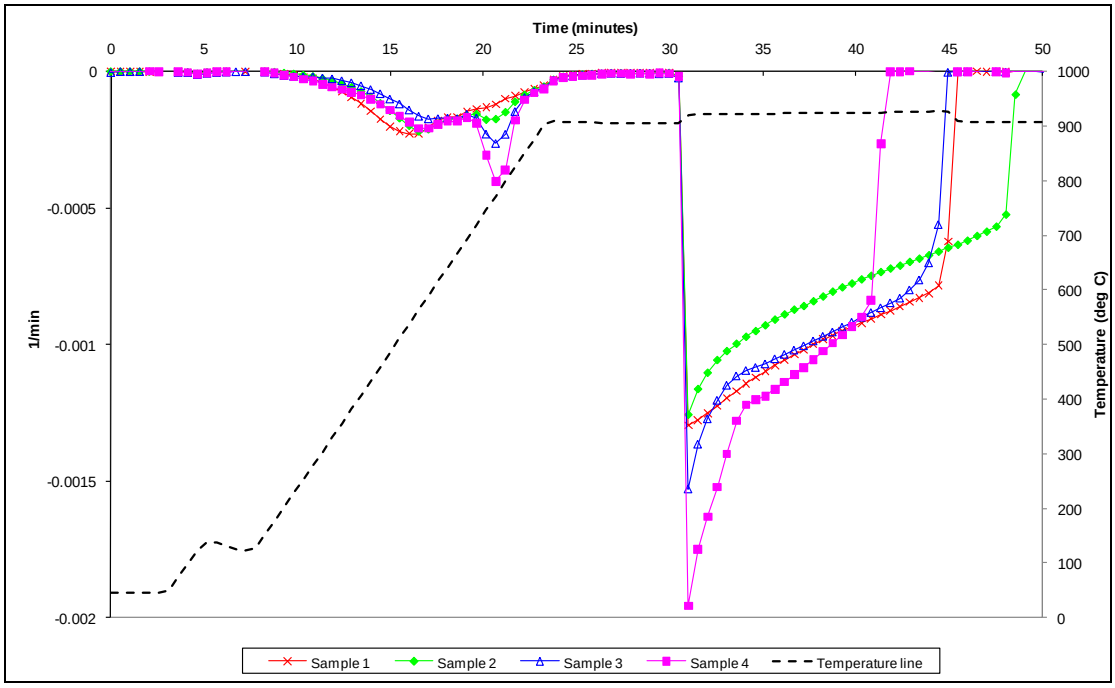

Figure 6-7 Differential Thermogravimetry (DTG multiple run average) of Waxy Oil green cokes

The proximate analysis shows an increase of the ash content with a corresponding decrease in the carbon residuum from Sample 1 to Sample 4 as indicated previously in Table 6-1. Figure 6-6 shows the mass loss of moisture and devolatlisation of VCM [starting at 8 min (≈ 150 °C) and terminating at just over 30 min (900 °C)] prior to the change in atmospheric conditions (nitrogen to air). With the change to an oxidative atmosphere, the fixed carbon is consumed until a stable residuum mass is indicated (mostly attributable to the ash content).

The DTG (Figure 6-7) shows all four cokes yielding a broad devolatlisation peak which is initiated at 150 °C and levels off at 900 °C in a nitrogen atmosphere. When the atmosphere is then changed to air, there is a steep peak of maximum reaction rate which increases in initial intensity as the catalyst concentration increases. The termination of these peaks is correlated to an increase of the catalyst content due to ash occlusion of the remaining carbon.

6.4.2 Influence of iron oxide or elemental iron on the oxidative consumption and carboxy reactivity of Waxy Oil coke

Previous research has determined that an increase in both calcium content (Boero *et al.*, 1987; Oya *et al.*, 1984; Lang & Neavel, 1982) and elemental iron (Walker *et al.*, 1983; Jenkins *et al.*, 1973) is linked to an increase in the rate of oxidative consumption and carboxy reactivity of coke.

As shown in Figure 6-7, Sample 4 (with the highest iron content) exhibited the highest initial air reactivity, followed by Sample 3 and then by Samples 1 and 2 which have lower iron and calcium contents.

The carboxy reactivity (69.78–87.02% respectively) of Waxy Oil calcined coke reported in Table 6-3 increases as the ash content (3.02–13.51%) increases from Sample 1 to Sample 4. Research conducted with petroleum sponge cokes (in the aluminium industry) confirms the catalytic effect of sodium and calcium on the carboxy reactivity of calcined coke (Hume *et*

al., 1993). The calcium content of Samples 1 to 4 increases (0.0931–0.1521%) with a corresponding increase in the carboxy reactivity. Indeed, the catalytic effect of calcium on the carboxy reactivity of petroleum cokes, coals and chars has previously been established by several authors, including Walker *et al.* (1993), Hippo and Walker (1975) and Lang and Neavel (1982). However, the increase in the calcium content may not be the only contributor to the increase in the carboxy reactivity from Sample 1 to Sample 4.

Apart from the influence of the higher comparative macroporosity, it is suggested that the unusually high iron content of the Waxy Oil calcined coke will catalyse carboxy reactivity. Iron is, by far, the element that contributes the greatest mass percentage to the ash component, on an elemental basis (Sample 1: 93.36%; Sample 2: 93.49%; Sample 3: 94.79%; Sample 4: 95.29%). It would seem unlikely that at these elevated concentrations there would be no effect (of elemental iron) on the reactivity of the coke. The author suggests three possible mechanisms by which large catalyst concentrations in the Waxy Oil coke may influence both the carboxy reactivity and the oxidative consumption.

- **As a reactivity catalyst:** Jenkins *et al.* (1973) determined that iron oxide (α-Fe_2O_3) is a poor catalyst for air and carboxy reactivity, while in its elemental form iron (Fe) is a good catalyst for both carboxy and air reactivity, in agreement with Hippo and Walker (1975) and Walker *et al.* (1983). In the Waxy Oil and during carbonisation, iron is present as Fe_3O_4, while at calcination temperatures of 1 400 °C iron oxide is partially reduced to elemental iron or Fe_3C, Fe_3O_4 and Fe_2O_3 as shown in Figure 6-15 and previously reported by Wang *et al.* (2001). Thus with increasing percentages of elemental iron in the calcined coke from Sample 1 to Sample 4, catalytic carboxy reactivity should increase as confirmed by the results shown in Table 6-3.

- **As a physical barrier:** Wang *et al.* (2001) have shown the effect of iron oxide particles presenting physical occlusions to the carbon microstructure during carbonisation. This serves to inhibit coke swelling, allowing the escape of gases and thus increasing the surface area. This characteristic has been demonstrated in the evaluation of the effect of the catalyst on the microstructure of calcined coke in the current study. Carbonisation of pitch in the presence of θ-Fe_2O_3 is known to increase the yield and decrease the anisotropy of coke due to oxidative dehydrogenation reactions (Wang *et al.*, 2001).

- **As an "oxygen reservoir":** The partial reduction of Fe_3O_4 to θ-Fe_3C and α-Fe during calcination would release oxygen, which may increase the consumption of carbon released as carbon monoxide. The potential of Fe_3O_4 to act as an "oxygen reservoir" within green coke cannot be corroborated in any of the literature cited and thus may be of a speculative nature. However, the author suggests that the unusually high catalyst concentration of the Waxy Oil and the fact that the dominant contaminant is Fe_3O_4 would indicate that within the *g*reen coke, there is a substantial oxygen concentration.

6.5 Waxy Oil calcined coke

In order to investigate exclusively the effect of metal contaminants on the characteristics of the calcined coke, the Waxy Oil green coke samples were calcined in a muffle oven (with a nitrogen flux) at an extremely low temperature ramp rate (from ambient to 1 300 °C) as given in Chapter 5.3.2.

6.5.1 Influence of increasing catalyst content on the microstructure of Waxy Oil calcined coke

6.5.1.1 Comparative summary of the effect of the catalyst content (catalyst agglomerates[17]) on the microstructure of Waxy Oil calcined coke

A series of comparative micrographs of Waxy Oil calcined coke are shown in Figure 6-8 to Figure 6-11, corresponding to Samples 1 to 4 respectively. While each of the cokes presented a fair degree of heterogeneity (examined in more detail in Figure 6-14 to Figure 6-17), the micrographs shown in Figure 6-8 to Figure 6-11 are representative of the average microstructure of each of the four coke samples.

A micrograph of Sample 1 Waxy Oil calcined coke with an ash content of 3.02% is shown in Figure 6-8.

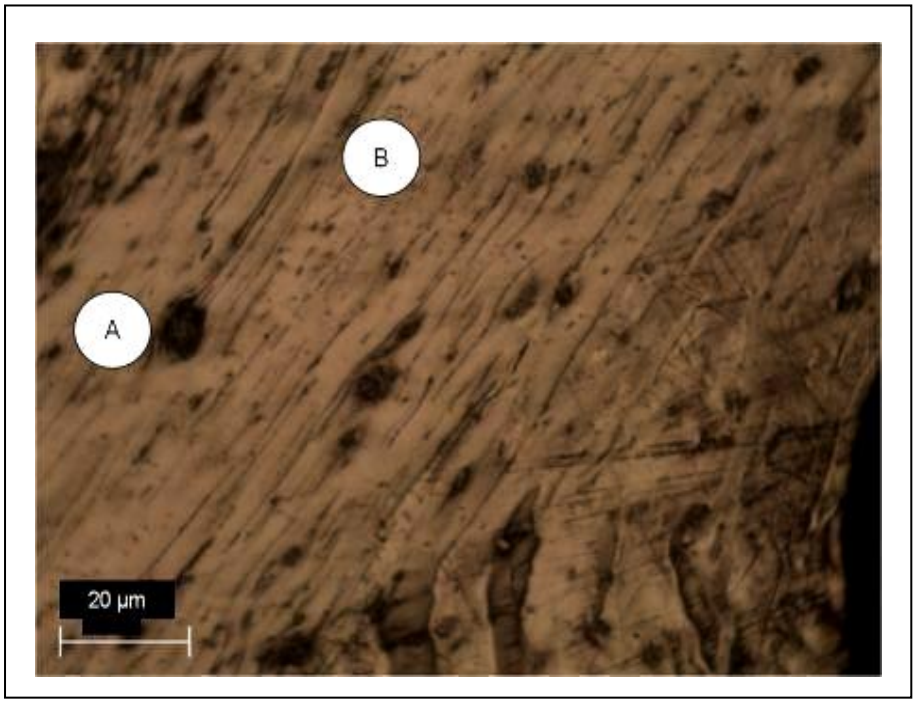

Figure 6-8 Optical micrograph of Sample 1 Waxy Oil calcined coke

The microstructure of Sample 1 is dominated by microstructural flow domains of indeterminable length as shown in Position B. The iron catalyst (appearing as black areas except for the pore on the bottom right of the micrograph) is embedded within the carbon microstructure with sizes up to 6 µm shown in Position A. The iron catalyst particles act as an obstacle to the microstructure, around which flow domains are formed.

[17] The generic term "catalyst agglomerate/s" is used to describe the presence of catalyst particles within the carbon microstructure. Given the particle size distribution of the catalyst, the agglomerate should be read as consisting of either a singular catalyst particle or a grouping of catalyst particles in the same localised vicinity. It is not possible to distinguish the difference using optical microscopy.

A micrograph of Sample 2 calcined Waxy Oil calcined coke with an ash content of 5.42% is shown in Figure 6-9.

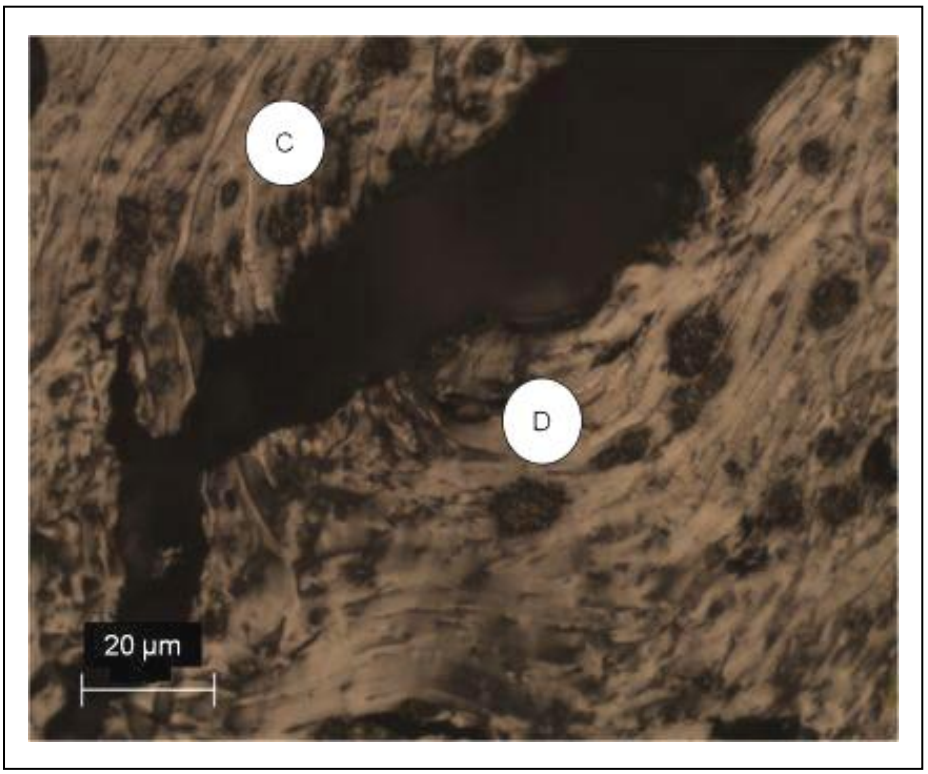

Figure 6-9 Optical micrograph of Sample 2 Waxy Oil calcined coke

As the catalyst content increases, so does the particle size (up to approximately 15 µm) and frequency as seen in the micrograph. The increase in the catalyst size may be due either to catalyst agglomeration or solely to the size of the catalyst particles. As seen in the micrograph, there is a transverse shrinkage crack separating the domain flow (Positions C and D).

A micrograph of Sample 3 calcined Waxy Oil calcined coke with an ash content of 8.66% is shown in Figure 6-10.

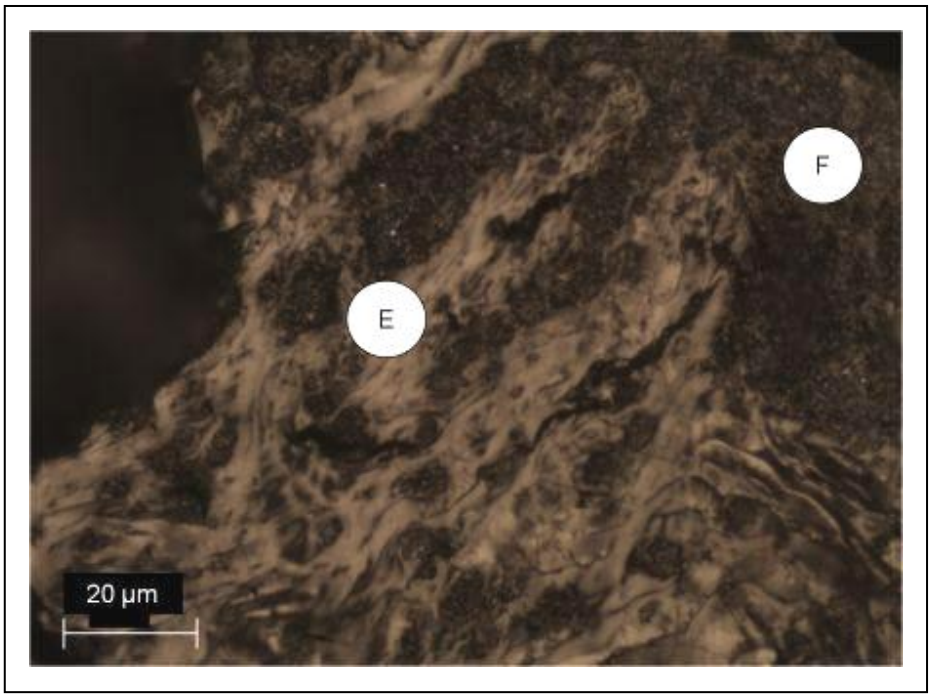

Figure 6-10 Optical micrograph of Sample 3 Waxy Oil calcined coke

Further increasing the catalyst content results in catalyst agglomerations of over 60 µm (Position F). The microstructure now represents elongated domains as shown by Position E, with smaller areas showing mosaic microstructures.

A micrograph of Sample 4 calcined Waxy Oil calcined coke with an ash content of 13.51% is shown in Figure 6-11.

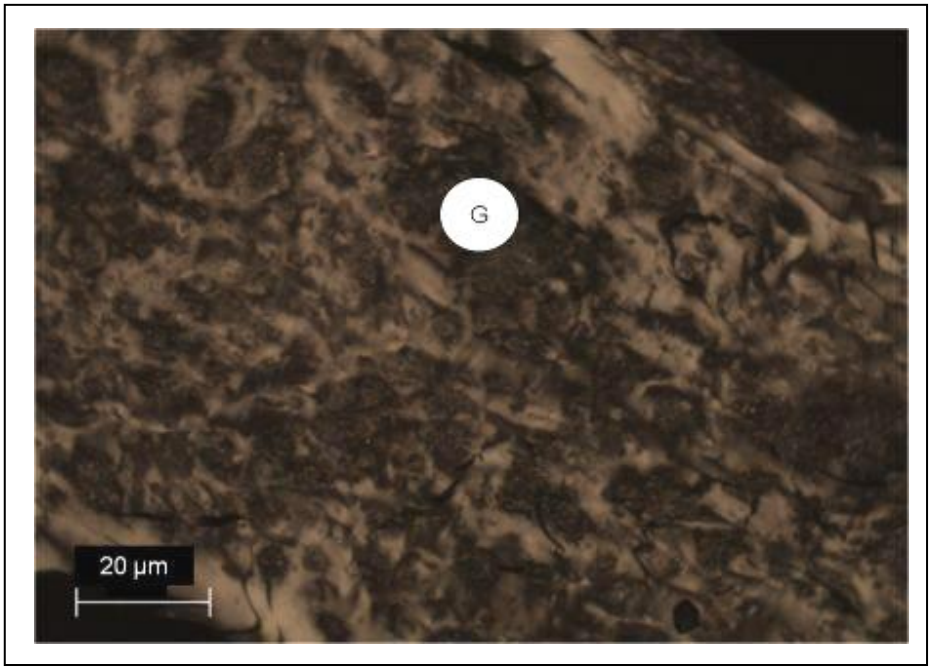

Figure 6-11 Optical micrograph of Sample 4 Waxy Oil calcined coke

In Sample 4, which has the highest catalyst content, the carbon micrograph is almost totally occluded by the matrix of catalyst agglomerates (Position G). The microstructure is heterogeneous with areas of elongated flow, coarse flow and coarse mosaic structures.

A bit map trace of catalyst agglomerates within the carbon microstructure Samples 1 to 4 of Waxy Oil calcined coke is shown in Figure 6-12.

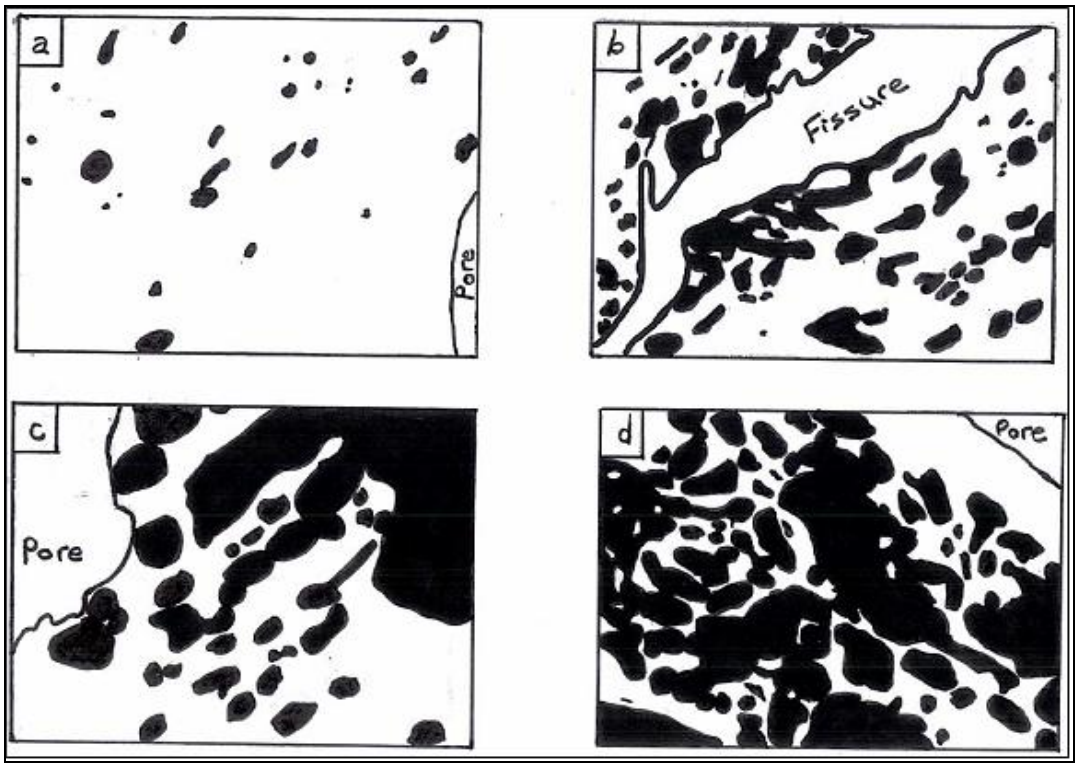

Figure 6-12 Diagram showing contamination of calcined coke by catalyst agglomerates of Samples (a) 1, (b) 2, (c) 3 and (d) 4

The catalyst content is shaded in black and shows clearly the influence of the catalyst on the spatial distribution of the carbon macrostructure. This is important when evaluating the effect of thermal graphitisation on the crystal development, discussed later in the chapter (Section 6.5.3.1).

Apart from the long-range effects of the catalyst concentration on the carbon microstructure, the internal structure of these catalyst agglomerates warrants further investigation. The internal structure of the catalyst agglomerates showing the formation of carbon mosaic microstructures is shown in Figure 6-13.

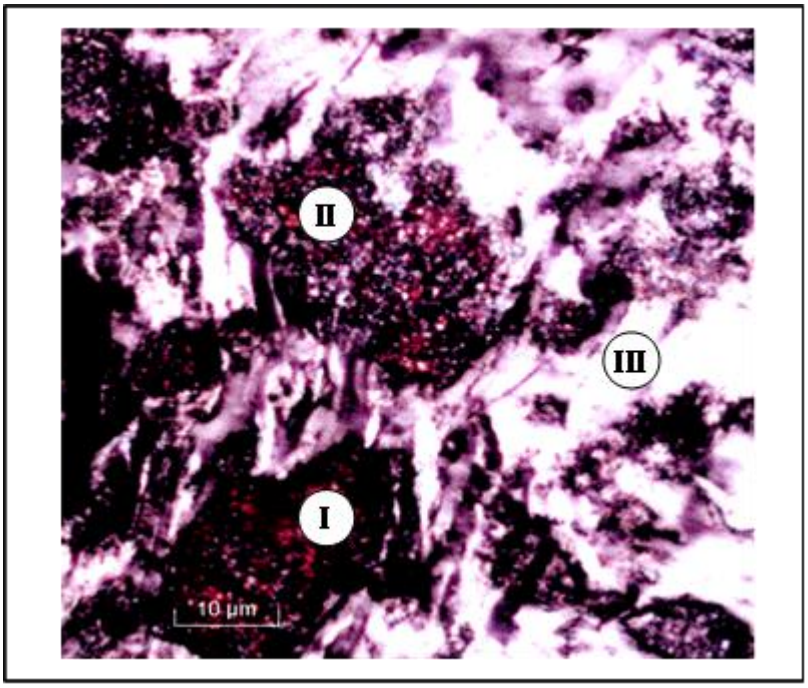

Figure 6-13 Polarised micrograph of catalyst agglomerates within the carbon microstructure

The form of the catalyst in the green coke is Fe_3O_4. Inert calcination (1 400 °C) liberates much of the volatile carbon matter (probably by devolatlisation) and partially reduces the catalyst to a mixture of Fe_3O_4, Fe_2O_3, Fe or Fe_3C. The "grainy" texture of the calcined coke would provide evidence for the loss of carbon. However, the visible dominance of catalyst agglomerates in the calcined coke is expected, given that calcination was conducted under inert and not oxidative conditions. The partial reduction of Fe_3O_4 to Fe may serve as a source of oxygen for carbon burn-off. As shown in Figure 6-13, within the catalyst agglomerate there is evidence of iron oxide (Position I) appearing as a brownish-red shade with mosaic microstructures (Position II) formed by catalysed oxidative polymerisation, in agreement with the findings of Wang *et al.* (2001), as opposed to the laminar flow domains (Position III) outside the immediate vicinity of the catalyst agglomerate.

An SEM image taken at 8 KV and a magnification of 15 000 times is shown in Figure 6.14.

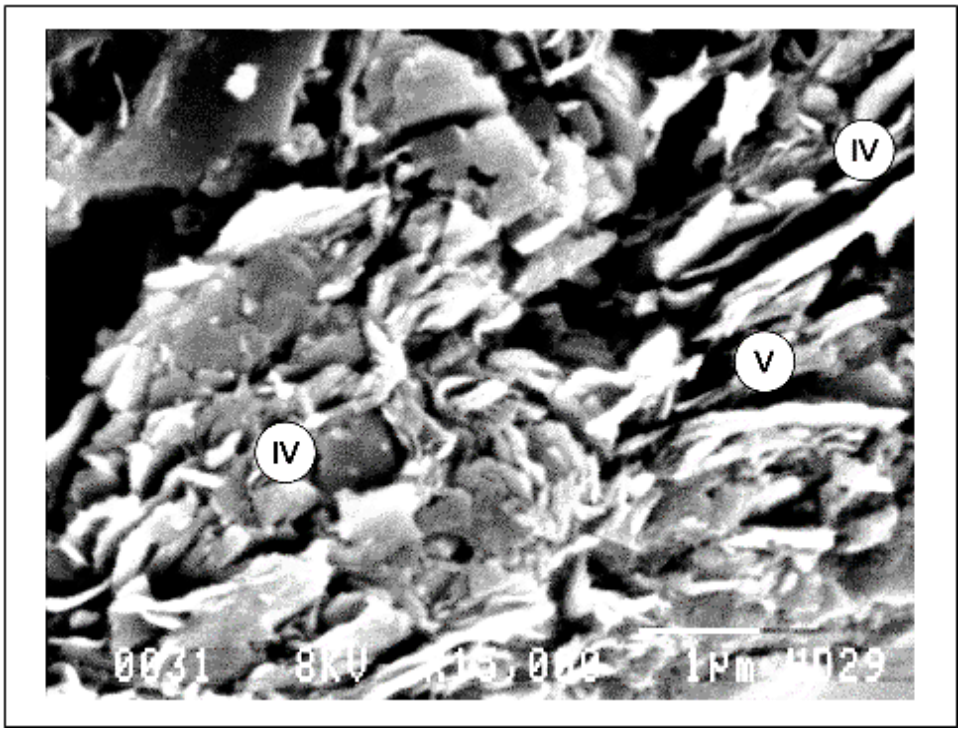

Figure 6-14 Scanning electron micrograph of ash agglomerate within the carbon microstructure of Sample 3, Waxy Oil calcined coke

The smaller catalyst particles would not be visible using optical microscopy. As shown in Figure 6-14, smaller catalyst particles less than 1 µm in diameter (Position IV – identified by their spherical nature compared to the flake like nature of the carbon microstructure) can be seen using SEM, embedded in the flake-like flow patterns of the carbon microstructure (Position V).

The author suggests that given the unusually high concentration, the catalyst (Fe_3O_4) in the green coke may serve as an "oxygen reservoir". It is further suggested that on reduction of the metal oxide, elemental oxygen will react with any carbon molecules either within the catalyst or around the immediate perimeter and be liberated as carbon monoxide. This localised carbon burn-off in addition to the reported effect of iron (Fe) as an oxidation catalyst is in agreement with the work of Jenkins *et al.* (1973), Hippo and Walker (1975) and Walker *et al.* (1983) and is suggested as the probable cause of the high concentration. Thus the fine mosaics visible within the inner structure of the catalyst agglomerate may be partially a result of oxidative polymerisation, but may also be the carbon remnants of oxidation during calcination.

6.5.1.2 Identification of phases of the iron-based catalyst in Waxy Oil calcined coke and pre-graphite

The XRD trace of the four Waxy Oil calcined coke samples showing phases of iron is shown in Figure 6-15.

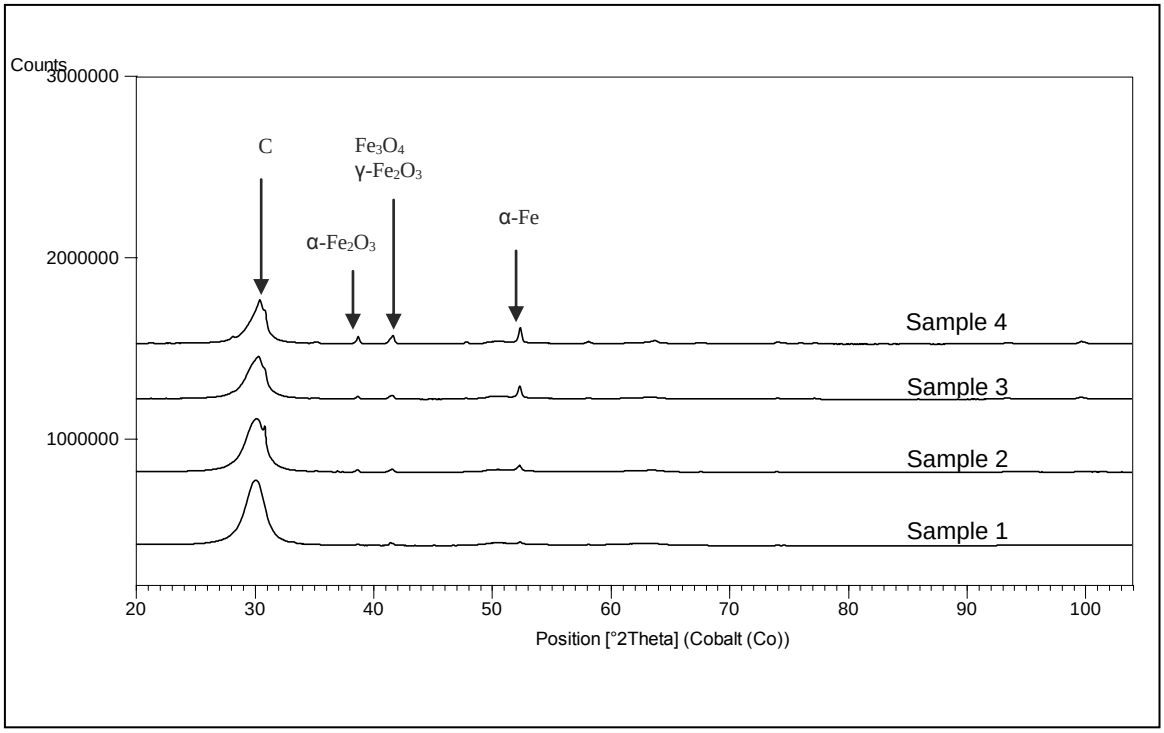

Figure 6-15 XRD trace of Waxy Oil calcined coke showing forms of the iron catalyst

Calcination induces a modification of the catalyst (Fe_3O_4) in the green coke to a mixture of Fe_3O_4, Fe_2O_3 and Fe. However, it can be seen that as the catalyst content of the calcined coke increases (from Sample 1 to Sample 4), the peaks on the trace (allocated to the various phases of the iron-based catalyst) are more intense.

The variability of iron oxide reduction with thermal treatment has been previously reported by several authors as follows:

1. Wang *et al.* (2001) showed thermal treatment at 1 000 °C to reduce iron oxide completely to elemental iron and iron carbide. However, the surface area of the iron oxide powder (0.1–1.0 µm) may be the reason for the complete reduction at a comparatively low temperature.
2. Dhakate *et al.* (1997) showed thermal treatment at 1 400 °C to reduce iron oxide completely to elemental iron.
3. Ugarkovic and Legin (1986) showed thermal treatment at 1 500 °C to present a mixture of iron phases, including Fe_3O_4, Fe_2O_3 and Fe.

The XRD trace of the four Waxy Oil pre-graphites showing the phases of iron is shown in Figure 6-16.

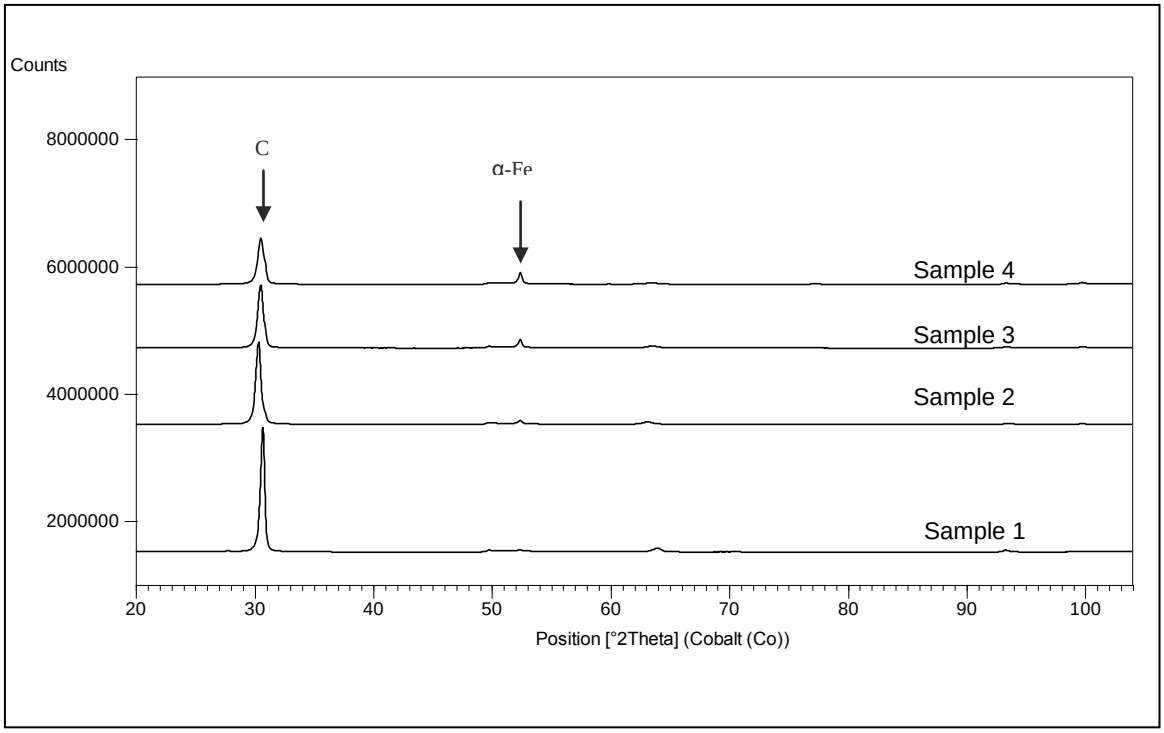

Figure 6-16 XRD trace of Waxy Oil pre-graphites showing phases of iron

Thermal treatment (2 000 °C) induced a complete reduction of the catalyst (Fe_3O_4), only yielding a peak for elemental iron. As the catalyst content of the pre-graphite increases (from Sample 1 to Sample 4), the Fe peak becomes sharper, which is expected.

It is further evident from the XRD trace that the peak in the graphite region is broader in the pre-graphite with the highest catalyst concentration and that as the concentration reduces, so the peak becomes narrower and more intense. As the catalyst concentration decreases, the spatial area for the development of microstructural anisotropy increases. This would thus indicate that the dominant graphitisation mechanism (during thermal treatment to 2 000 °C) may be thermal (depending on the microstructure) rather than catalytic, as is the case with thermal treatment at a lower temperature (1 300 °C).

6.5.1.3 Detailed examination of the heterogeneous variation in the microstructure of Waxy Oil calcined coke

While the micrographs shown in Figure 6-8 to Figure 6-11 show a representative microstructure for the four cokes, evidence of substantial microstructural variation within each of the coke samples serves to confirm the heterogeneous nature of the calcined coke samples. For this reason a more detailed analysis of the carbon microstructures is shown in Figures 6-17 to 6-20. The variation in the microstructure of Sample 1 is shown in Figure 6-17 (a–c).

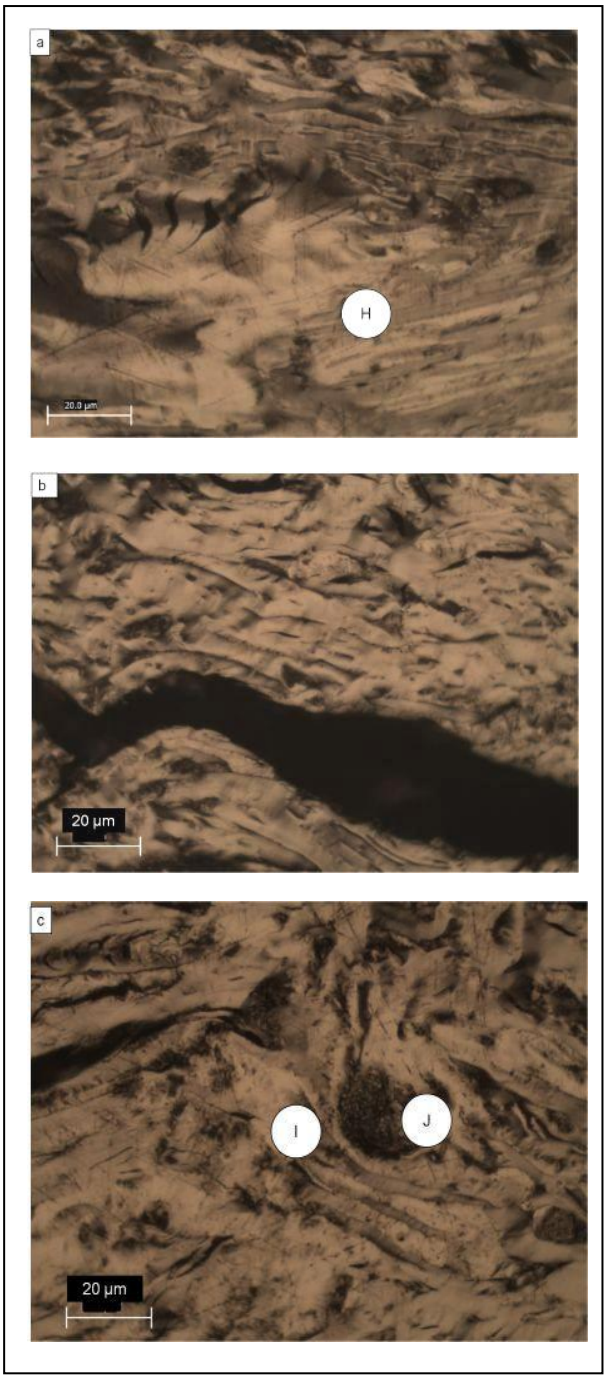

Figure 6-17 Optical micrographs (a–c) of Sample 1 of Waxy Oil calcined coke

The anisotropy of Sample 1 is dictated by the pore morphology which is parallel to the flow domains, either curved or straight (Figure 6-17a and 6-17b) respectively. However, in contrast to the "ribbon-like" morphology of needle coke, the flow domains appear shorter while the width is greater. During calcination, densification of the carbon microstructure creates ridges and valleys parallel to the flow domain (Position H). The presence of catalyst agglomerates (Position J) partially determines the morphology of the longer-range flow domains (Position I). The other contributor to the morphology of the microstructure would be the release of gases during carbonisation. Although the microstructure is dominated by acicular and elongated flow domains, there is evidence of both elongated medium and coarse

flow anisotropy. The variation in the microstructure of Sample 2 is shown in Figure 6-18 (a-c).

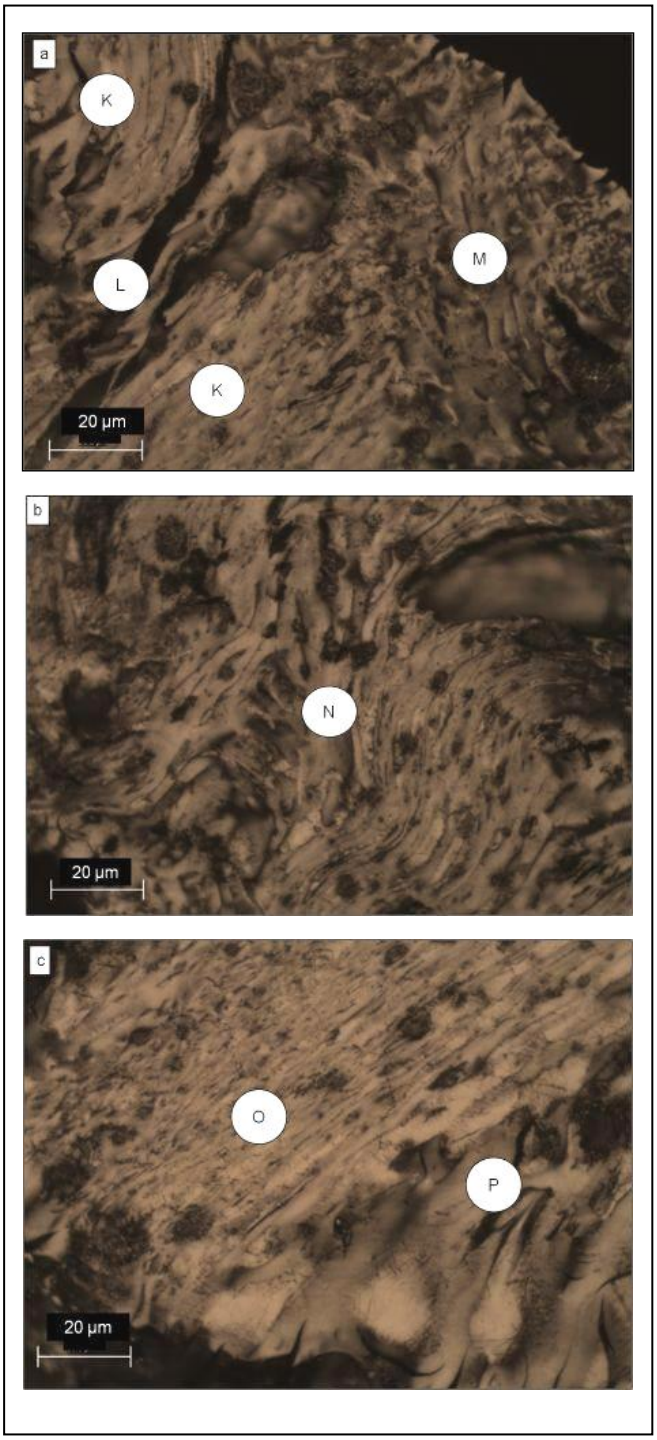

Figure 6-18 Optical micrographs (a–c) of Sample 2 of Waxy Oil calcined coke

The microstructure of Sample 2 ranges from elongated flow domains (Position K) to domains (Position M). Position N shows a central elongated domain with curved parallel domains converging from both the left and right of the micrograph. Position L shows a fissure aligned with the flow domain. Position N shows a convergence of flow domains from the left and right sides of the micrograph, with a habitual frequency of smaller catalyst particles. The

difference in the types of flow domain is seen by contrasting the longer thinner domains (Position O) and the larger wider domains (Position P).

The variation in the microstructure of Sample 3 is shown in Figure 6-19 (a–c).

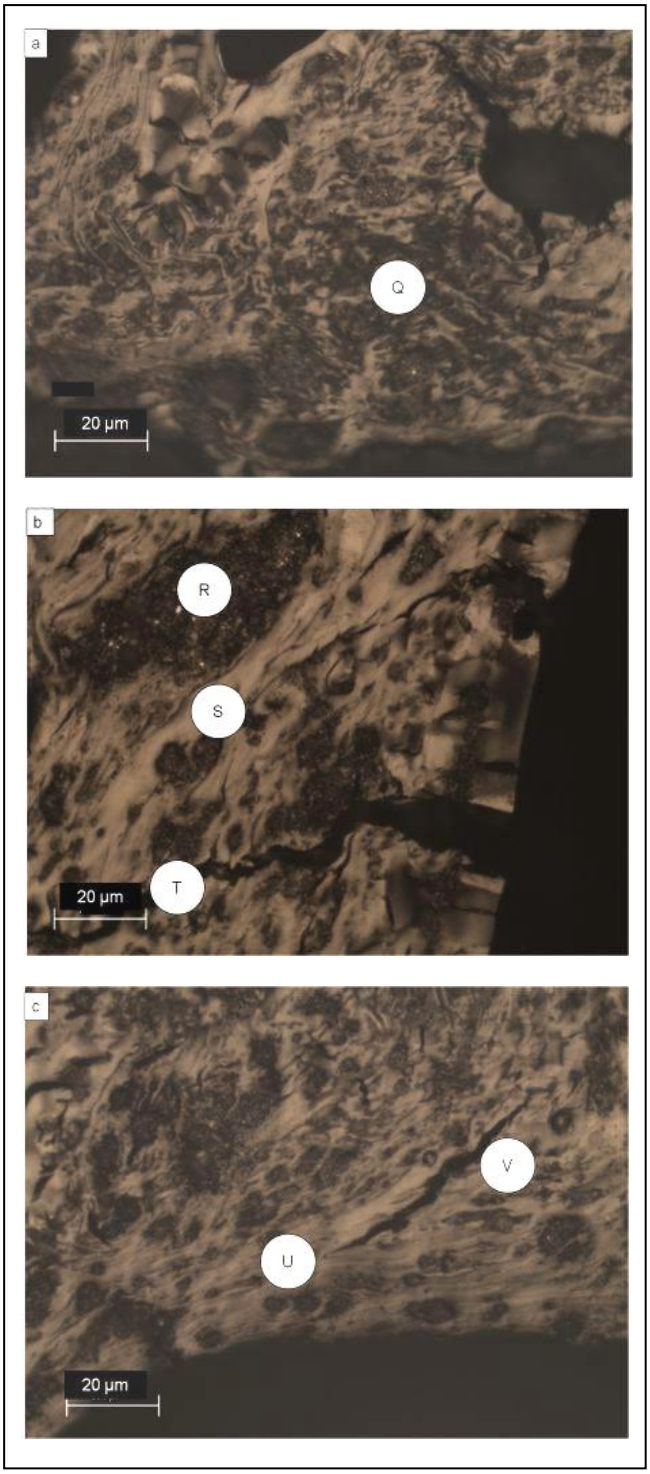

Figure 6-19 Optical micrographs (a–c) of Sample 3 Waxy Oil calcined coke

Sample 3 shows the appearance of larger catalyst agglomerates, both densely packed (Positions Q and R) and interspersed by coarse grain mosaics. As the density and size of the

catalyst agglomerates increase, the overall anisotropy of the microstructure reduces (in some areas into the mosaic range). However, in areas of the micrograph where the size and density of the ash agglomerates is low (Position S), the dominant microstructure is still elongated flow domains. The appearance of shrinkage fissures both parallel to the flow domain (Position T) and perpendicular to the flow domain (Position V and U) are similar to those described for Sample 2.

The variation in the microstructure of Sample 4 is shown in Figure 6-20 (a–c).

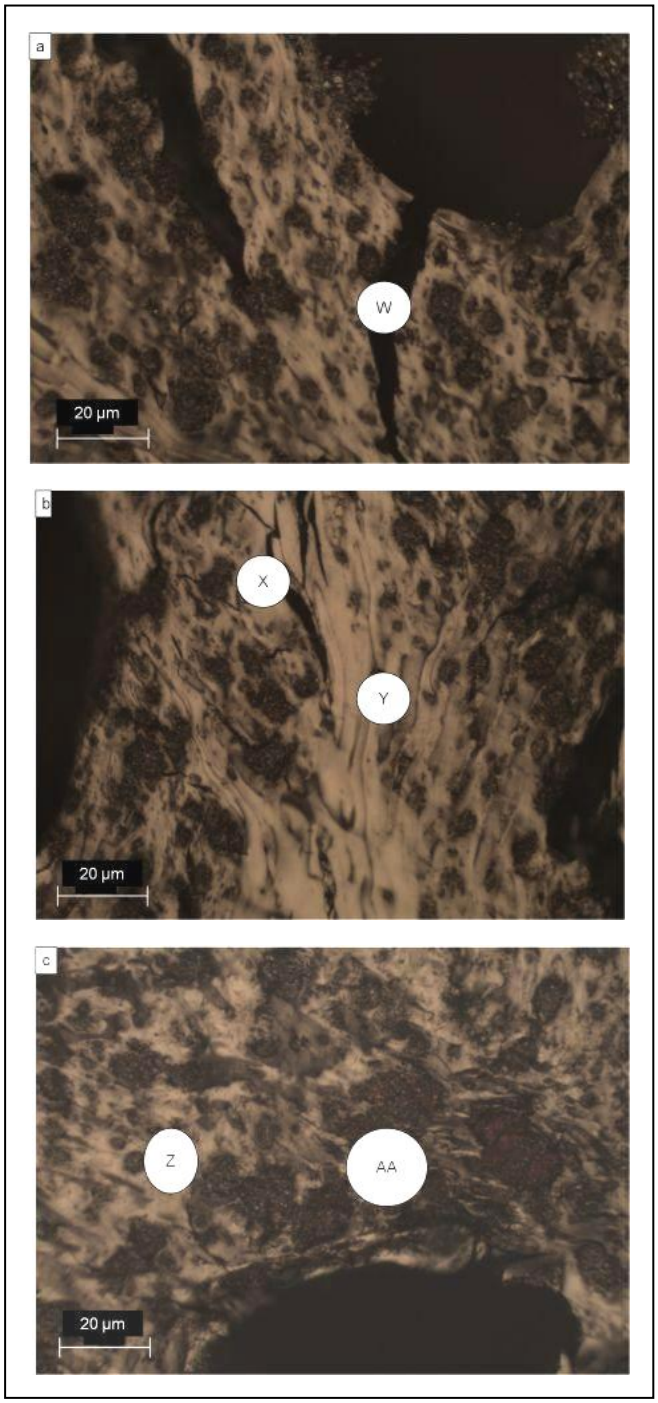

Figure 6-20 Optical micrographs (a–c) of Sample 4 of Waxy Oil calcined coke

The microstructure of Sample 4 calcined coke is highly variable, again determined by the size and density of the catalyst agglomerates, ranging from elongated flow (Position Y) to medium-grain mosaic (Position AA). Both transverse (Position W) and parallel (Position X) shrinkage fissures to the alignment of the carbon microstructure are observed. Position Z shows the close packing arrangement of the catalyst agglomerates of over 10 µm in diameter.

Thus apart from mosaic microstructures in the immediate vicinity of the catalyst agglomerate, the general microstructure appears locally anisotropic. It may therefore be argued that removing the catalyst alone would yield the anisotropic microstructure desired. However, as shown in Chapters 7 and 8, organic molecular thermal instability has a substantial effect on the microstructure. It is not seen in the above micrographs as delayed coking effectively distributes the mosaic microstructures.

6.5.2 Chemical analysis of Waxy Oil calcined cokes

The analysis of the calcined coke (Samples 1 to 4) is shown in Table 6-3.

Table 6-3 Analysis of Waxy Oil calcined cokes

	Units	Sample 1	Sample 2	Sample 3	Sample 4
Calcined coke yield	**Mass%**	90.6	90.5	89.4	86.5
Carbon	**Mass%**	97.109	95.863	94.343	92.882
Hydrogen	**Mass%**	0.130	0.110	0.130	0.120
Nitrogen	**Mass%**	0.020	0.020	0.020	0.020
Sulphur	**Mass%**	0.017	0.024	0.032	0.056
Real density (-75 µm; He)	**$g.cm^{-3}$**	2.1024	2.1087	2.1124	2.1220
Volatile Carbon Matter (VCM)	**Mass%**	0.57	0.47	0.38	0.59
Fixed carbon[1]	**Mass%**	96.41	94.11	90.96	85.90
CO_2 reactivity	**Mass%. $100\ min^{-1}$**	69.78	77.88	81.13	87.02
Ash content	**Mass%**	3.02	5.42	8.66	13.51
Metal content:					
Calcium (Ca)	**Mass%**	0.0931	0.1380	0.1473	0.1521
Iron (Fe)	**Mass%**	1.8365	2.6882	3.7474	4.7624
Silicon	**Mass%**	0.0308	0.0437	0.0535	0.0800
Vanadium (V)	**Mass%**	0.0001	0.0001	0.0001	0.0001
Nickel (Ni)	**Mass%**	0.0005	0.0001	0.0001	0.0001
TOTAL METALS IN COKE	**Mass%**	1.9671	2.8755	3.9533	4.998

Although the VCM of the four samples is relatively consistent, it does indicate slight under calcining. As expected, the ash content increases from Sample 1 to Sample 4, in agreement with the trend of the ash contents of the green coke.

The hydrogen content (0.110–0.130%) of the calcined coke shows a substantial decrease from that of the green coke (3.52–3.68%) due primarily to destructive cracking of hydrogen from the defective edges of carbonaceous layers. The nitrogen content of the calcined coke shows a slight decrease and the sulphur content a slight increase from those of the green coke form.

The real density increases from Sample 1 to Sample 4. This appears to be in contrast to the accepted relationship between a higher degree of anisotropy and higher real densities, as described by Frohs *et al.* (2007). The opposite trend is indicated in this study and is considered to be a "pseudo effect" due to the unusually high catalyst content and the smaller PSD (-75 µm) used for the analysis. As the major elemental contaminant is iron (which has a substantially higher molecular weight than carbon: 55.847 vs. 12.011 amu respectively), this is the probable cause of this unusual trend. It is also probable that given the catalyst concentration, not all the Fe_3O_4 would have been converted to either Fe_3C and Fe, which would further add to the comparative influence on the real density (as shown in the XRD of the calcined coke – Figure 6-15).

The correlation of the ash content with the real density yields a linear regression with an R^2 value of 0.9862. By using the equation to determine the regression, it is possible to predict a value for the real density (2.0974 $g.cm^{-3}$), assuming that the ash content of the coke was zero. Using the ash analysis to represent the form of the catalyst in the green coke (Fe_3O_4) may be questionable as during the ashing of the coke, Fe_3O_4 would be oxidised to Fe_2O_3. However, it is the closest comparison. The correlation of the iron content with the real density yields a linear regression with an R^2 value of 0.9684. By using the equation to determine the regression, it is possible to predict a value for the real density (2.0901 $g.cm^{-3}$), assuming the iron content of the coke was zero. The minimal difference between both the R^2 values for the linear regressions may indicate that there is a mixture of iron compounds present (i.e. Fe_3O_4, Fe_2O_3, Fe_3C and Fe), as confirmed by the XRD analysis shown in Figure 6-19.

6.5.3 X-ray diffraction of Waxy Oil calcined coke

X-ray diffraction was conducted on samples of Waxy Oil calcined coke to determine the influence of the catalyst on the ordering of the crystal structure. A detailed description of the experimental protocol is given in Chapter 5, Section 5.1.5.3.

6.5.3.1 Analysis of peaks in the graphite region of Waxy Oil calcined cokes

An XRD trace of the graphite region of Waxy Oil calcined cokes is shown in Figure 6-21.

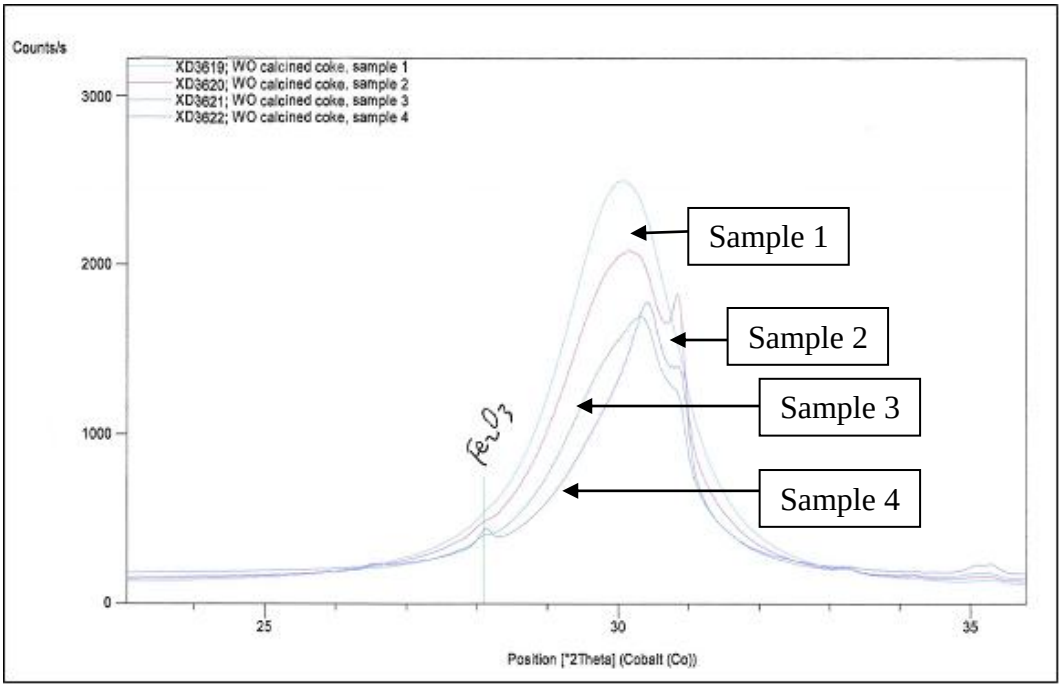

Figure 6-21 XRD trace showing graphite peaks between a 2θ angle of 25 and 35° in the Waxy Oil calcined cokes

The XRD trace of the four Waxy Oil calcined cokes presents broad peaks (within the graphite region) which are without doubt the product of overlapping individual peaks (as shown later in Figure 6-22).

Sample 1, with the lowest catalyst content, yields a broad Gaussian curve. As the catalyst content increases (Sample 2), the trace develops a small peak at a higher 2θ angle on the right shoulder. The XRD trace of Samples 3 and 4 indicates a broadening of the shoulder peak to the right of the trace.

As shown in Figure 6-15, the presence of elemental iron increases as the catalyst content increases. Both Ugarkorvic and Legin (1986) and Wang *et al.* (2001) have reported that an increase in the iron content of calcined petroleum coke lowers the temperature at which graphitisation occurs, presenting **two** overlapping peaks in the graphite region. Wang *et al.* (2001) identify these peaks as a thermal peak at a lower 2θ angle (depending on the original microstructural carbon anisotropy) and a peak at a higher 2θ angle due to catalytic "graphitisation".

However, previous research by Wang *et al.* (1995) identified the presence of a third broad peak within the graphite region at a lower 2θ angle, ascribed to more disordered carbon. Baraniecki *et al.* (1969) refer to the development of multiple peaks in the graphite region as being a result of "multi-phase graphitisation".

While the XRD trace of the Waxy Oil calcined cokes thus provides evidence of multi-phase graphitisation, the substantial overlapping of the 002 peaks warrants further investigation. In literature previously cited, Wang *et al.* (2001) used a narrow PSD for the iron additive (0.1-1.0 µm), which was equally dispersed within the carbon matrix. As the iron content increased, the microstructure trended towards a uniform mosaic microstructure.

In general terms, the increase in the catalyst concentration from Sample 1 to Sample 4 [as given by the chemical analysis (Table 6-3) and in the micrographs (Figure 8-11)] would support the development of the catalytically derived 002 peak.

The XRD trace of Waxy Oil calcined coke (Sample3) showing the three deconvoluted peaks named G1, G2 and G3 in the graphite region is shown in Figure 6-22. The interlayer spacings of the three peaks are shown in Table 6-4.

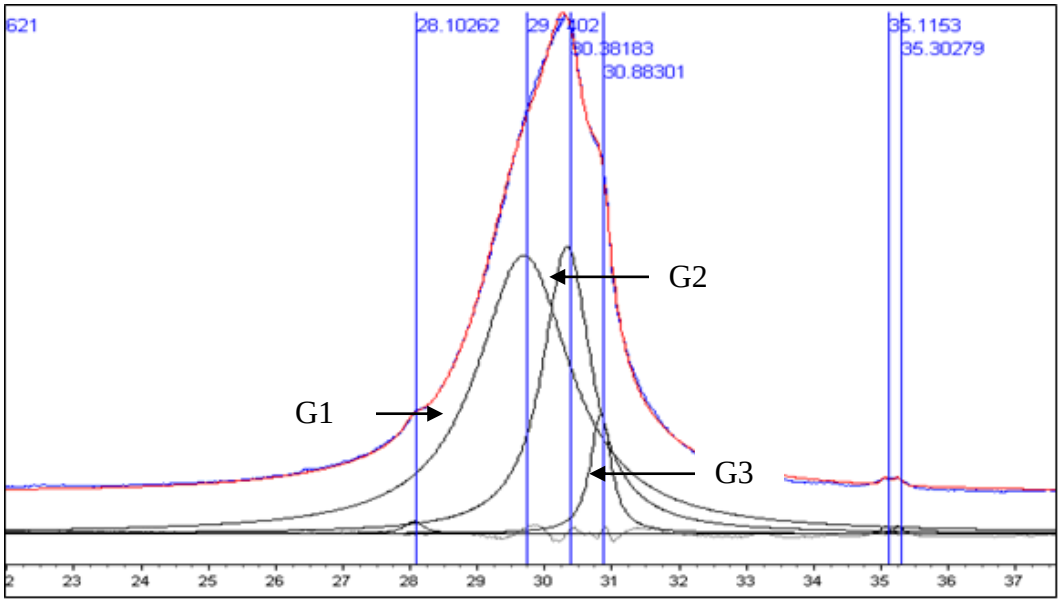

Figure 6-22 XRD trace showing graphite peaks G1, G2 and G3 in the Waxy Oil calcined coke

A description of the peaks to which random numbers G1, G2 and G3 were ascribed is given below:

- **G1:** This peak appears at a 2θ angle of 29.74 °. As it appears at the lowest 2θ angle of the three peaks and is the broadest, it is thought to be associated with the least ordered carbon. As shown in Figure 6-13, mosaic microstructures are present in the immediate vicinity of the catalyst.

- **G2:** This peak appears at a 2θ angle of 30.38 °. It is indicative of the improved development of the crystal structure, based on thermal treatment of the more anisotropic microstructures in the calcined coke.

- **G3:** This peak appears at a 2θ angle of 30.88 °. As this peak is the sharpest, yielding the lowest d_{002} interlayer spacing, it is suggested that it is due to catalysed graphitisation (as a result of the iron content in the coke).

Table 6-4 Interlayer spacing of G1, G2 and G3 graphite peaks in Waxy Oil calcined cokes

Peak	Units	Sample 1	Sample 2	Sample 3	Sample 4
G1	**Å**	3.5040	3.4880	3.4850	3.4830
G2	**Å**	3.4410	3.4180	3.4140	3.4090
G3	**Å**	3.3760	3.3590	3.3600	3.3590

Å= $1x10^{-10}$ m

The ability of thermal treatment (in this case calcination) to increase the density of carbon depending on the microstructure of the coke is evident in the variation of the interlayer spacing of the G1 and G2 peaks. Although mosaic carbon microstructures (G1) are graphitisable, the microdomain boundaries limit the range within which crystal development occurs and thus present with higher interlayer spacings than G2 where there are fewer microdomain boundaries, allowing crystal development over a longer range.

The substantially lower interlayer spacing of the G3 002 peak is due to the mechanism of catalytic graphitisation which converts the carbon into quite highly ordered graphite, which is in agreement with the results of Wang *et al.* (1995).

Weismuller *et al.* (1995) suggest that carbon is catalytically transformed into highly ordered graphite by one of two mechanisms:

- Dissolution of carbon in the molten metal until super-saturation is reached, after which carbon precipitates in the form of crystalline graphite
- The formation of a metal carbide intermediate which decomposes to form crystalline graphite

As shown in Table 6-4, the interlayer spacing of the G1 and G2 peaks decreases slightly with increasing catalyst content. There is a substantial reduction of the interlayer spacing of G3 from Sample 1 to Sample 2, after which it remains constant for Samples 3 and 4.

While the degree of catalytic graphitisation is dependent on the concentration of iron (at least until the point of saturation) as reported by Wang *et al.* (2001) and Dhakate *et al.* (1997), it is the author's opinion that this may also be highly dependent on the PSD of the catalyst as smaller catalyst particles have a higher ratio of surface area to volume (compared with larger catalyst particles). Thus, with smaller catalyst particles the surface area contact with carbon in their direct vicinity is greater.

The interlayer spacing of the disordered (G1) and the thermal (G2) peaks in the graphite region decreases with an increasing catalyst content and a decrease in the overall anisotropy of the microstructure from Sample 1 to Sample 4. Although unexpected, this result is in agreement with that of Wang *et al.* (2001). This would suggest that the dominant graphitisation mechanism at 1 300 °C is catalytic.

6.5.4 Raman spectroscopy of Waxy Oil calcined coke

Raman spectroscopy was conducted on samples of Waxy Oil calcined coke in order to determine the influence of the catalyst content on the average ordering of the crystal structure. A detailed description of the experimental protocol is given in Chapter 5, Section 5.1.5.4.

Raman spectroscopy can distinguish between the various carbon phases and has been used to investigate the degree of crystallinity of carbonaceous materials (Sadezky *et al.*, 2005; Beyssac *et al.*, 2003). In the Raman spectrum both first- and second-order bands are observed in the region 200–4000 cm^{-1}. Five first-order bands have been identified and are designated the G, D1, D2, D3 and D4 bands (Sadezky *et al.*, 2005). The G band (1580 cm^{-1}) has E_{2g} symmetry as a result of the ideal graphitic lattice. It is therefore indicative of the degree of

graphitisation in the sample. The D bands are associated with disorder and defects present in the graphite layers (Sadezky *et al.*, 2005). The D1 (1350 cm^{-1}, A_{1g} symmetry) and D2 (1620 cm^{-1}, E_{2g} symmetry) bands indicate disorder in the graphene layers at the edges and on the surface layers respectively. The D3 band (1500 cm^{-1}) is indicative of the amount of amorphous carbon present in the sample, and the observation of the usually Raman inactive D4 band (1200 cm^{-1}) indicates disorder due to the presence of polyenes and ionic impurities.

Several ratios of the Raman bands have been proposed by Sadezky *et al.* (2005) and Beyssac *et al.* (2003) to give structural information regarding carbon samples. $R_1 = I_{D1}/I_G$ and $R_1' = I_{D2}/I_G$ are an indication of the relative disorder that exists within the graphene layers (Sadezky *et al.*, 2005), whereas $R_2 = I_{D1}/ (ID_1 + I_{D2} + I_G)$ gives information regarding the degree of organisation that exists in the sample (Beyssac *et al.*, 2003).

The Raman spectra of the four Waxy Oil calcined coke samples are shown in Figure 6-23 and the R_1, R_1' and R_2 ratios in Table 6-5.

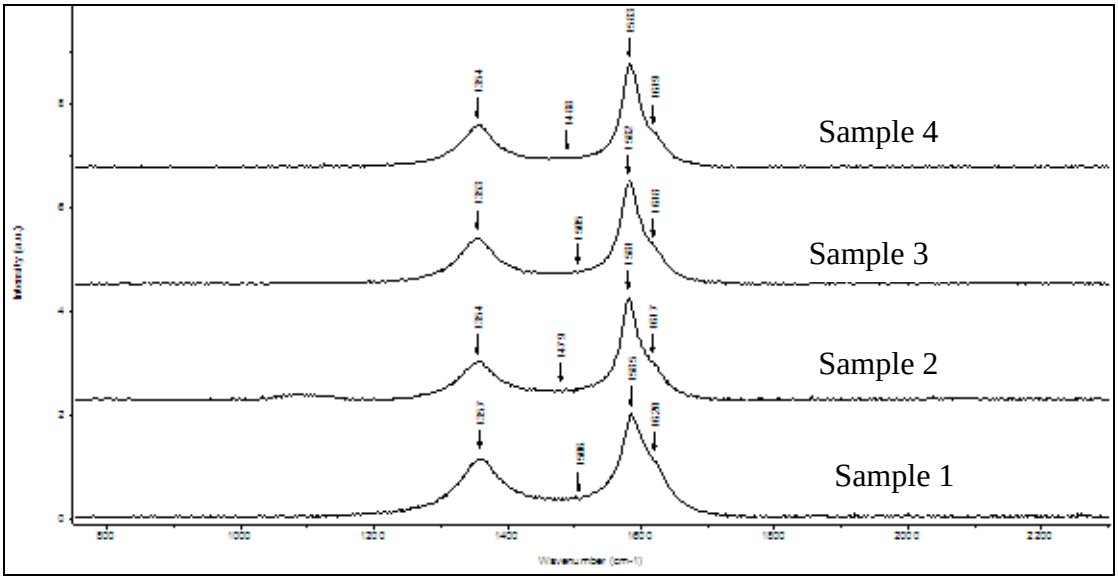

Figure 6-23 Raman spectra of Waxy Oil calcined cokes

Table 6-5 Comparative table of Raman spectra ratios (R_1, R_1' and R_2) for Waxy Oil calcined cokes

	Calcined coke				References	
Ratio	**Sample 1**	**Sample 2**	**Sample 3**	**Sample 4**	**Needle Coke**	**Graphite**
R_1	0.624	0.357	0.452	0.400	0.769	0.062
R_1'	0.332	0.203	0.195	0.169	-	-
R_2	0.319	0.229	0.275	0.255	0.435	0.058

$R_1 = I_{D1}/I_G$

$R_1' = I_{D2}/I_G$

$R_2 = I_{D1}/(I_{D1} + I_{D2} + I_G)$

For the calcined needle coke no separate D2 band could be observed, but this does not mean that it has infinite graphitic domain, as the broad band at 1602 cm^{-1} probably represents both the G and D2 bands of calcined needle coke.

The calcined coke samples all have large R_1 values, but appear more ordered than the calcined needle coke. The R_1' ratio indicates that the crystallite width of the calcined cokes increases with increasing catalyst concentration. This is further evidence to support the dominance of catalytic graphitisation within the calcined cokes.

It is also interesting to note that the R_1 ratio of the calcined needle coke (Table 6-5; 0.769) is higher than that of any of the Waxy Oil calcined cokes. As the needle coke specification requires an ash content of less than 0.2%, the effect of catalytic graphitisation will be negligible and the crystal order will be determined by the development of the thermal graphite peak which, in turn, will depend on the microstructure. As the crystal development due to catalytic graphitisation will produce near-perfect graphite, the effect on the overall crystal structure will be both substantial and dominating.

6.6 Waxy Oil pre-graphite

Samples (1–4) of Waxy Oil green coke (> 2.0 mm, approximately 17 g) were thermally treated in a medium-frequency induction furnace to 2 000 °C with a soaking time of 5 min. Analyses conducted on the pre-graphites included real density, proximate analysis, XRD and Raman spectroscopy.

The proximate analysis of the pre-graphites is shown in Table 6-6.

Table 6-6 Analysis of Waxy Oil pre-graphites

	Units	Sample 1	Sample 2	Sample 3	Sample 4
VCM	**mass%**	0.6	0.8	0.6	0.4
Fixed carbon	**mass%**	97.5	95.2	93.0	88.4
Ash content	**mass%**	1.9	4.0	6.4	11.2

As the sample mass (approximately 17 g) for heat treatment (2 000 °C) of the Waxy Oil green coke was limited by the size of the graphite crucible, the ash content was estimated using TGA. The ash content of the pre-graphites is similar to that of the green coke and suggests that, even given the 82.0–84.6% yield, there was minimal iron sublimation.

6.6.1 Effect of catalyst content on the real density of Waxy Oil green and thermally treated cokes

The relationship between the catalyst concentration (Samples 1–4) and the corresponding real densities of the green and thermally treated cokes is shown in Table 6-7.

Table 6-7 Real density of Waxy Oil green coke, calcined coke and pre-graphite

	Units	Sample 1	Sample 2	Sample 3	Sample 4
Green coke	**g.cm^{-3}**	1.3879	1.4237	1.456	1.4792
Calcined coke	**g.cm^{-3}**	2.1024	2.1087	2.1124	2.1220
Pre-graphite	**g.cm^{-3}**	2.2113	2.1886	2.1774	2.1470

Increasing the catalyst content increases the real densities of the green and calcined coke. However, the real density of the pre-graphites decreases as a function of increasing catalyst concentration.

When proposing an explanation for these trends, it is necessary to consider both the yield and the effect of the phase of the iron-based catalyst in the green coke, calcined coke and pre-graphite.

The molecular weight of Fe_3O_4 (231.537) is considerably higher than that of carbon (12.011). As the bulk of the catalyst has a PSD below 75 µm (the particle size used to determine the real density of the coke), its effect is likely to be included. This would thus explain the increase in the real density as the ash content of the green coke increased. With regard to the calcined coke, the yield as shown in Table 6-3 (86.5–90.6%) will increase the real density due to partial gasification of the carbon volatiles. However, as the calcination was conducted in nitrogen, it is suggested that the heavier components of the volatile carbon matter would carbonise to form solid carbon. As indicated in Figure 6-15, XRD data shows the presence of Fe_3O_4, Fe_2O_3 and Fe. It is further suggested that the reduction of Fe_3O_4 would be only partial given the particle size range of the catalyst.

6.6.2 X-ray diffraction of Waxy Oil pre-graphite

XRD was conducted on samples of Waxy Oil pre-graphite in order to determine the influence of the catalyst concentration on the interlayer spacing of peaks in the graphite region. A detailed description of the experimental protocol is given in Chapter 5, Section 5.1.5.3.

6.6.2.1 Identification of peaks within the graphite region for Waxy Oil pre-graphites

An XRD trace of the graphite region of Waxy Oil pre-graphites is shown in Figure 6-24.

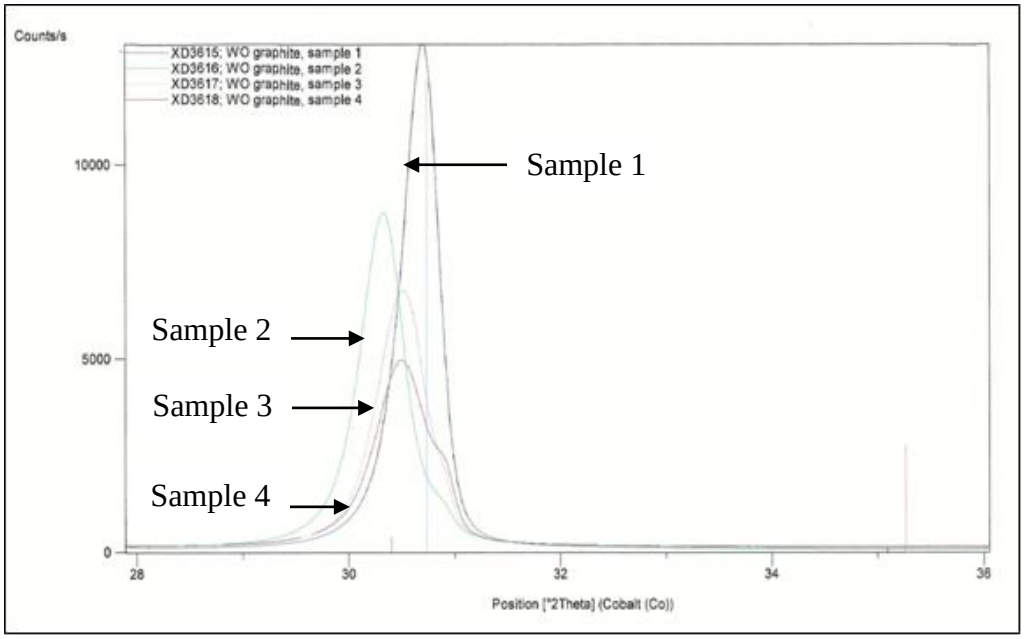

Figure 6-24 XRD trace showing peaks in the graphite region between a 2θ angle of 28 and 32° in the Waxy Oil pre-graphite

In comparison with the calcined coke (shown in Figure 6-21), the peaks in the graphite region of the Waxy Oil pre-graphites appear narrower and more intense. Sample 1 shows a narrow thermal peak. The peaks associated with Sample 2 to Sample 4 decrease in comparative (as the same amount of sample was used for the analysis) intensity and broaden while shifting to a higher 2θ angle.

There is a substantial difference in the 2θ angle of the thermal graphite peak between Sample 1 and Sample 2 of the pre-graphites. The shift towards a lower 2θ angle in the thermal graphite peak of Sample 2 indicates that Sample 1 shows a lower interlayer spacing. The apex of the thermal graphite peak for Samples 3 and 4 shifts to a higher 2θ angle (than Sample 1), which may indicate a co-dependence on both thermal and catalytic graphitisation mechanisms.

The XRD trace of Waxy Oil pre-graphites showing the three deconvoluted peaks in the graphite region identified as G1, G2 and G3 is shown in Figure 6-25.

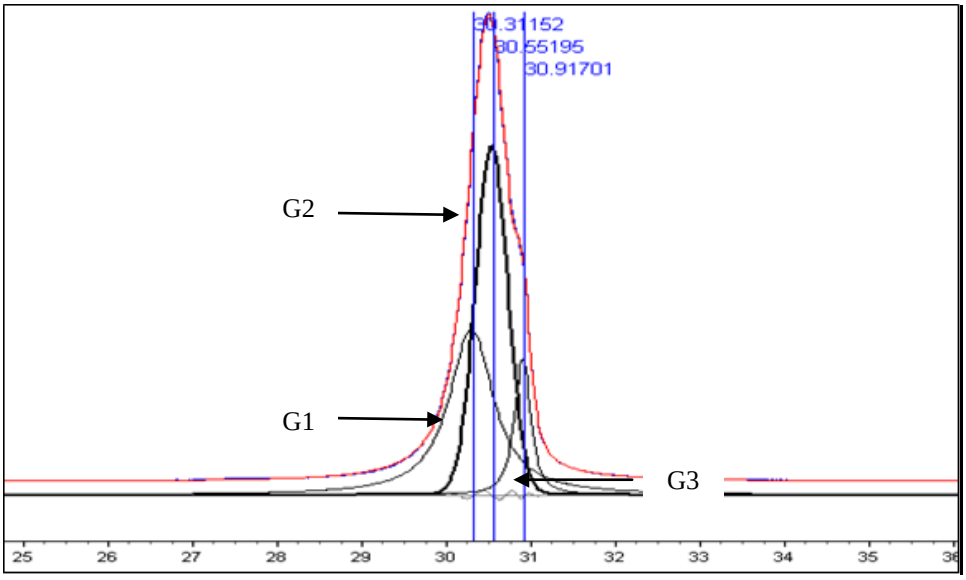

Figure 6-25 XRD trace showing graphite peaks G1, G2 and G3 in the Waxy Oil pre-graphites

For example, the three graphite peaks identified in Sample 1 calcined coke (G1, G2 and G3) are present in the Waxy Oil pre-graphites, but appear to have shifted to a higher 2θ angle. However, the 2 000 °C thermal treatment appears to narrow the width and increase the intensity of the thermal graphite peak (G2). This variation in the shape of the peaks as a result of thermal treatment is consistent with observations by Wang *et al.* (1995):

1. The disordered peak (G1) for calcined coke appears at a 2θ angle of 29.74° vs. the peak for pre-graphite which appears at a higher 2θ angle of 30.31°.
2. The thermal peak (G2) for calcined coke appears at a 2θ angle of 30.38° vs. the peak for pre-graphite which appears at a higher 2θ angle of 30.55°.
3. The catalytic peak (G3) for calcined coke appears at a 2θ angle of 30.88° vs. the peak for pre-graphite which appears at a higher 2θ angle of 30.92°.

The 2θ angle shifts for the disordered peak (G1; 0.57°) and the thermal peak (G2; 0.17°) are substantially greater than the shift for the catalytic peak (G3; 0.03°). This would indicate that

the thermal treatment (2 000 °C) had a more substantial effect on the development of the former peaks. Thus, in terms of the driving force for crystallographic development, it appears that thermal rather than catalytic graphitisation may be the driving force, especially in the pre-graphites where the catalyst concentration is lower. This is confirmed by studying the interlayer spacings associated with the peaks in the graphite region (G1, G2 and G3) shown in Table 6-8.

Table 6-8 Interlayer spacing of G1, G2 and G3 in the Waxy Oil pre-graphites

Peak	Units	Sample 1	Sample 2	Sample 3	Sample 4
G1	Å	3.348	3.429	3.417	3.422
G2	Å	3.360	3.404	3.390	-
G3	Å	3.355	3.357	3.354	3.357

Å= $1x10^{-10}$ m

The interlayer spacing of the G1 and G2 peaks are substantially lower in the pre-graphite coke than in the calcined coke, indicative of the effect of a temperature increase.

The increase in the interlayer spacing of Sample 1 to Samples 2 to 4 is caused partially by graphitisation due to thermal treatment and partially by catalytic graphitisation. As the catalyst concentration increases, the overall anisotropy of the carbon microstructure diminishes. Furthermore, when once the carbon immediately adjacent to the catalyst has been catalytically graphitised, it is not further graphitised by increasing thermal treatment; this is especially true in Samples 3 and 4.

The saturation of catalytic graphitisation for Samples 1 and 2 is thought to be due to the lower catalyst content. Both Mochida *et al.* (1980) and Wang *et al.* (2001) suggest that once carbon is catalytically graphitised, it is hardly graphitised further by the same catalyst even at a higher temperature.

6.6.3 Raman spectroscopy of Waxy Oil pre-graphite

The Raman spectrographic trace of the four Waxy Oil pre-graphites is shown in Figure 6-26. The intensities of the G, D1, D2, D3 and D4 peaks were used to determine the R_1, R_1' and R_2 ratios shown in Table 6-9.

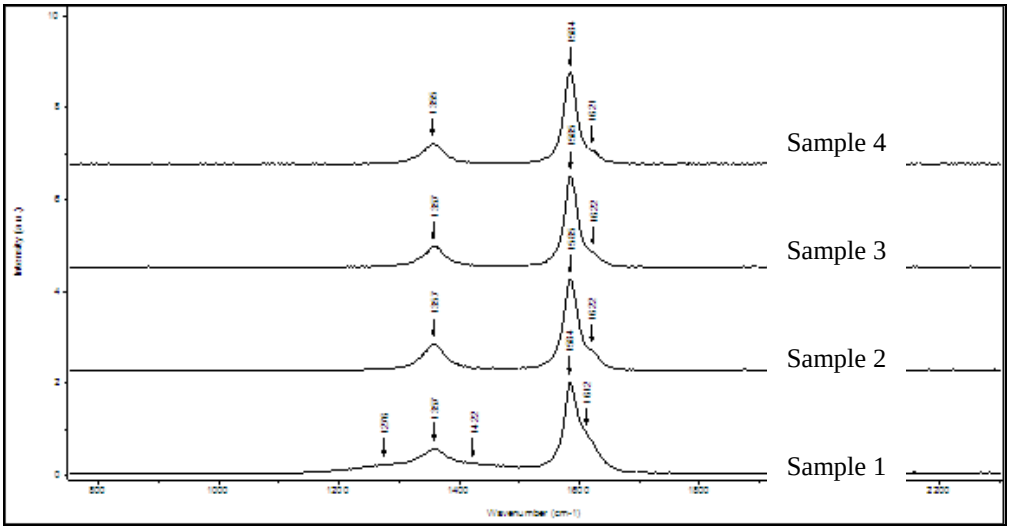

Figure 6-26 Raman spectra of Waxy Oil pre-graphites

Table 6-9 Comparison of Raman spectra ratios (R_1, R_1' *and* R_2) for Waxy Oil pre-graphites

	Pre-graphites				References	
Ratio	**Sample 1**	**Sample 2**	**Sample 3**	**Sample 4**	**Needle Coke**	**Graphite**
R_1	0.206	0.284	0.225	0.225	0.769	0.062
R_1'	0.321	0.118	0.086	0.074	-	-
R_2	0.135	0.203	0.172	0.173	0.435	0.058

R1 = *ID1/IG*

*R*1' = *ID2/IG*

R2 = *ID1*/(*ID1* + *ID2* + *IG*)

The pre-graphite samples have lower R_1 values (Table 6-9) than the calcined cokes (Table 6-5), showing that they have more ordered graphitic structures, which is expected as a result of thermal graphitisation, as indicated by the XRD data.

In comparison with the disordered and thermal peaks for the pre-graphite, the R_1 ratio (indicating the thickness of the crystallite) shows a similar trend between Samples 1 and 2, with Samples 3 and 4 being very much the same. The R_1' ratio indicates a decrease in the overall order as the catalyst content increases from Sample 1 to Sample 4. The increase in the order of pre-graphite Samples 3 and 4 compared with Sample 2 may indicate that saturation of catalytic graphitisation has not been reached.

6.7 Graphitisation of Waxy Oil green coke

This section examines the efficacy of catalyst sublimation from Waxy Oil green coke at a temperature of approximately 3 000 °C.

6.7.1 Analysis Waxy Oil green coke

Samples of Run of Coker (ROC)[18] Waxy Oil green coke were obtained from the commercial delayed coker at Secunda, South Africa. After the green coke sample had been dried, it was sieved to produce the following particle size fractions:

- 0–1 mm
- 1–2 mm
- 2–4 mm
- 4–8 mm
- > 8 mm

A composite sample (2 200 g) composed of known masses of the size fractions was produced for the graphitisation experiment. The chemical analysis of the size fractions is shown in Table 6-10.

Table 6-10 Chemical analysis of Waxy Oil green coke particle size fractions

	Units	0–1 mm	1–2 mm	2–4 mm	4–8 mm	> 8 mm
Real density	**g.cm^{-3}**	1.4378	1.4564	1.4485	1.4774	1.4802
VCM	**Mass%**	10.79	12.23	12.01	12.34	9.82
Ash	**Mass%**	7.39	7.68	8.10	8.93	8.77
Iron (Fe)	**Mass%**	3.3467	3.5486	3.7163	3.8475	3.8419
Nickel (Ni)	**Mass%**	0.0001	0.0001	0.0001	0.0001	0.0001
Vanadium (V)	**Mass%**	0.0001	0.0001	0.0001	0.0001	0.0001
Calcium (Ca)	**Mass%**	0.1222	0.1158	0.1130	0.1094	0.1055
Silicon (Si)	**Mass%**	0.0386	0.0362	0.0035	0.0359	0.0380
Sodium (Na)	**Mass%**	0.0081	0.0044	0.0043	0.0047	0.0052

The VCM of the various size fractions ranges between 9.82 and 12.34%. Given the process of delayed coking, cutting and crushing, there is no specific evidence that VCM is in any way correlated to PSD variation.

The chemical analysis of Waxy Oil graphites is shown in Table 6-11.

Table 6-11 Chemical analysis of Waxy Oil graphite

	Units	0–1 mm	1–2 mm	2–4 mm	4–8 mm	> 8 mm
Carbon	**Mass%**	98.000	98.000	97.060	97.280	97.600
Hydrogen	**Mass%**	0.120	0.100	0.170	0.160	0.160
Nitrogen	**Mass%**	0.020	0.020	0.020	0.020	0.020
Sulphur	**Mass%**	0.003	0.003	0.002	0.004	0.011
Fixed carbon	**Mass%**	98.14	98.12	97.25	97.46	97.79
VCM	**Mass%**	0.03	0.01	0.14	0.17	0.14
Real density	**g.cm^{-3}**	2.2734	2.2722	2.2517	2.245	2.2597
CO_2 reactivity	**Mass%. 100 min^{-1}**	81.25	82.81	-	78.49	77.45
Air reactivity	**Mass%**	0.42	0.42	0.49	0.51	0.47

[18] Run of Coker (ROC) refers to the full PSD of green coke after cutting and crushing and before any sieve screening.

	Units	0–1 mm	1–2 mm	2–4 mm	4–8 mm	> 8 mm
Resistivity	**μΩ.m^{-1}**	324	307	298	318	323
Ash	**Mass%**	6.70	5.57	5.88	6.99	8.22
Iron (Fe)	**Mass%**	3.2310	2.9691	3.0762	3.3443	3.6012
Nickel (Ni)	**Mass%**	0.0001	0.0001	0.0001	0.0001	0.0001
Vanadium (V)	**Mass%**	0.0001	0.0001	0.0001	0.0001	0.0001
Calcium (Ca)	**Mass%**	0.0019	0.0019	0.0019	0.0018	0.0022
Silicon (Si)	**Mass%**	0.0585	0.0468	0.0509	0.0453	0.0507
Sodium (Na)	**Mass%**	0.0001	0.0010	0.0001	0.0001	0.0001
Total metals	**Mass%**	3.292	3.019	3.129	3.392	3.654

The percentile ash and iron loss vs. resistivity of Waxy Oil graphites is shown in Figure 6-27.

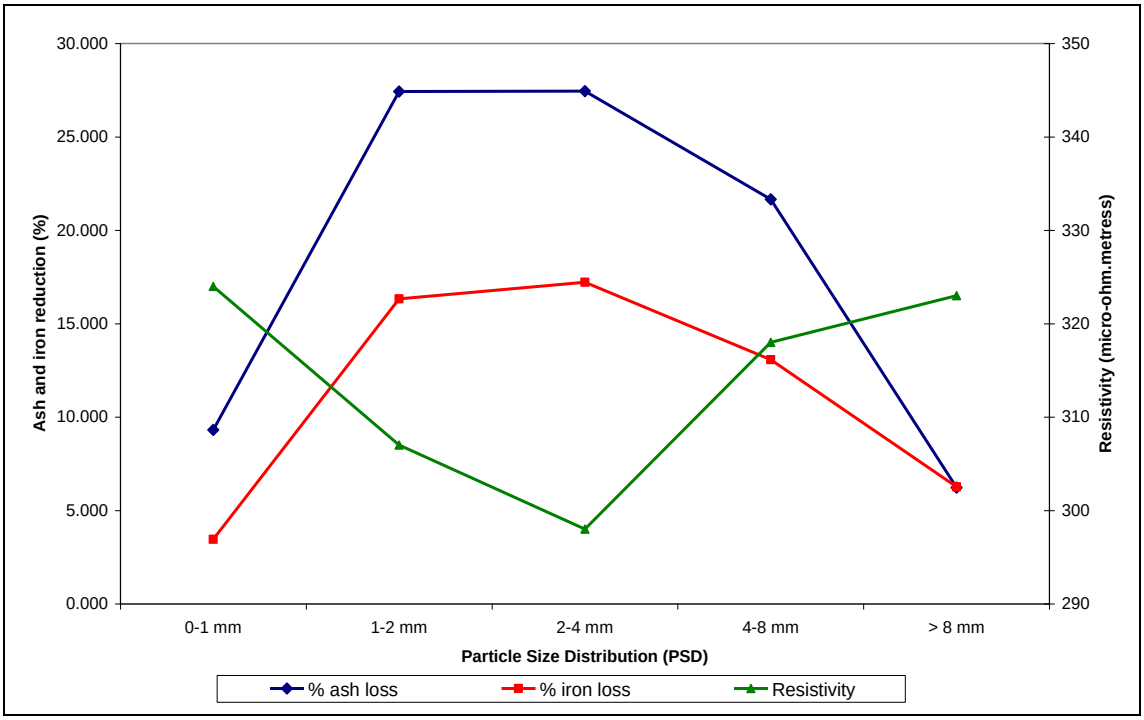

Figure 6-27 Graph showing the percentile loss of ash and iron from the green coke (during graphitisation) on the left axis vs. the resistivity of the graphite on the right axis

The ash reduction in Waxy Oil graphites is between 6 and 28%. The greatest percentile ash and iron loss occurs in the 1–2 mm and 2–4 mm particle size range with a reciprocal decrease in the resistivity. At both the ends of the particle size spectrum indicated (0-1 and > 8 mm) opposing forces of carbon surface area and catalyst exposure to the atmosphere may limit ash and iron reduction.

It was decided not to conduct further analysis on the Waxy Oil graphite samples (inclusive of optical microscopy, Raman spectroscopy and X-Ray diffraction) as it is evident from the results shown in Figure 6-7 that graphitisation would not be capable of removing the catalyst content to appropriate needle coke specification levels.

The discussion of the graphitisation section is limited due to the fact that it is the authors opinion that graphitisation was employed as a potential method to reduce the catalyst content. As it is clearly evident that this only occurred with a limited degree of success, further experimental analysis would not seem logical.

6.8 Conclusions – Influence of catalyst concentration on the characteristics of Waxy Oil coke

The current study presents data showing the effect of catalyst concentration (dominated by iron oxides) on the structural and reactivity profiles of commercial Waxy Oil green cokes, thermally treated to 1 400 °C (calcined cokes) and 2 000 °C (pre-graphites) .

The conclusions drawn from the current study of commercial Waxy Oil coke are:

- The real density of the green and calcined coke increases with increasing catalyst content due to the higher molecular weight of iron oxide compared with carbon. However, the contrary is true for the real densities of the pre-graphites, which decrease with increasing catalyst content due to reduction and partial sublimation of elemental iron.

- The oxidative consumption and carboxy reactivity is increased with increasing iron content as it acts as a promoter for both of these reactions.

- The catalyst obscures the formation of microstructural flow domains, acting predominantly as an inert barrier. As the catalyst size decreases, there is evidence of isotropic mosaic microstructures produced as iron oxide catalyses oxidative polymerisation.

- The reduction of iron oxide to elemental iron releases molecular oxygen which probably reacts with carbon to form carbon monoxide.

- The dominant crystal development mechanism during heat treatment of Waxy Oil coke to 1 300 °C is that of catalytic graphitisation, which is promoted by increasing iron content. However, further heat treatment of the Waxy Oil coke to 2 000 °C promotes a thermal graphitisation mechanism.
- Thermal treatment of Waxy Oil coke to 3 000 °C is not capable of reducing the ash content to needle coke specifications.

6.9 Recommendations – Influence of catalyst concentration on the characteristics of waxy oil coke

Based on the evidence provided in this chapter, a number of recommendations in respect of the production of needle coke from Waxy Oil can be made.

This option evaluates a process by which the catalyst is removed from Waxy Oil prior to carbonisation, followed by processes to decrease the catalytic oxidative polymerisation and the ash content.

It is further recommended that modification of the Waxy Oil be effected by means of a process called “sequential optimisation”. One or a combination of these processes will be employed to produce a modified carbonisation precursor in order to produce a more needle-like coke.

The recommended processes include:

1. Filtration of the Waxy Oil to remove the catalyst
2. Distillation of the filtered Waxy Oil
3. Thermal treatment of the filtered Waxy Oil
4. Thermal treatment and distillation of the filtered Waxy Oil

The modified Waxy Oils will be evaluated to determine the effect of the variation in chemical structure caused by the various processes. These results are discussed in Chapters 7 and 8.

7 WAXY OIL MODIFICATION

7.1 Introduction

The modification procedures employed to increase the anisotropy of the coke serve to retard the onset of carbonisation, allowing for maximum fluidity of the system during mesophase formation. This is achieved by stabilising thermally reactive organic moieties prior to carbonisation. Due to the complexity of comparing analyses of the modified Waxy Oil, the analyses have been colour coded as shown in Table 7-1.

Table 7-1 Experimental conditions and colour coding for modified Waxy Oils[19]

Sample	Waxy Oil modification	Colour coding
A	No modification	Orange
B	Sample A filtered through 0.5 µm sieve	Blue
C1	Sample B distilled (480 °C at -0.9 kPa)	Red
C2	Sample B distilled (440 °C at -0.9 kPa)	Grey (80%)
D1	Sample B thermally treated (400 °C, 5 bar, 2 h)	Dark yellow
D3	Sample B thermally treated (410 °C, 5 bar, 2 h)	Bright green
D4	Sample B thermally treated (420 °C, 5 bar, 2 h)	Dark red
E2	Sample B thermally treated (410 °C, 1 h at 5 bar and 1 h at 1 bar)	Pink
E1a	Sample B thermally treated (410 °C, 1 h at 5 bar and 1 h at 1 bar)	Black
E1b	Sample E1a distilled (325 °C under nitrogen)	Sky blue

7.2 Modification of Waxy Oil

7.2.1 No modification of Waxy Oil (Sample A)

This sample is used as a reference against which filtered Waxy Oil (Sample B) is compared. The description of the catalyst's effect on the quality of Waxy Oil coke (discussed in Chapter 6, Section 6.5.1) was based on commercial samples. Sample A was carbonised in a test tube and the coke will be compared with those produced by the other modifications discussed in Chapter 8. Thus, Sample A excludes any potential variability between commercial and laboratory process conditions.

[19] Apart from Sample A, all the samples in Table 7-1were filtered prior to any further modification.

7.2.2 Waxy Oil Filtration (Sample B)

A sample (40 ℓ) of Waxy Oil was obtained from the commercial delayed coker at Secunda, South Africa. As it was not possible to determine the Particle Size Distribution (PSD) of the solids in the Waxy Oil sample, this analysis was conducted on the Synthol Decant Oil (SDO).[20] The solids include any minerals and carbonaceous solids. The PSD is shown in Figure 7-1.

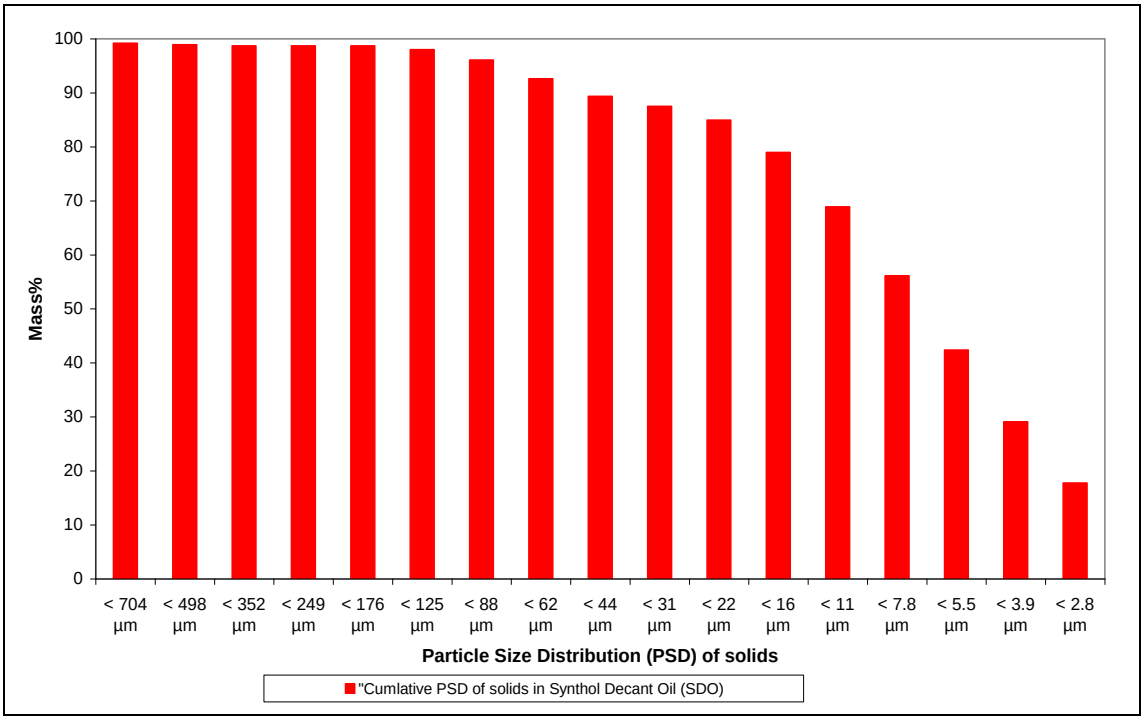

Figure 7-1 Particle Size Distribution (PSD) of solids in Synthol Decant Oil (SDO)

The PSDs of Waxy Oil catalyst particles and carbonaceous solids are less than 100 µm. It is possible to remove the catalyst partially by centrifugation, but not with the efficiency required for needle coke specifications. The effect of filtration on the levels of catalyst (as determined by the ash content) in Waxy Oil filtrates is discussed below.

Waxy Oil was heated to 90 °C and filtered through various sintered metal plates (2.0–0.5 µm). The ash and carbonaceous Mass Insoluble in Quinoline (MIQ) were determined on three samples of the virgin Waxy Oil feed and a series of filtrates. A detailed experimental procedure and description of the filtration apparatus is given in Chapter 5, Section 5.4.1. The results are shown in Table 7-2.

[20] The Synthol Decant Oil (SDO) is the heavy residue product of the Synthol reaction; it is distilled to form the Waxy Oil, which is the residue of the distillation (as shown in Figure 3-1).

Table 7-2 Ash and carbonaceous MIQ[21] content of Waxy Oil blanks and filtrates [obtained through a series of sintered metal plates (2.0–0.5 µm)]

Sample	Units	Filter description	Ash content 1	Ash content 2	Carbonaceous MIQ
Waxy Oil blank 1	**Mass %**	**None**	1.649	1.694	1.065
Waxy Oil blank 2	**Mass %**	**None**	1.699	1.673	0.916
Waxy Oil blank 3	**Mass %**	**None**	1.609	1.593	0.802
Test 1	**Mass %**	**2 µm filter**	0.132	0.139	0.336
Test 2	**Mass %**	**1.0 µm filter**	0.076	0.085	0.153
Test 3	**Mass %**	**0.5 µm filter**	0.006	0.006	not determined
Test 4[22]	**Mass %**	**0.5 µm filter**	0.004	0.003	not determined

Three different samples of Waxy Oil were independently obtained from the 40 ℓ sample. This was done to establish a level of confidence in the determination of the ash content of Waxy Oil, which is dependent on obtaining representative samples. All the Waxy Oil blank samples (named Test 1, 2 and 3) yield ash contents between 1.6 and 1.7%, with carbonaceous MIQ contents between 0.8 and 1.1%.

The use of a 2.0 µm sintered metal plate (Test 1) reduced the ash content to 0.134% (or a 92% reduction) based on the average of the two duplicate results. The 1 µm sintered metal plate (Test 2) reduced the ash content further to 0.081% (or a 95.1% reduction), and the 0.5 µm sintered metal plate (Tests 3 and 4) reduced the ash content further to between 0.004 and 0.006% respectively (or a 99.6% reduction).

It was decided to produce the feed for distillation and thermal treatment (3 ℓ) using the 0.5 µm sintered metal plate to achieve the maximum ash reduction. Furthermore, based on the requirement of needle coke specifications (ash content 0.2% maximum), only the filtrate from Tests 3 and 4 would yield a calcined coke with an acceptable ash content (based on an estimated 10% yield from the fresh Waxy Oil feed).

7.2.2.1 Analysis of unfiltered and filtered Waxy Oil[23]

TGA[24] and DTG were conducted on Samples A and B. The results are shown in Figures 7-2 and 7-3 respectively. A detailed discussion of the experimental procedure is given in Chapter 5, Section 5.4.3.

[21] The determination of the ash content to three decimal places for Waxy Oils with high catalyst concentrations is not as accurate as indicated. This procedure is, however, followed to show the comparative ash contents of the filtered Waxy Oil.
[22] Test 4 is a duplicate of Test 3 conducted to establish a level of confidence.
[23] The research for Chapter 7 (Sections 7.2.2.1–7.5) was conducted by the author at the Instituto Nacional del Carbón (INCAR) in Oviedo, Spain under the tutorship of Dr Ricardo Santamaria.
[24] TGA of Waxy Oil is not to be read as a distillation reaction. Although the mass loss in the initial temperature range is a result of distillation, at 400–430 °C (depending on the stability of the molecules) thermal cracking occurs, releasing lighter hydrocarbon distillates and gas. Between 450 and 500 °C carbonisation occurs. Both these reactions involve a chemical change in the molecular composition of the feed.

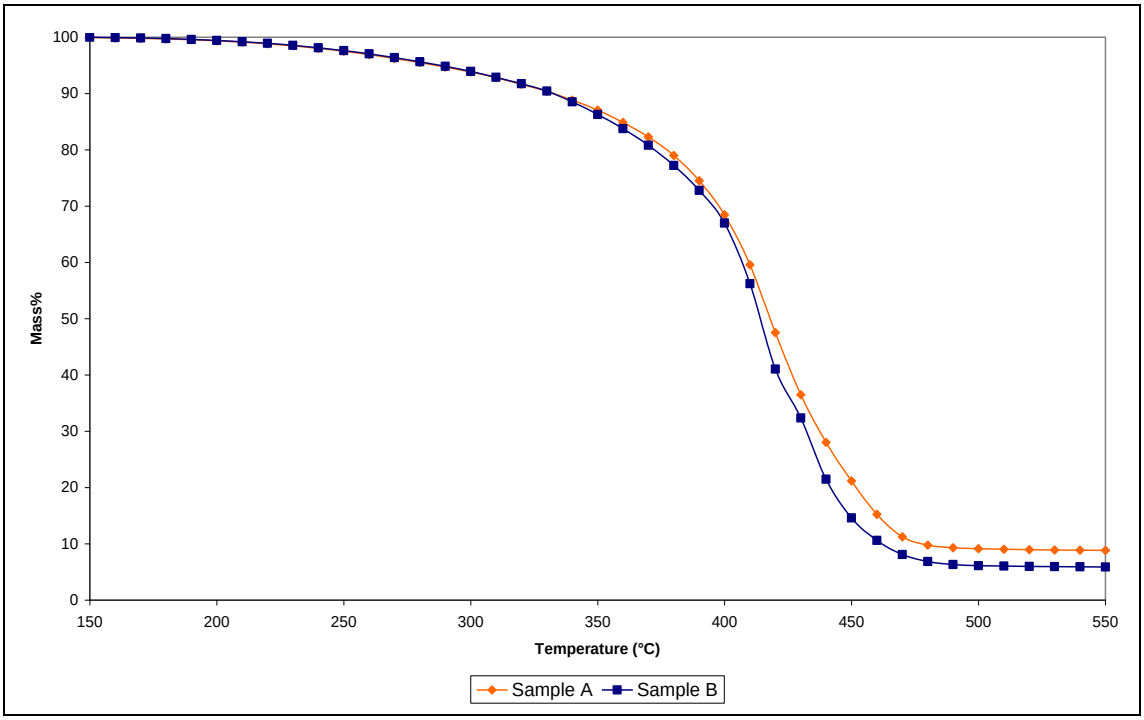

Figure 7-2 Thermogravimetric Analysis (TGA) of Samples A and B

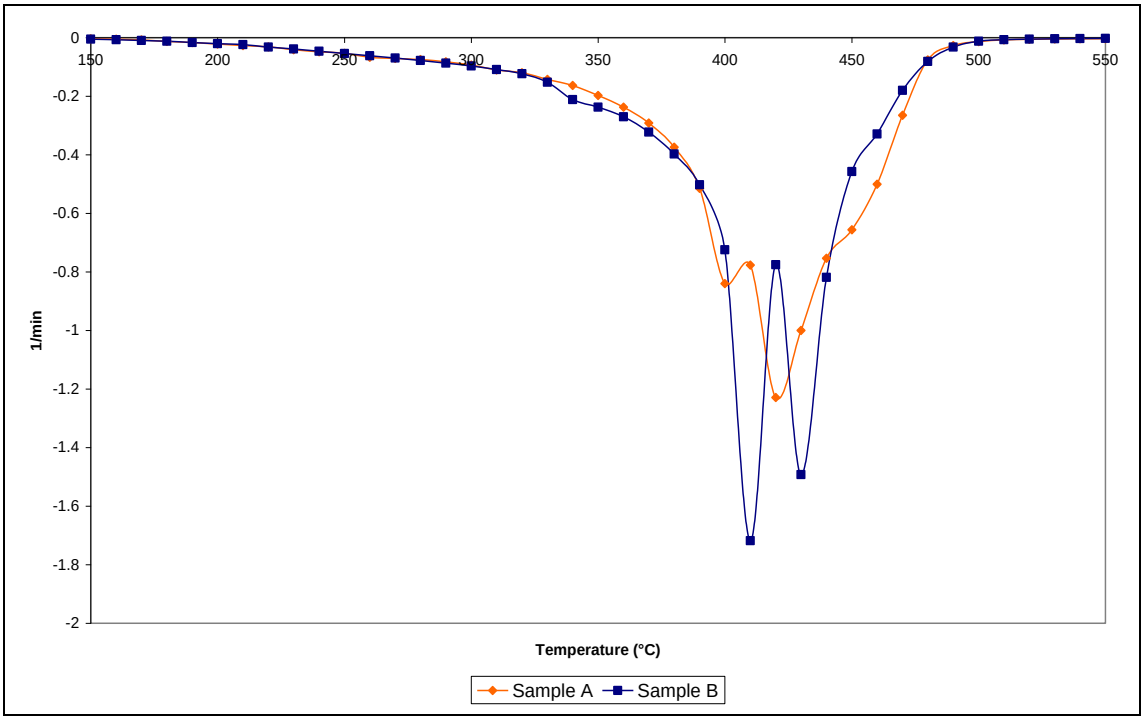

Figure 7-3 Differential Thermogravimetry (DTG) of Samples A and B

The TGA curves of Samples A and B (Figure 7-2) are similar between 200 and 340 °C (which is not unexpected as the only variant is the catalyst content). However, as Waxy Oil is the product of a flash distillation, there is a small percentage of lighter boiling components as witnessed by a 5% mass reduction to 290 °C. The residuum of Sample A (9.34%) is higher than that of Sample B (6.30%), both being determined at 500 °C. The difference between the residua of Sample A and B is ascribed partly to the mass contribution of the catalyst (1.67%).

With regard to the remaining 1.37% differential, this is ascribed to the effect of iron catalysis in promoting oxidative polymerisation and thus increasing the carbon yield, as described by Wang *et al.* (2001).

The DTG (Figure 7-3) of Sample B indicates two peaks at 410 and 430 °C. Given their proximity, they may constitute only one peak. While Waxy Oil and petroleum pitches differ vastly in respect of their composition, a similar DTG behaviour (including one peak which is the product of both endothermic distillation and exothermic cracking reactions) has been previously reported by Perez *et al.* (2002) using petroleum residues. The peak for Sample A at 420 °C is shallower than that for Sample B. The probable reason is that due to the higher ash content of Sample A, there is a smaller percentage of organic residue and thus the intensity of cracking based on the relative mass percentage is lower.

As it was not possible to conduct a GCMS on Sample A (due to the ash content), Sample B was refluxed in toluene (which was used as a solvent for the GCMS). The whole of Sample B was soluble in toluene. The GCMS of filtered Waxy Oil (Sample B) is shown in Figure 7-4 and the procedure explained in greater detail in Chapter 5, Section 5.4.5.

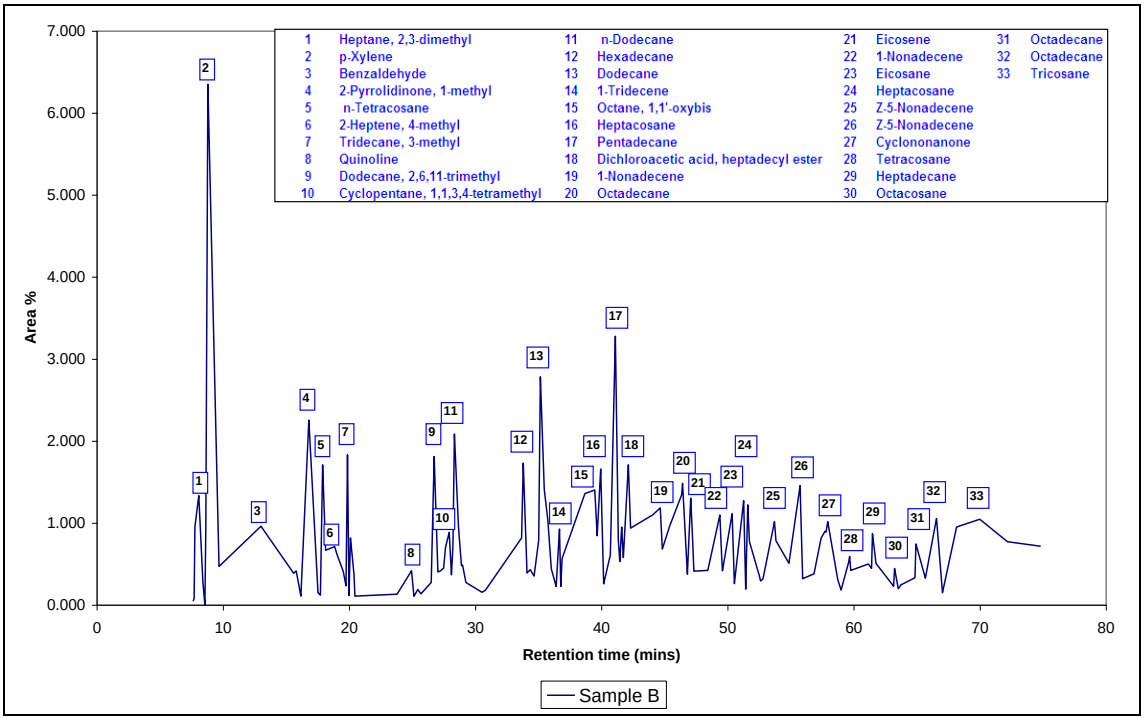

Figure 7-4 Gas Chromatography–Mass Spectroscopy (GCMS) of Sample B

The GCMS trace (Figure 7-4) shows the elution of many hundreds of organic molecules within a retention time of up to 70 min. Molecules identified in the index of the GCMS trace (shown in Figure 7-4) have area percentages of half a per cent or greater. Of particular importance is the variance in the molecular weight of oxygenates. Within the first 20 min only 24% of oxygenates elute and similarly between 20 and 40 min (16%), between 40 and 60 min (52%) and finally above 60 min (8%). The major oxygenate groups in Sample B (total 13.12%) include esters (3.94%), ketones (3.28%), alcohols or phenolics (2.07%) and epoxides (1.32%). Peaks 1 to 10 are composed largely of alkylated aromatics and alkanes. In the latter portion of the trace (Peaks 11 to 33) there is a predominance of normal alkanes ranging from C_{10} to C_{30}.

The composition of molecules eluting within the first 30 min include cyclo-aliphatics and iso-alkanes typically lower than tridecane (C_{13}). While not specifically indicated in the figure, there is a host of alkylated aromatics which present in smaller concentrations eluting within this time period. The higher molecular weight molecules eluting after 30 min comprise mainly normal alkanes and alkenes (C_{10}–C_{30}). The area percentage of normal alkanes (especially in the C_{20}–C_{30} range) is of particular importance to this study. However, in Sample B, although their presence is identifiable, they do not emerge as dominating peaks in the GCMS trace.

The GCMS trace of a single sample of filtered Waxy Oil heavy residue has limited value. However, as discussed later, by overlaying the traces of two samples it is possible to determine general **qualitative** differences in their molecular composition.

In the study of how the composition of heavy residues affects the microstructure of the green coke produced, the concentration of single components is of lesser importance than that of "families" of components into which they may be grouped, specifically in relation to their thermal reactivity (during the onset of carbonisation) and thus their propensity to produce cokes with either mosaic or domain flow microstructures.

The individual components have been classified[25] into "families" or groups of similar composition for Sample B and are shown in Table 7-3.

Table 7-3 Molecular compound groups in Sample B filtrate

Molecules	Unit	Sample B
Alkylated aromatics	**Area %**	9.13
Pure aromatics	**Area %**	0.84
Iso-alkanes	**Area %**	14.10
Normal alkanes	**Area %**	38.18
Oxygenates	**Area %**	13.12
Cyclo-alkanes	**Area %**	2.02

The organic composition of Sample B is dominated by both normal alkanes and alkylated homologues thereof. While there is a comparatively small concentration of pure aromatics, the concentration of alkylated aromatics is comparatively large. However, of particular interest is the concentration of oxygenates, which is not unexpected as oxygen functionalities may be introduced from carbon monoxide during the Fischer-Tropsch reaction with hydrogen.

The change in the concentration of alkylated aromatics, alkylated alkanes and especially oxygenates as a result of Waxy Oil modification is key to controlling the reaction rate during carbonisation as all of the abovementioned groups are known to increase the reaction rate during carbonisation, as previously described by Obara *et al.* (1981) and Sima *et al.* (2003). This promotes the formation of mosaic microstructures which, in the current study, is deemed detrimental. While the removal of reactive molecular components is important, the increase in the concentration of thermally "stable" molecules is of equal interest. The totals of all pure

[25] The classification of molecules into similar groups was conducted in line with the requirements of this study and does not represent all possible classifications. The area percentage contribution of each molecular component was manually calculated from the GCMS data table.

normal alkanes (C_{10}–C_{30}) were manually calculated from the GCMS data table and are shown in Table 7-4.

Table 7-4 Normal alkanes (C_{10}–C_{30}) in Sample B residue

Molecule description	Carbon number	Unit	Sample B
Decane	**C10**	**Area %**	0.00
Undecane	**C11**	**Area %**	0.00
Dodecane	**C12**	**Area %**	7.69
Tridecane	**C13**	**Area %**	2.78
Tetradecane	**C14**	**Area %**	0.76
Pentadecane	**C15**	**Area %**	3.54
Hexadecane	**C16**	**Area %**	2.83
Heptadecane	**C17**	**Area %**	4.14
Octadecane	**C18**	**Area %**	4.64
Nonadecane	**C19**	**Area %**	1.05
Eicosane	**C20**	**Area %**	2.86
Heneicosane	**C21**	**Area %**	1.58
Docosane	**C22**	**Area %**	0.00
Tricosane	**C23**	**Area %**	1.82
Tetracosane	**C24**	**Area %**	0.00
Pentacosane	**C25**	**Area %**	0.38
Hexacosane	**C26**	**Area %**	0.72
Heptacosane	**C27**	**Area %**	2.94
Octacosane	**C28**	**Area %**	0.45
Nonacosane	**C29**	**Area %**	0.00
Contane	**C30**	**Area %**	0.00
TOTAL		**Area %**	**38.18**

As Waxy Oil is the commercial residue product of flash distillation to remove lighter petrol and diesel intermediates, it is not unexpected that Sample B would contain small amounts of typical normal alkanes in the diesel range. However, at a combined concentration of approximately 12%, these alkanes are unexpectedly high. The normal alkanes constitute only a total of 38.18%, being dominated by lighter fractions (26.39%; C_{12}–C_{18}).

With regard to the iso-alkanes and oxygenates identified, it is necessary to determine methods of stabilisation to decrease their potential reactivity during carbonisation. At the same time it is necessary to identify and maximise molecules with a higher thermal stability that promote the formation of the anisotropic flow patterns previously discussed in Chapter 6. The concentration of heavier normal alkanes (typically from eicosane [C_{20}] to contane [C_{30}]) may present the best option for aromatisation and the subsequent formation of flow domains during carbonisation.

The influence of highly aliphatic residues, e.g. petroleum vacuum residues, on the quality of coke (and thus the necessity for stabilisation) was argued previously by Marsh *et al.* (1999) who linked the reactivity of these residues to a premature increase in the matrix viscosity, smaller optical textures and the resultant increase in the CTE. However, reactivity is not linked solely to the aliphatic nature of feeds, as shown by Calemma & Rausa (1997) who studied highly aromatic asphaltene feeds.

7.2.3 Waxy Oil filtration and distillation

Filtration of Waxy Oil is a necessity in connection with the ash content requirement of needle coke. Sample B is thus considered the base product against which all other modifications of the organic composition of Waxy Oil are compared. In terms of potential pre-carbonisation costs (not including filtration), distillation to produce a heavier Waxy Oil would be the most viable and least capital-intensive method of modification on a commercial scale as the distillation temperature of the existing column could merely be increased. The efficacy of distillation would rely on the molecules that serve to increase the reactivity of the Waxy Oil being concentrated within the lower molecular weight fractions and thus reporting to the distillate.

The distillation of Waxy Oil was conducted in the laboratory using approximately 250 g of filtered Waxy Oil (Sample B) at the maximum vacuum pressure achievable of -0.9 kPa. Waxy Oil was distilled to residue temperatures of 340 °C (Sample C2) and 380 °C (Sample C1) respectively. A detailed description of the distillation procedure is provided in Chapter 5, Section 5.2.2.

The residue and distillate yields of the vacuum distillations are shown in Table 7-5.

Table 7-5 Waxy Oil residue and distillate yields from vacuum distillation of Sample B

Experiment No.	Sample	Residue temperature (°C)	Vacuum (kPa)	Residue (%)	Distillate (%)
C1	**Filtered Waxy Oil**	**380**	**-0.9**	87.0	13.0
C2	**Filtered Waxy Oil**	**340**	**-0.9**	94.3	5.7

The distillation of Waxy Oil proved problematic as the maximum vacuum achievable (-0.9 kPa) provided only a small amount of distillate before the residue started cracking at approximately 350 °C. Sample C1 is thus not a “true distillation” but rather a mild thermal treatment reaction. Mild thermal cracking serves to increase the distillate[26] yield (compared with Sample C2 distillate) due to the production of lighter cracked molecules. However, the Waxy Oil residue produced from the distillation reaction of Waxy Oil at 380 °C is not insignificant, with specific reference to the amount of oxygenates left in the residue, shown in Table 7-6 and discussed later in this section. Much of the wax distillate of Sample C2 solidified in the condenser, causing blockages as shown in Figure 7-5.

[26] The distillate yield is calculated as 100% minus the residue yield. The distillate is the product of both lighter liquid hydrocarbons and hydrocarbon gases. The GCMS analysis on the distillate pertains only to the liquid distillate. The same holds true for all distillates produced by Waxy Oil modifications discussed in this chapter.

Figure 7-5 Photo of solidified wax distillate in the condenser

TGA and DTG were conducted on Samples C1 and C2 and compared with Sample B as shown in Figures 7-6 and 7-7 respectively.

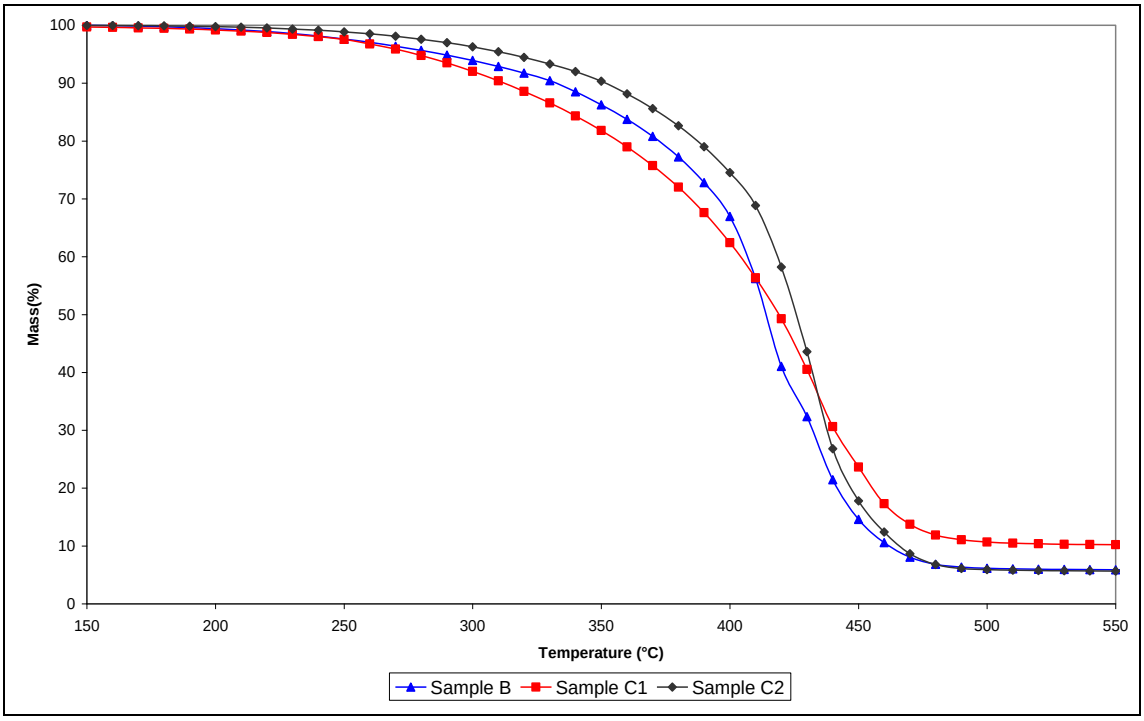

Figure 7-6 Thermogravimetric Analysis (TGA) of Samples B, C1 and C2 residues

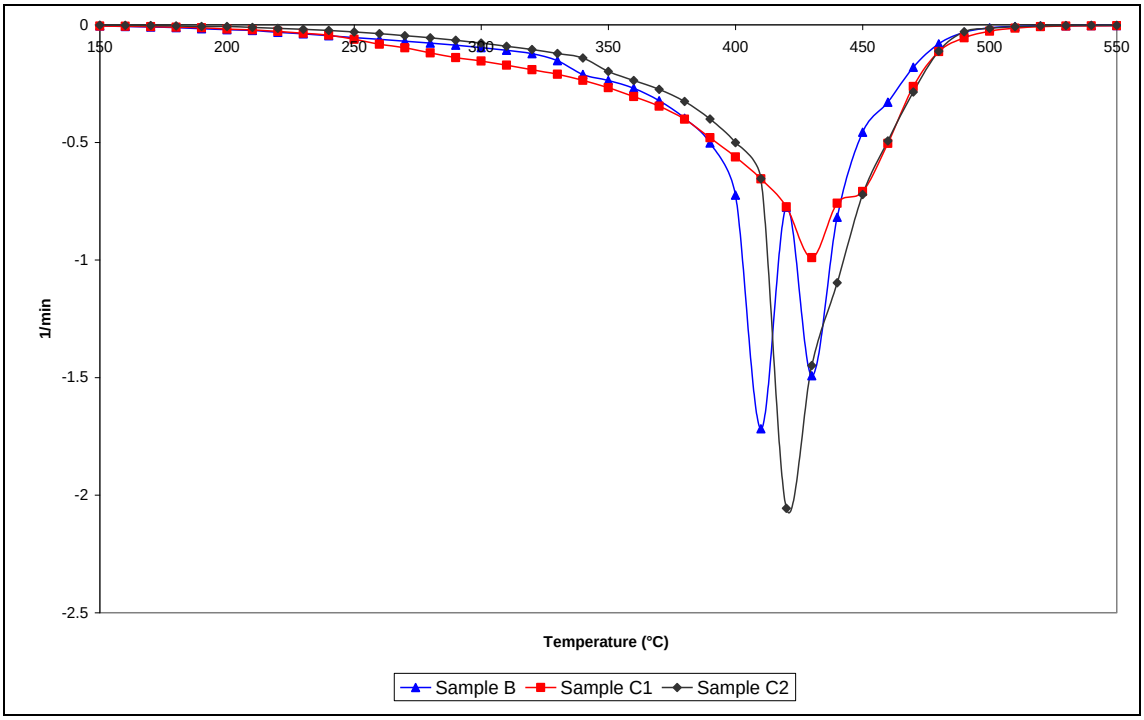

Figure 7-7 Differential Thermogravimetry (DTG) of Samples B, C1 and C2 residues

Both Samples C1 and C2 show an initial mass loss at approximately 200 °C (Figure 7-6). However, compared with Sample B, Sample C2 distillation removes lower molecular weight molecules above 250 °C, as indicated by the slightly steeper mass loss curve of Sample B within this temperature range. However, the opposite is true for Sample C1: the initial mass loss curve is steeper than that of Sample B, indicating that the planned "distillation" turned into a mild thermal treatment producing a small increase in the concentration of lower molecular weight hydrocarbons. Thus, even though the mass loss curve of Sample C1 is steeper than that of the other samples within the lower temperature range, the residuum of Sample C1 (10.68%) is greater than that of Sample C2 (5.90%).

In the corresponding DTG (Figure 7-7), Sample C2 exhibits a single peak of maximum mass loss rate at 420 °C (similar to Sample B). The first peak for Sample C1 is associated with mass loss of lighter cracked hydrocarbons below 350 °C; given the even distribution, a definable peak is not visible. The second is a more intense peak at 430 °C. The second peak (for Sample C1) is less intense than the singlet peak corresponding to Sample C2 due to the higher dilution factor of Sample C1. It also occurs at a slightly higher temperature (430 °C) compared with the second peak of Sample C2 at 420 °C.

Distillation to pre-cracking temperatures (below 350 °C) is a physical reaction, removing molecules without chemical reaction. However, the mild thermal treatment producing Sample C1 involves a small degree of molecular breakdown. The second mass rate peak (for Sample C1) is of great interest and is described throughout the course of this chapter for all the modifications. In general, the intensity of the carbonisation peak is inversely comparable to the amount of lighter cracked hydrocarbons remaining in the residue (i.e. the first peak). The temperature of the second peak in the cracking region (approximately 420–460°C) is dependent on the concentration of higher molecular weight, thermally stable normal alkanes.

Comparing the GCMS traces of Sample B with those of Samples C1 and C2 is useful for determining the effect of distillation on the general molecular composition. However, as the GCMS traces are complex, comparing more than two samples in the same figure may prove confusing. Thus the GCMS of Sample B and Sample C2 residues are initially compared as shown in Figure 7-8.

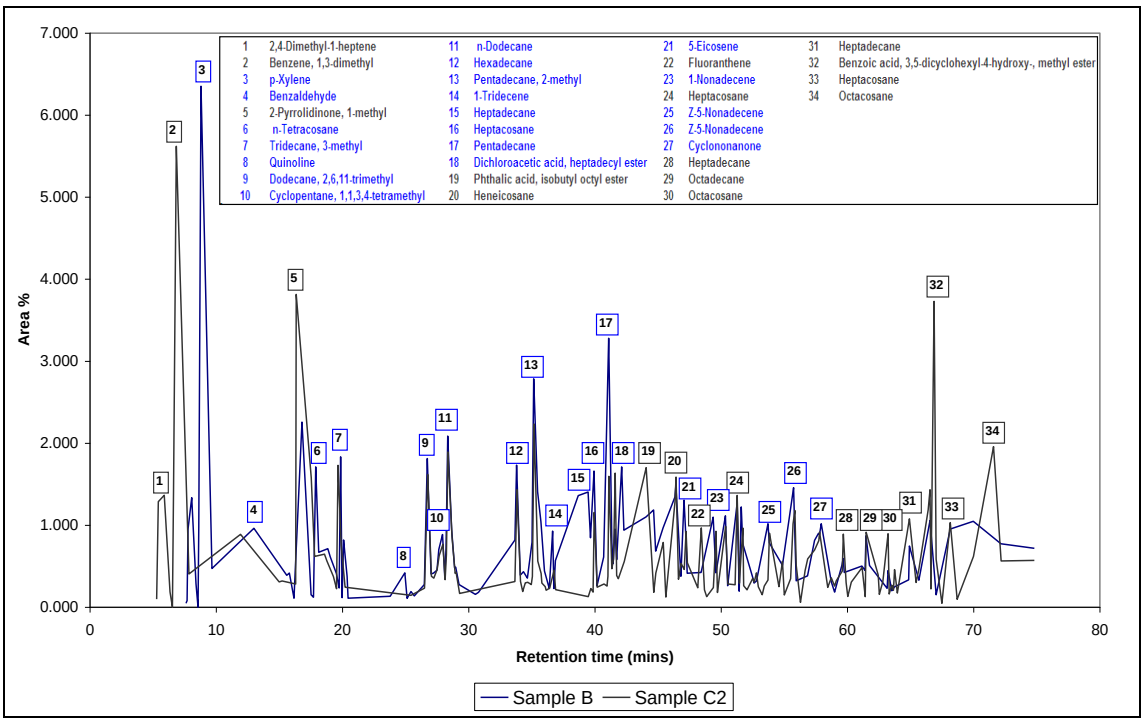

Figure 7-8 Gas Chromatography–Mass Spectroscopy (GCMS) of Samples B and C2 residues[27]

As the residue yield of Sample C2 is 94.3%, it stands to reason that a qualitative GCMS comparison of the trace (with Sample B) would be similar. As shown in Figure 7-8, the distillate component of Sample C2 indicates the removal of a small concentration (approximately 1%) of alkanes from C_{10} to C_{28}. It should be noted that the distillation (below cracking temperatures) to produce Sample C2 involves no chemical modification of Waxy Oil molecules.

The GCMS of Sample B and Sample C1 residues are compared in Figure 7-9.

[27] The GCMS traces of the two samples have been overlaid for comparative purposes and each sample is represented by a different colour as previously mentioned. The numbers identifying the peaks are related to the individual molecules in the index. Both the peak numbers and their corresponding descriptions in the index are colour coded in terms of the sample they represent. When the peaks of the two samples overlap, the peak is colour coded according to the sample with the largest comparative area percentage for that specific molecule.

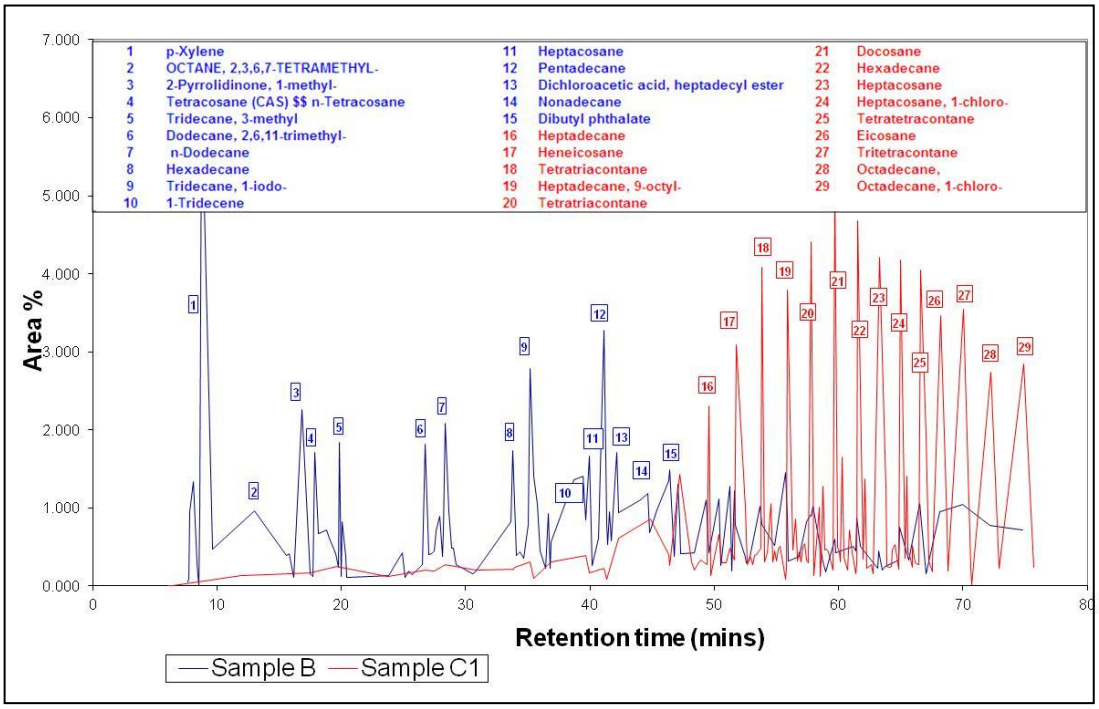

Figure 7-9 Gas Chromatography–Mass Spectroscopy (GCMS) of Samples B and C1 residues

There is a substantial difference in the GCMS traces of Samples B and C1. Compared with Sample B, the trace of Sample C1 shows substantial depletion of lighter hydrocarbons below a retention time of 40 min (peaks 1–15). The lower concentration of molecules within this area of the trace indicates the propensity of thermally unstable molecules to pyrolyse, forming lower molecular weight organics which distil below a temperature of 380 °C. This may include the distillation of a small amount of pure aliphatics. However, in comparison with Sample B, there is evidence of an increase in the area percentage of heavier molecular weight normal alkanes after a retention time of 50 min (peaks 16–29) in the C_{17} to C_{28} range. This range of pure normal alkanes increases from less than 1% (Sample B) to between 2 and 5% in Sample C1. The increase is due mainly to a reduction of the dilution factor (i.e. the removal of lighter hydrocarbons at lower retention times) and bears further witness to the relative stability of this group of heavier normal alkanes.

As Sample B does not have a distillate fraction, it is only possible to compare the GCMS traces of the distillates from Samples C1 and C2 shown in Figure 7-10.

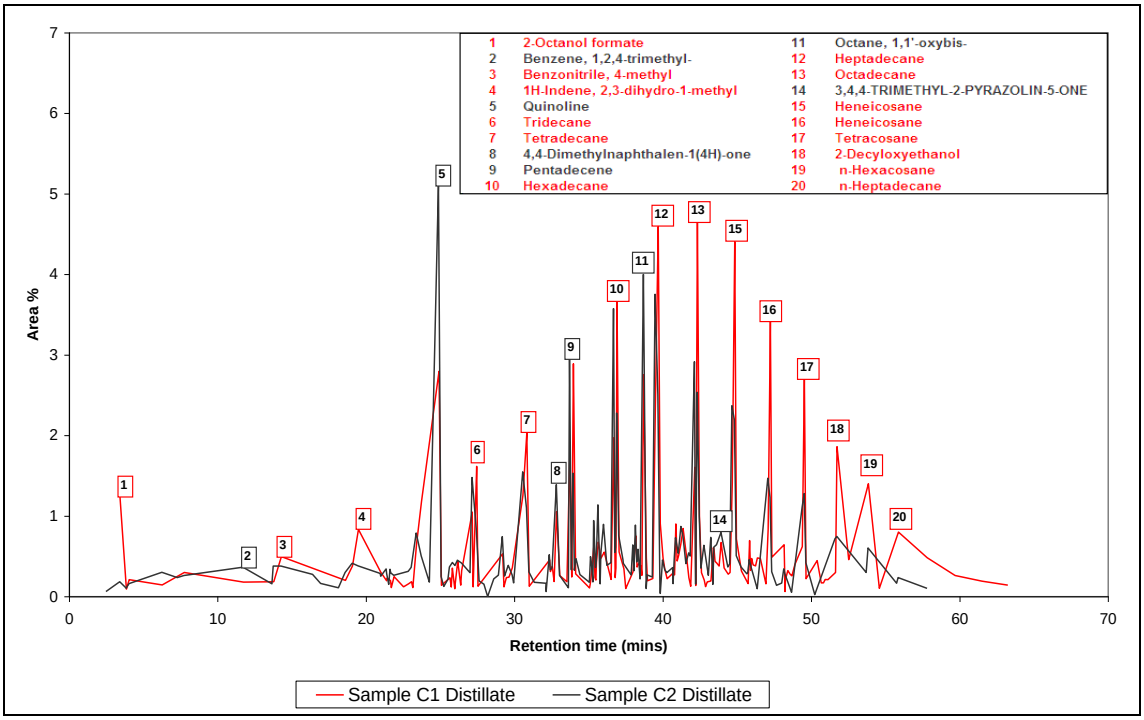

Figure 7-10 Gas Chromatography–Mass Spectroscopy (GCMS) of Samples C1 and C2 distillates

Within the first 20 min the distillate of Sample C1 appears to contain a similar, if not slightly higher, concentration of lighter components than the distillate of Sample C2. This may be due to the distillation of lighter cracked hydrocarbons. However, the major peaks identified do not indicate a complete dealkylation reaction. Given the higher reaction temperature, it is not unexpected that the Sample C1 distillate would contain a greater proportion of heavier aliphatics (peaks 12–20).

The Sample C1 reaction produces a heavier Waxy Oil residue, thus increasing the concentration of higher molecular weight components (especially normal alkanes from C_{17} and higher) under mild thermal cracking conditions. However, what a comparison of the GCMS trace is incapable of determining is the quantitative variation in groups of similar molecules. For this reason the individual components have been classified into "families" or groups of similar composition for Samples C1 and C2 and are shown in Table 7-6.

Table 7-6 Molecular compound groups in Samples C1 and C2 residues

Molecules	Unit	Sample C1	Sample C2
Alkylated aromatics	**Area %**	1.00	7.18
Pure aromatics	**Area %**	0.00	6.31
Iso-alkanes	**Area %**	5.33	14.10
Normal alkanes	**Area %**	46.39	30.12
Oxygenates	**Area %**	10.34	11.05
Cyclo-alkanes	**Area %**	0.00	0.30

Sample C2 shows a greater area percentage of both pure and alkylated aromatics in comparison with Sample C1. A greater amount of alkylated aromatics may have been dealkylated and the aromatics produced removed in the distillate of Sample C1. The same

holds true to a lesser degree when comparing the relative concentrations of alkylated alkanes. This results in a reciprocal increase in the concentration of normal alkanes in Sample C1.

Although Sample C1 was initially considered a "mistake" in terms of the original planned distillation, it is included in the discussion as it holds a wealth of information. Mild cracking (at 380 °C) has a substantial effect on the aliphatic to aromatic ratio, but there is only a slight decrease in the concentration of oxygenates. Very much the same holds true for Sample C2. Thus in terms of stabilising the Waxy Oil, both distillations were unsuccessful in reducing the oxygenate concentration substantially.

The major oxygenate groups present in Sample C2 (total 11.05%) include alcohols/phenolics (5.31%), carboxylic acids (3.52%) and ethers (0.49%). The major oxygenate groups present in Sample C1 (10.34%) include carboxylic acids (5.37%), alcohols/phenolics (1.33%) and phthalates (0.49%).

In order to study the nature of the oxygenate molecules in Sample C1 in greater detail they have been listed (along with their retention times and area percentages) in Table 7-7.

Table 7-7 Oxygenate molecules in Sample C1 residue

Molecules	Retention time (min)	Area (%)
Benzaldehyde	11.93	0.129
2-Butyn-1-OL, 4-Methoxy-	17.45	0.168
2-Butyn-1-OL, 4-Methoxy	19.60	0.244
3,3-Bis(methoxymethyl)oxacyclobutane	27.45	0.188
Phthalic acid, monoamide, N-ethyl-N-(3-methylphenyl),-undecyl ester	46.35	0.406
Hexyl octyl ether	48.41	0.196
2-Pentadecanol	49.39	0.274
Hexyl octyl ether	50.66	0.296
1-Octanol, 2-butyl	52.95	0.365
7-Hydroxy-3-(1,1-dimethylprop-2-enyl)coumarin	53.41	0.398
1-Eicosanol	54.24	0.419
1-Hentetracontanol	56.29	0.460
Ethanol, 2-(dodecyloxy)	57.10	0.495
(meso)-3,4-dihydroxymethyl-3,4-dimethylhexane	57.41	0.329
Ethanol, 2-(dodecyloxy)	58.47	1.005
Ethanol, 2-(dodecyloxy)	58.57	0.342
Ethanol, 2-(dodecyloxy)	59.00	0.468
9,10-Secochola-5,7,10(19)-triene-3,24-diol	59.54	0.204
Nonahexacontanoic acid	60.44	0.370
Nonahexacontanoic acid	60.75	0.198
Nonahexacontanoic acid	60.83	0.721
7-Hydroxy-3-(1,1-dimethylprop-2-enyl)coumarin	61.36	0.157
1a,9b-dihydro-4-methyl-1H-phenanthro[9,10-b]azirine	66.42	0.268
Nonahexacontanoic acid	67.06	1.920
Nonahexacontanoic acid	67.56	0.316

The bulk of oxygenates (93%) elute after 46 min. Thus even though mild cracking (380 °C) and distillation may increase the coking residue (as established in Figure 7-6), these

experimental conditions do not serve to stabilise the residue in terms of substantially reducing the oxygenate content. As previously mentioned, oxygenates are distributed throughout the molecular weight range of Waxy Oil. Thus even if the vacuum pressure were to be increased (to reduce cracking), the residue would still contain substantial amounts of oxygenates, which is contrary to the aim of this set of experiments. This is seemingly in contradiction to the findings of Perez *et al.* (2002) who determined that the bulk of oxygenates identified within petroleum residues were concentrated in the lower molecular weight molecules. However, given the difference in the origins of the two feeds, it is not entirely unexpected. Another factor to consider is that temperatures greater than 380 °C would need to be employed to destroy the concentration of oxygenates. This presents a challenge as not only are oxygenate molecules eluted at higher retention times, but also they do not appear to have been reduced to any substantial degree by mild cracking and distillation at 380 °C. Quite apart from the quality of the residues, the quality of the distillates is core to the production of petrol and diesel intermediates for the refinery. If distillation were able to increase the concentration of higher molecular weight molecules in the distillate, this may induce challenges in keeping the diesel intermediate fractionation cut within specification.

The concentrations of normal alkanes in Samples C1 and C2 are shown in Table 7-8.

Table 7-8 Normal alkanes (C_{10}-C_{30}) in Sample C1 and C2 residues

Molecule description	Carbon number	Unit	Sample C2	Sample C1
Decane	**C10**	**Area %**	0.00	1.73
Undecane	**C11**	**Area %**	0.00	0.00
Dodecane	**C12**	**Area %**	0.00	2.94
Tridecane	**C13**	**Area %**	0.00	0.00
Tetradecane	**C14**	**Area %**	0.21	3.21
Pentadecane	**C15**	**Area %**	0.27	2.77
Hexadecane	**C16**	**Area %**	6.32	1.42
Heptadecane	**C17**	**Area %**	4.84	3.46
Octadecane	**C18**	**Area %**	0.00	4.01
Nonadecane	**C19**	**Area %**	0.22	0.77
Eicosane	**C20**	**Area %**	4.15	6.43
Heneicosane	**C21**	**Area %**	4.64	6.37
Docosane	**C22**	**Area %**	5.26	3.36
Tricosane	**C23**	**Area %**	0.00	0.13
Tetracosane	**C24**	**Area %**	0.00	0.30
Pentacosane	**C25**	**Area %**	0.00	1.86
Hexacosane	**C26**	**Area %**	0.00	0.51
Heptacosane	**C27**	**Area %**	4.21	2.93
Octacosane	**C28**	**Area %**	0.00	3.93
Nonacosane	**C29**	**Area %**	0.00	0.00
Contane	**C30**	**Area %**	0.00	0.26
TOTAL		**Area %**	**30.12**	**46.39**

Apart from the obvious increase in the area percentage of normal alkanes in Sample C1 compared with Sample C2, for reasons discussed earlier (with the exception of heptacosane), the bulk of Sample C2 normal alkanes appear to be concentrated in the C_{16} to C_{22} range. In contrast, Sample C1 normal alkanes appear over a greater carbon number distribution, if not slightly higher as well.

7.2.4 Waxy Oil filtration and thermal treatment

Filtered Waxy Oil was thermally treated in a Pyrex glass test tube inside a reactor connected to a smaller vessel to collect distillates. A complete description of the experimental procedure is given in Chapter 5, Section 5.2.3. The aim of thermally treating Waxy Oil is:

- Cracking Waxy Oil to produce both stable heavier alkanes and lighter hydrocarbon distillates
- Destruction of reactive hydrocarbons, especially iso-alkanes organics and oxygenates at pre-carbonisation temperatures (400–430 °C), thus reducing the propensity of the residue to produce mosaic microstructural domains during the onset of carbonisation
- Increasing the green coke yield
- Decreasing the temperature range over which carbonisation occurs, which means increasing the temperature of initial poly-condensation reactions

7.2.4.1 Waxy Oil thermal treatment at 5 bar pressure

Waxy Oil (approximately 50 g) was thermally treated for 2 h in a Pyrex glass test tube at temperatures of 400, 410, 420 and 430 °C.

The yields of the thermal treatment experiments at 5 bar pressure are shown in Table 7-9.

Table 7-9 Waxy Oil residue and distillate yields from thermal treatment reactions at 5 bar pressure

Experiment number	Temperature (°C)	Time [1] (h)	Pressure (bar)	Residue (%)	Distillate (%)	Distillation coefficient (%)
D1	**400**	**2**	**5**	73.1	26.9	87.0
D3	**410**	**2**	**5**	58.7	41.3	62.2
D4	**420**	**2**	**5**	45.2	54.8	57.1

[1] Duration of thermal treatment at maximum heat treatment temperature

A notable exclusion from the experimental data in Table 7-9 is the reaction conducted at 430 °C (Sample D2). At this temperature small amounts of mosaic semi-coke (secondary QI) were observed in the modified Waxy Oil residue. The sample was discarded and no analyses were conducted. The philosophy of this chapter is the production of modified residues with no QI. From an experimental viewpoint the production of mosaic QI from highly reactive species followed by filtration is possible, as described by Calemma and Rausa (1997) who studied residues with high concentrations of asphaltenes. However, it is the author's opinion that such a process would have very limited potential for commercial application.

A temperature increase from 400 to 420 °C during thermal treatment serves to decrease the residue yield. Due to the production of a greater concentration of lighter hydrocarbons, the distillate yield is similarly increased. The "distillation coefficient" (referred to in Table 7-9) is defined as the percentage of lighter hydrocarbons produced by cracking reactions yet remaining in the residue below a temperature of 320 °C and corresponding to the maximum mass loss rate in Sample D4 (prepared under the most severe thermal conditions). The efficiency with which lighter cracked hydrocarbons are removed from the residue is reduced

as the soaking temperature increases from 400 ^{o}C (87%) in Sample D1 to 420 °C (57.1%) in Sample D4.

With regard to the thermal treatment experiments at 5 bar pressure, two variables need to be discussed. The first variable is the residue yield and the second variable is the concentration of lighter hydrocarbons that remain in the residue. To demonstrate this, the TGA and DTG of Samples D1, D3 and D4 are shown in Figures 7-11 and 7-12 respectively. Sample B is included as a comparison.

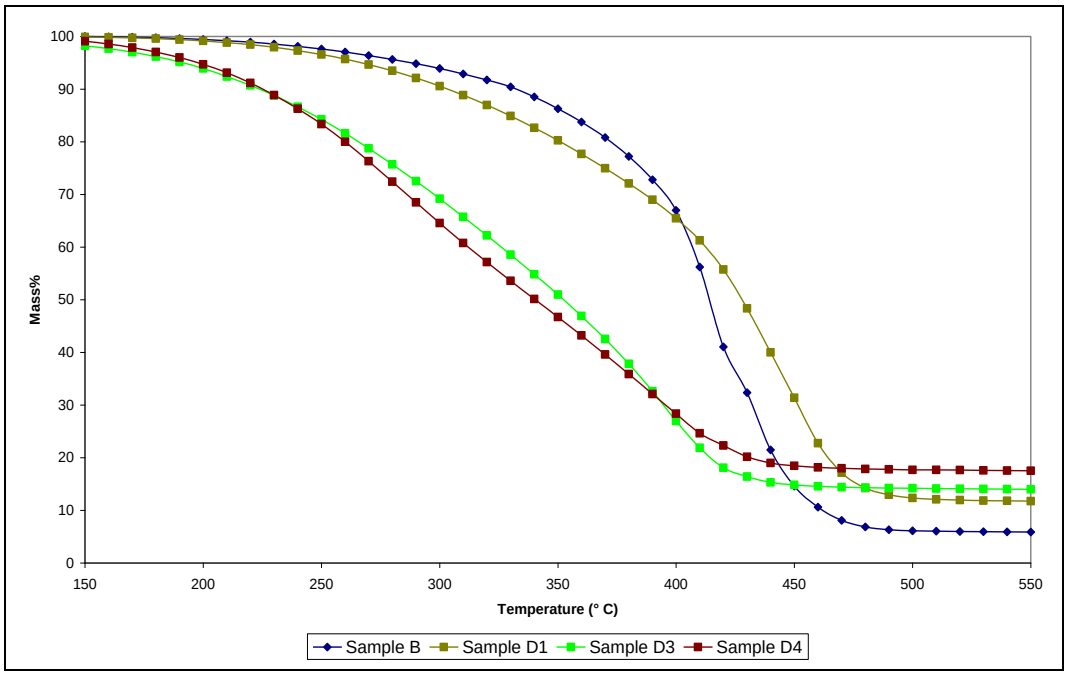

Figure 7-11 Thermogravimetric Analysis (TGA) of Samples B, D1, D3 and D4 residues

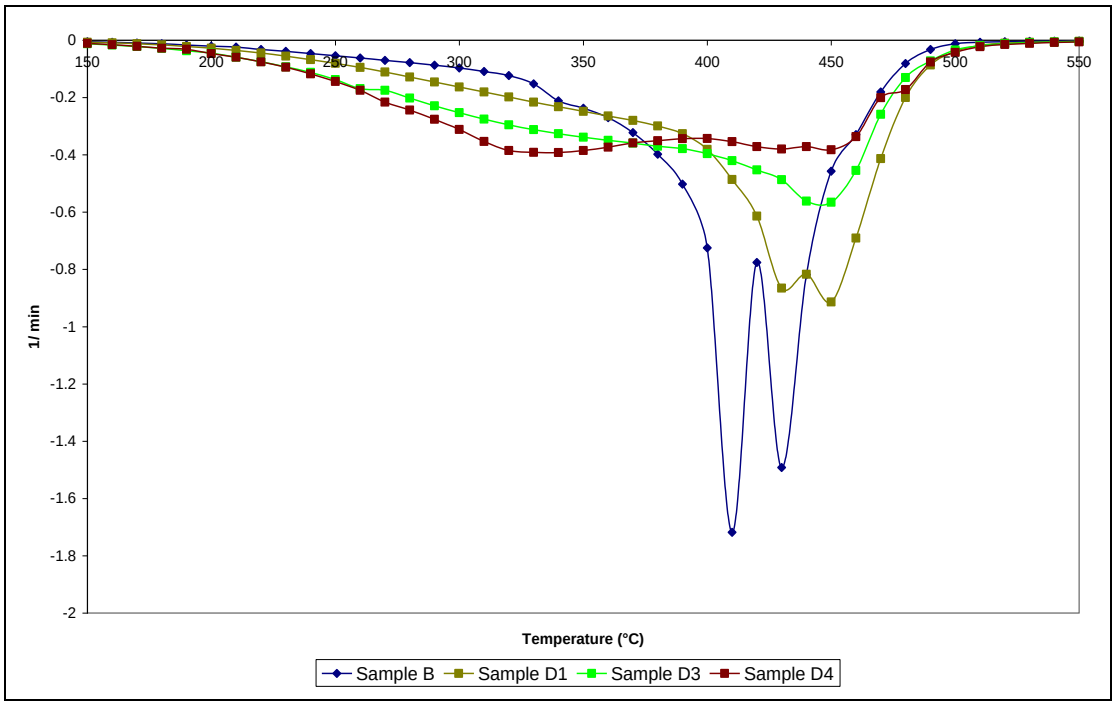

Figure 7-12 Differential Thermogravimetry (DTG) of Samples B, D1, D3 and D4 residues

Increasing the thermal severity of cracking reactions increases the percentage of lighter hydrocarbons produced, thus indicating a steeper distillation gradient of the traces in the lower temperature range of the TGA (Figure 7-11) from Samples D1 to D4. Samples D4 and D3 exhibit initial mass loss at 110 and 130 °C respectively, while Sample D1 exhibits initial mass loss at approximately 200 °C. The increase in mass loss between 200 and 400 °C with thermal severity has quite the opposite effect on the residuum percentages of Sample D1 (12.35%), Sample D3 (14.18%) and Sample D4 (17.70%).

Thermal treatment under pressure increases the percentage of both the lighter hydrocarbons, which cannot escape, and the heavier thermally stable hydrocarbons. The DTG (Figure 7-12) of the three samples is therefore characterised by increased rates of mass loss below 320 °C and two more intense peaks, corresponding to carbonisation reactions, between 440 and 450 °C. As the thermal severity of cracking increases, so the intensity of the first peak increases and that of the second peak diminishes. This is in general agreement with the findings of Perez *et al.* (2002) who observed a similar relationship between the first and second reaction peaks when studying thermal cracking of petroleum pitches. As the mass of lighter hydrocarbons increases (from Samples D1 to D4), Sample D4 produces a shallow broad peak at 320 °C. Given the increased thermal stability of the heavier molecules, it is not surprising that the second peaks are at a higher temperature corresponding to greater thermal severity (Sample B – 420 °C; Sample D1 – 430 °C; Sample D3 – 440 °C; Sample D4 – 450 °C). An increase in thermal treatment severity (Samples D1 to D4) also decreases the intensity of the second series of peaks. This loss of intensity of the second peak is due to higher dilution effects caused by the first peak, especially in Sample D4 in which the intensity of the first and second peaks is similar.

The GCMS of Sample D1 residue is initially compared with Sample B residue in Figure 7-13 and Sample D3 residue with that of Sample D4 in Figure 7-14.

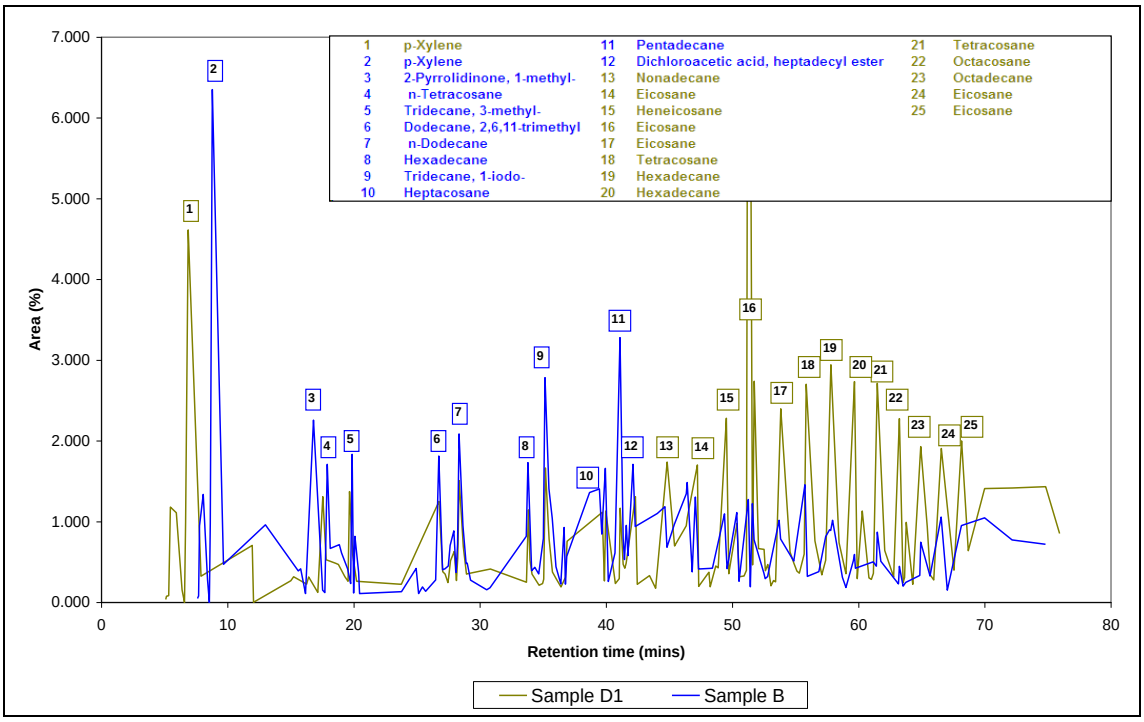

Figure 7-13 Gas Chromatography–Mass Spectroscopy (GCMS) of Samples D1and B residues

The major distinction of Sample D1 (compared with Sample B) is the emergence of a dominant "crest" pattern of stable normal alkanes, ranging from nonadecane (C_{19}) to octacosane (C_{28}) between peaks 13–25. As previously mentioned, these normal alkanes do not necessarily elute at exactly the same retention time, so it is not unexpected to see two peaks of the same normal alkane (e.g. eicosane, hexadecane and octacosane) at different retention times. This is the reason that the comparison of the GCMS traces is merely qualitative and does not have an exact quantitative value. Although in the first 40 min Sample B shows peaks with a comparatively higher area percentage, there is evidence of the lighter molecules in Sample D1; these are present due to the lower distillation coefficient.

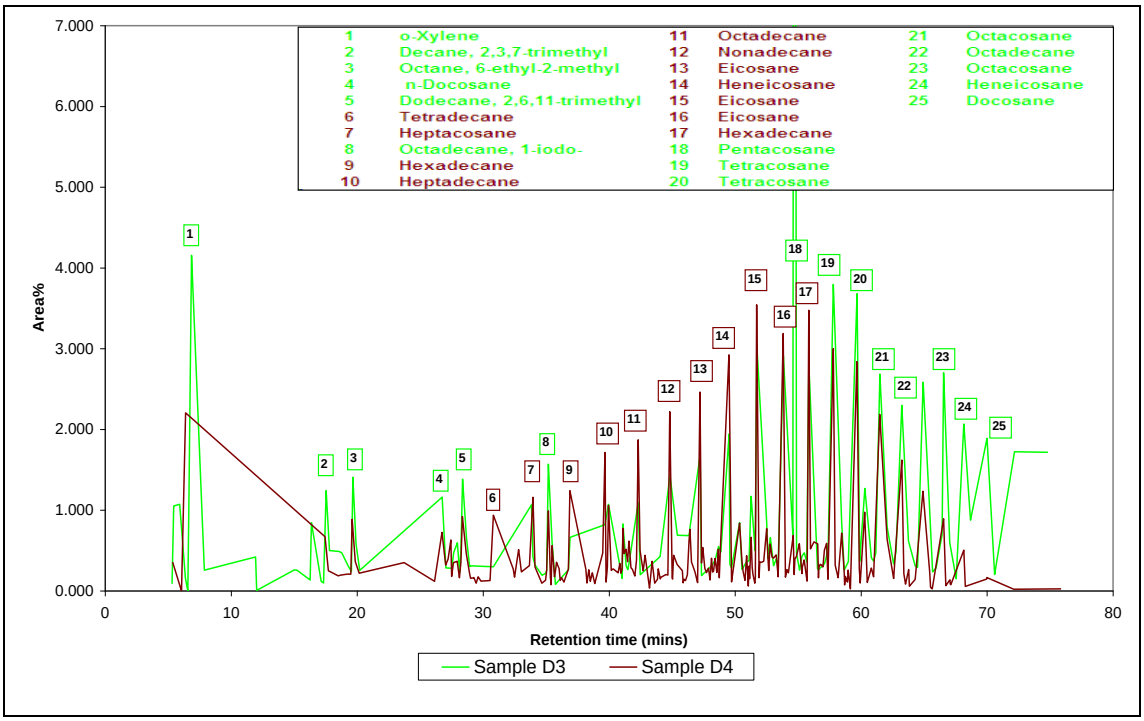

Figure 7-14 Gas Chromatography–Mass Spectroscopy (GCMS) of Samples D3 and D4 residues

When the GCMS traces of Samples D3 and D4 are compared, once again a dominant "crest" of normal alkanes is evident between 40 and 70 min (peaks 10–25). Surprisingly, Sample D3 indicates a higher area percentage of normal alkanes between 60 and 70 min, which is not consistent with an increase in thermal severity under ideal distillation conditions. The reason for this is the higher area percentage of lighter molecules within the initial retention time range (Sample D4), indicating a higher dilution factor in the lower temperature range.

In order to compare the GCMS traces of the distillates from Samples D1 and D3, they are plotted against one another in Figure 7-15. Similarly, the distillates from Samples D3 and D4 are compared in Figure 7-16.

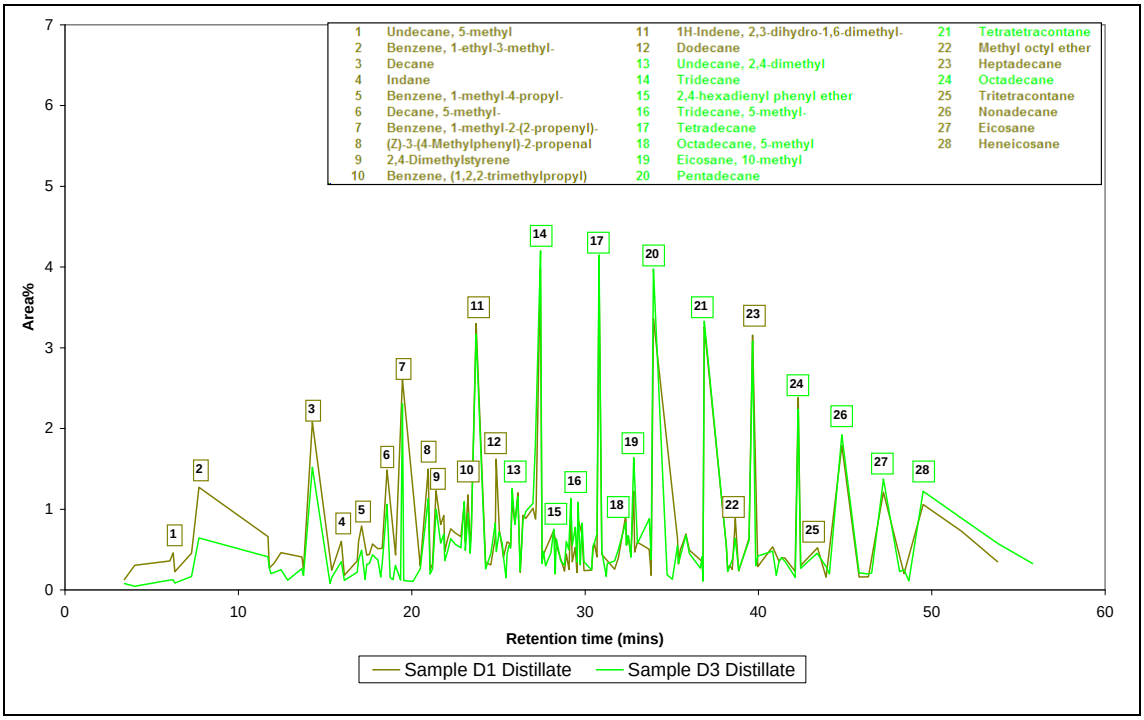

Figure 7-15 Gas Chromatography–Mass Spectroscopy (GCMS) of Samples D1 and D3 distillates

The GCMS traces of Sample D1 and D3 distillates appear similar. However, the elution of lighter molecules from Sample D1 appears to be more prominent in the first 20 min (peaks 1–7). Between 25 to 40 min, heavier molecules within Sample D3 distillate appear to have the greater area percentage, which is not unexpected given the higher reaction temperature.

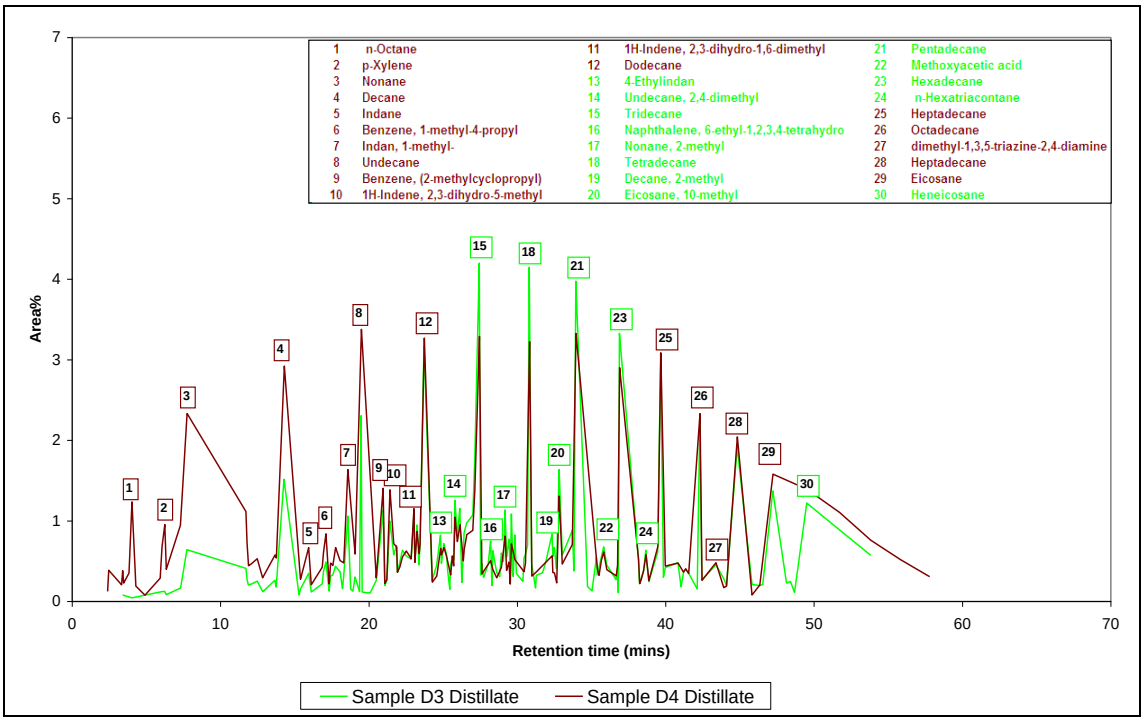

Figure 7-16 Gas Chromatography–Mass Spectroscopy (GCMS) of Samples D3 and D4 distillates

A comparison of the distillates of Samples D3 and D4 shows that Sample D4 distillate is composed of a greater percentage of lighter molecules which elute in the first 20 min (peaks 1–8). The distillate of Sample D4 (within the first 20 min) also shows the presence of pure lower normal alkanes (e.g. octane, nonane and decane) and alkylated homologues of benzene which are more than likely the stabilised products of the cracking reaction. The TGA (Figure 7–12) is proof of the lower distillation coefficient of lighter hydrocarbons, especially from Sample D4 residue. Under ideal distillation conditions the area percentage of molecules eluting in the initial retention time of 20 min would be higher than shown above.

As previously indicated, it is easier to determine the variation in the molecular composition of the thermal treatment residues when similar compounds are grouped, as shown in Table 7-10.

Table 7-10 Molecular compound groups in Sample D1, D3 and D4 residues

Molecules	Unit	Sample D1	Sample D3	Sample D4
Alkylated aromatics	**Area %**	5.37	5.42	6.18
Pure aromatics	**Area %**	0.00	0.71	0.57
Iso-alkanes	**Area %**	13.54	15.14	11.16
Normal alkanes	**Area %**	66.85	63.27	58.68
Oxygenates	**Area %**	1.71	1.57	2.85
Cyclo-alkanes	**Area %**	2.54	0.46	1.52

The percentage of normal alkanes produced decreases from Sample D1 to D4. Although this trend may initially appear to contradict the effect of thermal severity on the area percentage of higher molecular weight normal alkanes, this is not correct. The trend indicated is due to an increased percentage of lighter cracked hydrocarbons which form as the temperature increases. However, at 5 bar pressure the lighter hydrocarbons do not escape the residue, which in turn serves to dilute the area percentage of heavier normal alkanes.

Apart from the somewhat unexpected trend described above, one of the most important results is the reduction of the oxygenate concentration (1.71–2.85%) in the three thermally treatment residues (compared with Samples B: 13.12%; C1: 10.34%; and C2: 11.05%).

The concentrations of normal alkanes (C_{10}–C_{30}) in Sample D1, D3 and D4 residues are shown in Table 7-11.

Table 7-11 Normal alkanes (C_{10}–C_{30}) in Samples D1, D3 and D4 residue

Molecule description	Carbon number	Unit	Sample D1	Sample D3	Sample D4
Decane	**C10**	**Area %**	0.00	0.00	0.00
Undecane	**C11**	**Area %**	0.00	0.10	0.21
Dodecane	**C12**	**Area %**	4.32	1.96	1.94
Tridecane	**C13**	**Area %**	0.25	0.00	0.63
Tetradecane	**C14**	**Area %**	0.79	1.46	1.32
Pentadecane	**C15**	**Area %**	2.16	0.42	1.57
Hexadecane	**C16**	**Area %**	9.00	5.16	8.42
Heptadecane	**C17**	**Area %**	4.84	2.17	5.99
Octadecane	**C18**	**Area %**	4.27	7.09	5.18
Nonadecane	**C19**	**Area %**	3.61	3.78	6.92
Eicosane	**C20**	**Area %**	12.76	4.93	14.51
Heneicosane	**C21**	**Area %**	8.26	7.41	6.49
Docosane	**C22**	**Area %**	1.91	3.30	0.53
Tricosane	**C23**	**Area %**	0.00	0.42	0.00
Tetracosane	**C24**	**Area %**	5.42	9.67	0.00
Pentacosane	**C25**	**Area %**	3.32	3.95	1.02
Hexacosane	**C26**	**Area %**	0.88	2.04	0.26
Heptacosane	**C27**	**Area %**	1.12	3.78	2.42
Octacosane	**C28**	**Area %**	3.94	5.62	1.28
Nonacosane	**C29**	**Area %**	0.00	0.00	0.00
Contane	**C30**	**Area %**	0.00	0.00	0.00
TOTAL		**Area %**	**66.85**	**63.27**	**58.68**

The data presented in Table 7-11 are important in that they demonstrate the effect of the dilution factors on the area percentage of higher molecular weight normal alkanes. For comparing the results of normal alkanes within the residues of Sample D1 to D4, the data are of little value given the dilution factor involved. However, all three thermal treatment residues indicate an increase in the concentration of normal alkanes (C_{10}–C_{30}) compared with distillation (Sample C2) and mild thermal treatment (Sample C1).

The aromatics in Sample D1 are largely alkylated or oxygenated homologues of benzene (e.g. ortho- and para-xylene and benzaldehyde). At the maximum thermal treatment temperature, Sample D4 shows that the aromatic molecules are largely based on two to four benzyl ring structures (e.g. 1-(propenyl) naphthalene, 9-H fluorene, 1-methyl 9-H fluorene, 4-methyl phenanthrene and 1-methyl pyrene). This increases the probability that a certain amount of cyclisation of aliphatics, coupled with dehydrogenation, may have occurred. To some degree the increase in the size of the aromatic rings between Sample D1 and D4 decreases the problematic nature of accounting for alkylated aromatics previously mentioned. Furthermore, the ratio of alkylated aromatics to non-alkylated aromatics decreases from Sample D1 (3.2) to D3 (1.7) and finally D4 (1.5).

It could very well be argued that the presence of lighter molecular weight components within the thermal treatment residues would be of little consequence as they would be expected to distil off during carbonisation. However, as discussed in Chapter 8, they prove to have a substantial effect on the microstructure of the coke. In Chapter 7 the *actual reactivity* of the residue is of less importance than the *potential for reactivity* of the residue at carbonisation temperatures. The "potential for reactivity" is defined (in this study) as the quantitative

identification of molecules (or families of molecules) with a known propensity to decrease the temperature of the onset of poly-condensation, producing semi-carbons which gravitate towards the bottom of the test tube and form mosaic microstructures.

Thermal treatment of filtered Waxy Oil (under pressure) very broadly produces two types of organic molecules in the residue: firstly, the lighter hydrocarbons (which did not escape) and secondly, the stabilised long-chain normal alkanes. To demonstrate the effect of lighter hydrocarbons as potential reactivity promoters, the residue of Sample D3 is analysed in greater detail.

It was noted in Figure 7-14 that the second peak of maximum mass loss rate of the DTG was at approximately 420 °C for Sample B and at 440 °C for Sample D3, thus implying that as the area percentage of heavier long-chain alkanes increases, the thermal stability also increases. However, it is important to note that this does not refer to the thermal stability of Sample D3 residue in its entirety, but only to the stabilised heavier normal alkanes, as the lighter molecules had already been distilled.

Thus in order to examine potential reactivity promoters, the GCMS for Sample D3 (Figure 7-16) can be split into two approximate regions. The first region (below 30 min retention time) is ascribed to lighter hydrocarbons and the second region (after 30 min retention time) to heavier normal alkanes as this is where the “crest” begins to show.

To identify potential reactivity promoters, the first region of lighter hydrocarbons is therefore examined. A breakdown of potential reactivity promoters in this region has been manually calculated from the GCMS data for Sample D3 and divided into groups of molecules as shown in Figure 7-17.

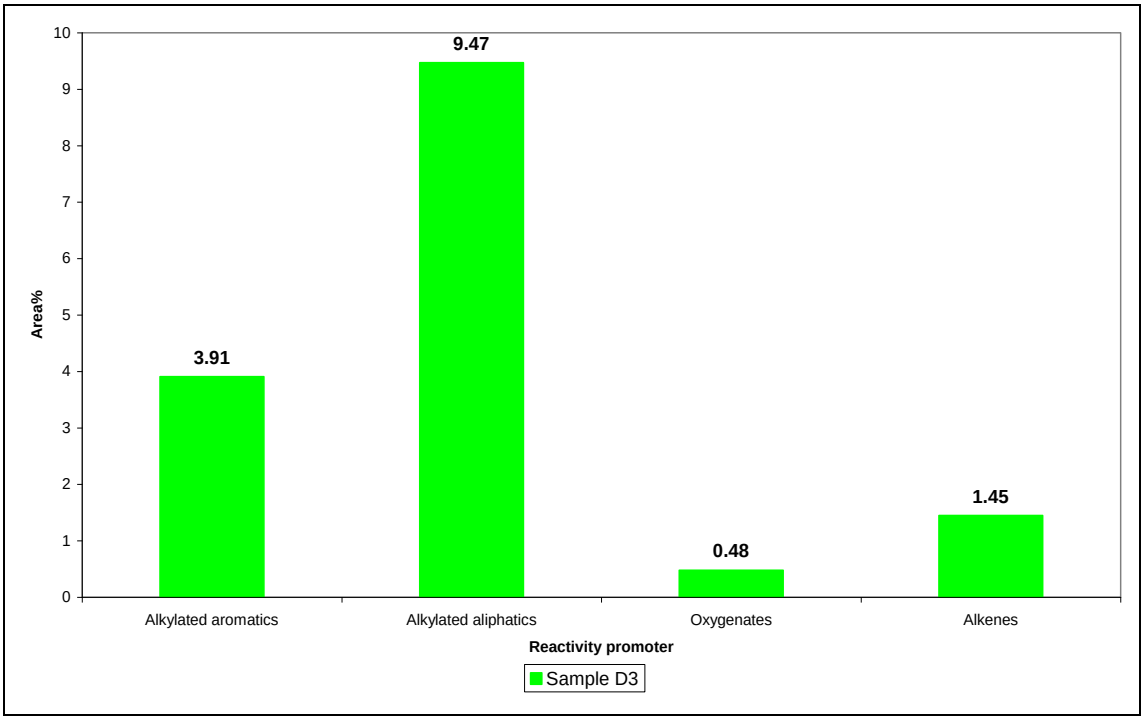

Figure 7-17 Histogram of potential reactivity promoters subdivided into groups of Sample D3 residue (eluting before 30 min according to Figure 7-16)

The dominant group of potential reactivity promoters is iso-alkanes (9.47%), which include methyl to tetra-methyl side chains on parent aliphatics from heptane to decane. Other substituents include a small amount of ethyl and propyl substituents on heptane. In order to substantiate the potential reactivity of hydrocarbons in this region, a comparison is made with the findings of Obara *et al.* (1981) who, while studying the reactivity of Ethylene Tar Pitch (ETP), noted the scission of aliphatic side chains at 400 °C and the formation of reactive radicals to lower the temperature of poly-condensation, thus promoting the formation of mosaic microstructures. This is further substantiated by Mochida *et al.* (1990), also investigating the thermal stability of ETP, who ascribed the higher reactivity to 1-methyl or ethyl substitutions to the aromatic ring.

In Sample D3 the area percentage of alkylated aromatics (3.91%) is lower than that of alkylated aliphatics. In order to differentiate between the thermal stability of pure and alkylated aromatics the results of Perez *et al.* (2002) may be studied. This research compared the variance of composition and reactivity of thermally treated petroleum residues with those of distilled petroleum residues. In this research physical distillation did not dealkylate the aromatics (due to resonance stabilised benzyl radicals), leading to a higher reactivity, compared with thermal treatment which did dealkylate the aromatics. Similarly, during a study of model compounds, Lewis *et al.* (1987) further argued for the activating effect of methyl substituents causing dimethyl naphthalene to carbonise at a faster rate than naphthalene. While the concentration of alkylated aromatics (3.91%) is certainly lower than that of the alkylated aliphatics, the same dealkylation mechanisms should apply to both, which makes Sample D3 relatively thermally unstable. Although the small percentage of alkenes (1.45%) is of comparatively less concern, Mochida *et al.* (1990) previously argued for the effect of olefins in increasing the reaction rate during carbonisation and inhibiting the formation of anisotropic microstructures.

As with the thermal treatment at 5 bar, there is no reason to believe that these lighter compounds would not be present in residue during “static” coking (also conducted at 5 bar). The time differential between the increase in typical thermal treatment temperatures (in this case 410 °C) and the onset of carbonisation (approximately 460 °C) is small. It is therefore concluded that the groups of compounds discussed above possess substantial potential to increase the reactivity of the residue during carbonisation and thus the formation of mosaic microstructures. The effect on the microstructure is further discussed in Chapter 8.

A similar exercise has been conducted with Sample E1b, from whose residue the lighter hydrocarbons were removed after thermal treatment by distillation. This is further discussed below in Section 7.4.2.3.

7.2.4.2 Waxy Oil thermal treatment at lower pressure

Given the challenges presented by the distillation coefficient of the initial thermal treatment experiments at 5 bar, it was decided to repeat the experiments at one of the temperatures (namely 410 °C, Sample D3), but to reduce the pressure of thermal treatment after 1 h from 5 bar to 1 bar (Sample E1a) and 0 bar (Sample E2) to determine the efficacy of removing distillate from the residue. The yields of the isothermal thermal treatment reactions are shown in Table 7-12 and compared with Sample D3 as a reference.

Table 7-12 Waxy Oil yields from thermal treatment reactions at lower system pressure

Experiment number	Temperature	Time [1]	Pressure	Residue	Distillate	Distillation coefficient
	(°C)	(h)	(bar)	(%)	(%)	(%)
D3	**410**	**2**	**5**	58.7	41.3	62.2
E1a	**410**	**2**	**1 h at 5 bar; 1 h at 1 bar**	54.4	45.7	68.3
E2	**410**	**2**	**1 h at 5 bar; 1 h at 0 bar**	49.6	50.4	84.6

As expected, the yield of the thermally treated residues is reduced as the reaction pressure (after 1 h) is reduced. Similarly, because the reaction was conducted under isothermal conditions, the reduction in the residue yield is accompanied by an increase in the distillation coefficient.

In order to study the effect on the concentration of lighter hydrocarbons in the residues produced, the TGA and DTG for Samples E1a and E2 are shown in Figures 7-18 and 7-19 respectively. Samples B and D3 are included as references.

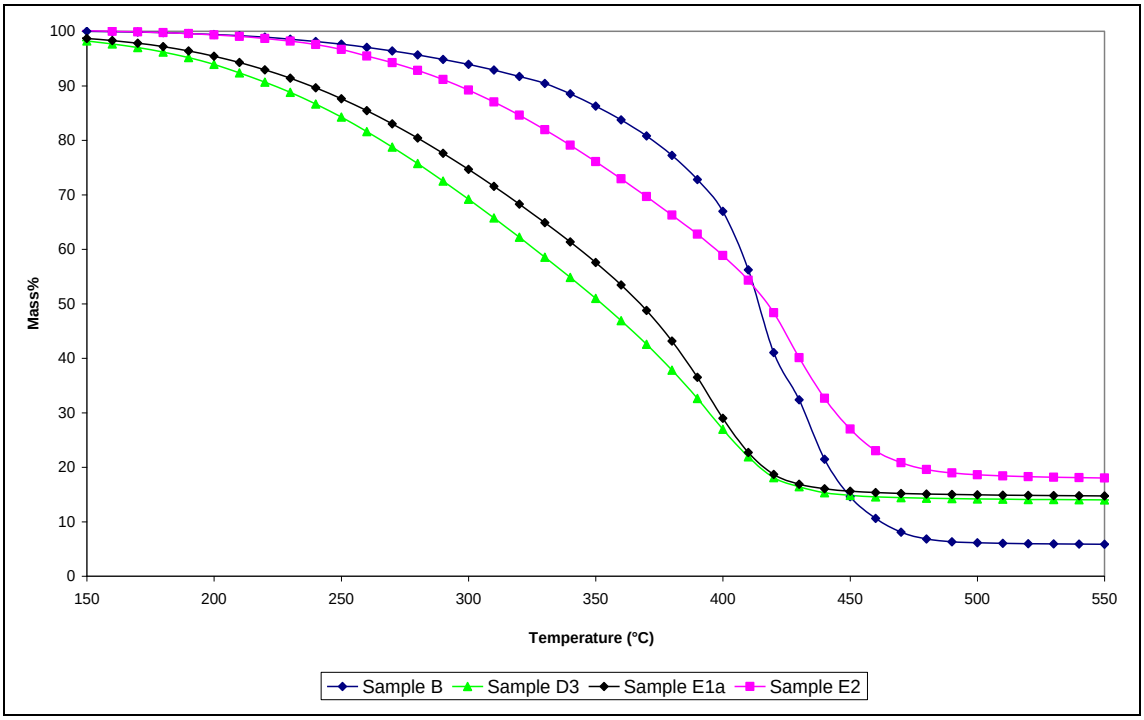

Figure 7-18 Thermogravimetric Analysis (TGA) of Samples B, D3, E1a and E2 residues

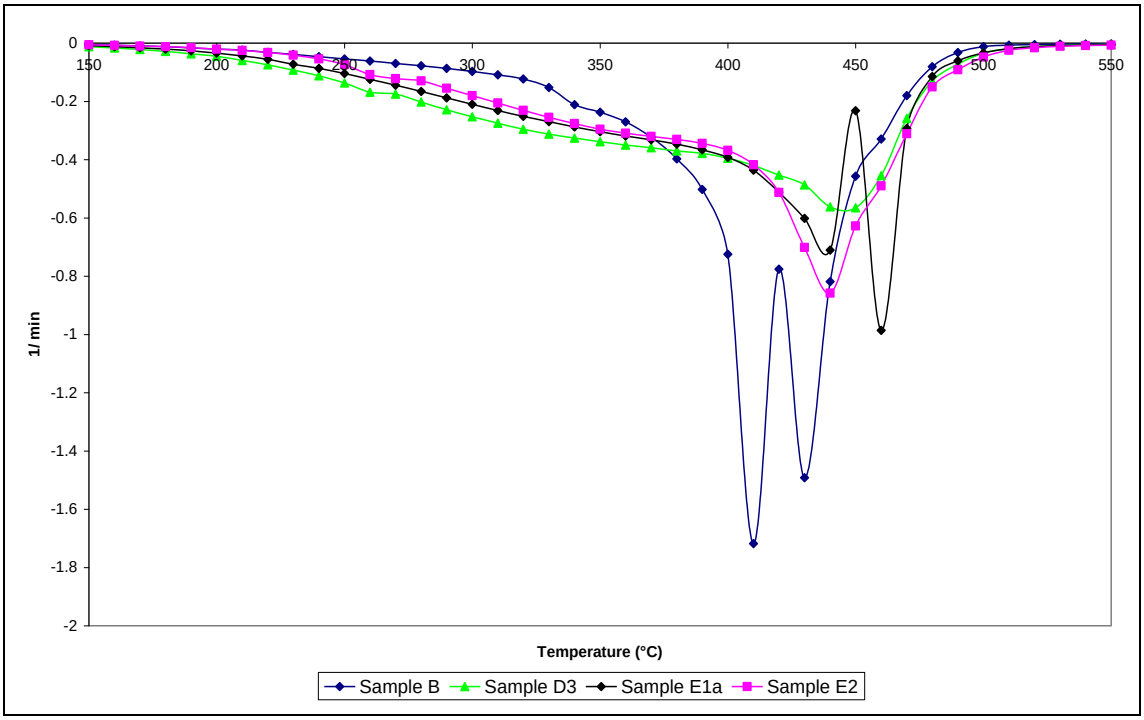

Figure 7-19 Differential Thermogravimetry (DTG) of Samples B, D3, E1a and E2 residues

As shown in Figure 7-18, reducing the pressure (after 1 h to 1 bar; Sample E1a) does not substantially reduce the amount of lighter cracked hydrocarbons in the residue, as indicated by the mass loss between 200 and 370 °C and compared with Sample D3. The efficiency with which lighter hydrocarbons are removed from the residue also serves to increase the residuum yield at 500 °C. However, a further pressure drop (to 0 bar for 1 h; Sample E2) does further reduce the amount of lighter hydrocarbons but retains almost 50% thereof.

The increased efficiency of lighter hydrocarbon removal in the 200–370 °C range promotes the shift of the second peak of maximum rate of mass loss to a higher temperature for Sample E2 (470 °C) compared with Sample D3 (440°C) as shown in Figure 7-21.

The GCMS trace of Sample D3 residue is compared with that of Sample E1a residue in Figure 7-20 and their distillates are compared in Figure 7-21.

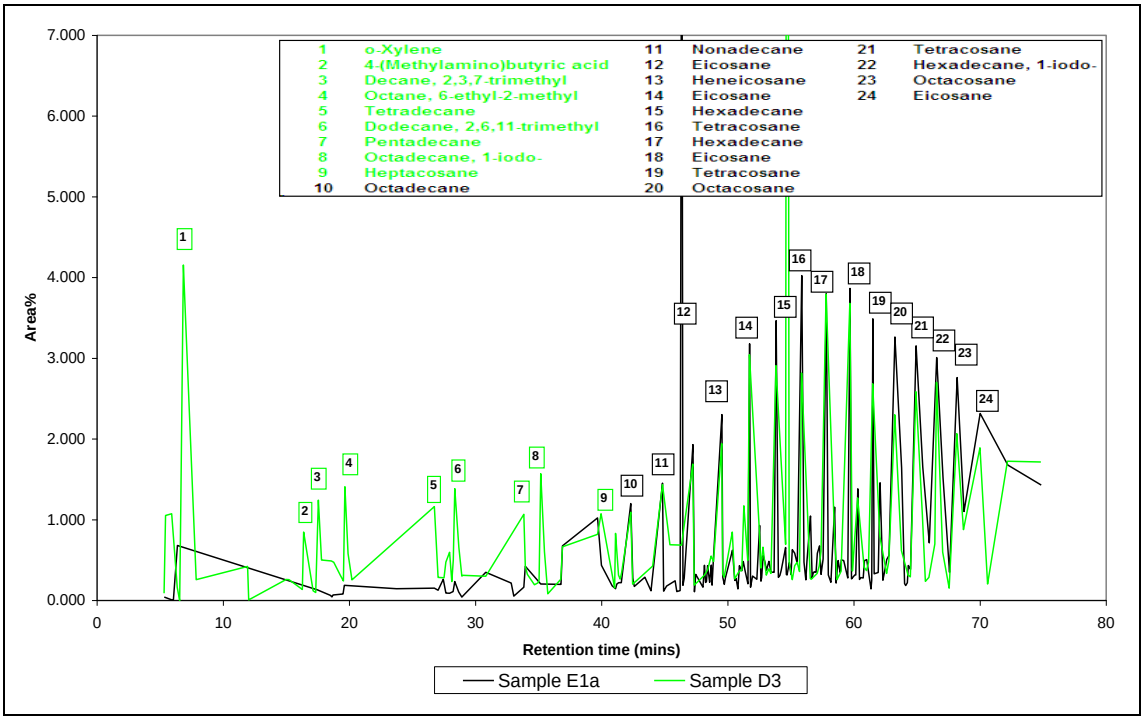

Figure 7-20 Gas Chromatography–Mass Spectroscopy (GCMS) of Samples D3 and E1a residues

As shown in Figure 7-20, there is a substantial reduction in lighter hydrocarbons eluted below a retention time of 35 min for Sample E1a residue compared with Sample D3 residue. The increase in the distillation efficiency involves the removal of ortho-xylene, alkylated and normal alkanes below C_{18} (peaks 1–8). There is a reciprocal increase in the area percentage of the stable normal alkanes after a retention time of 40 min (peaks 10–24).

The removal of lighter hydrocarbons from Sample E1a compared with Sample D3 is perhaps better described by comparing the GCMS traces of their respective distillates, shown in Figure 7-21.

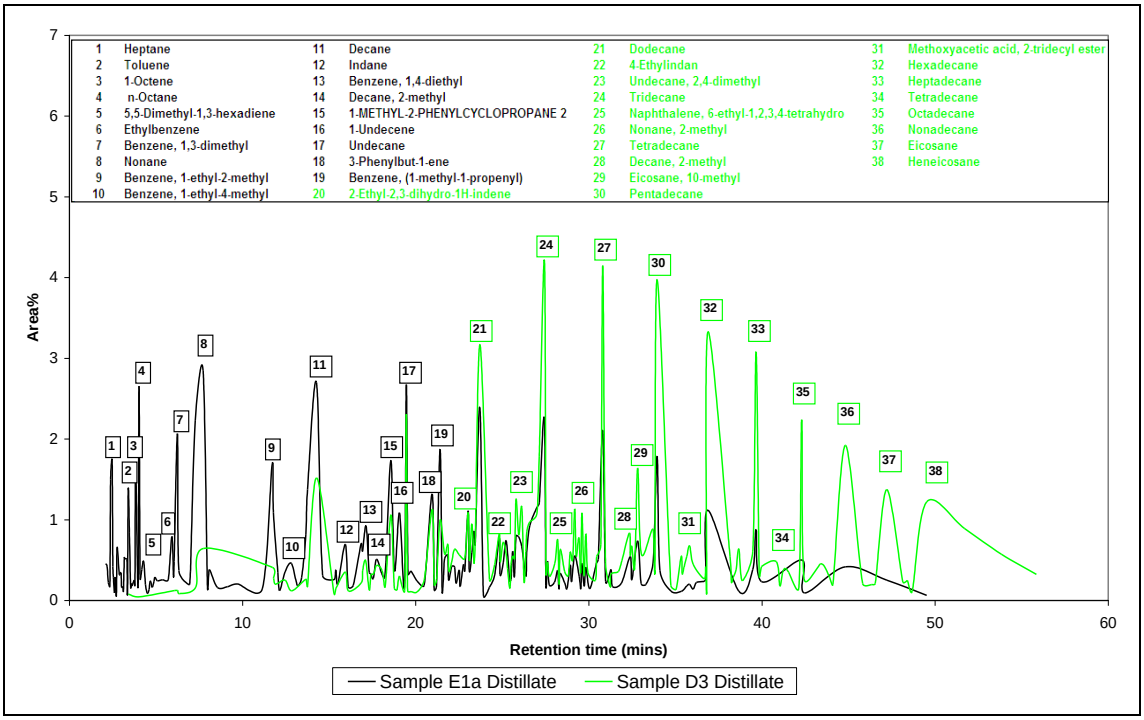

Figure 7-21 Gas Chromatography–Mass Spectroscopy (GCMS) of Samples D3 and E1a distillates

The distillate fraction of Sample E1a shows a higher area percentage of lighter hydrocarbons eluted in the first 20 min (peaks 1–17) compared with Sample D3. The lighter molecules in Sample E1a distillate include both alkylated homologues of benzene, lower molecular weight pure alkanes (e.g. octane, nonane, decane and undecane) and alkenes (e.g. 1-octene and 1-undecene) as the major peaks. Sample D3 distillate, in turn, shows a higher area percentage of higher molecular weight pure and alkylated aliphatics after an elution time of 25 min. This is merely a function of the greater concentration of lighter hydrocarbons reporting to the residue and not the distillate of Sample D3.

The effect on the comparative GCMS traces of Samples E1a and E2 residues of further reducing the system pressure (to 0 bar) is shown in Figure 7-22 and the effect on their respective distillates in Figure 7-23.

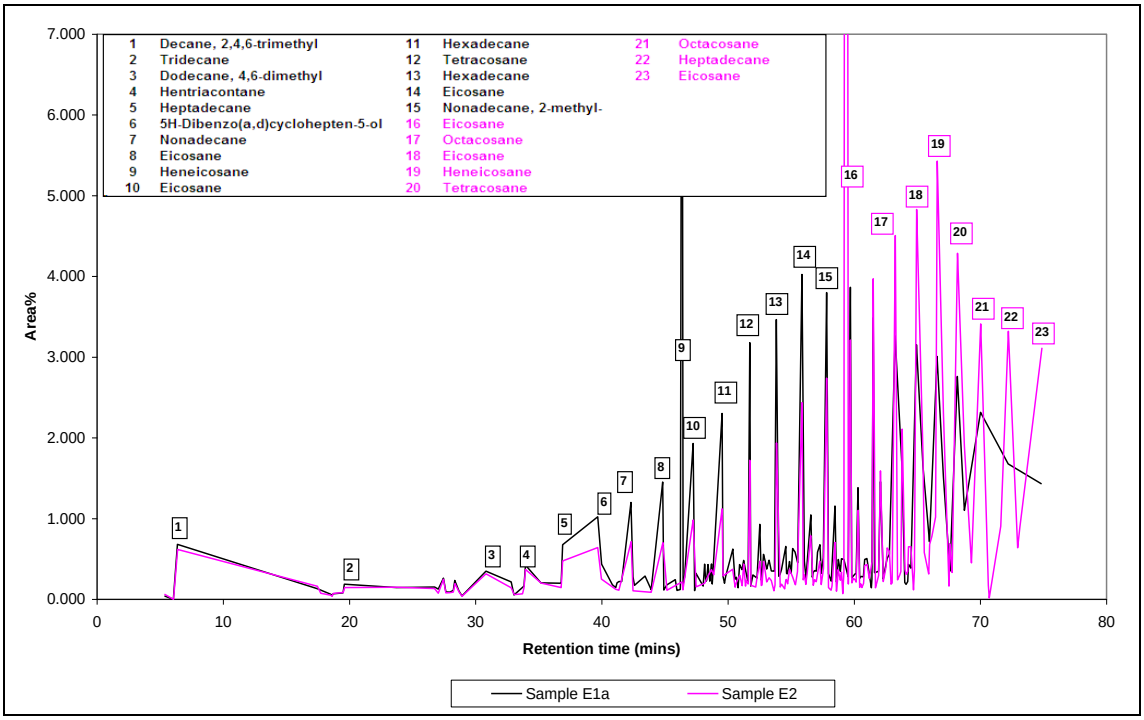

Figure 7-22 Gas Chromatography–Mass Spectroscopy (GCMS) of Samples E1a and E2 residues

Both Samples E1a and E2 residues show a similar elution trend for the first 35 min of retention time. However, between 35 and 55 min Sample E1a shows individual component peaks with a higher area percentage when compared with Sample E2 (peaks 7–14; C_{16}–C_{21}), with the exception of peak 12. The reciprocal effect is evident between an elution time of 60 and 70 min when Sample E2 yields peaks with a higher area percentage (peaks 16–23; C_{20}-C_{28} normal alkanes).

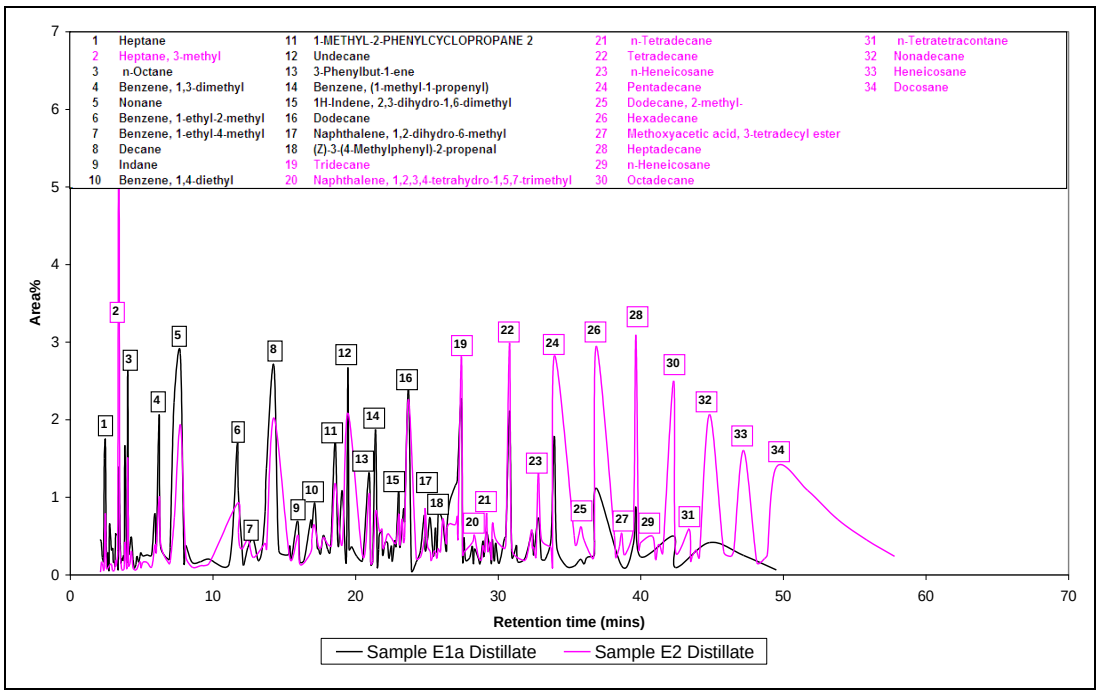

Figure 7-23 Gas Chromatography–Mass Spectroscopy (GCMS) of Samples E1a and E2 distillates

Sample E2 distillate is a heavier fraction than Sample E1a distillate, especially with regard to the "crest" of heavy normal alkanes shown in peaks 19–34 (C_{13}–C_{22}) which emerge within a retention time of 25–50 min. The reverse is true for the first 25 min when peaks 1–15 show a higher retention time for Sample E1a (with the exception of peak 2).

In terms of the groups or families of products for the three thermal treatments, a comparison is shown in Table 7-13.

Table 7-13 Molecular compound groups in Samples D3, E1a and E2 residues

Molecules	Unit	Sample D3	Sample E1a	Sample E2
Alkylated aromatics	**Area %**	5.42	2.71	3.60
Pure aromatics	**Area %**	0.71	0.29	1.19
Iso-alkanes	**Area %**	15.14	1.77	3.03
Normal alkanes	**Area %**	63.27	74.61	74.93
Oxygenates	**Area %**	1.57	1.38	2.28
Cyclo-alkanes	**Area %**	0.46	0.55	0.19

The removal of lighter cracked material is evident in the percentage increase of normal alkanes when Sample D3 residue is compared with Samples E1a/E2 residue. Both Samples E1a and E2 show a considerable decrease in the component percentage of iso-alkanes, with minimal difference in the oxygenate concentration. It is surprising that the component percentages of pure alkanes in Samples E1a and E2 are so similar. To evaluate this further it is necessary to consider the spread of normal alkanes (C_{10}–C_{30}) in the two samples, which is shown in Table 7-14.

Table 7-14 Normal alkanes (C_{10}–C_{30}) in Samples D3, E1a and E2 residues

Molecule description	Carbon number	Unit	Sample D3	Sample E1a	Sample E2
Decane	**C10**	**Area %**	0.00	0.00	0.00
Undecane	**C11**	**Area %**	0.10	0.08	0.08
Dodecane	**C12**	**Area %**	1.96	0.32	0.51
Tridecane	**C13**	**Area %**	0.00	0.26	0.25
Tetradecane	**C14**	**Area %**	1.46	0.35	0.57
Pentadecane	**C15**	**Area %**	0.42	0.29	0.45
Hexadecane	**C16**	**Area %**	5.16	12.11	5.39
Heptadecane	**C17**	**Area %**	2.17	1.42	6.53
Octadecane	**C18**	**Area %**	7.09	2.37	4.95
Nonadecane	**C19**	**Area %**	3.78	3.91	1.16
Eicosane	**C20**	**Area %**	4.93	21.20	29.28
Heneicosane	**C21**	**Area %**	7.41	6.04	8.26
Docosane	**C22**	**Area %**	3.30	3.34	1.04
Tricosane	**C23**	**Area %**	0.42	1.10	1.10
Tetracosane	**C24**	**Area %**	9.67	12.05	3.22
Pentacosane	**C25**	**Area %**	3.95	0.84	0.54
Hexacosane	**C26**	**Area %**	2.04	0.39	1.34
Heptacosane	**C27**	**Area %**	3.78	0.14	0.00
Octacosane	**C28**	**Area %**	5.62	8.39	10.26
Nonacosane	**C29**	**Area %**	0.00	0.00	0.00
Contane	**C30**	**Area %**	0.00	0.00	0.00
TOTAL		**Area %**	**63.27**	**74.61**	**74.93**

The probable reason for this similarity is the substantial influence of hexadecane in Sample E1a.

7.2.4.3 Waxy Oil filtration, thermal treatment and distillation.

As the sample quantities were limited, only Sample E1a could be distilled (by bubbling under nitrogen to 325 °C) to determine the effect of lighter hydrocarbon removal from the residue. The yields of residue and distillate are shown in Table 7-15. Sample E1a is shown for comparison purposes.

Table 7-15 Yields from the distillation of Sample E1a producing distillate and residue (named Sample E1b)

Experiment number	Temperature (°C)	Time [1] (h)	Pressure (bar)	Residue (%)	Distillate (%)	Distillation coefficient (%)
E1a	**410**	**2**	**1 h at 5 bar; 1 h at 1 bar**	54.4	45.7	68.3
E1b	**none**	**none**	**Sample E1a N_2 stripped to max. 325 °C**	43.0	57.0	93.2

The nitrogen-strip distillation of Sample E1a increased the distillate fraction, producing a heavier Waxy Oil residue (Sample E1b) accompanied by an increase in the distillation coefficient.

The TGA and DTG of these samples are shown in Figures 7-24 and 7-25 respectively.

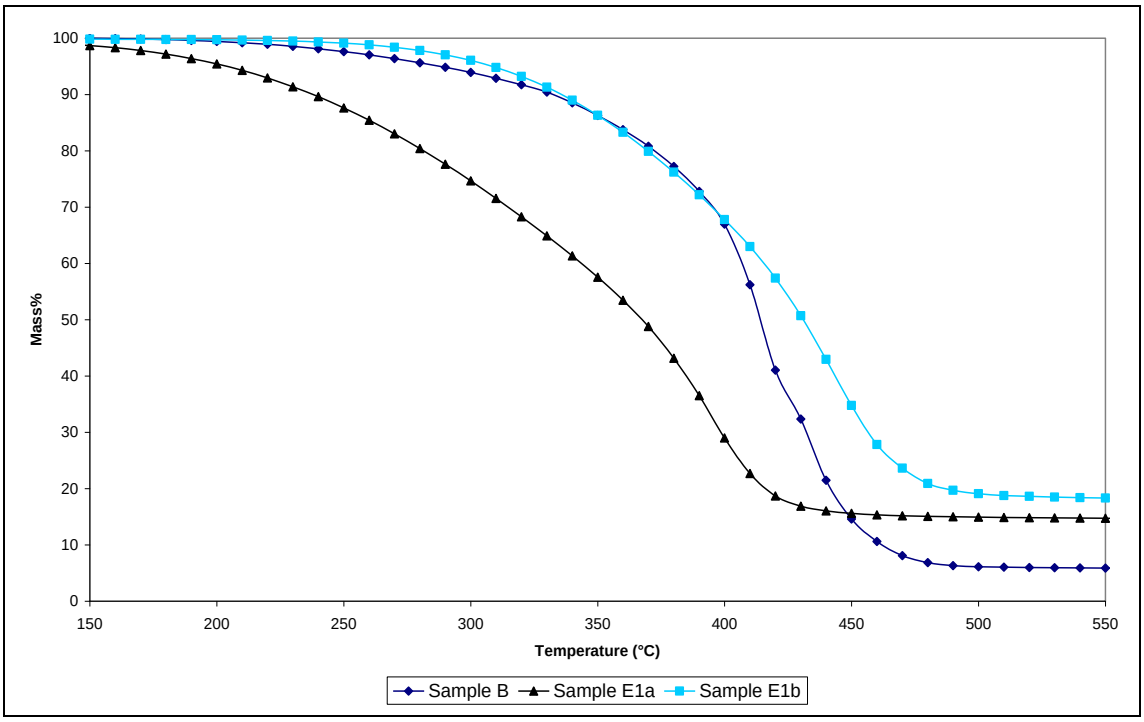

Figure 7-24 Thermogravimetric Analysis (TGA) of Samples B, E1a and E1b residues

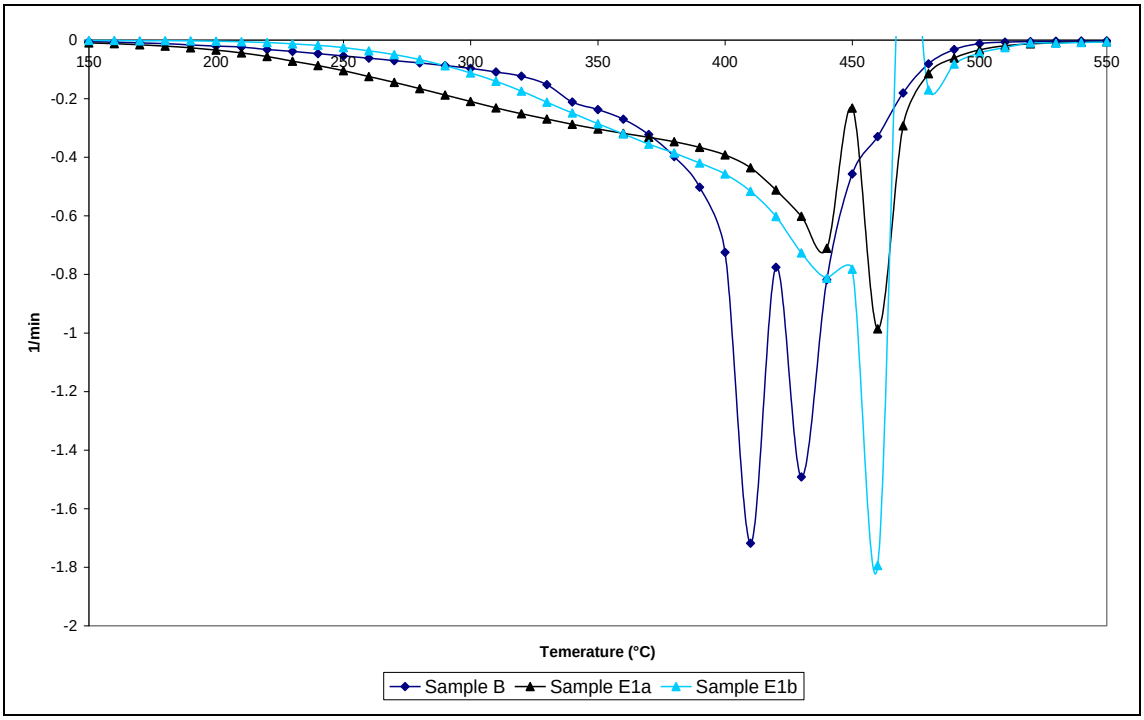

Figure 7-25 Differential Thermogravimetry (DTG) of Samples B, E1a and E1b residues

As shown in Figure 7-24, not only is the amount of lighter hydrocarbons in Sample E1b reduced (compared with Sample E1a), but there is a similar, if not lower, mass loss compared with Sample B within the 200–370 °C region of the TGA. The removal of lighter material from Sample E1a also serves to increase the residue of E1b (17%) compared with E1a (14%) and B (5%). The greater amount of carbon residue in Sample E1b is comparable to the reduction in mass loss in the initial region of the TGA. The distillation coefficient is also increased from 84.6% (Sample E1a) to 93.2% (Sample E1b) as shown in Table 8-17.

With regard to the DTG (Figure 7-25), Sample E1b shows a more intense (second) peak at a higher carbonisation temperature than either Samples B or E1a. The rate of mass loss between Samples E1b and B is similar between 200 and 370 °C. The higher temperature at which the second peak occurs (Sample E1b) again indicates an increase in the concentration of thermally stable heavier normal alkanes. However, what is very apparent is the substantial increase in the intensity of the second peak, indicating that a greater percentage of the residue is reacting at this temperature. This is not unexpected given the lower dilution factor. The effect of the distillation on the molecular composition of Sample E1b residue (compared with Sample E1a residue) is shown in Figure 7-26 and the effect on their respective distillates in Figure 7-27.

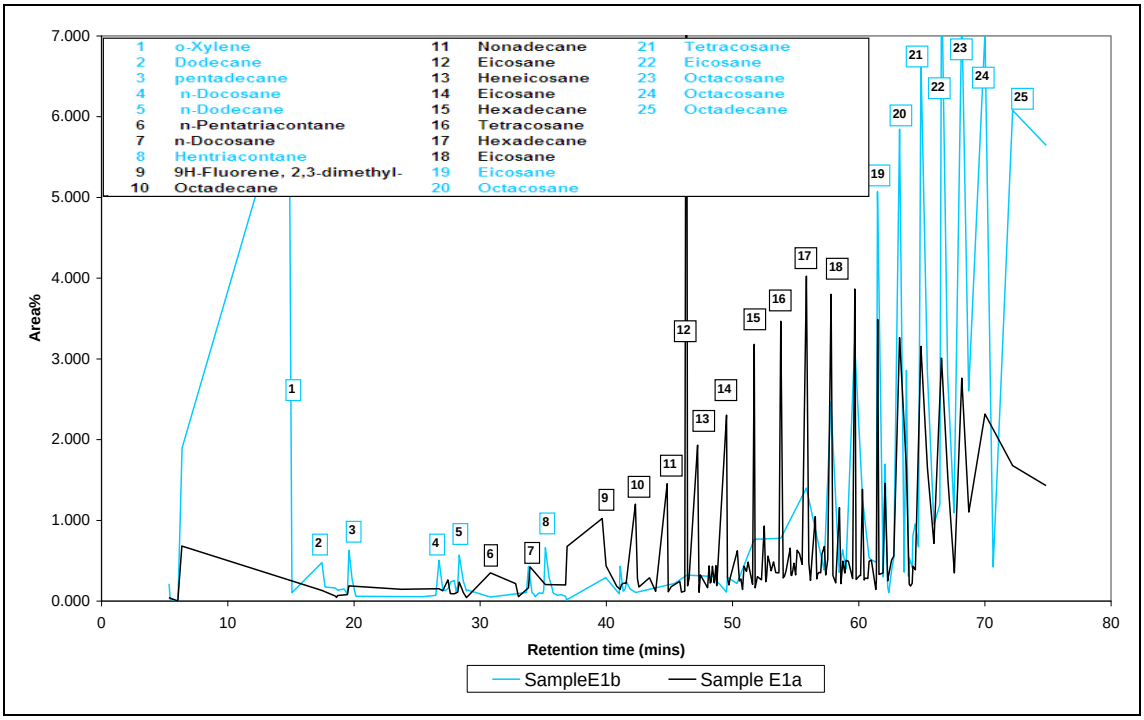

Figure 7-26 Gas Chromatography–Mass Spectroscopy (GCMS) of Samples E1a and E1b residues

While Sample E1b residue does show a slight increase of peaks 1–5, the greatest effect of distillation is to remove components with a retention time between 40 and 60 min, specifically molecules below C_{21} (peaks 10–18), and there is a reciprocal increase in the area percentage of higher molecular weight pure aliphatics (C_{20}–C_{28}; peaks 19–25).

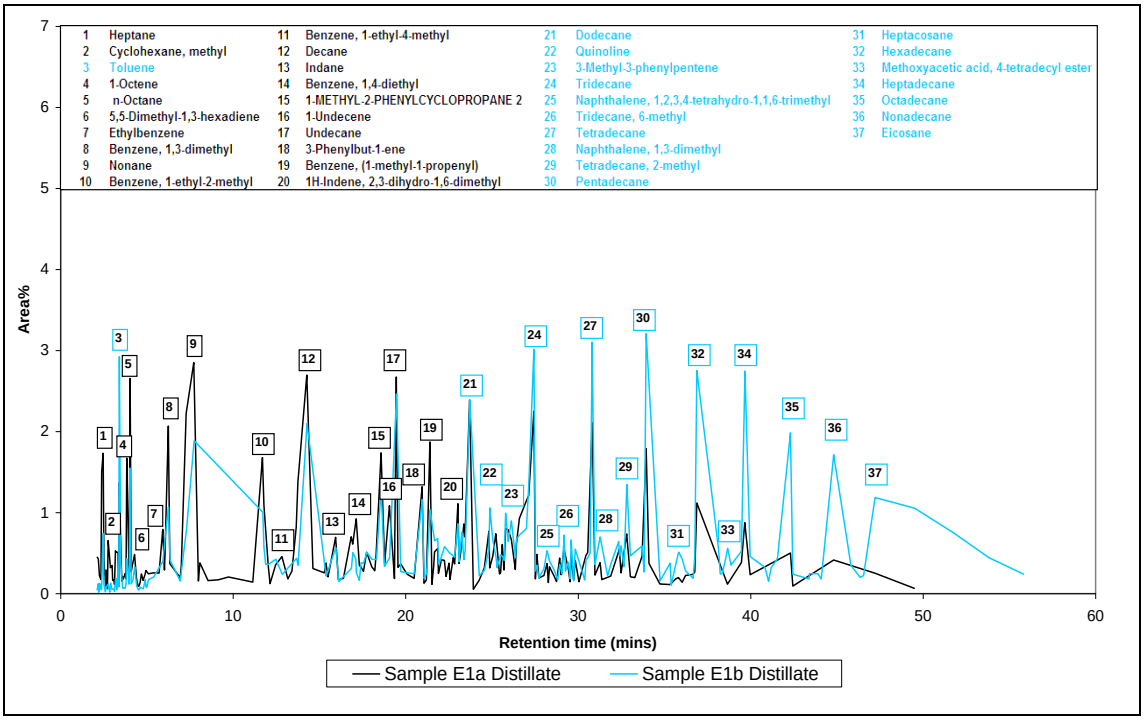

Figure 7-27 Gas Chromatography–Mass Spectroscopy (GCMS) of Samples E1a and E1b distillates

Compared with the distillate of Sample E1a, Sample E1b shows an increase in the concentration of heavier pure aliphatics, specifically C_{13}–C_{21} (peaks 21–37) and, on average, a decrease in the area percentage for the products eluting before 25 min retention time (peaks 1–20).

In terms of the groups or families of products for Samples E1a and E1b residues, a comparison is shown in Table 7-16.

Table 7-16 Molecular compound groups in Samples E1a and E1b residues

Molecules	Unit	Sample E1a	Sample E1b
Alkylated aromatics	**Area %**	2.71	1.89
Pure aromatics	**Area %**	0.29	0.83
Iso-alkanes	**Area %**	1.77	2.61
Normal alkanes	**Area %**	74.61	85.82
Oxygenates	**Area %**	1.38	1.31
Cyclo-alkanes	**Area %**	0.55	0.02

Sample E1b shows the highest concentration of normal alkanes of any of the modified Waxy Oil residues discussed in this chapter. It is suggested that, with minimal contributions from any of the other alkylated compounds and a low oxygenate concentration, Sample E1b should produce the highest coke yield and the greatest concentration of stable molecules; it is thought that this will promote flow domains in the coke.

In terms of the distribution of normal alkanes (C_{10}–C_{30}), Samples E1a and E1b residues are compared in Table 7-17.

Table 7-17 Normal alkanes C_{10}–C_{30}) in Samples E1a and E1b residues

Molecule description	Carbon number	Unit	Sample E1a	Sample E1b
Decane	**C10**	**Area %**	0.00	0.00
Undecane	**C11**	**Area %**	0.08	0.05
Dodecane	**C12**	**Area %**	0.32	1.93
Tridecane	**C13**	**Area %**	0.26	0.00
Tetradecane	**C14**	**Area %**	0.35	0.16
Pentadecane	**C15**	**Area %**	0.29	0.63
Hexadecane	**C16**	**Area %**	12.11	2.44
Heptadecane	**C17**	**Area %**	1.42	3.55
Octadecane	**C18**	**Area %**	2.37	14.35
Nonadecane	**C19**	**Area %**	3.91	0.00
Eicosane	**C20**	**Area %**	21.20	24.76
Heneicosane	**C21**	**Area %**	6.04	3.71
Docosane	**C22**	**Area %**	3.34	1.11
Tricosane	**C23**	**Area %**	1.10	1.63
Tetracosane	**C24**	**Area %**	12.05	6.71
Pentacosane	**C25**	**Area %**	0.84	0.43
Hexacosane	**C26**	**Area %**	0.39	2.31
Heptacosane	**C27**	**Area %**	0.14	0.00
Octacosane	**C28**	**Area %**	8.39	20.42
Nonacosane	**C29**	**Area %**	0.00	0.00
Contane	**C30**	**Area %**	0.00	1.63
TOTAL		**Area %**	74.61	85.82

The three molecules that are in the greatest concentration in Sample E1b are eicosane (C_{20}), octacosane (C_{28}) and octadecane (C_{18}), making up 59.53% of the total percentage of the sample. Sample E1b also shows a reduction in the area percentage contribution of molecules with a lower molecular weight than octadecane (C_{18}) compared with Sample E1a.

In the same way as lighter hydrocarbons in Sample D3 were shown to have the potential to act as reactivity promoters, the effect of their removal is considered when evaluating Sample E1b. Following the procedure used to determine the reactivity potential of Sample D3, the presence of lighter compounds eluting within the first 30 min is considered and shown in Figure 7-28.

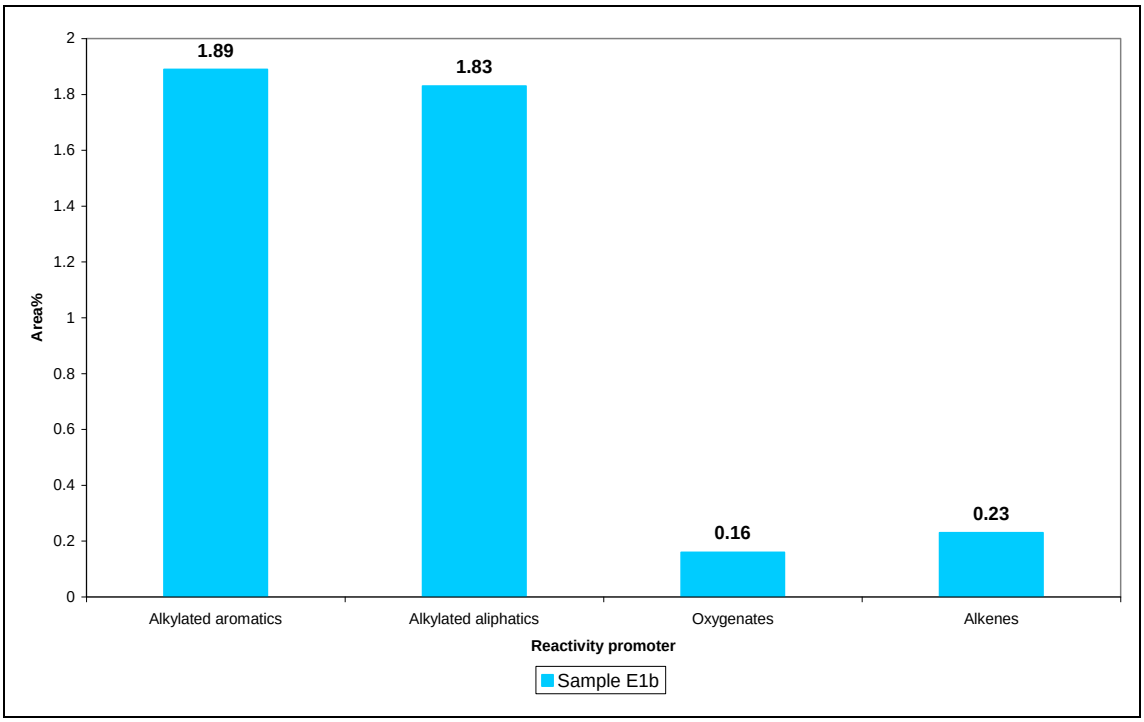

Figure 7-28 Histogram of potential reactivity promoters subdivided into groups of Sample E1b residue (eluting before 30 min according to Figure 7-28)

Compared with Sample D3 (Figure 7-19), Sample E1b shows a substantial reduction in the concentration of iso-alkanes and alkylated aromatics which were previously identified as potential reactivity promoters. Thus, it would be expected (if this theory is correct) that the coke residue formed from Sample E1b would thus be more anisotropic than that of Sample D3 coke. This is further discussed in Chapter 8.

7.3 Hydrogen (^{1}H) Nuclear Magnetic Resonance (NMR) and Aromatic Index (I_{ar}) of modified Waxy Oils

The research detailed in Chapter 7 showed GCMS evidence of a substantial increase in the concentration of normal alkanes, based on a series of experimental interventions. However, the question may well be asked whether the GCMS data are representative of the whole residue. In other words, were there heavier aromatics which did not elute? For this reason a

comparison between the ^{1}H (aliphatic to aromatic ratio) and the Aromatic Index (I_{ar}) of the residues is shown in Table 7-18.

Table 7-18 Comparison between the ^{1}H (aliphatic to aromatic ratio) and the Aromatic Index [$I_{ar}=Abs_{3050}/(Abs_{3050}+Abs_{2920})$] of modified Waxy Oils

Residue	^{1}H (aliphatic to aromatic) ratio	Aromatic Index (I_{ar})
Sample B	26.50	*
Sample C1	18.62	0.0041
Sample C2	23.75	*
Sample D1	16.17	*
Sample D3	12.45	0.0046
SampleD4	8.58	0.0079
Sample E2	10.97	0.0110
Sample E1b	9.93	0.0118

*Data not detected

The data in Table 7-18 provide a general comparison between the ^{1}H Nuclear Magnetic Resonance (NMR) and Aromatic Index (I_{ar}) of modified Waxy Oils. In general, as the ^{1}H (aliphatic to aromatic) ratio decreases, there is an increase in the I_{ar}, which would be expected. Given the low aromaticity of the modified Waxy Oils, ^{1}H NMR is more of a quantitative analysis method due to the problems encountered in determining the absorbance of the FTIR band around 3500 cm^{-1}.

^{1}H NMR was preferred over ^{13}C NMR for two reasons. Firstly compared to coal-tar pitches, Waxy oil is not in the amorphous fused state at room temperature but is a liquid. Secondly, given the abundance of hydrogen compared to carbon, quantitative analysis was easier using ^{1}H NMR. While the aromatic index is a less quantitative measure of the aromaticity it is shown in Table 7-18 to indicate only a slight increase in the absorbance of the 3050 cm^{-1} band. this is relevant to show that thermal treatment does not induce substantial increases in the aromaticity due to a lack of activation energy

Samples B and C2 indicate a relatively high ^{1}H (aliphatic to aromatic) ratio since their preparation does not involve chemical cracking and dealkylation. As the severity of thermal treatment increases, so the ^{1}H (aliphatic to aromatic) ratio further decreases due to dealkylation with a corresponding increase in the I_{ar}. However, the results indicate that the slight increase in the I_{ar}, which corresponds to a reduction of the ^{1}H (aliphatic to aromatic) ratio, is related to the dealkylation of aromatics or aliphatics and not to the aromatisation of thermally stable normal alkanes. It is proposed that aromatisation of the stabilised normal alkanes in Waxy Oil would require a greater activation energy and would take place within the initial phase of carbonisation.

In order to put the I_{ar} for the modified Waxy Oils, which range from 0–0.012, into perspective, the I_{ar} of other feedstocks available from the cited literature (Sima *et al.*, 2003; (Perez *et al.*, 2002) are listed, namely coal-tar binder pitch (0.63), Ashland petroleum pitch (0.41), low-temperature gasification pitch (0.37), distilled petroleum vacuum residue (0.38) and thermally treated petroleum vacuum residue (0.45). Similarly, the ^{1}H (aliphatic to aromatic) ratio for the modified Waxy Oils ranges from 9 to 26, whereas that of other feedstocks available from the cited literature (Alcaniz-Monge *et al.*, 2001) is substantially

lower, including that of thermally treated coal-tar pitch (0.25) and distilled coal-tar pitch (0.63).

7.3.1 The question of aromaticity

Although the literature cited in this chapter mostly confirms the dependence of anisotropicity on the increase in the concentration of aromatic compounds, in all the modified Waxy Oils the concentration of such compounds was found to be negligible. So the question must be asked: Were the optimum reaction conditions utilised? Thus, the thermal treatment temperature and duration need to be discussed.

As reported, Sample D2 showed small pieces of solid carbon at the bottom of the test tube after thermal treatment. Thus 420 °C is considered a maximum temperature.

In the same way, it may be possible to increase the aromaticity by extending the duration of thermal treatment, as suggested by Eser *et al.* (1989) who studied petroleum residues. While the author is in complete agreement with the work of Eser *et al.*, Waxy Oil is a vastly different residue. During a failed experiment, increasing the duration of thermal treatment resulted in a heavy polymer gum forming and gravitating to the bottom of the test tube. This is probably due to dehydrogenation and polymerisation, which are not beneficial.

Although it is the author's opinion that the carbonisation of Waxy Oil does include an aromatisation step prior to mesophase formation, it is more than likely that this occurs at higher temperatures and thus close to the onset of carbonisation.

7.4 Influence of Waxy Oil modification on the distillate fractions of Samples C2, E1a and E1b

Inasmuch as the emphasis of this study is focused on the quality of the residue and subsequent coke formation, the influence of hydrocarbon distillates produced during Waxy Oil modifications cannot be ignored as they have a substantial influence on the revenue generated from the value chain. While it would have been possible to compare the distillate fractions of all the samples, the major difference between a distillation approach and a thermal treatment approach can be determined by studying the distillate fractions of two samples:

- **Sample C2 distillate:** This is the product of physical distillation and does not include chemical modification of Waxy Oil.
- **Samples E1a and E1b distillate:** This is the product of a chemical cracking reaction and the removal of lighter hydrocarbons. As the residue of Sample E1a was distilled to produce Sample E1b, the relative distillate fractions of both samples are added together to represent one combined fraction.

7.4.1 Intermediate[28] distillation fractions[29] of Samples C2, and E1a and E1b

The composition of product yields for Samples C2, and E1a and E1b are shown in Table 7-19.

Table 7-19 Distribution of product yields of Samples C2, and E1a and E1b

Sample	Unit	Distillate fractions			Residue
		Petrol intermediate	Diesel Intermediate	Heavy fuel oil	
Sample C2	**mass %**	0.4	5.1	0.2	94.3
Sample E1b	**mass %**	32.7	11.6	0.3	43.0

1 All distillate fractions are shown as a mass percentage of the filtered Waxy Oil.

2 The cumulative distillate fraction of Samples E1a and E1b are shown. The distillate fractions of Sample E1a have been corrected for a 15% mass loss due to the production of hydrocarbon gas.

As previously mentioned, Waxy Oil is the product of a flash distillation of SDO. Thus it contains a negligible naphtha (petrol intermediate) concentration but more coker oil (diesel intermediate). This is evidenced by the large temperature increase between the Initial Boiling Point (IBP) and the 5% distillate removal (179–311 °C), as shown in Chapter 3 (Table 3-1). The same relationship between distillation and low-temperature pyrolysis was noticed by Martinez-Escandell *et al.* (1999) in their study of long-chain aliphatic waxes. The study reported no distillates up to 360 °C, compared with distillates of lower molecular weight products of up to 59% when the wax was thermally treated.

Vacuum distillation to pre-cracking temperatures is a physical reaction in that it removes the small amount of lower molecular weight hydrocarbons remaining in the Waxy Oil given the inaccurate nature of flash distillation. Thus the petrol intermediate (0.4%) is negligible and the bulk of the distillate is composed of the diesel intermediate (5.1%), with a small contribution from the production of heavy fuel oil. As distillation is a *physical* reaction and not a *chemical* reaction, there is no need to account for hydrocarbon gas and thus the mass balance is complete.

Thermal treatment (at 410 °C) or low-temperature thermal pyrolysis[30] is a chemical reaction which increases the percentage of stable high molecular weight normal alkanes and of lighter molecular weight hydrocarbons, as well as producing gas. The production of 15% gas yield from the low-temperature pyrolysis of Waxy Oil is in general agreement with the results of Martinez-Escandell *et al.* (1999) who obtained similar gas yields when studying the low-temperature pyrolysis of aliphatic petroleum vacuum residues. The distillation of thermally treated residue thus substantially increases the distillate yield. There is also a larger percentage of petrol intermediates (32.7%) produced compared with that of the diesel

[28] The term "intermediate" is defined in this study as a product produced in the refinery which requires further downstream processing before it can be sold.

[29] Manual calculation of the GCMS data was done to estimate the quantitative amount of various distillation fractions. The petrol fraction is based on molecules between C_4 and C_{12}. The diesel fraction is calculated based on molecules between C_{12} and C_{21}. The heavy fuel oil fraction is calculated based on molecules greater than C_{21}.

[30] For the purpose of this study thermal treatment at 410 °C is referred to as "low-temperature thermal treatment" compared with carbonisation at 480 °C which may be comparatively referred to as "high-temperature thermal treatment".

intermediates (11.6%). As thermal treatment involves the production of hydrocarbon gas, this has been accounted for in the mass balance.

In summary, the production of a substantially higher percentage of petrol and diesel intermediates would be beneficial to the refinery in terms of the need for fuel additives and reducing the amount of residue as feed for carbonisation.

7.4.2 Molecular grouping of intermediate petrol distillation fraction of Samples C2, and E1a and E1b

As both the petrol and diesel distillate fractions are only intermediate products requiring downstream processing, a comparison with the typical molecular groupings of saleable fuel products is not applicable. However, what is apparent is the effect of low-temperature pyrolysis on the typical spectrum of the lower molecular weight breakdown products produced which report to the distillate fraction. Low-temperature pyrolysis of a complex mixture of organic molecules (e.g. Waxy Oil) has the potential for billions of individual reactions. By way of example, Domine *et al.* (2002) calculated 156 individual reactions for the pyrolysis of normal hexane alone. As Waxy Oil is composed predominantly of iso and normal alkanes, the typical reactions may be modelled on these groups of molecules.

Low-temperature pyrolysis of normal alkanes involves a myriad of potential reactions. However, starting from the most basic of cleavage mechanisms, the aliphatic C-C bond (bond enthalpy of 348 $kJmol^{-1}$) is more readily cleaved than the C-H bond (bond enthalpy of 412 $kJmol^{-1}$), as argued by Saunders (2003). Thus lysis of an alkane by a radical formation mechanism to form lower alkanes is slightly preferred to initial dehydrogenation. The process may be represented in the simplified reaction mechanism provided by Domine *et al.* (2002) shown in Figure 7-29. A similar reaction mechanism for the production of lower molecular weight intermediates during low-temperature pyrolysis has previously been reported by Rodriguez-Reinoso *et al.* (2001).

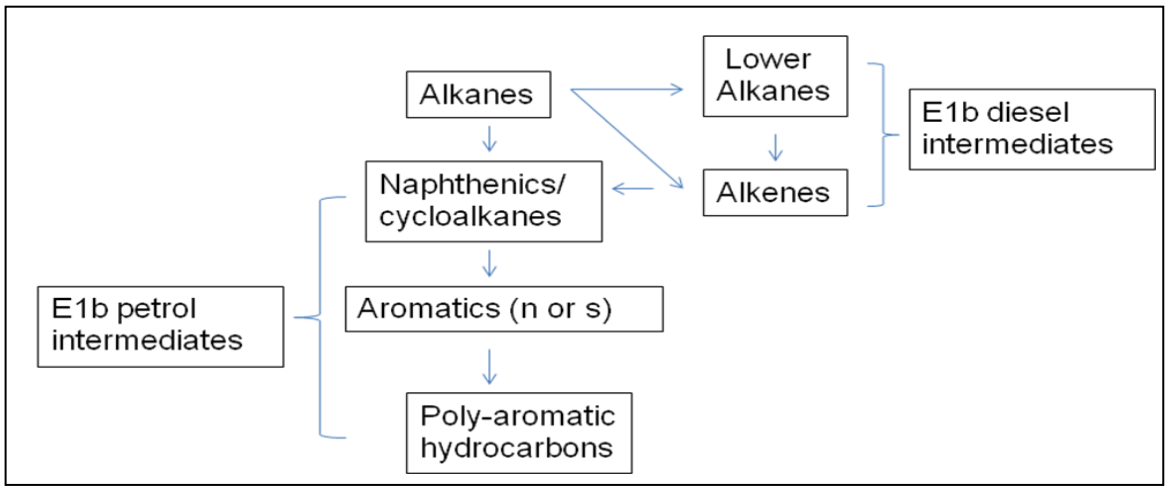

Figure 7-29 Simplified reaction model of exchanges between molecular families during thermal pyrolysis (modified from Domine *et al.*, 2002)

In line with the simplified reaction model shown in Figure 7-29, the percentages and types of molecular family shown in the product spectrum of the petrol intermediate distillate of Samples E1a and E1b can be described as shown in Figure 7-30.

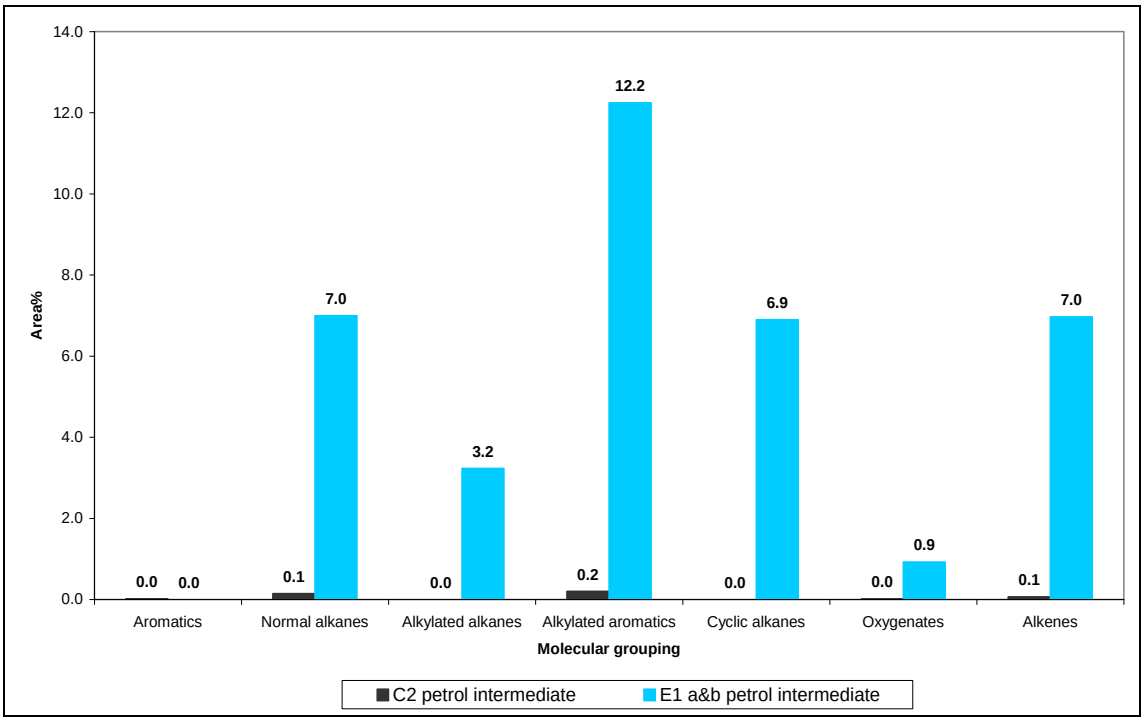

Figure 7-30 Quantitative analysis of molecular groups comprising the petrol fraction of Samples C2, and E1a and E1b distillates[31]

Low-temperature pyrolysis produces a host of different lower molecular weight families (Figure 8-32), dominated by alkylated aromatics (12.2%), normal alkanes (7.0%), alkenes (7.0%), cyclic alkanes (6.9%) and alkylated alkanes (3.2%). The normal and iso-alkanes have a higher molecular weight compared with that of most of the other families and are probably relatively unreactive. The alkenes formed are the larger normal alkane fragments of C-C bond homolytic cleavage which have been dehydrogenated, in agreement with the study of pyrolytic cracking of *n*-hexadecane by Tsuzuki *et al.* (1999). The smaller alkane fragments are probably removed as hydrocarbon gases. However, there is also a substantial percentage of cyclic alkanes which are either the product of cyclo addition reactions or, more likely, due to self-condensation of normal alkanes as they mostly contain long alkyl substitutions on the alicyclic ring. This compounding effect of reactions has also been studied by Bounaceur *et al.* (2002) who described them as "H-transfer, decomposition by B-scission, radical isomerisation, addition and termination". Although the formation of cyclic alkanes is a slow reaction, their dehydrogenation is rapid, which would explain the relatively high percentages of alkylated aromatics. The absence of oxygenates is probably due to lysis of the carbonyl or hydroxyl function and the formation of water.

The substantially higher percentage of lower molecular weight petrol intermediates compared with diesel intermediates (shown in Table 7-19) from low-temperature pyrolysis may also be affected by the distillation efficiency of the reactive system (as in Sample E1a). The longer the breakdown products remain in the reactor at temperature (as opposed to distilling off), the

[31] All distillate fractions are shown as a mass percentage of the filtered Waxy Oil.

higher the percentage of lower molecular weight products, as also observed by Martinez-Escandell *et al.* (1999). This may also serve to explain the relatively high percentage of alkylated aromatics produced by the dehydrogenation of alkylated cyclic alkanes as shown in Figure 7-30.

7.4.3 Molecular grouping of intermediate diesel distillation fraction of Samples C2, and E1a and E1b

By means of comparison with Figure 7-30 the percentages and types of molecular family shown in the diesel intermediate distillate of Samples E1a and (E1) can be described as in Figure 7-31.

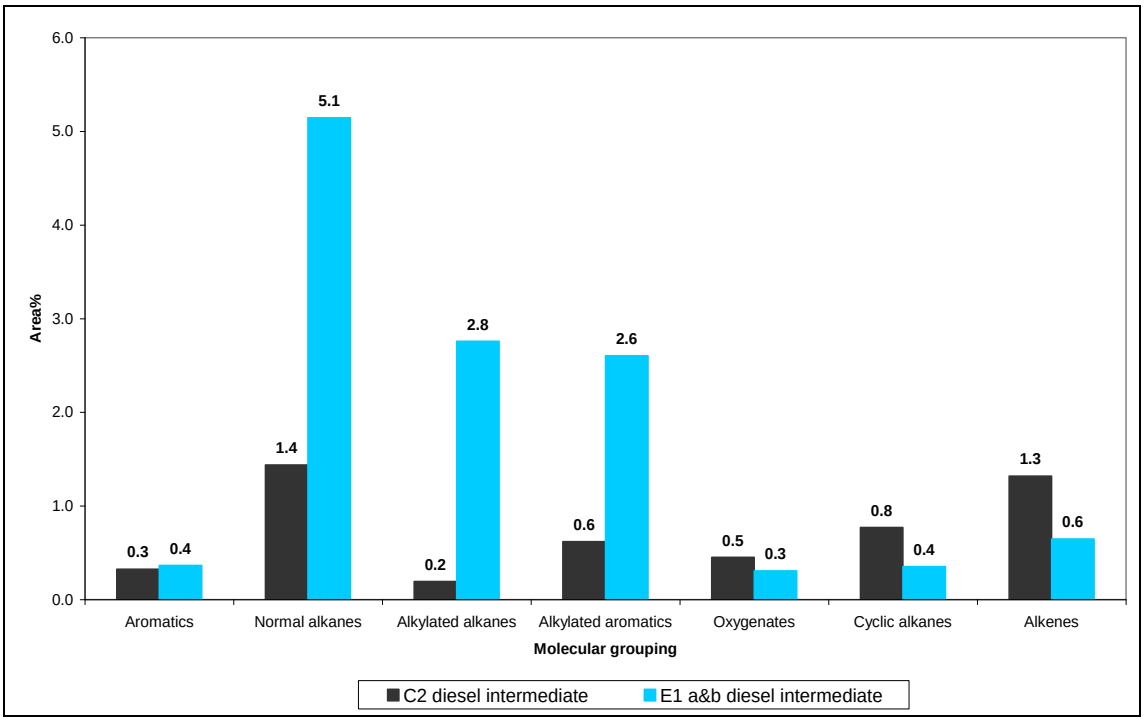

Figure 7-31 Quantitative analysis of molecular groups comprising the diesel fraction of Samples C2, and E1a and E1b distillates[32]

The diesel intermediate fraction presents a less "mature" spectrum of breakdown molecules (Figure 7-31) when compared with the petrol intermediate fraction (Figure 7-30). The "maturity" of the product spectrum is defined in this study as the distribution of intermediate products formed by low-temperature thermal pyrolysis as shown in Figure 7-29.

The product spectrum (Figure 7-31) of the diesel intermediate fraction is dominated by normal alkanes (5.1%), with smaller contributions from alkylated alkanes (2.8%) and alkylated aromatics (2.6%). The higher thermal stability of this fraction is based on the dominance of normal alkanes and the relatively low percentages of the primary breakdown products, namely cyclic alkanes (0.4%) and alkenes (0.6%).

[32] All distillate fractions are shown as a mass percentage of the filtered Waxy Oil.

Compared with the petroleum intermediate fraction of Sample C2 distillates, the diesel intermediate fraction is composed predominantly of normal alkanes (1.4%) and alkenes (1.3%).

7.4.4 Importance of distillate breakdown products to the mechanism of carbonisation

The importance of a detailed discussion of the breakdown product spectrum from low-temperature thermal pyrolysis of Waxy Oil (described above) is that it sheds light on the probable reaction mechanism of the higher molecular weight normal alkanes during carbonisation (otherwise stated as high-temperature thermal pyrolysis).

The lower reactivity of higher molecular weight normal alkanes discussed above and proposed by Domine *et al.* (2002) explains the "crest" of normal alkanes (C_{21}–C_{30}) shown in the GCMS of Sample E1b residue (Figure 7-26). Low-temperature thermal pyrolysis of Waxy Oil does not induce thermal breakdown of these higher molecular weight normal alkanes and thus as the distillate is removed, their concentration increases due to a reduction in the dilution factor. In support of this, Bounaceur *et al.* (2002) also determined the increase in the activation energy required to breakdown *n*-tetradecane compared with *n*-hexane.

Throughout Chapter 7 it has been seen that the thermal stability of normal alkanes limits the concentration of aromatic molecules (be they pure or alkylated). However, to show that a small amount of aromatisation does occur (especially in the distillate fraction of E1b) a simple calculation is possible as shown in Table 7-20.

Table 7-20 Comparison of the total aromatics (including pure and alkylated aromatics) in Sample B (residue) and Sample E1b (residue and distillate)

Fraction	Unit	Sample B	Sample E1b
Aromatics in distillate	**Area%**	0.0[1]	15.2[3]
Aromatics in residue	**Area%**	10.0[2]	1.2[4]
Total aromatics	**Area%**	**10.0**	**16.4**

- Sample B does not have a distillate fraction.
- Cumulative value of both alkylated and pure aromatics in Sample B as given in Table 8.3
- Cumulative value of both alkylated and pure aromatics in petrol and diesel intermediates calculated from Figures 8-23 and 8-33 respectively
- Cumulative value of both alkylated and pure aromatics in Sample E1b residue corrected by the residue yield factor of 0.43

The total area percentage of aromatics in the filtered Waxy Oil (Sample B) is 10.0%. If Sample B is used as a reference, then by calculating the total aromatic area percentage of Sample E1a residue and distillate (16.4%), it is determined that a small amount of aromatisation has occurred. It is further evident that the aromatics are the product of low temperature as the greater percentage thereof is present in the distillate fraction of Sample E1b. This essentially proves that aromatics are formed according to the product breakdown mechanism shown in Figure 7-29.

Both thermal treatment at 410 °C (low-temperature thermal pyrolysis) and carbonisation at 480 °C (high-temperature thermal pyrolysis) are the same types of reaction; it is only that the latter has a higher energy input. At carbonisation temperatures, the normal alkanes (C_{21}–C_{30})

will react by much the same reaction mechanism, forming substituted cyclic alkanes and then substituted aromatics. Complete or incomplete lysis of alkyl substitution on the aromatic ring increases the percentage of pure aromatics which provide the primary "building blocks" for poly-condensation to form poly-aromatic hydrocarbons.

7.5 Conclusions – Waxy Oil modification

This chapter presents data showing the effect of Waxy Oil modification on the molecular composition.

The conclusions drawn are as follows:

- Waxy Oil filtration to less than 0.5 µm is effective in removing the required amount of catalyst to meet the needle coke specification. The lower the micron aperture of the sintered metal filter, the lower the ash content of the Waxy Oil.
- Filtration would be better conducted on the SDO and not the Waxy Oil.
- Distillation of the Waxy Oil would be better conducted at higher vacuum pressure to allow the removal of a greater volume of lighter molecules prior to cracking.
- Distillation (even at higher vacuums) is, however, not considered a viable option due to the distribution of oxygenates throughout the molecular weight range of Waxy Oil. Furthermore, a substantial increase in the molecular weight of the diesel intermediate fraction may present quality problems.
- Thermal treatment at 400–420 °C is effective in the partial destruction of iso-alkanes aliphatic and aromatics, as well as of oxygenates.
- An increase in the thermal treatment temperature serves to increase the cracking severity. However, the experimental set-up used does not promote efficient removal of lighter hydrocarbons from the residue, especially noticeable at 5 bar pressure.
- Reducing the system pressure after 1 h during thermal treatment does increase the removal of lighter hydrocarbons from the residue.
- Lighter cracked molecules remaining in the residue may act as reactivity promoters during carbonisation.
- Distillation of thermally treated residues is the most effective method for removing lighter cracked hydrocarbons from the residue. By using this method it is possible to increase the concentration of normal alkanes to 85% in the residue. This is also effective in reducing the yield of the residue to 45%, based on the virgin filtered Waxy Oil.
- The modification techniques used are not dissimilar to those in the cited literature on aromatic coal tar or petroleum-based residues. However, while dealkylation and the destruction of oxygenated molecules are common goals, the stabilisation of Waxy Oil includes the concentration of long-chain normal alkanes as opposed to aromatics.
- Another difference is that the carbonisation of Waxy Oil will involve an extra aromatisation step.
- Thermal treatment induces the formation of pre-carbonisation products which decrease as the molecular weight increases, thus explaining the stability of the high molecular weight normal alkanes in Waxy Oil.

7.6 Recommendations – Waxy Oil modification

Based on the evidence provided in this chapter, the following recommendations are made:

- The modified Waxy Oils produced should be subject to "static" carbonisation in a test tube to determine the effect of Waxy Oil modification on the anisotropy of the carbon.
- "Static" carbonisation will further test the theory that distillation after thermal treatment is necessary to remove reactivity promoters and thus reduce the anisotropicity of the carbon.
- "Static" carbonisation will promote a layered coke deposition with mosaic microstructures (formed from the more reactive components) at the bottom of the test tube, and flow domains (from the more stable components) higher up the test tube.
- The anisotropicity of the cokes produced will be determined using optical microscopy.

8 "STATIC" CARBONISATION OF MODIFIED WAXY OILS

8.1 Introduction[33]

The aim of this chapter is to provide a correlation between the chemical composition of modified Waxy Oils (produced in Chapter 7) and the microstructure of coke produced by "static" carbonisation.

The chapter is divided into two main themes:

- Firstly, the effect of **catalyst concentration** on various characteristics of Waxy Oil coke is determined, including the coke yield, macrostructure, microstructure, crystal development, carboxy reactivity and air reactivity. The carbonised products of Sample A (unfiltered Waxy Oil) and Sample B (filtered Waxy Oil) are therefore compared.

- Secondly, the effect of **organic modification** of filtered Waxy Oil on the green coke yield, macrostructure and microstructure is determined. The carbonised products of Samples C1, C2, D1, D3, D4, E2 and E1b are compared. The substantial effect of organic modification on the microstructural characteristics of the cokes produced is determined.

The unmodified and modified Waxy Oils produced in accordance with the procedures previously described (Chapter 7) were subjected to **"static" carbonisation** at 480 °C and 5 bar in a test tube, with a heat soaking time of 2 h. A detailed description of the procedure is given in Chapter 5.

Small quantities of the unmodified and modified Waxy Oil samples (approximately 100 g) were placed in separate Pyrex glass test tubes. The modified Waxy Oil samples were carbonised in the same reactor used for the thermal treatments (discussed in Chapter 7). Green cokes A and B were removed from the Pyrex glass tubes and calcined in a muffle furnace at 1 350 °C in argon.

8.2 The role of "static" carbonisation

The mode of carbonisation has a distinct influence on the characteristics of coke produced. In this chapter the fundamental effect of Waxy Oil composition on the coke microstructure is determined and thus "static" carbonisation was preferred to "dynamic" or delayed coking. "Static" carbonisation of heavy residues is by no means novel, neither is the expression of overall anisotropy based on the height percentage of a piece of coke against the longitudinal plane produced in a tube bomb, as determined by Mochida *et al.* (1989). During "static" carbonisation, molecules with a higher reactivity polycondense, initially forming a semi-solid second phase of slightly higher density. The molecules gravitate towards the bottom of the test tube, in much the same way as asphaltenes have been noted to precipitate out of ethylene

[33] The research for Chapter 8 was conducted by the author at the Instituto Nacional del Carbón (INCAR) in Oviedo, Spain under the tutorship of Dr. Ricardo Santa-Maria Ramirez.

tars, as determined by Obara *et al.* (1981), or out of low-sulphur petroleum residues, as determined by Mochida *et al.* (1989).

Although the molecular composition of Waxy Oil is certainly different from that of better known needle coke precursors, certain molecular families (included in Waxy Oil) have previously been shown to increase the reactivity during the onset of carbonisation and tend to form mosaic microstructures at the bottom of the longitudinal plane of the green coke sample. These families include oxygenates, as determined by Dumont *et al.* (2005) and Sima *et al.* (2003), and multi-alkylated hydrocarbons, as determined by Guo *et al.* (2010). In contrast, thermally stable molecules react at higher temperatures within the carbonisation cycle, producing anisotropic coke towards the top of the coke section, as described by Mochida *et al.* (1989).

"Static" carbonisation thus shows the effect of these reactivity promoters (discussed in Chapter 7) in forming a layered microstructure with isotropic coke at the bottom of the test tube and anisotropic coke towards the top of the test tube.

8.3 Effect of catalyst removal on coke characteristics

8.3.1 Green and calcined coke yields of filtered and unfiltered Waxy Oil

The yields of green and calcined cokes from "static" test tube carbonisation and calcination of Samples A and B are shown in Table 8-1.

Table 8-1 Yield of green and calcined cokes from Samples A and B modified Waxy Oil

Experiment number	Sample	Residue yield (%)[1]	Green coke yield (%)[1]	Green coke yield (%)[2]	Calcined coke yield from green coke (%)	Calcined coke yield from Waxy Oil (%)
A	Unfiltered Waxy Oil	100	22.5	22.5	92.0	20.7
B	Filtered Waxy Oil	98.3	19.8	19.8	91.2	18.1

1 Based on carbonisation residue feed

2 Base on fresh Waxy Oil feed

The green coke yield of unfiltered Waxy Oil (Sample A) is slightly higher than that of filtered Waxy Oil (Sample B) which may be ascribed to both the influence of the catalyst and its propensity to increase the coke yield during carbonisation, as previously determined by Wang *et al.* (2001). The calcined coke yield (from green coke) is similar for both A and B. Due to the reactive nature, molecular composition and lower viscosity of Waxy Oil, the green coke yield is low compared with that of better known needle coke feedstocks. With the exception of Low Sulphur Vacuum Residue (23%), the yields of Waxy Oil green cokes are notably lower, e.g. FCCDO (40%) (Mochida *et al.*, 1989).

8.3.2 Macrostructure of Waxy Oil green cokes A and B

There is substantial evidence in the literature to show the effect of precursor molecular composition (specifically utilising co-carbonisation of feeds) on the micro- and macrostructure of green coke (Mochida *et al.*, 1989; Clark *et al.*, 2002). The effect of process conditions, including the introduction of a steam or nitrogen "chaser" on the macropore morphology, has previously been reported (Fu & Newman, 1989; Karacan & Badger, 2003) during dynamic or delayed coking.

To determine whether catalyst removal from Waxy Oil prior to carbonisation has an effect on the comparative macrostructure, photos at different height sections of the coke (formed in the test tube) were taken. A diagrammatic representation of the position of the photos taken in relation to the coke height is shown in Figure 8-1. The experimental procedure is described in Chapter 5, Section 5.3.3.1.

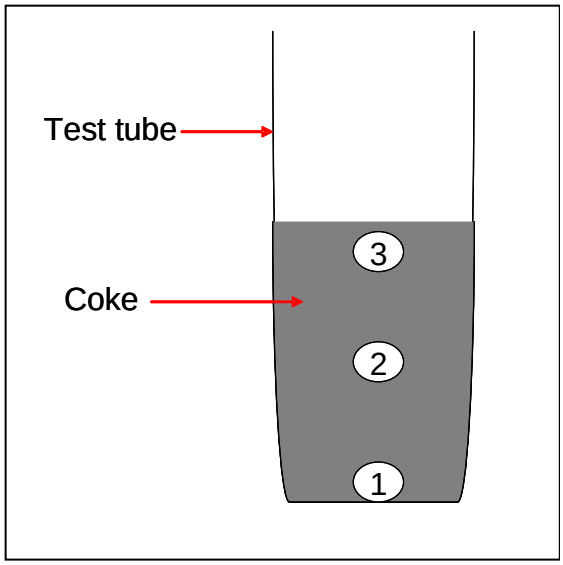

Figure 8-1 Diagram showing the height zones within the coke bed at which photos of the macrostructure were taken

Photos of the coke macrostructure were taken at the bottom (Position 1), middle (Position 2) and top (Position 3) of the coke tube.

The macromorphology of green coke A at the top, middle and bottom of the coke section are shown in Figure 8-2 (a–c) respectively and that of green coke B in Figure 8-2 (e–f) respectively.

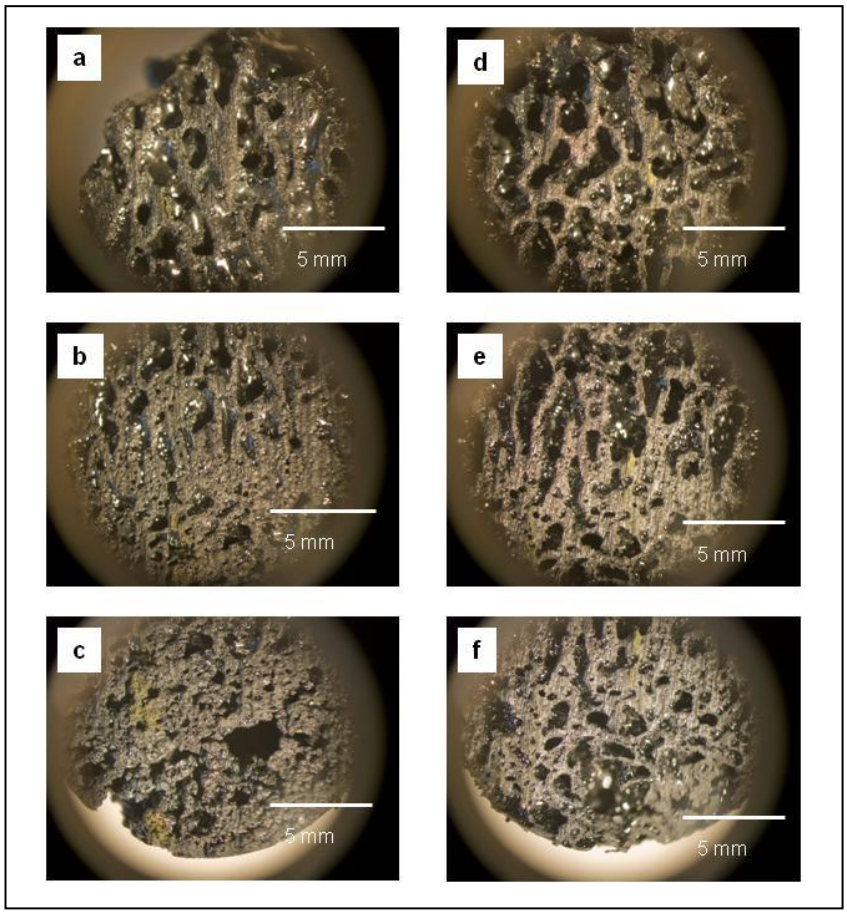

Figure 8-2 Macromorphology of green coke A at the top, middle and bottom of the coke section (a–c) respectively and of green coke B at the top, middle and bottom of the coke section (d–f) respectively

Comparing the macropore morphology of cokes A and B at the top of the coke section (Figures 8-2a and d); green coke B shows a minimal difference in visible macroporosity compared with its green coke A counterpart. The same is true for the middle sections of both green cokes (Figures 8-2b and e). At the bottom of the coke section, however, there is a discernable difference in the macrostructure of the cokes. Green coke A (Figure 8-2c) exhibits a macrostructure that resembles clusters of coke agglomerates, with a grainy texture loosely bonded together, reminiscent of shot coke formation. By contrast, the bottom section of green coke B (Figure 8-2e) shows macrodomain flow.

8.3.3 Optical microscopy of Waxy Oil green cokes A and B

Optical microscopy was used as the method of determining the relative degree of anisotropy through the height of the coke formed in the test tube. The optical micrographs presented **do not**, however, represent the quality of the coke that would be produced by delayed coking. As reactive molecules react to form semi-carbons at a lower temperature than thermally stable molecules, examination of a longitudinal section of the **whole piece of green coke (from bottom to top)** provides an indication of the overall reactivity of the feed from the green coke microstructure which deposits in horizontal layers. As the optical microscopic procedure is central to the determination of the coke microstructure, it is described (in full detail) below and a photo depicting an example of a longitudinal coke section is provided for reference in Figure 8-3.

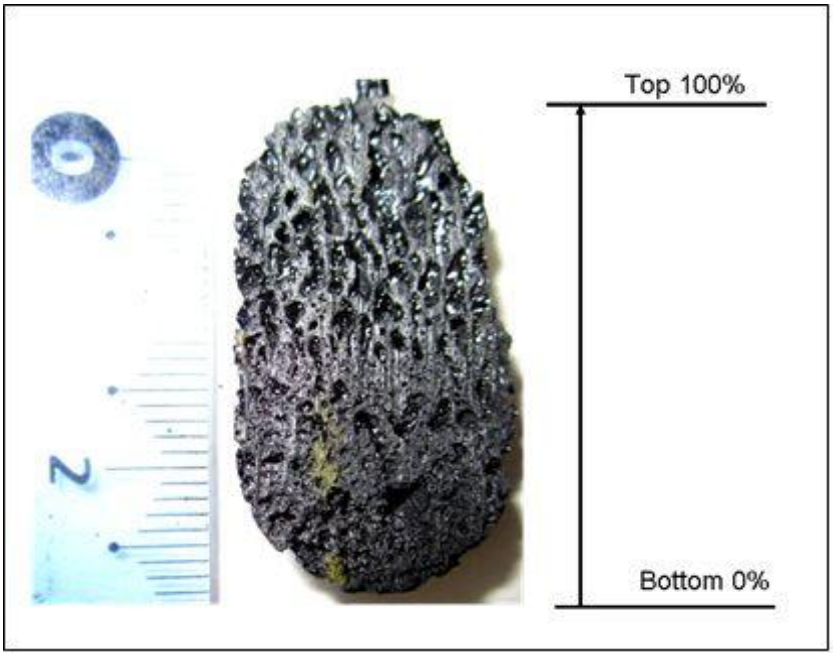

Figure 8-3 Photo of a longitudinal section of green coke

Optical microscopy was done using the longitudinal plane of the whole green coke particle which was mounted in epoxy resin using a Buehler mounting press (150 °C; 29 MPa; 15 min). It was conducted on polished samples using a Zeiss Axioplan microscope with a Liera DC100 monitor. Micrographs were taken of the coke particle from the bottom (0%) to the top (100%), as represented in Figure 8-3, using an automatic step counter every 14 µm along the length. Where the micrograph either contained totally mosaic microstructures or was a mixture of mosaic and flow domains, it was determined to be mosaic. Where the microstructure of the coke (towards the top of the coke section) contained only flow domains, it was determined to have a domain microstructure.

The relative height percentages of mosaic vs. domain flow microstructures for green cokes A and B are shown in Table 8-2.

Table 8-2 Percentages of mosaic vs. domain flow microstructures within a longitudinal section of green cokes A and B

Sample	Waxy Oil modification	Green coke Microstructure	
		Mosaic (%)	Domain (%)
A	No modification	78	22
B	Filtered through 0.5 µm sieve	46	54

A comparison of the quantitative microstructural development of green cokes A and B (Table 8-2) shows that the removal of catalyst from Waxy Oil substantially reduces the height percentage of mosaic microstructures. The dominance of mosaic microstructures in green coke A (78%) is ascribed to the compound effect of the iron oxide catalyst and the thermal reactivity of Waxy Oil molecules. The iron-based catalyst promotes an increase in the height percentage of mosaic microstructures by two means: firstly as an inert barrier to mesophase

formation (specifically visible in Figure 8-5c), limiting the amount of hydrogen transfer, as described by Obara *et al.* (1985) and Menendez *et al.* (1997); and secondly by promoting catalytic dehydrogenation, as described by Wang *et al.* (2001).

Catalyst filtration (green coke B) removes one of the reactivity promoters, as evidenced by the reduction in the height percentage of mosaic microstructures to 46% (ascribed solely to the thermal instability of organic molecules in Waxy Oil) during carbonisation.

8.3.3.1 Optical microscopy of green coke A

Optical micrographs of the top and bottom sections of green coke A are shown in Figure 8-4. Figure 8-4a–c shows micrographs of green coke A at the **bottom** of the longitudinal section of coke with increasing magnification. Figure 8-4d–f shows micrographs of green coke A at the **top** of the longitudinal section of coke with increasing magnification.

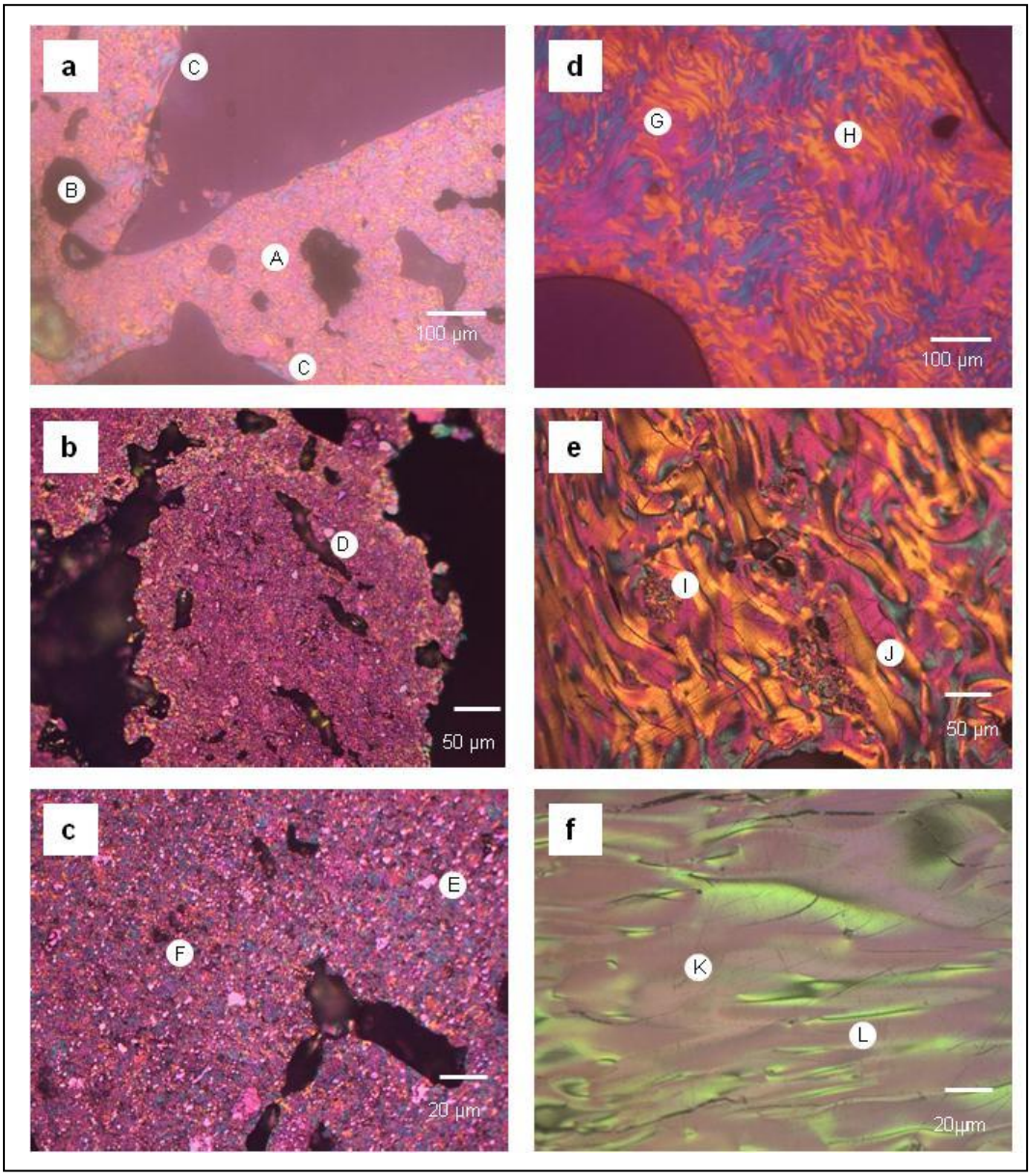

Figure 8-4 Optical micrographs of green coke A at the bottom (a–c) and top (d–f) of the coke section

At the bottom of the coke section, Figure 8-4a shows green coke A to have a fine to medium mosaic microstructure (Position A), with small areas of coarse flow domains (Position B) at the extinction contours of the pores, probably caused by shear forces (attributable to escaping gas) during solidification of the mesophase. There is also evidence of substantial porosity, as shown by Position B. At higher magnification (Figure 8-4b), green coke A displays a "grainy" texture composed of catalyst embedded in the mosaic carbon microstructure (Position D). At the highest magnification (Figure 8-4c), the variance in the size of the catalyst can be differentiated from fine (Position F) to over 6 µm (Position E) as shown by white areas.

The nomenclature used to differentiate between the mosaic and flow domain microstructures of Waxy Oil green coke in Chapter 8 is in accordance with that of Obara *et al.* (1981).

At the top of the coke section (Figure 8-4d), the microstructure is dominated by flow domains. These are composed of a collection of independent micro-domains (approximately 200 x 200 µm) surrounding Positions G and H. They are not axially orientated with one another. The lack of axial orientation (between micro-domains) at lower magnification is probably linked to the low shear rate which allows deformation due to the absence of a dominating flow vector, as previously described by Mochida *et al.* (1994). This is the result of "static" carbonisation. Obviously, as the magnification is increased (Figure 8-4e), the micrograph covers a smaller area and thus the degree of axial orientation appears greater. Also visible in the micrograph are smaller regions of mosaic microstructures (Position I) which are thought to be associated with agglomerations of very fine catalyst. However, the micrograph is dominated by flow domains of indeterminable length (Position J). At the highest magnification (Figure 8-4f), the microstructure of green coke A presents as flow domains (Position K) with uni-axial orientation. The pores (Position L) have a high aspect ratio and run parallel to the domain flow.

The formation of flow domains within the top section of green coke A shows the segregation of carbon microstructures even with the maximum reactivity promoters present during carbonisation.

8.3.4 Optical microscopy of green coke B

Optical micrographs of the top and bottom sections of green coke B are shown in Figure 8-5. Figure 8-5 (a–c) shows micrographs of green coke B at the **bottom** of the longitudinal section of coke with increasing magnification. Figure 8-5 (d–f) shows micrographs of green coke B at the **top** of the longitudinal section of coke with increasing magnification.

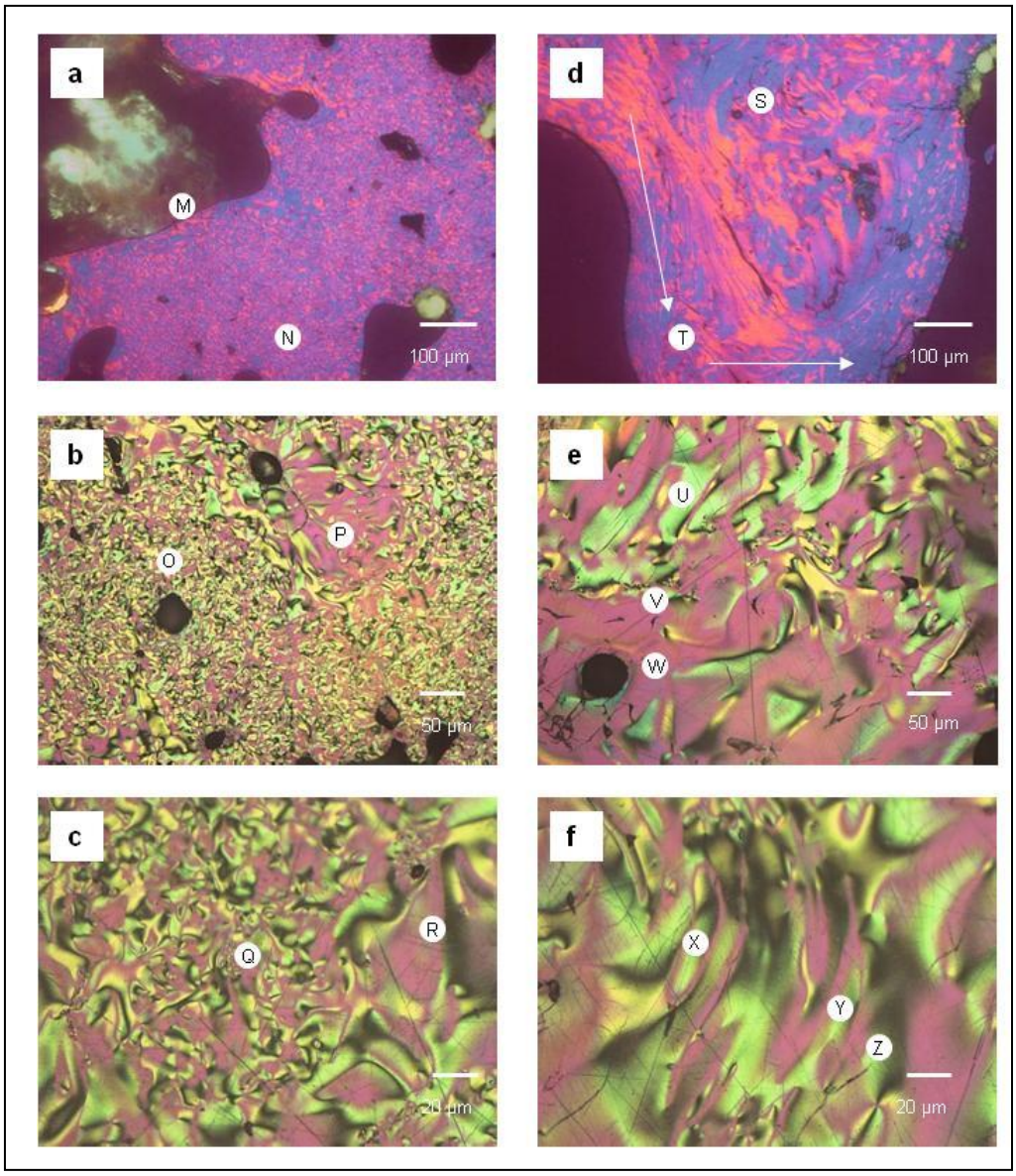

Figure 8-5 Optical micrographs of green coke B at the bottom (a–c) and top (d–f) of the coke section

Whereas the quantitative and qualitative effect of both the catalyst and thermally unstable organics during carbonisation have been established by the microstructure of green coke A, the microstructure of Sample B green coke largely eliminates the effect of the catalyst during carbonisation and therefore its effect on the microstructure.

At the lowest magnification at the bottom of green coke B (Figure 8-5a), the microstructure is a mixture of fine to coarse mosaics (Position N). Independent areas of flow domains (Position M) are evident at the extinction contour of the pores. In comparison with green coke A (Figure 8-4a), there is a notable increase in the frequency of these flow domains around the pores. At higher magnification (Figure 8-5b), the micrograph presents a heterogeneous assembly of microstructural domains of both coarse flow (Position P) and fine to medium mosaics (Position O). At the highest magnification (Figure 8-5c), the most notable omission compared with green coke A (Figure 8-5c) is the catalyst. Again the microstructure shows flow domains (Position R) and more isotropic coarse mosaic microstructures (Position Q).

At the lowest magnification at the top of green coke B (Figure 8-5d), the microstructure is dominated by flow domains of indeterminable length, either straight (Position T) or with a curved geometry (Position S). At higher magnification, the top section of green coke B (Figure 8-5e) shows a general axial flow orientation from the top right to the bottom left of the micrograph (Position U) interspersed with pores which, although possessing a high aspect ratio (Position V), are perpendicular to the flow domain. Of interest is Position W where the domain flow is concentric around a small transverse pore.

The higher reactivity of the molecular composition of Sample B is similar to that reported by Martinez-Escandell *et al.* (1999) who found the formation of very small spheres in the early stages of mesophase development, leading to the formation of coarse mosaics when highly aliphatic vacuum residues were carbonised without prior thermal stabilisation (as seen at the bottom of the coke section).

8.3.4.1 Value of microstructural classification of green cokes A and B

The microstructure of green cokes A and B has been discussed in detail, but their exact classification is perhaps of less importance than the trend that they show. The concept of "reactivity promoters" is defined in this thesis as any compositional characteristic of the Waxy Oil that increases the carbonisation temperature range (by decreasing the temperature at which carbonisation is initiated), increasing the reactivity of the whole system.

Sample A has two reactivity promoters (the iron oxide and the thermal instability of the Waxy Oil organic molecules), while Sample B has one reactivity promoter (the thermal instability of the Waxy Oil organic molecules). However, both Samples A and B are composed of a percentage of thermally stable alkanes which form domains within the higher carbonisation temperature range and are clearly distinguished from the mosaics which form at lower temperatures, falling to the bottom of the test tube due to their increased density. It is this characteristic of Waxy Oil "static" carbonisation that allows the quantitative differentiation of the microstructure based on the height of the green coke section as reported in Table 8-2. The same procedure is used to differentiate between the organic modifications of Waxy Oil, reported in later in Section 8.4.

8.3.5 Analysis of calcined cokes A and B

8.3.5.1 EDX of Waxy Oil Sample A calcined coke

The EDX of Sample A green coke is shown in Figure 8-6.

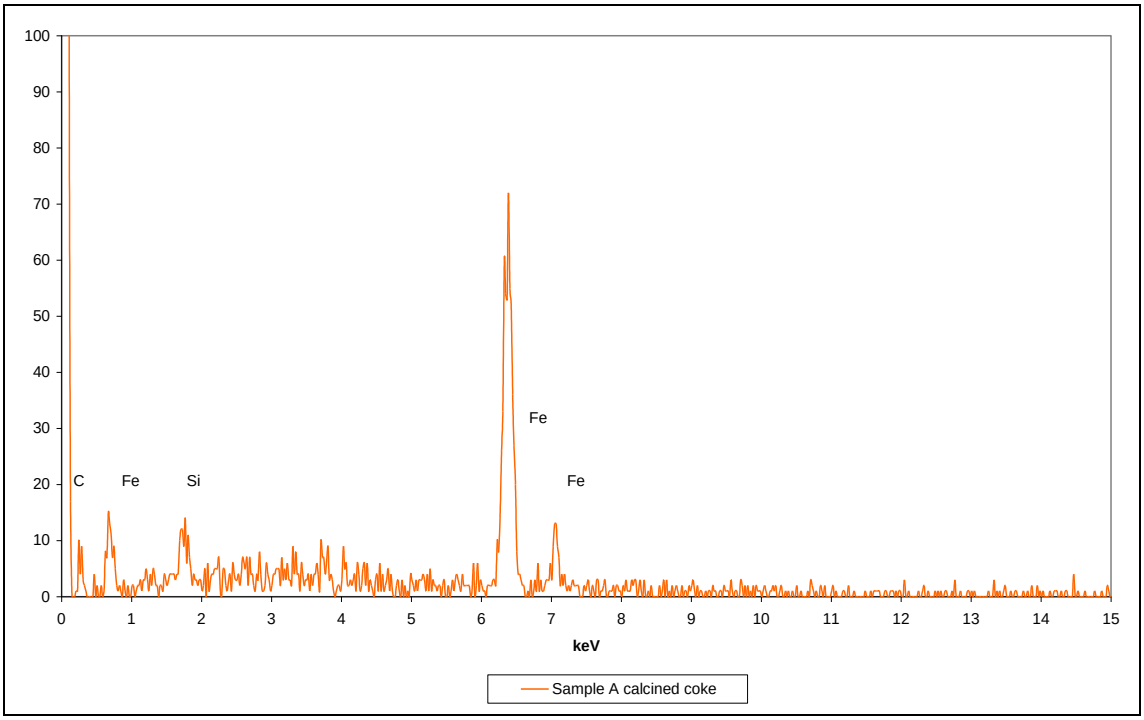

Figure 8-6 EDX of Sample A Waxy Oil calcined coke

Figure 8-6 shows that the mineral composition of the lower portion of calcined coke A is dominated by iron (at approximately 6.5 and 7.1 keV). Another mineral at lower intensity is silicon (approximately 1.7 keV).

8.3.5.2 Scanning Electron Microscopy of Waxy Oil calcined cokes A and B

Scanning Electron Microscopy (SEM) was conducted down a longitudinal section on both Samples A and B calcined coke. The same numbering system used in Figure 8-1, namely Positions 1, 2 and 3, was utilised.

SEM images of Sample A calcined coke at Position 1 are shown in Figure 8-7.

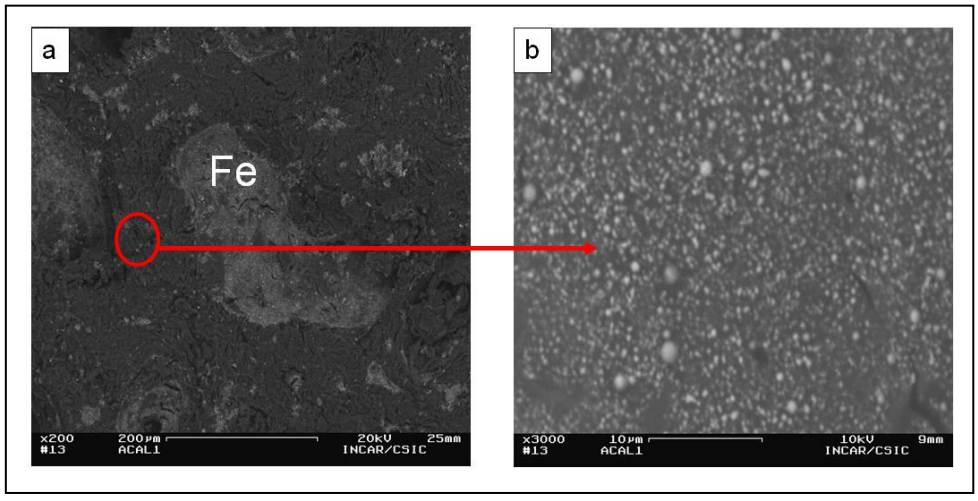

Figure 8-7 Scanning electron micrographs of Sample A calcined coke at Position 1 (bottom) with increasing magnification from (a) to (b)

Figure 8-7 (a) shows agglomerates of catalyst particles of various sizes (the largest being approximately 300 µm in length and 50 µm in width) visible at low magnification in Position 1 (bottom) of Sample A calcined coke, indicated by the lighter shade of grey. However, shown in Figure 8-7b is a region of the coke at higher magnification showing the frequency of smaller catalyst particles (less than 10 µm) embedded in the carbon microstructure.

SEM images of Sample B calcined coke are shown in Figure 8-8 (Position 1) at the bottom of the coke section.

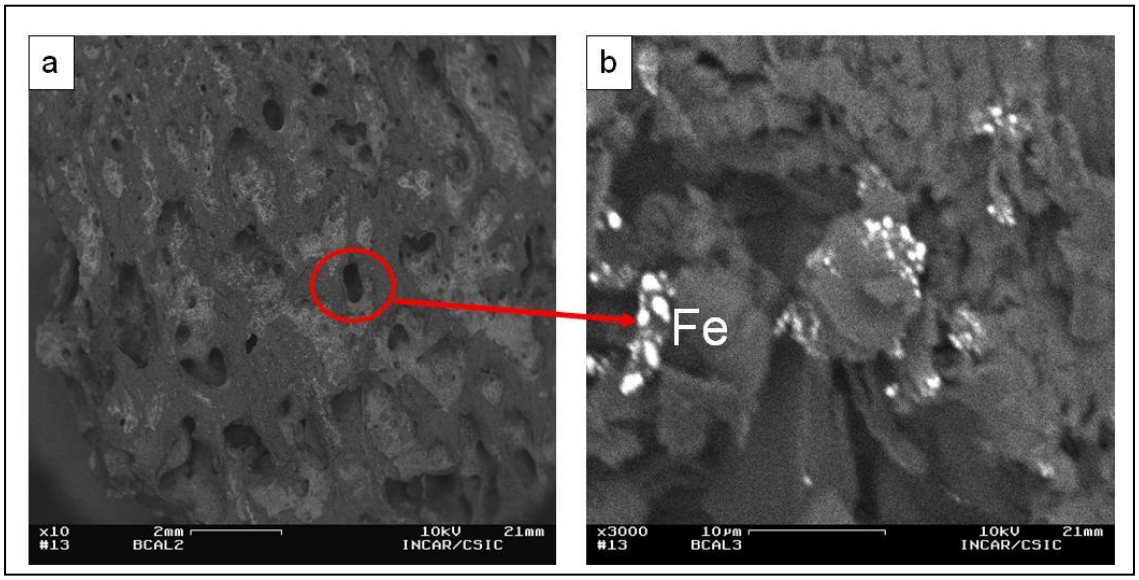

Figure 8-8 Scanning electron micrographs of Sample B calcined coke at Position 1 (a) and (b)

Figure 8-8a shows a substantially lower amount of iron (especially higher PSD particles) with lower agglomeration sizes at lower magnification. At higher magnification, Figure 8-8b shows sparsely populated agglomerates of smaller catalyst particles (appearing as white areas), but far fewer than shown for calcined coke A (Figure 8-7b).

8.3.6 Raman spectroscopy of Waxy Oil calcined cokes

Raman spectroscopy was conducted on samples of calcined coke A and B at various height positions along the longitudinal plane of the piece of coke (as previously defined in Figure 8-1). The degree of disorder was estimated from the relationship I_D:I_T, where I_D corresponds to the intensity of the D band (1350 cm^{-1}) and I_T corresponds to the total intensity of all first-order region bands (D, G, D´ at 1350, 1580 and 1620 cm^{-1} respectively). The I_D:I_T ratio is shown as an insert to Figures 8-9, 8-10 and 8-11.

A comparison of the bottom zone of calcined cokes A and B is shown in Figure 8-9.

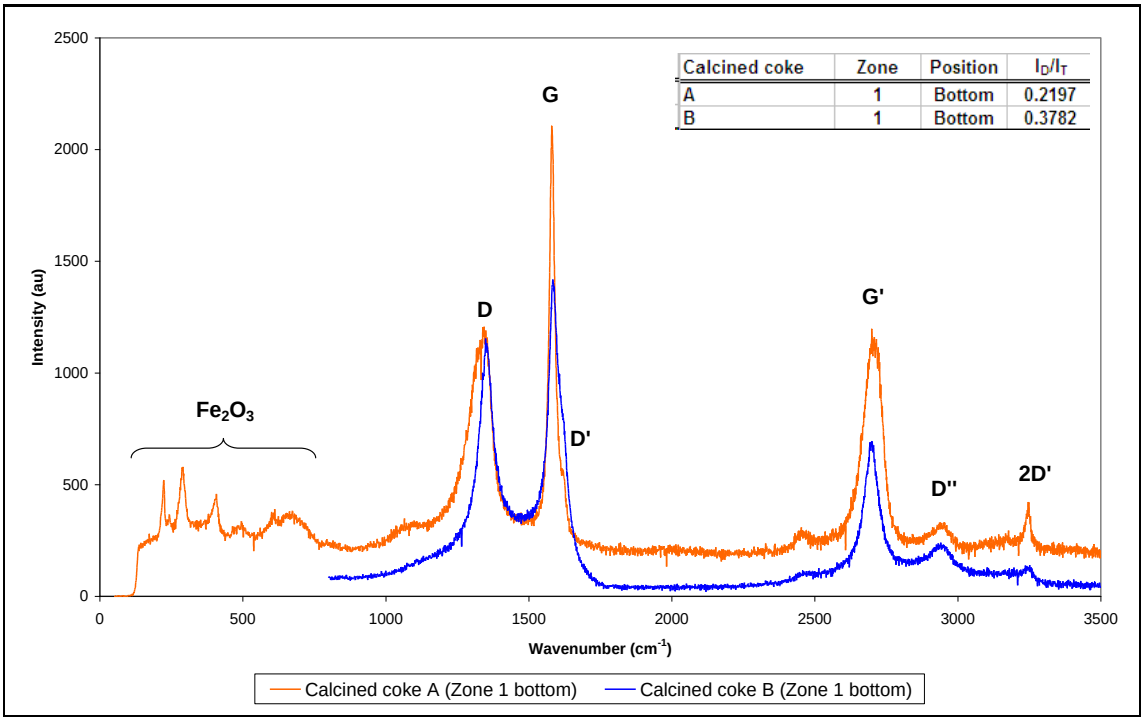

Figure 8-9 Raman spectroscopy trace of calcined coke A (zone 1 bottom) vs. calcined coke B (zone 1 bottom)

The bottom part of calcined coke A shows evidence of the iron catalyst at lower wave numbers (100–750 cm^{-1}) which is absent in calcined coke B. Furthermore, calcined coke A shows well-defined first- and second-order spectra with a high degree of order. The second-order spectrum for calcined coke B is less defined. In terms of the degree of order (shown as an insert to Figure 8-9), calcined coke A is substantially more ordered than calcined coke B. Although both samples possess a mosaic microstructure at the bottom of the coke, calcined coke A has a high iron concentration. The graphitisation mechanism is consequently dominated by catalysis forming relatively pure graphite, therefore on average increasing the order compared with calcined coke B with little or no catalyst.

In order to evaluate the structural order through the height of **calcined coke A**, the spectra obtained from the bottom, middle and top zones of the coke are shown in Figure 8-10.

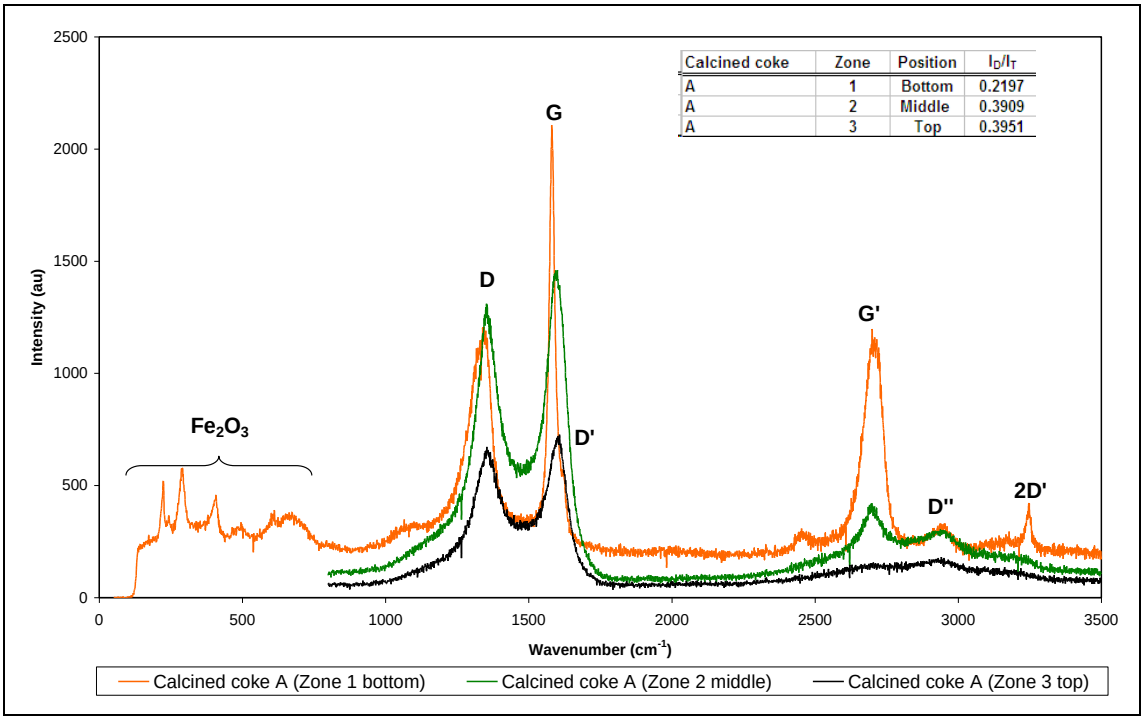

Figure 8-10 Raman spectroscopy trace of calcined coke A (zone 1 bottom), zone 2 (middle) and zone 3 (top)

The second-order spectrum of the middle (zone 2) and top (zone 3) of calcined coke A is less well defined as the catalyst concentration within these zones is lower than in the bottom of the coke (zone 1). The degree of order (shown as an insert to Figure 8-10) shows that the effect of catalytic graphitisation is severely diminished in zones 2 and 3 due to the catalyst gravitating towards the bottom of the test tube (zone 1) during the initial heating phase of carbonisation. A comparison between zones 2 and 3 is perhaps confusing as the effects of both catalytic graphitisation and crystal order development as a function of thermal treatment (and depending on the anisotropy of the microstructure) need to be considered. From the micrographs (Figure 8-4d–f) and the quantitative analysis of microstructural anisotropy (Table 8-2) it is clear that flow domains preside at the top of calcined coke A, while in the middle the microstructure is more isotropic. However, in the middle there is more likely to be fine catalyst which influences the degree of order. Thus it is more correct to make a comparison only between zone (1) and zones (2 and 3).

In order to evaluate the structural order through the height of calcined coke B, the spectra obtained from the bottom, middle and top zones of the coke are shown in Figure 8-11.

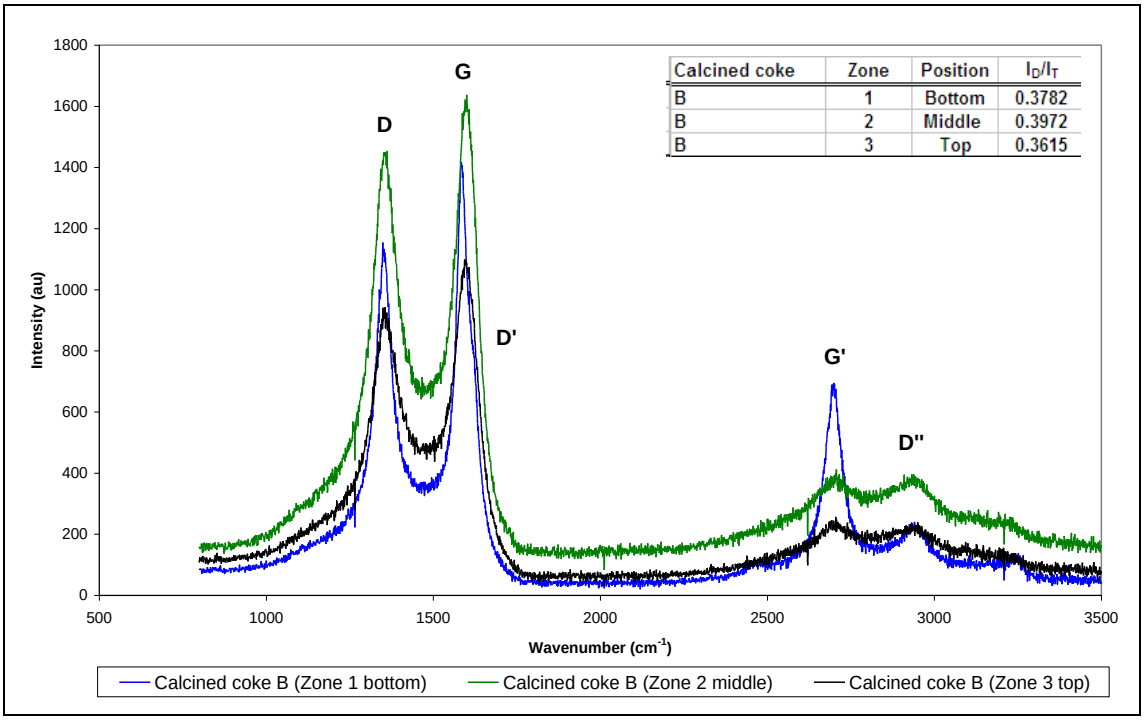

Figure 8-11 Raman spectroscopy trace of calcined coke A (zone 1 bottom), zone 2 (middle) and zone 3 (top)

Within the bottom section (zone 1) of calcined coke B there is SEM evidence of a miniscule amount of catalyst (Figure 8-8b), at least when compared with calcined coke A (Figure 8-7b). While microstructurally both the bottom (zone 1) and middle (zone 2) have a mosaic microstructure, based on a comparison of the micrographs there do appear to be isolated areas of domain flow within the middle section. So although from a microstructural analysis the Raman order should be higher in the middle section, it is not. Even the miniscule amount of catalyst in the bottom section, which from the SEM would appear insignificant, promotes catalytic graphitisation and therefore, on average, the order is higher. Comparison of zone 2 (middle) with zone 3 (top) is the only comparison where the effect of the catalyst can be discounted; the higher order reported for zone 3 (top) is based on its greater anisotropy and hence the higher Raman order due to thermal graphitisation.

8.3.7 Carboxy (CO_2) reactivity of Waxy Oil calcined cokes

Samples of Waxy Oil calcined coke (-200 µm) were heated in a thermogravimetric analyser to 1 000 °C (10 °C.min^{-1}) with continued isothermal conditions for 1 h in the presence of carbon dioxide (150 ml.min^{-1}) and nitrogen (150 ml.min^{-1}). The carboxy reactivity profile was determined for calcined cokes A and B. The graph of the TGA reactivity profiles is shown in Figure 8-12 and the DTG reactivity profiles in Figure 8-13.

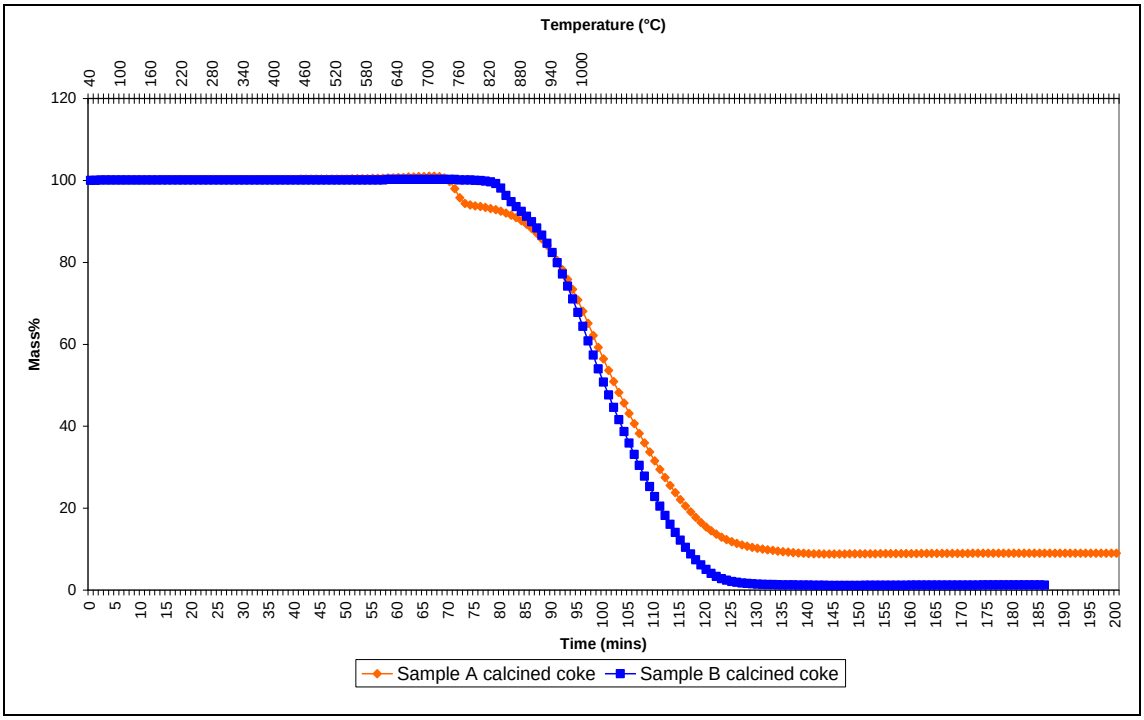

Figure 8-12 TGA carboxy (CO_2) reactivity profile of calcined cokes A and B

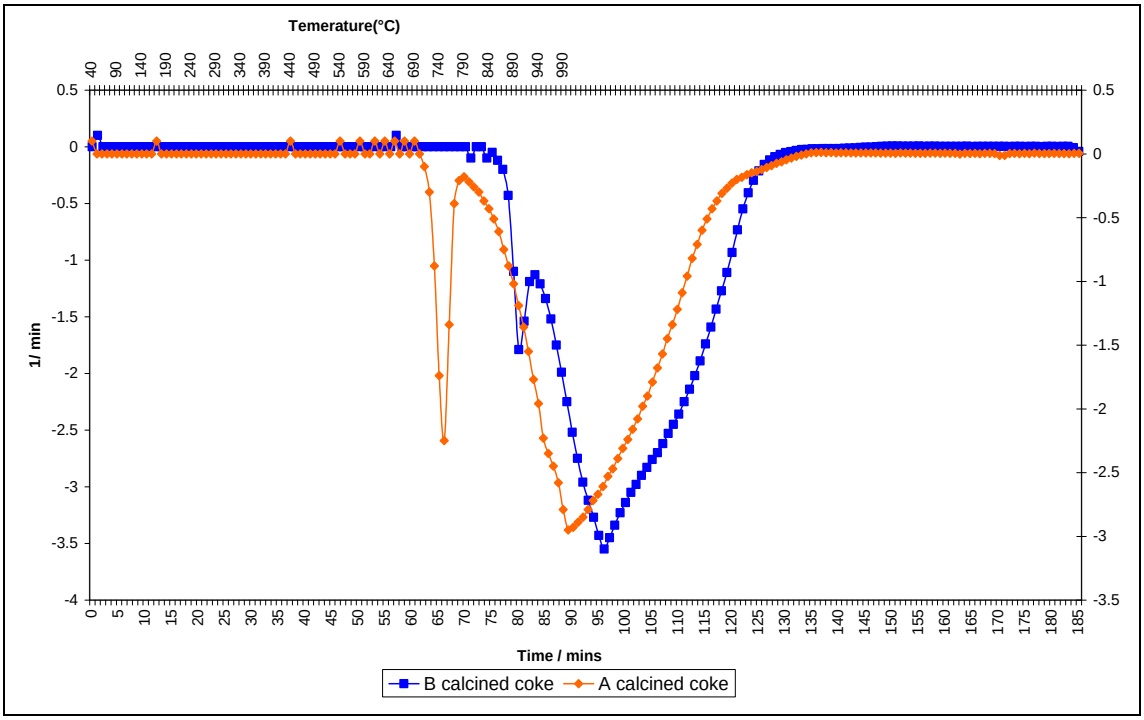

Figure 8-13 DTG carboxy (CO_2) reactivity profile of calcined cokes A and B

In general, Sample A shows a mass loss of approximately 10% initiated at a temperature of 730 °C (Figure 8-12). Further substantial mass loss is then only evident at 860 °C. The residuum of calcined coke A is approximately 10%. The initial mass loss for Sample B (Figure 8-12) occurs at a higher temperature (850 °C). However, the next gradient of mass loss is steeper than for calcined coke A. The residuum of calcined coked B is negligible.

It is convenient to calculate the reactivity in two ranges, i.e. **before 1 000 °C** and **after 1 000 °C under isothermal conditions.**

As shown in Figure 8-12, the mass loss from calcined coke A is in a window of 270 °C (between 730 and 1 000 °C; 32.6% mass loss), while the mass loss window for calcined coke B is 210 °C (between 790 and 1 000 °C; 36.0% mass loss).

As shown in Figure 8-12, the second mass loss range of calcined coke A at isothermal conditions is in a time window of 43 min (between 96 and 143 min; 59.05%) until a stable residuum mass is attained, while that of calcined coke B is in a time window of 47 min (between 96 and 143 min; 63.2%) until a stable residuum mass is attained. The mass loss rates for calcined cokes A and B are similar (1.37 and 1.34%.min^{-1} respectively). In summary, the initial DTG reactivity peak for calcined coke A (Figure 9-13) is probably enhanced by iron catalysis compared with the lower-intensity initial peak at a higher temperature for calcined coke B.

8.3.8 Air reactivity of Waxy Oil calcined cokes

Samples of Waxy Oil calcined coke (-200 µm) were heated in a thermogravimetric analyser to 1 000 °C with an air flow of 150 ml.min^{-1} and a nitrogen flow of 150 ml.min^{-1}. The air reactivity profile was determined for the calcined cokes A and B. The graph of the TGA reactivity profiles is shown in Figure 8-14 and the DTG reactivity profiles in Figure 8-15.

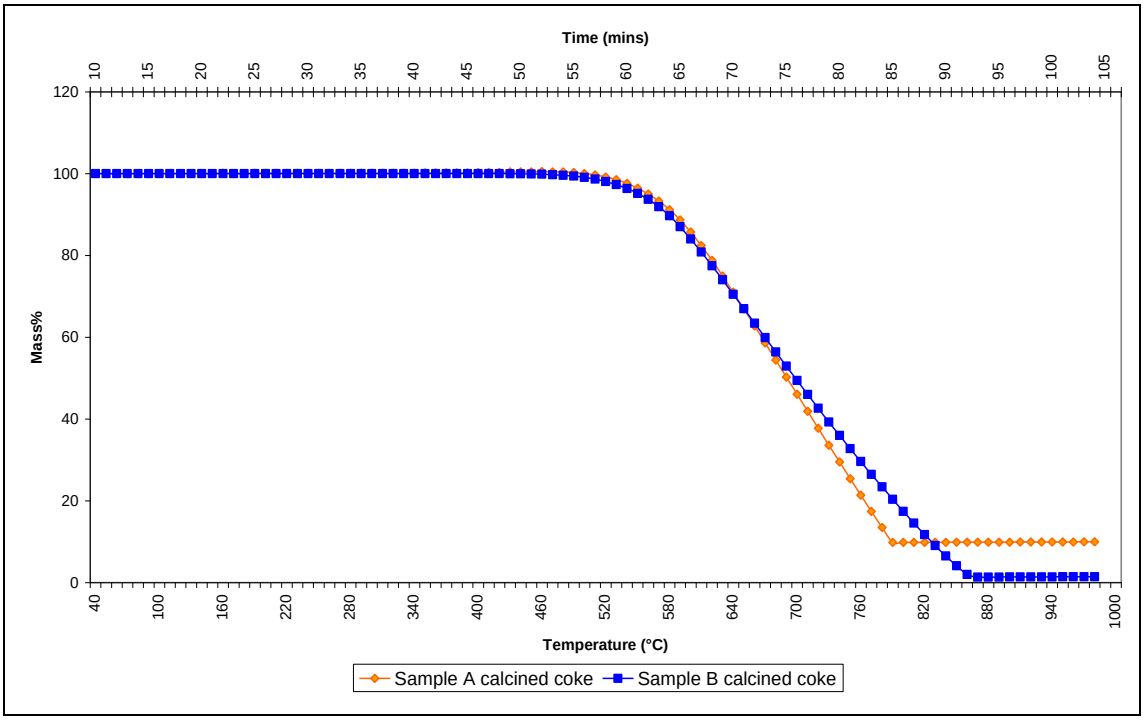

Figure 8-14 TGA air reactivity profile of calcined cokes A and B

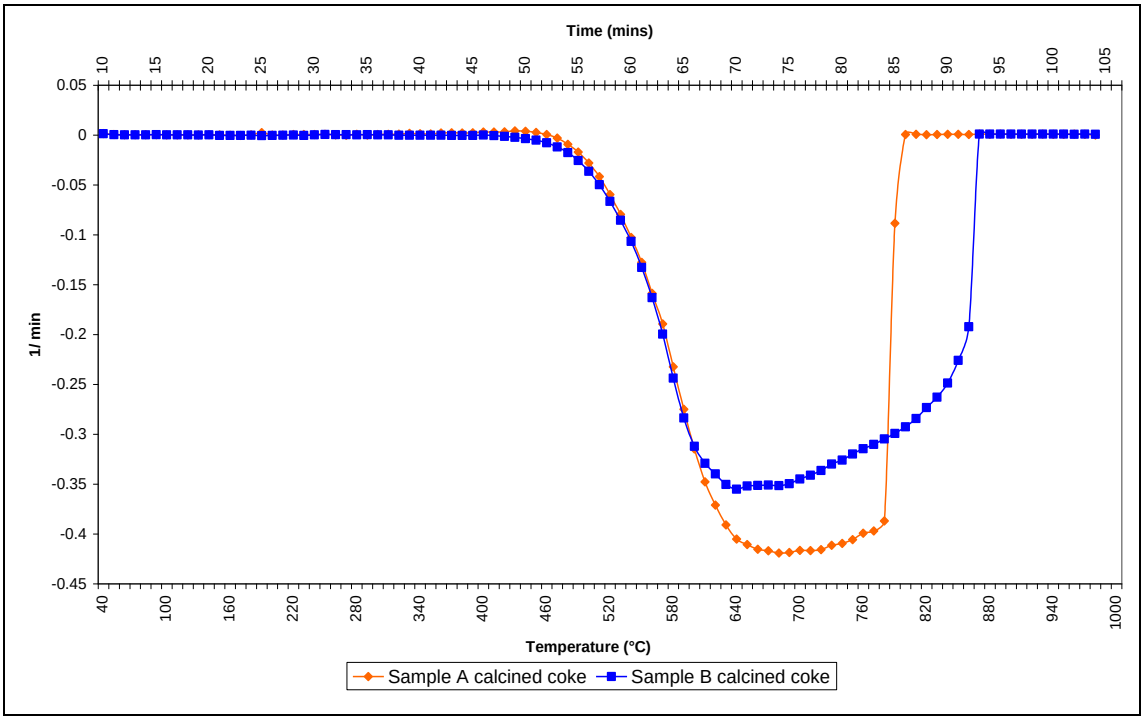

Figure 8-15 DTG air reactivity profile of calcined cokes A and B

As shown in Figure 8-14, calcined coke A shows an initial slight mass increase between 400 and 490 °C, which is probably due to the oxidation of iron. Calcined coke A shows an oxidation window of 290 °C (between 500 and 790 °C), whereas calcined coke B has a larger oxidation temperature window of 460 °C (between 410 and 870 °C). The reactivity profile of both samples (from onset of mass loss to equilibrium) indicates that the reactivity of calcined coke A (0.31%.°C^{-1}) is slightly higher than of calcined coke B (0.21%.°C^{-1}). The higher stable residual mass of calcined coke A is accounted for mainly by the higher catalyst content.

The DTG analysis of the reactivity profiles shown in Figure 8-15 indicates a similar initial reaction rate for both calcined cokes A and B, between 450 and 600 °C, which indicates that the iron does not catalyse an increase in the reactivity of calcined coke A in this temperature range.

8.3.9 The difference in the profiles of air and carboxy reactivity

As determined in Chapter 6, calcination induces a substantial reduction of iron oxide to elemental iron, which has previously been described as a good catalyst for both carboxy and air reactivity.

In carbon dioxide, minimal oxidation of the catalyst would occur so the sharp mass loss peak is attributed to iron catalysis. In air, the elemental iron portion of the catalyst is slowly re-oxidised as the temperature increases, which may account for the absence of a sharp peak as seen for the carboxy reactivity since iron oxide is a poor catalyst for both reactivities.

8.4 The effect of molecular modification of Waxy Oil on green coke microstructure and yield

8.4.1 Waxy Oil green coke yield and quantitative optical microscopy

The green coke yield and quantitative microscopic analysis of the carbonisation of Samples C1, C2, D1, D3, D4, E2 and E1b are shown in Table 8-3.

Table 8-3 Green coke yield and quantitative optical microscopic analysis of carbonised samples of distilled and thermally treated, filtered Waxy Oil

Sample	Waxy Oil modification	Residue yield (%)[2]	Green coke			
			Yield[1]	Yield[2]	Microstructure[3]	
			(%)	(%)	Mosaic (%)	Domain (%)
C1	Sample B distilled (480 °C at -0.9 kPa)	87.0	21.9	26.0	41	59
C2	Sample B distilled (440 °C at -0.9 kPa)	94.3	20.8	22.0	50	50
D1	Sample B thermally treated (400 °C, 5 bar, 2 h)	73.1	19.7	27.0	38	62
D3	Sample B thermally treated (410 °C, 5 bar, 2 h)	58.7	17.5	29.8	36	64
D4	Sample B thermally treated (420 °C, 5 bar, 2 h)	49.6	15.2	30.6	36	64
E2	Sample B thermally treated (410 °C, 5 bar, 1 h at 5 bar and 1 h at 1 bar)	45.2	14.9	32.9	22	78
E1b	Sample B thermally treated (410 °C, 5 bar, 2 h, distilled to 325 °C under nitrogen)	43.0	15.5	36.3	0	100

1 Based on carbonisation residue feed

2 Based on fresh Waxy Oil feed

3 The percentage of the flow domain and isotropic areas of the micrographs are representative of the middle of the coke section and the left and right adjacent to the Pyrex glass tube

Before the effect of the modifications on the green coke yield **based on the residue** is determined, it is important that it is initially determined **based on the fresh Waxy Oil feed** (iron free). The green coke yield of the carbonisation of the two distilled samples (C1 and C2) is similar to that of Sample B. Thereafter there is a decreasing green coke yield (based on fresh Waxy Oil feed) as the temperature increases and the pressure of the modification temperatures is reduced. This is not unexpected as when the thermal treatment temperature increases and the pressure drops, lighter molecules are produced and, secondly, report to the

distillate fraction. The discussion of the effect of Waxy Oil pre-carbonisation modification on the green coke yield (discussed below) is **based on the residue and not the fresh feed.**

The distillation of filtered Waxy Oil to 440 °C (Sample C2) produced a green coke with approximately the same yield as that of the filtered Waxy Oil (Sample B). This is not unexpected as only 5% of the mass was removed. Sample C1 produced a green coke with a slightly higher yield, which can be ascribed to the mild thermal treatment conditions and removal of lighter cracked hydrocarbons. This is evident in the lower residue mass. The green coke yield for the thermal treatments at 5 bar indicates that as the temperature is increased (producing lighter distillates), the residue is reduced and so the carbon residuum yield increases.

The experiment aimed at removing lighter cracked hydrocarbons from the residue (Sample E2) by reducing the pressure during thermal treatment resulted in an increase in the green coke yield.

Sample E1a was not subjected to "static" carbonisation but rather was distilled under nitrogen to effect complete removal of the lighter cracked hydrocarbons in the residue. Thus it is not surprising that the residue percentage relative to the Waxy Oil is reduced whereas the green coke yield of Sample E1b increases to 36.3%. The yield of Sample E1b is similar to those obtained from the pyrolysis and distillation of a highly aliphatic vacuum residue, as reported by Martinez-Escandell *et al.* (1999) who determined coke yields of between 30 and 40%.

Thus, while it is possible to increase the green coke yield of filtered Waxy Oil from 22.0% to 36.3%, the yield is still comparatively low compared with residues with a greater aromaticity, as described by Mochida *et al.* (1989) and Marsh *et al.* (1999). Although Fanjul *et al.* (2002) used air blowing to increase the carbonisation yield and Wang *et al.* (2001) achieved the same by the addition of iron oxide, both of these methods also decrease the anisotropy of the coke and are thus not viable for this study.

Another possible method would be to conduct the carbonisation at a lower temperature, as previously reported by Eser *et al.* (1989). However, all the cited literature refers to highly aromatic feeds. Waxy Oil, being a highly aliphatic feedstock, is subject to cracking reactions (even of thermally stable molecules) at carbonisation temperatures. Historically, the cited literature (Sangrama *et al.*, 2010; He *et al.*, 2003) using long-chain paraffins as a feed has been dedicated to the formation of lower molecular weight alkenes from higher molecular weight normal alkanes. It is therefore suggested that lower carbonisation temperatures may not completely effect aromatisation of the normal alkanes and thus promote polymerisation of the alkenes.

Samples C1 and C2 modified Waxy Oils are clearly very different (in terms of their respective concentrations of both alkylated and pure aliphatic/aromatic molecules, as described in Chapter 7, Section 7.2). The quantitative comparison of their microstructure (Table 8-3) indicates that while C1 green coke does show a marginal improvement in the height percentage of domain flow (59 vs. 50% for C1 and C2 green cokes respectively), there is still a substantial percentage of carbon at the bottom of the coke section with a mosaic microstructure. One similar characteristic both these modified Waxy Oils share is the relatively high concentration of oxygenates [Sample C1 (10.34%) and Sample C2 (11.05%)], which may explain the height percentage of mosaic microstructures (41–50%).

Thermal treatment at 5 bar pressure between 400 and 420 °C did increase the relative percentage of domain microstructures [D1, D3 and D4 (62–64%) respectively] in comparison with the distillation experiments. However, there was no specific conclusive evidence to suggest a substantial influence of thermal treatment temperature (within this group of samples) on the microstructure. As discussed in Chapter 7, Section 7.2.4, thermal treatment does substantially reduce the effect of two of the reactivity promoters, namely oxygenates and multi-alkylated alkanes, and thus the increase in the overall anisotropy of the green coke is validated. As there is still a substantial percentage of mosaic microstructures (36–38%) within these three cokes, it is concluded that the lighter hydrocarbons remaining in Samples D1–D4 act as reactivity promoters, as discussed in Chapter 7, Section 7.2.4.

Reducing the pressure during thermal treatment removes much of the lighter hydrocarbons from the residue (Sample E2). This increases the degree of anisotropy to 78%. Distillation of the residue after thermal treatment at 410 °C removes the great majority of lighter hydrocarbons from the pre-carbonisation residue. The microstructural anisotropy of green coke E1b consequently increases to 100% domain flow. The microstructural analysis of green coke E1b is discussed in greater detail below.

8.4.2 Optical microscopy of Waxy Oil green coke E1b

Although a microstructural classification of all the green cokes was conducted (in order to determine the relative quantitative anisotropy listed in Table 8-3), it would be of little benefit to describe the micrographs in detail (as was done for green cokes A and B) as they all show similar isotropic microstructures towards the bottom of the coke section and anisotropic microstructures towards the top of the coke section. The only variance is the height percentage at which there is a change in the morphology of the microstructure.

However, as the aim of this study is to increase the anisotropy of the green coke and it is reported that green coke E1b is composed solely of flow domains, a comparative microstructural description between the bottom and top of the coke section is provided in Figure 8-16. Figure 8-16 (a) shows the microstructure of green coke E1b at the bottom of the coke section, while Figure 8-16 (b) is also a micrograph of the bottom section of green coke E1b, just at a higher magnification. Figures 8-16 (c and d) show micrographs of the top section of green coke E1b.

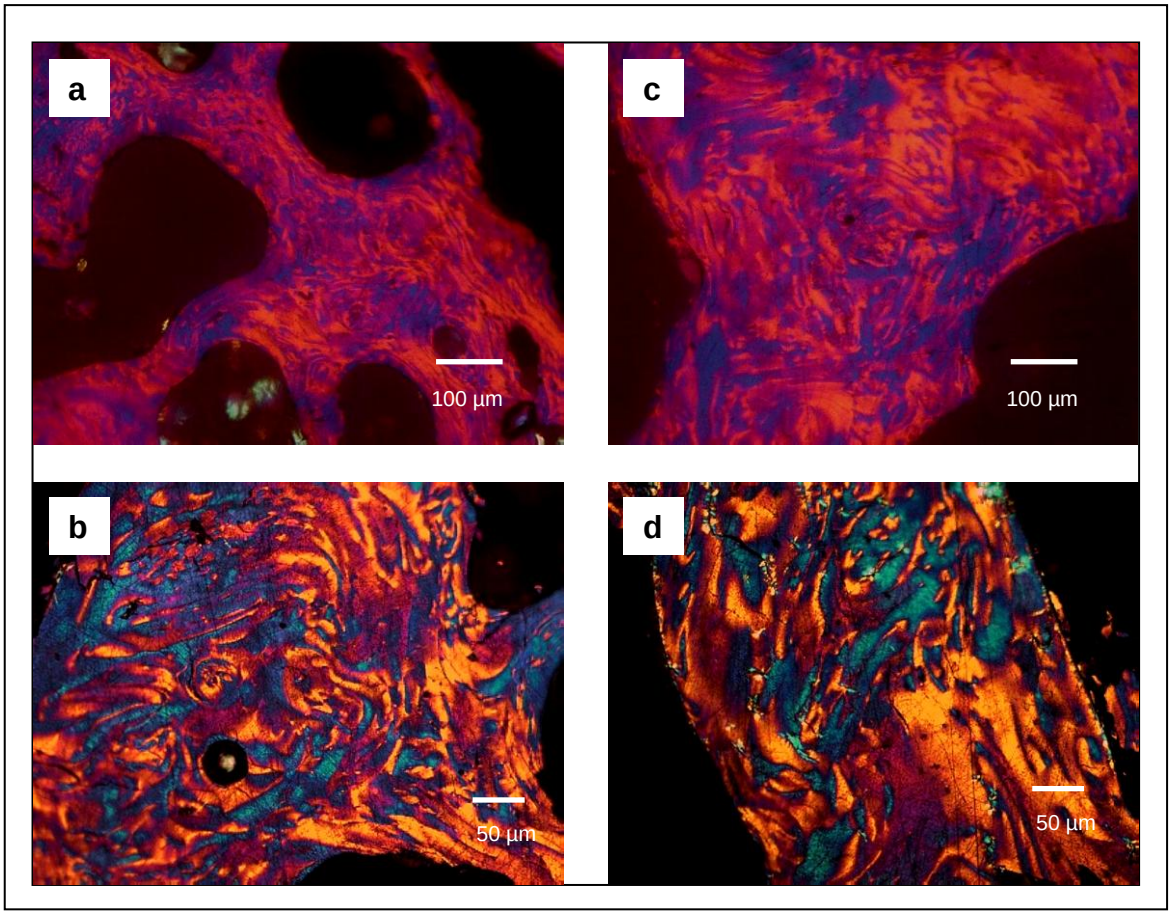

Figure 8-16 Optical micrographs of the bottom (a–b) and top (c–d) sections of green coke E1b

As has been observed in the preceding micrographs of green cokes A and B (Figures 8-4 and 8-5 respectively), the more reactive species form mosaic coke at the bottom of the coke section and with an increase in height the microstructure becomes all the more anisotropic.

Thus it is interesting to note that micrographs taken of the bottom (Figure 8-16a) and top (Figure 8-16c) of E1b green coke have a similar domain flow microstructure. One notable difference is that at the bottom of E1b there appears to be a greater porosity, which dictates the flow vector of the domains. The similarity in the microstructure is also evident when micrographs of the top (Figure 8-16b) and bottom (Figure 8-16 (d)) of green coke E1b are compared at higher magnification.

The micrographs of green coke E1b at the bottom of the coke section (0%) and at the top (100%) shown above in Figure 8-16a–d have flow domain microstructures. A series of micrographs showing the microstructure of green coke E1b through the longitudinal height section of the coke is shown in Figure 8-17a–d, in accordance with a similar procedure described by Mochida *et al.* (1989) when examining the effect of co-carbonising blends of LSVR and FCCDO.

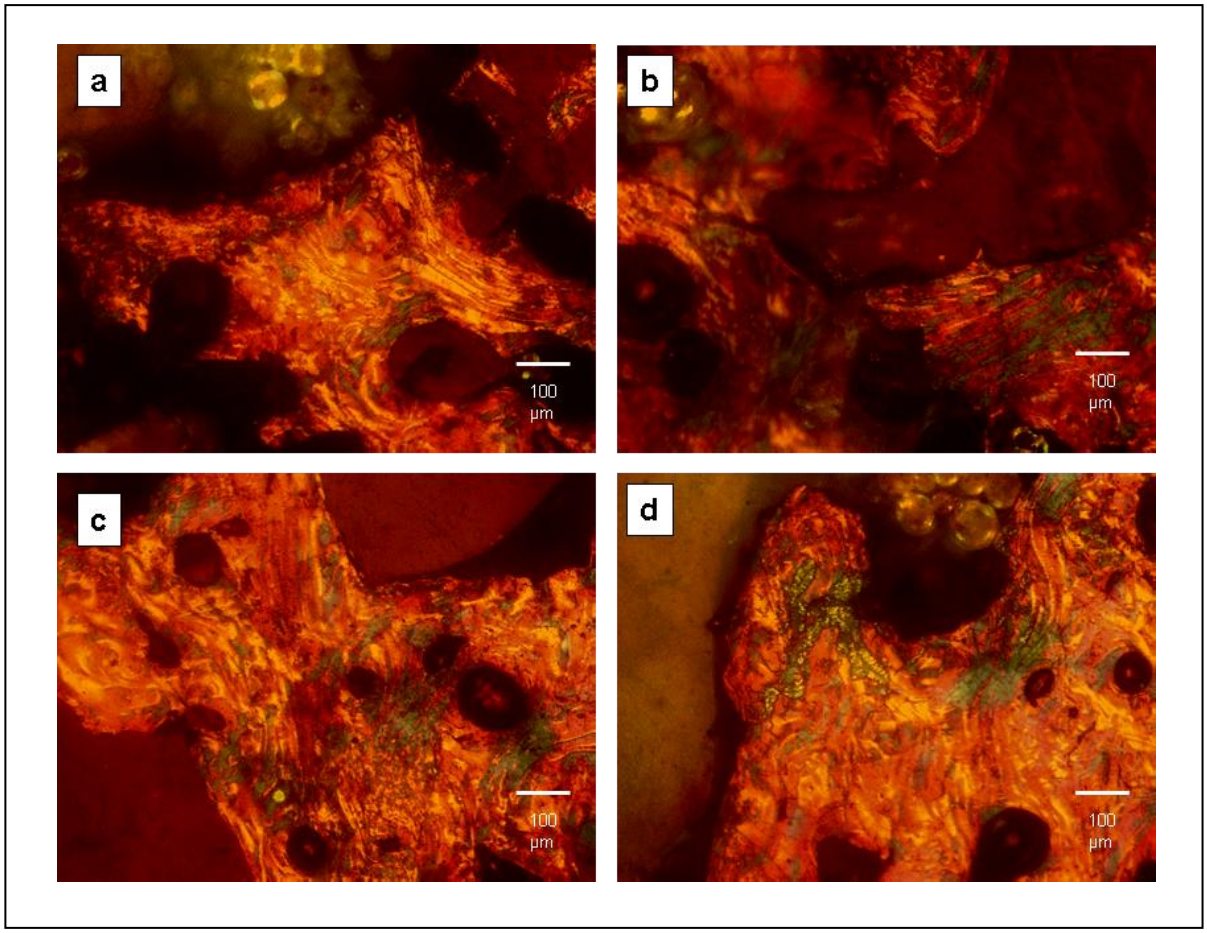

Figure 8-17 Series of micrographs of green coke E1b with increasing height percentage: (a) 13%; (b) 30%; (c) 60%; and (d) 80%

Throughout the height percentage of green coke E1b, the dominating microstructure is one of flow domains. However, what is evident is the substantial porosity in all of the micrographs (Figure 8-17a–d).

The necessity for stabilising Waxy Oil for the production of anisotropic coke has been demonstrated above. However, it must be realised that not all residues need to undergo this intermediate reaction. Generally, the more aromatic a residue (without asphaltenes), the greater the ease with which the self-assembly of mesogens occurs, leading to an anisotropic mesophase. This is substantiated by the difference in the carbonisation mechanisms of aromatic and aliphatic feeds described by Torregrosa-Rodriguez *et al.* (2000).

8.4.3 Macrostructure of Waxy Oil green cokes B and E1b

The macromorphology of green coke E1b at the top, middle and bottom of the coke bed is shown in Figure 8-18a–c respectively. The macromorphology of green coke B at the top, middle and bottom of the coke bed is shown in Figure 8-18e–f respectively. Green coke B is shown for comparison.

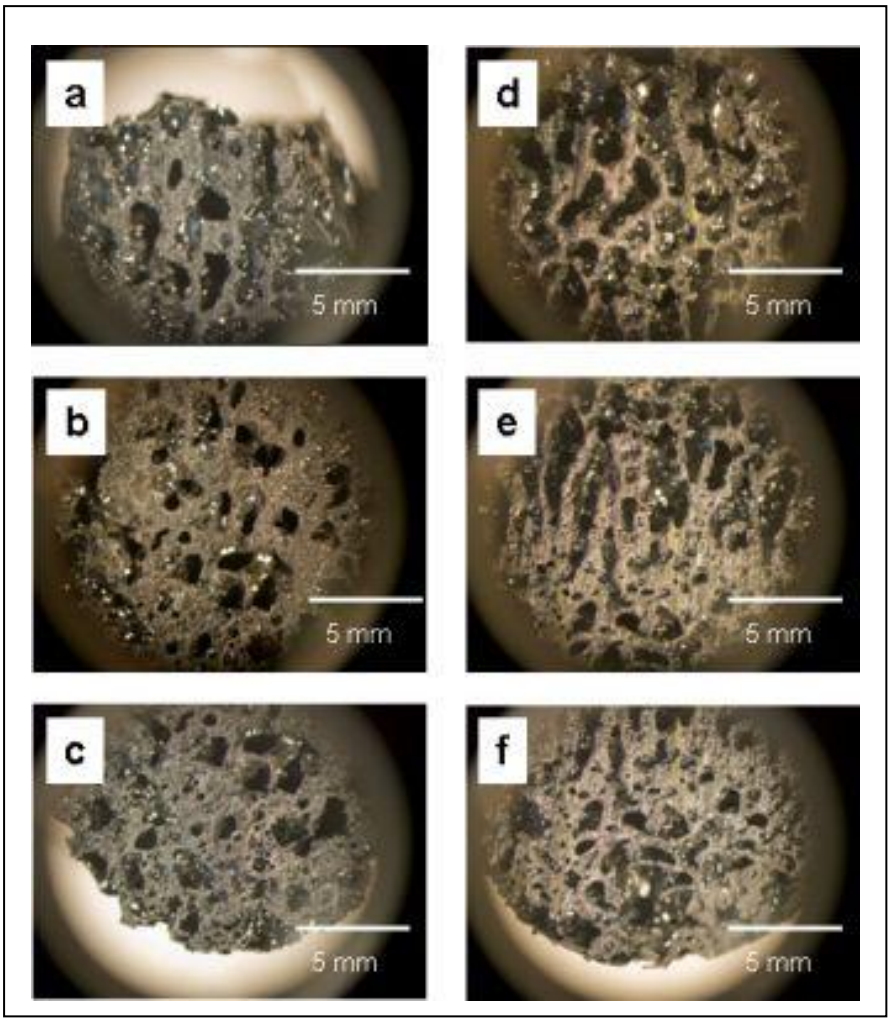

Figure 8-18 Macromorphology of green coke E1b at the top, middle and bottom of the coke bed (a–c) respectively and macro-morphology of green coke B at the top, middle and bottom of the coke bed (e–f) respectively

Green coke B is compared with green coke E1b to determine the difference of the most effective Waxy Oil modification (Sample E1b) against no molecular modification (Sample B).

In comparison with green coke B (Figure 8-18d–f), all the height sections of E1b (Figure 8-18a–c) contain similar visible porosity.

In Chapter 6 (Figures 6-1 to 6-4) the macromorphology of the pores (at least in one of the planes) did show a greater aspect ratio than Sample E1b. The aforementioned cokes were, however, produced by “dynamic” or delayed coking and there was a continual supply of gas

(and thus larger shear forces), which has the effect of "dragging" the mesophase at the solidification stage, thus increasing the aspect ratio.

8.5 Maximising the value of Waxy Oil modification

Maximising the value of Waxy Oil feed modification (in terms of needle coke) can be measured against:

- the residue yield (from modification of virgin Waxy Oil)
- the green coke yield (from the residue)
- the green coke anisotropy

A comparative histogram of these variables is plotted for each of the modifications conducted and shown in Figure 8-19.

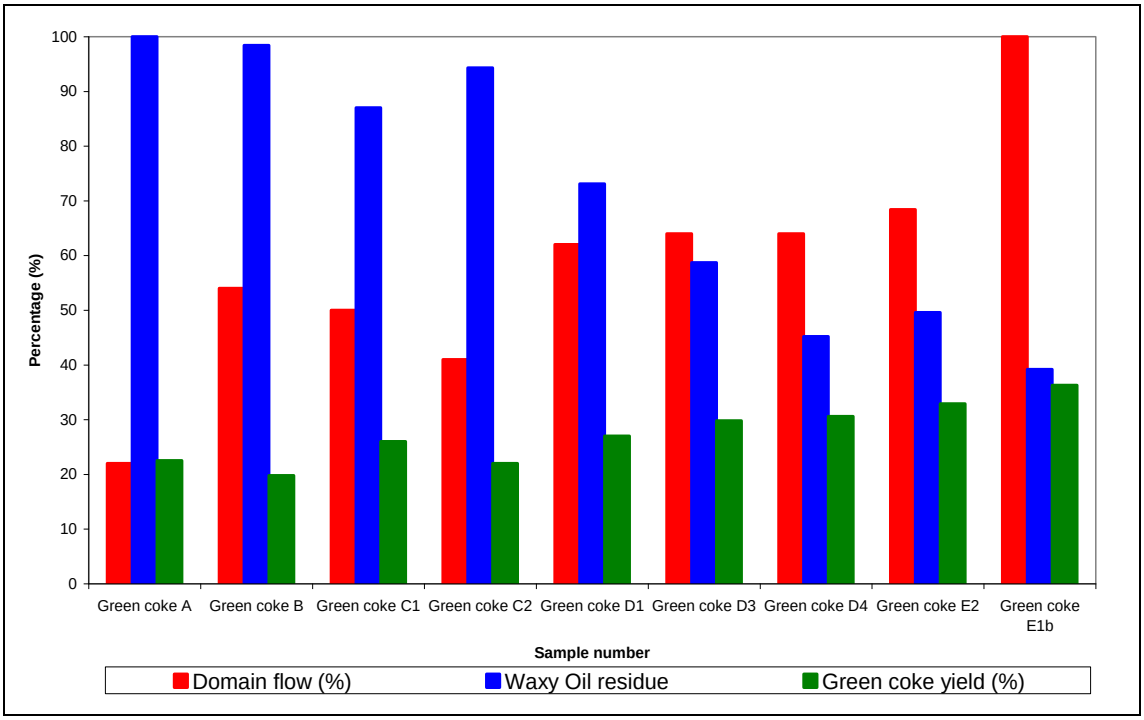

Figure 8-19 Histogram showing the influence of Waxy Oil modification on the residue yield, green coke yield and degree of green coke anisotropy (as measured by the percentage of flow domains)

In terms of the optimal Waxy Oil modification for needle coke production, it is clear that thermal treatment followed by distillation (Sample E1b) gives the maximum value.

It is possible to decrease the residue yield to 43% (Sample E1b) and by so doing maximise the green coke yield from approximately 20% (Sample B) to 36% (Sample E1b). The advantages thereof include:

- Maximising the green coke produced
- Maximising the green coke yield, which reduces porosity and increases the apparent density
- Increasing the capacity of the delayed coker to process feed

- Reducing the amount of cracked hydrocarbon distillates from the coker; it is more beneficial to remove the cracked hydrocarbons prior to carbonisation to limit dehydrogenation

In terms of importance, the microstructure of the coke produced defines the market to which the product can be allocated. The ability to remove the ash content to needle coke specifications has been shown and thus Sample A is automatically discounted as a possible feed. The microstructure domain flow can be increased to 100% (Sample E1b). Increasing the anisotropy of the coke would be expected to decrease the Coefficient of Thermal Expansion (CTE) of extruded artefacts, as previously established by Mochida *et al.* (1989).

In all aspects mentioned, Sample E1b is considered the optimum feedstock. The results of Chapter 8 do not include parameters such as CTE, VBD, etc. as delayed coking will influence the characteristics of the coke.

8.6 Is the low green coke yield of Waxy Oil carbonisation a potential problem?

The very simple answer is that the low green coke yield, even of Sample E1b (36%), is a cause for great concern and cannot be ignored.

Although stabilisation treatments accompanied by distillation do increase the green coke yield, the fact still remains that the residue is composed of long-chain normal alkanes which are more reactive than aromatic residues and thus will always produce a lower green coke yield. Thus all reasonable measures need to be considered to reduce further mass loss during calcination. Inert calcination of the green coke is strongly recommended to reduce the effect of air and carboxy reactivities. It should be possible to produce a calcined coke yield of approximately 32% (based on fresh Waxy Oil feed).

8.7 Conclusions – "Static carbonisation" of Waxy Oils

This chapter presents data showing the effect of Waxy Oil modification on the characteristics and yield of green coke produced by "static" test tube carbonisation.

The conclusions drawn are as follows:

- A reduction in the ash content of the Waxy Oil feed prior to carbonisation has the following effects on the coke quality:
    - There is only a slight decrease in the green and calcined coke yield.
    - There is a substantial decrease in the height percentage of mosaic microstructures in the green coke.
    - The oxidative consumption catalytic activity of the iron is only evident after 600 °C.
    - The carboxy reactivity mass loss is initially catalysed by the iron catalyst as it is in the form of the element (Fe) rather that the less reactive oxide.
    - The crystal structure is less dependent on multiphase graphitisation.

  - The crystal structure is less ordered due to the reduction of multi-phase graphitisation.

- The more reactive Waxy Oils have a higher percentage of mosaic microstructures than the less reactive Waxy Oils. The importance to the microstructure of removing cracked lighter material from the residue after thermal treatment has also been established.
- It is possible to produce a green coke with a domain flow structure through the length of the longitudinal section using thermal treatment followed by distillation.
- Thermal treatment followed by distillation provides the largest green coke yield.

8.8 Recommendations – "Static carbonisation" of Waxy Oils

Based on the evidence provided in this chapter, the following recommendation is made:

Although it has been established that the anisotropy of green coke can be substantially influenced by modification of the carbonisation precursor, the mechanism involved is not understood. It is therefore recommended that the carbonisation mechanism of Waxy Oil be studied to provide a reasonable answer and this is studied in Chapter 9.

9 CARBONISATION MECHANISM OF WAXY OIL[34]

9.1 Introduction

At the very heart of the transformation of a heavy residue through mesophase formation and finally solidification to form a green coke is a mechanism explaining the predisposition of a feed with a certain molecular composition to produce coke with particular characteristics.

Waxy Oil again presents an additional challenge in that the residue product of thermal treatment is composed of long-chain normal alkanes and not aromatics. The carbonisation of Waxy Oil (whether thermally treated or not) involves an extra intermediate step, including the formation of stable aromatics from long-chain normal alkanes prior to mesophase formation.

This chapter adopts a fairly simple approach to the carbonisation mechanism:

- Identifying molecular reaction intermediates during carbonisation
- Determining the effect of the pre-mesogens formed on mesophase development and coke microstructure

9.2 Low-temperature carbonisation[35] of filtered and thermally treated Waxy Oil

A comprehensive explanation of the experimental procedure is given in Chapter 5, but a short description is also provided below.

Filtered Waxy Oil was thermally treated in an autoclave (410 °C for 2 h at 5 bar) and the residue was vacuum distilled. Small quantities of the thermally treated Waxy Oil were carbonised for periods between 10 and 120 min in Pyrex glass test tubes at a comparatively low carbonisation temperature of 450 °C at 5 bar. The experimental procedure for analyses conducted on the carbonisation residues is shown in Figure 9-1.

[34] The research for Chapter 9 was conducted at the Instituto Nacional Del Carbón (INCAR) in Oviedo, Spain under the tutorship of Dr Ricardo Santamaria. The author designed the experiments and received raw data which were analysed, reviewed and written up in this chapter. The author was not present when the experiments were done as it was not possible to be in Spain

[35] "Low-temperature carbonisation" is defined in this study as taking place at 450 °C. This was done to allow comparison with the carbonisation temperature (480 °C) used in Chapter 8.

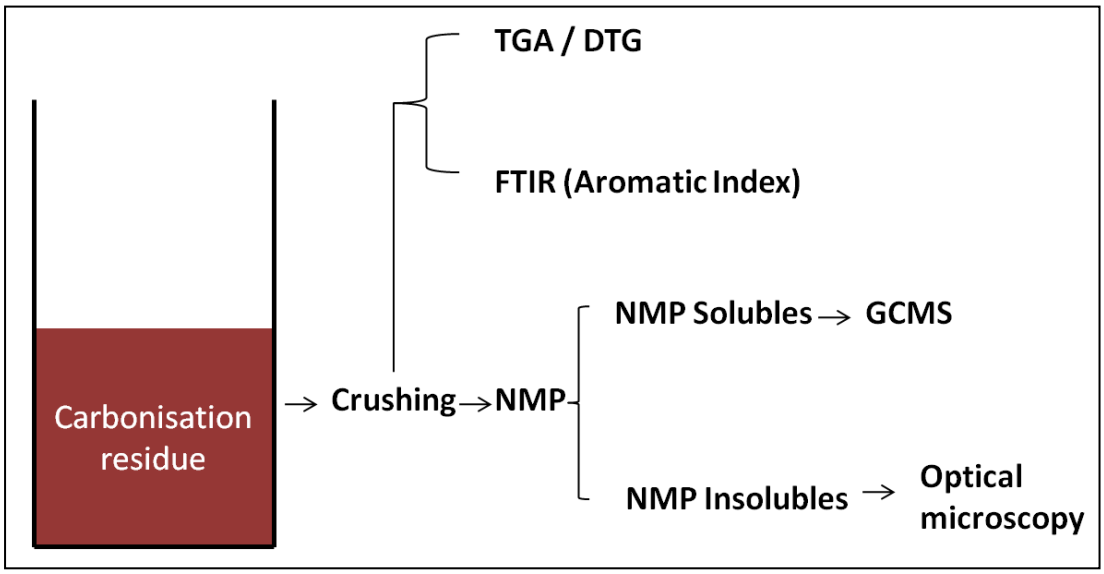

Figure 9-1 Procedure for processing the carbonisation residue and analysis

The residue left in the test tube after low-temperature carbonisation is a mixture of coke, mesophase and organics. The residue was crushed and samples were extracted for TGA/DTG[36] and FTIR analysis. The rest of the crushed residue was refluxed in N-methyl-2-pyrrolidone (NMP) and filtered to determine the yield of solubles and insolubles. The NMP-soluble fraction was used to conduct GCMS. The NMP-insoluble fraction was used to conduct optical microscopy on the mesophase and coke.

9.3 Residue yield and NMP (soluble and insoluble) fractions

The residue yields of the carbonisations and their NMP solubility are shown in Table 9-1.

Table 9-1 Determination of residue yield and NMP (soluble and insoluble) fractions

	Carbonisation time (min)	Residue Yield (%)	Solubility of residue in NMP[1]	
			NMP Insolubles Mass%	NMP Solubles Mass%
Sample C1	10	40.00	25.50	74.50
Sample C2	20	32.80	47.50	52.50
Sample C3	40	24.60	67.90	32.10
Sample C4	60	24.20	92.70	7.30
Sample C6	120	24.80	96.00	4.00

[1]The NMP-soluble and NMP-insoluble fractions are expressed as a percentage of the residue yield

The residue yield decreases with carbonisation duration from Sample C1 to Sample C3. Both Samples C1 and C2 contain a considerable amount of unreacted organics, which are denser than the coke formed during carbonisation, increasing the residue yield. This effect is also noticed in the comparatively large amount of NMP solubles. The residue yield of Samples C3 to C6 is fairly constant, being composed mainly of mesophase and coke solid carbon. The

[36] The TGA and FTIR analyses were conducted on the crushed residue. This could not be separated due to the presence of mesophase which would have affected the result.

increased mass of coke formed from Sample C3 to Sample C 6 is responsible for the reduction in the percentage of NMP solubles.

9.4 Thermogravimetry Analysis (TGA) and Differential Thermogravimetry (DTG) of the carbonisation residue

Representative samples of the crushed carbonisation residue were subjected to TGA and DTG. The TGA for the samples is shown in Figure 9-2.

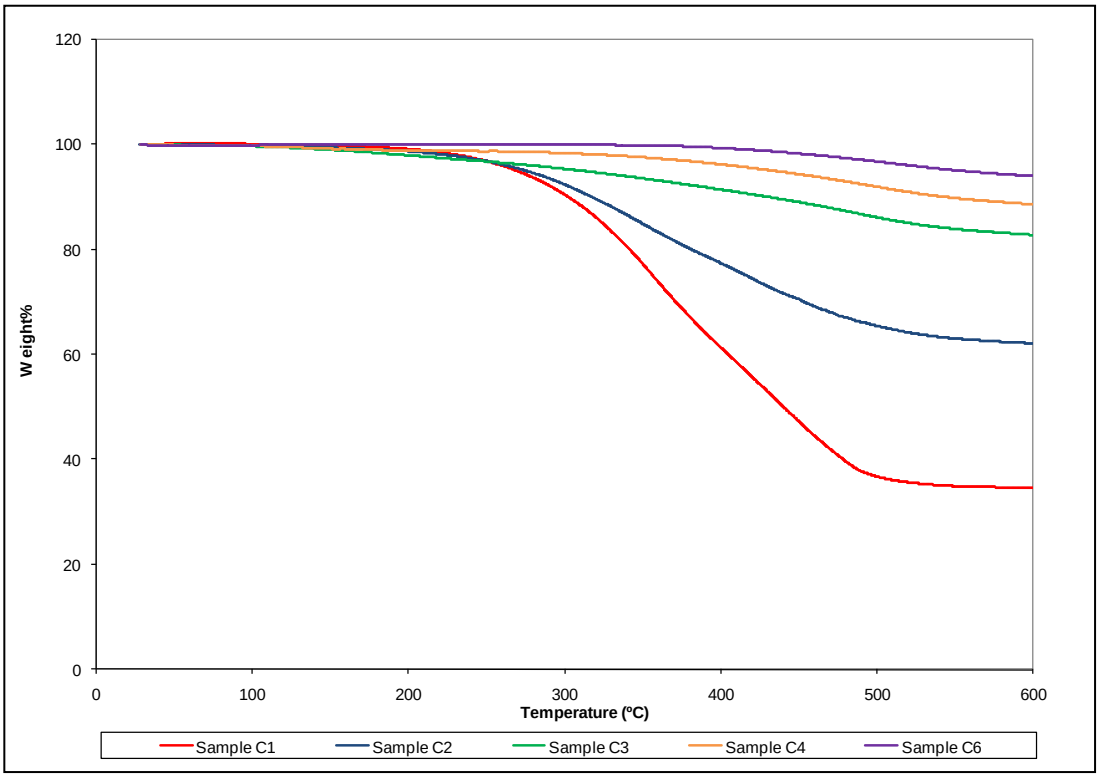

Figure 9-2 Thermogravimetric Analysis (TGA) of Samples C1, C2, C3, C4 and C6 as described in experimental conditions of Table 9-1

As the reaction time increases, so the gradient of the distillation curve becomes shallower as fewer light organics are distilled and the carbon residuum increases due to the greater mass of mesophase and coke in the TGA sample.

The DTG curves for the samples are shown in Figure 9-3.

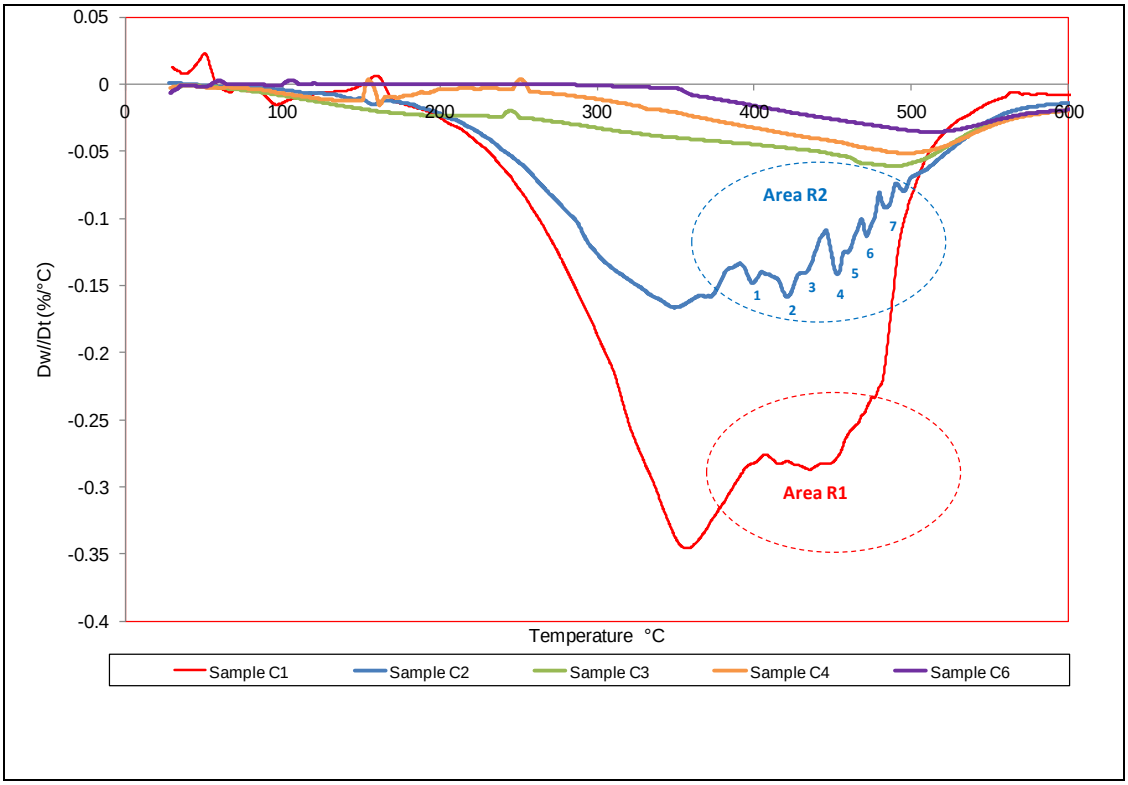

Figure 9-3 Differential Thermogravimetry (DTG) of Samples C1, C2, C3, C4 and C6 as described in experimental conditions of Table 9-1

Sample C1 shows two distinct peaks of maximum reaction rate. The first peak corresponds to the distillation of volatile matter below 350 °C and the second peak is both shallower and broader, corresponding to the carbonisation reaction between 400 and 500 °C. Sample C2 shows less intense distillation and carbonisation peaks (due to the higher percentage of coke formed during the carbonisation reaction). However, what is interesting is a comparison between the set of carbonisation sub-peaks (collectively shown as the carbonisation peak) of Samples C1 and C2 (in Figure 9-3, identified as Areas R1 and R2 respectively).

The broad carbonisation peak of Sample C1 extends from 411–443 °C. Sample C1 is also composed of a large percentage of molecules that are similar in that they are largely normal alkanes and therefore the intensity is greater than in Sample C2. Within Area R2 of the carbonisation peak of Sample C2, the trace presents seven separate sub-peaks. The first of these (as indicated by their numbers) includes Peak 1 (366 °C), Peak 2 (396 °C) and Peak 3 (417 °C), which are probably associated with initial cracking reactions. The other peaks include Peak 4 (451 °C), Peak 5 (470 °C), Peak 6 (481 °C) and Peak 7 (492 °C), which it is proposed are linked to different reactions of molecular composition ranging from cyclo-alkanes to aromatics. It is proposed that the seven sub-peaks indicated in the DTG of Sample C2 would correspond to the individual reactivities of these molecular families.

With regard to Samples C3, C4 and C6, the second carbonisation peak is increasingly less intense and occurs at higher temperatures. The lack of intensity may indicate that this sample is composed predominantly of mesophase and coke.

9.4.1 The effect of carbonisation time on the area percentage and molecular weight of normal alkanes

Increasing the duration of carbonisation between 10 and 40 min (Sample C1 to C3) at 450 °C increasingly cracks alkanes of higher molecular weight to form alkanes of lower molecular weight and hydrocarbon gases as shown in Figure 9-4.

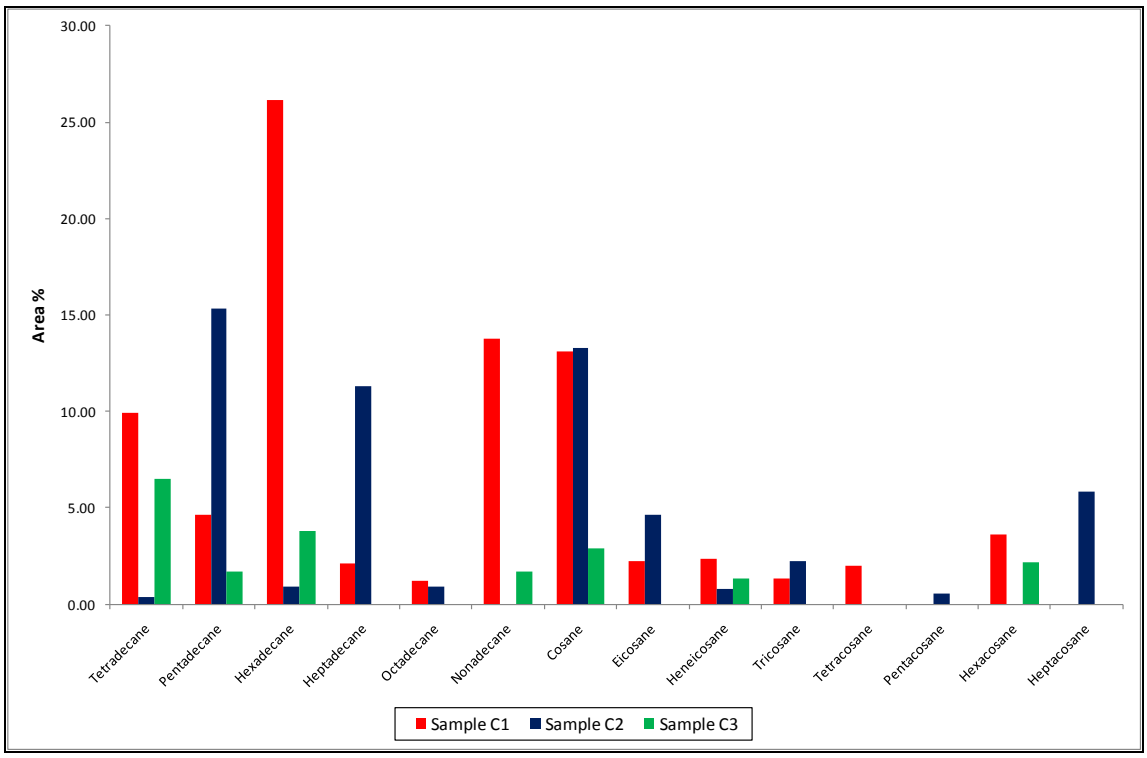

Figure 9-4 Quantification of the breakdown of normal alkanes during the low-temperature carbonisation of Waxy Oil (as described in experimental conditions of Table 9-1) as studied in Samples C1, C2 and C3[37]

Sample C1 shows the highest percentage of normal alkanes (total 83.8%), including tetradecane, hexadecane, nonadecane and cosane. The distribution of normal alkanes for Sample C2 shows an area percentage reduction in normal alkanes (total 56.89%), although the range is dominated by pentadecane, heptadecane, nonadecane and cosane. This may be caused by the breakdown of the higher normal alkanes above C_{20}.

The lowest percentage of normal alkanes is shown for Sample C3 (total 21.96%). However, the range of normal alkanes for Sample C3 is the highest between tetradecane and hexadecane, indicating, in general, a range of lower molecular weights compared with Samples 1 and 2. The percentile reduction in normal alkanes is also indicated by the comparatively increased aromaticity of Sample C3 shown in Table 9-2.

The reduction in molecular weight as the carbonisation time increases is probably caused by the production of C_1 to C_3 hydrocarbon gases, in agreement with the findings of Mochida *et al.* (1989).

[37] The range of normal alkanes in the three samples is calculated using GCMS data. The area % is calculated as a fraction of the total area % of the total GC-amenable molecules of the NMP-soluble fraction.

9.5 Aromaticity Index (I_{ar})

A comparison of the increase in the Aromaticity Index (I_{ar}) as a function of carbonisation time is shown in Table 9-2.

Table 9-2 Comparison of the Aromaticity Index [$I_{ar}=Abs_{3050}/ (Abs_{3050}+Abs_{2920})$] of the crushed carbonisation residues of Samples C1, C2, C3, C4 and C6

	Carbonisation duration (min)	Aromaticity Index (I_{ar})*
Sample C1	**10**	0.044
Sample C2	**20**	0.069
Sample C3	**40**	0.126
Sample C4	**60**	0.189
Sample C6	**120**	0.345

* Average of three measurements

The Aromaticity Index increases as a function of carbonisation time between 10 and 120 min. This is not unexpected given the reduction in the concentration of normal alkanes and the increase in the concentration of aromatic molecules as the duration increases.

In order to put the I_{ar} for the carbonised Waxy Oil into perspective, it should be possible to compare the indices with those of other heavy residues: coal-tar binder pitch (0.63), Ashland petroleum pitch (0.41), low-temperature gasification pitch (0.37), distilled petroleum vacuum residue (0.38) and thermally treated petroleum vacuum residue (0.45) (Sima *et al.*, 2003; Perez *et al.*, 2002). However, this comparison is inaccurate as the heavy residues listed are pre-carbonised residues and the carbonised Waxy Oil samples are more than likely concentrated with mesophase.

9.6 Typical molecular composition of pre-mesogen molecules produced by low-temperature carbonisation

The residue of the test tube was refluxed in NMP and filtered. The filtration residue contained both solid carbon and mesophase. The filtrate contained molecular intermediates of the carbonisation reaction. The composition of the filtrates from Sample C1 to Sample C6 was determined by GCMS (corrected for the presence of NMP). The GCMS traces of these samples are compared in Figures 9-5 to 9-8. Given the complexity of the traces, only two samples are compared in each figure. Comparison of the traces is qualitative and has not been corrected for the percentage of coke because in comparing the GCMS traces, what is important (for this chapter) is the type and not the concentration of organic molecules.

The purpose of the thermal treatment tests reported in Chapter 7 was to increase the area percentage of normal alkanes, appearing as a crest within an elution time of approximately 50 to 80 min. During low-temperature carbonisation the aim is to reduce the area percentage of normal alkanes as a function of time and produce aromatics or so called “pre-mesogens”.

A comparison of the GCMS traces of Samples C1 and C2 is shown in Figure 9-5.

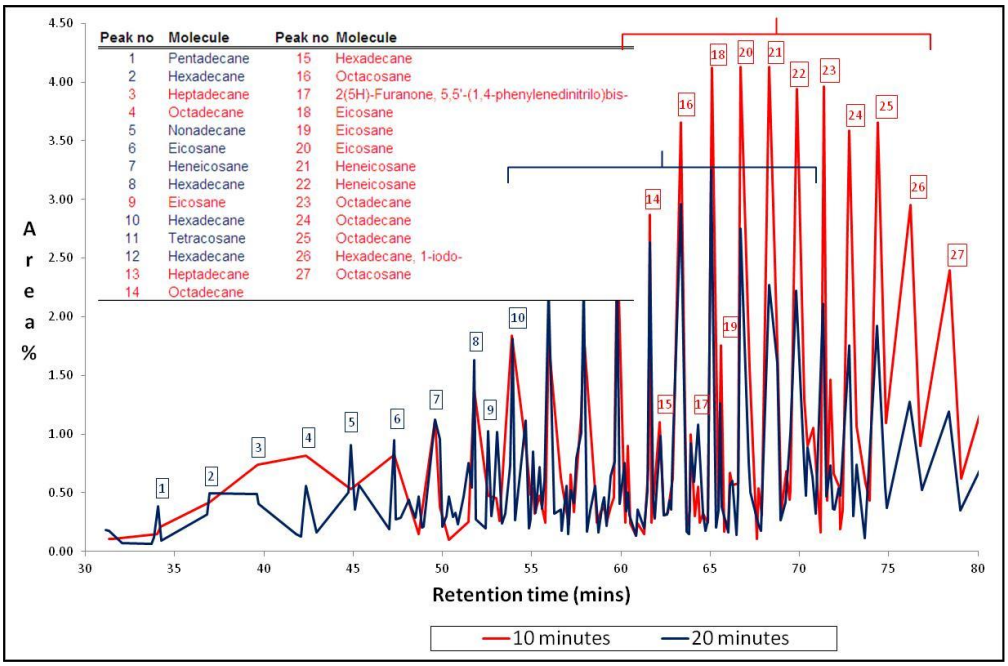

Figure 9-5 Gas Chromatography–Mass Spectroscopy of Samples C1 and C2 (NMP-soluble fraction) during low-temperature carbonisation at 10 and 20 min respectively

Sample C1 shows a crest of normal alkanes within an elution time of 50 to 80 min. These molecules are identified in the index (provided as an insert) as peaks 13–16 and 18–27. The crest of normal alkanes identified is the result of thermal treatment. By comparison, Sample 2 (carbonised for a longer time) shows a notable decrease in the area percentage of these molecules. This is due to increased cracking of normal alkanes and the production of hydro-aromatics (as seen in Table 9-3 and identified in Table 9-4). The "crest" (indicated in red blocks) of Sample C1 normal alkanes is also at a higher molecular weight than that of Sample C2 (indicated in blue blocks). This is due to the cracking of long-chain normal alkanes to lower chains. However, of importance is the absence of any substantial peaks representing aromatic molecules for either of the samples. The aliphatic nature of Samples C1 and C2 is substantiated by the I_{ar} values reported in Table 9-3.

A comparison of the GCMS traces of Samples C2 and C3 is shown in Figure 9-6.

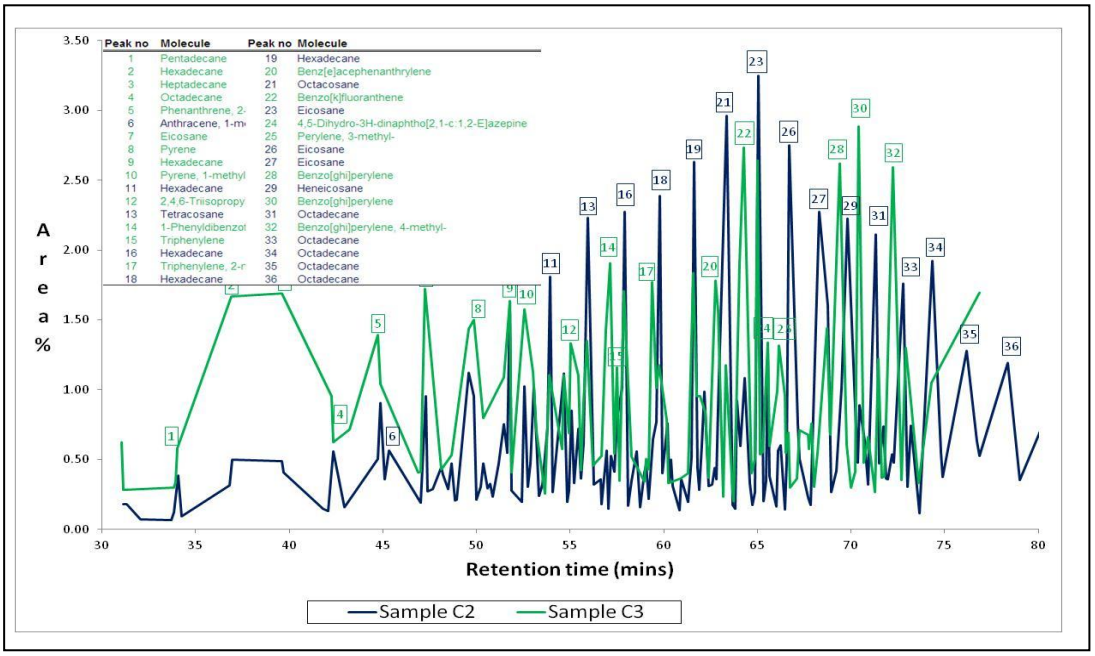

Figure 9-6 Gas Chromatography Mass Spectroscopy of Samples C2 and C3 (NMP soluble fraction) during low-temperature carbonisation at 20 and 40 min respectively

The "crest" of normal alkanes shown for Sample C2 within an elution time of 55 to 75 min is not present for Sample C3. Instead, Sample C3 shows the appearance of new peaks (often masked by the peaks of Sample C2), which indicate the formation of hydro, methyl and pure aromatics (identified in the index as peaks 5, 8, 10, 14, 15, 17, 20, 22, 24, 25, 28, 30 and 32). The substantial reduction in the area percentage of normal alkanes (56.89 to 21.96 area %) with an increase in hydro, methyl and pure aromatics (38.34 to 75.38 area%) when Sample C2 is compared with Sample C3 is substantiated in Table 9-3.A comparison of the GCMS traces of Samples C3 and C4 is shown in Figure 9-7.

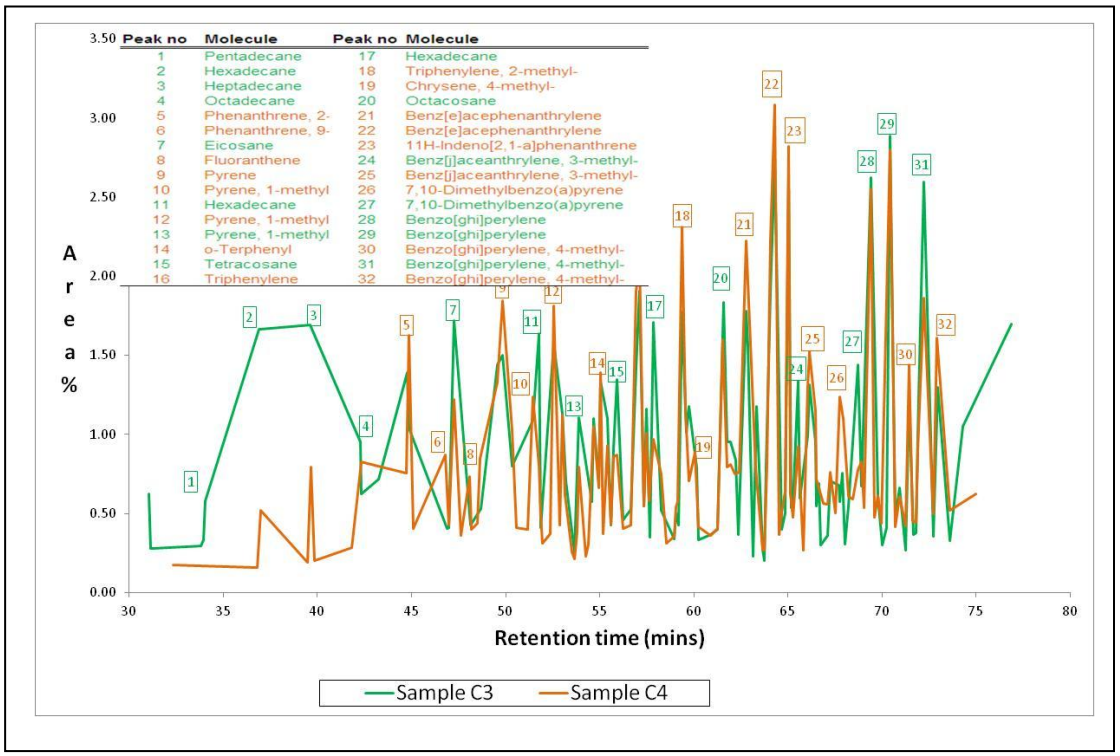

Figure 9-7 Gas Chromatography–Mass Spectroscopy of Samples C3 and C4 (NMP-soluble fraction) during low-temperature carbonisation at 40 and 60 min respectively

In Figure 9-5 the initial production of hydro, methyl and pure aromatics (Sample C3) was masked by normal alkanes (Sample C2). In Figure 9-7, the peaks of Sample C3 are again masked by those of Sample C4. However, these are not normal alkanes but rather alkylated two- to four-ring aromatics.

A comparison of the GCMS traces of Samples C4 and C6 is shown in Figure 9-8.

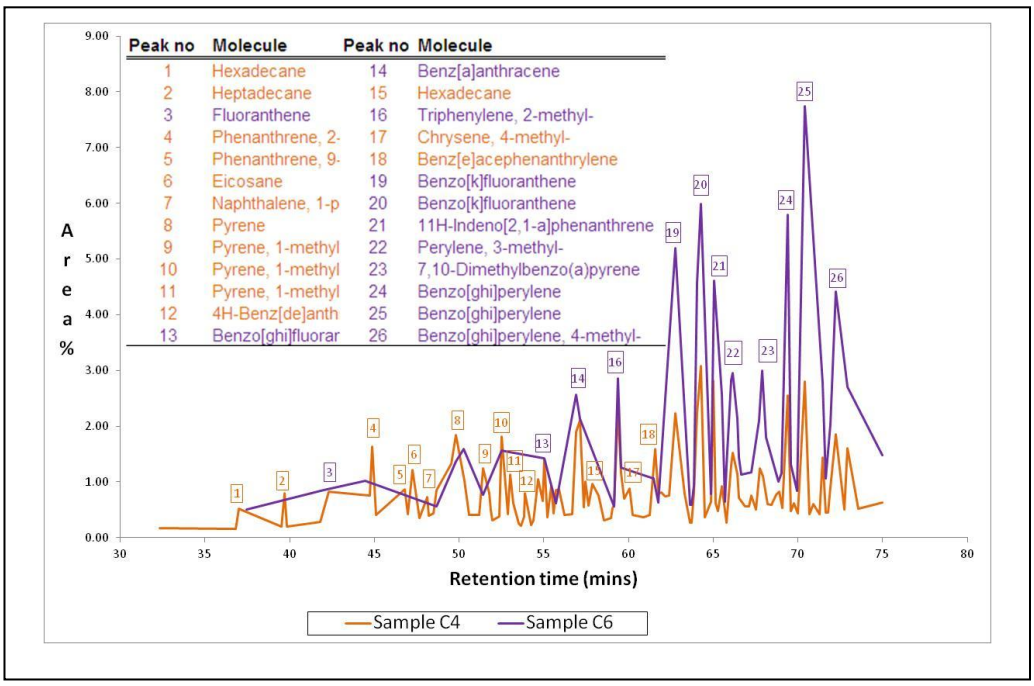

Figure 9-8 Gas Chromatography–Mass Spectroscopy of Samples C4 and C6 (NMP-soluble fraction) during low-temperature carbonisation at 60 and 120 min respectively

Compared with Sample C4, Sample C6 shows a substantial increase in the area % of pure aromatics, indicating dealkylation of the methyl aromatics which are more prevalent in Sample C4. Sample C4 shows larger peaks towards the lower retention times due to the lower molecular weight of the aromatics (predominantly two four-ring alkylated aromatics) vs. the higher molecular weight of the aromatics in Sample C6 (predominantly four six-ring pure and alkylated aromatics).

9.7 Pre-mesogen molecules produced during low-temperature carbonisation

A quantitative determination of molecular families as an area percentage of the NMP-soluble organics is shown in Table 9-3.

Table 9-3 Identification of typical molecular families produced in the NMP-soluble fraction during low temperature carbonisation, including Samples C1, C2, C3 C4, C6

Molecules	Unit	Sample C1	Sample C2	Sample C3	Sample C4	Sample C6
Normal alkanes	**Area %**	83.84	56.89	21.96	12.14	0.00
Iso-alkanes	**Area %**	2.29	3.25	1.77	2.53	0.00
Alkenes	**Area %**	1.48	2.43	3.37	0.53	0.00
Cycloalkanes or hydroaromatics	**Area %**	0.00	3.21	6.42	0.81	0.00
Alkylated aromatics	**Area %**	8.72	25.87	32.68	40.21	34.68
Pure aromatics	**Area %**	3.66	8.35	33.79	44.65	65.83

The determination of the molecular families in each sample was manually calculated from the area percentage in the GCMS data table. The area percentage given in Table 9-3 for each sample is the sum of the area percentage of similar molecules as defined by molecular families (e.g. normal alkanes, alkylated alkanes, etc.).

As shown in Table 10-6, as the duration of low-temperature carbonisation increases, there is a decrease in the area percentage of normal alkanes and an increase in the area percentage of alkyl and pure aromatics. The production of cyclo-alkanes/hydro-aromatics increases from Sample C2 to Sample C3, after which it decreases due to the formation of aromatics. As the duration of the low temperature increases, there is also an expected increase in the ratio of pure to alkylated aromatics.

9.8 Proposed reaction mechanism for the formation of pre-mesogens from high molecular weight normal alkanes

In attempting to establish the mechanism for the formation of aromatic hydrocarbons from long-chain normal alkanes, cognisance is taken of the general mechanism proposed by Domine *et al.* (2000) for *n*-hexane. However, it is used only as a guideline because the research done by Domine *et al.* (2000) was based on the reactions of single organic normal alkanes, whereas Waxy Oil is composed of a multitude of various alkanes.

It is proposed that the aromatisation may be broadly divided into four intermediate reaction steps:

- Stabilisation and concentration of normal alkanes
- Formation of cyclo-alkanes or hydro-aromatics
- Dehydrogenation to form alkylated aromatics
- Formation of aromatic pre-mesogens

Sample C1 was chosen to represent the typical distribution of alkanes as it was carbonised for the shortest duration and thus normal alkanes would be in the greatest concentration, compared with the longer reaction times.

The quantitative distribution of typical normal alkanes present in the NMP-soluble fraction of Sample C1 is as follows:

- Hexadecane (9.94 area %)
- Heptadecane (4.63 area %)

- Octadecane (26.16 area %)
- Eicosane (13.74 area %)
- Heneicosane (13.09 area %)
- Octacosane (3.60 area %)

The normal alkanes listed above represent a total of 71.16 area % of the total NMP-soluble fraction of Sample C1. Although there is a distribution between C_{16} and C_{28}, these molecules are concentrated in the C_{18} to C_{22} molecular weight range. Also noticeable is that, apart from heptadecane, all of these normal alkanes are even numbered.

9.8.1 Formation of cyclo-alkanes/hydro-aromatics[38]

The production of aromatic molecules from normal alkanes necessitates the production of intermediate cyclo-aliphatic or naphthenic molecules, as argued by Guillen *et al.* (2000) and Guo *et al.* (2010). However, the isolation of these intermediates is extremely difficult as although the cyclisation reaction is comparatively slow, the dehydrogenation reaction is immediate, as previously argued by Domine *et al.* (2000) when studying the thermolysis of *n*-hexane. It is thus not unexpected that these intermediates were present only in smaller area percentages in the GCMS data for this chapter. The area percentage of cyclo-alkanes/hydro-aromatics formed as a function of the duration of the low-temperature carbonisation is shown in Table 9-4.

Table 9-4 Cyclo-alkanes/hydro-aromatics formed in Samples C2 and C3[39;40]

Molecule	Units	Sample C2	Sample C3
Cyclohexane or hydrobenzenes	**Area %**	0.00	1.47
Hydronaphthalenes	**Area %**	1.16	2.51
Hydrochrysenes	**Area %**	1.39	2.22
Hydrobenzofluoranthenes	**Area %**	0.00	0.54
Hydropyrenes	**Area %**	0.00	1.66
Hydrobenzoanthracenes	**Area %**	0.66	0.00
TOTAL	**Area %**	**3.21**	**6.42**

As seen in Table 9-4, there is evidence of a small percentage of cyclo-alkanes/hydro-aromatics formed as intermediate products during the production of alkyl and pure aromatics from normal alkanes. Furthermore, these molecules span the range from one- to five-ring molecules. Sample C2 is populated with a greater total concentration of cyclo-alkanes/hydro-aromatics due to the longer duration of the reaction. The formation of the larger ring compounds is only present in any appreciable percentage in Sample C3.

Apart from the importance of the hydro-aromatic intermediates as a precursor for the aromatic ring structure, they also serve as important hydrogen donors which are able to liberate hydrogen, as argued by Diez *et al.* (1999), capping reactive radicals during the

[38] Given the rapid dehydrogenation reaction of cyclo-alkanes formed, they are grouped with hydro-aromatics.
[39] Cyclo-alkanes/hydro-aromatics may be pure or multi-alkylated. They may also be multi-hydrogenated.
[40] Only Samples C1 and C2 are evaluated as the area percentages of cyclo-alkanes/hydro-aromatics are the highest.

carbonisation reaction. This stabilises the reacting system and increases the duration of maximum fluidity of the mesophase, thus enabling the production of coke with flow domains.

9.8.2 Formation of alkylated aromatic molecules

A compilation of typical alkylated aromatics found in the NMP-soluble fraction of Sample C4 is shown in Figure 9-9.

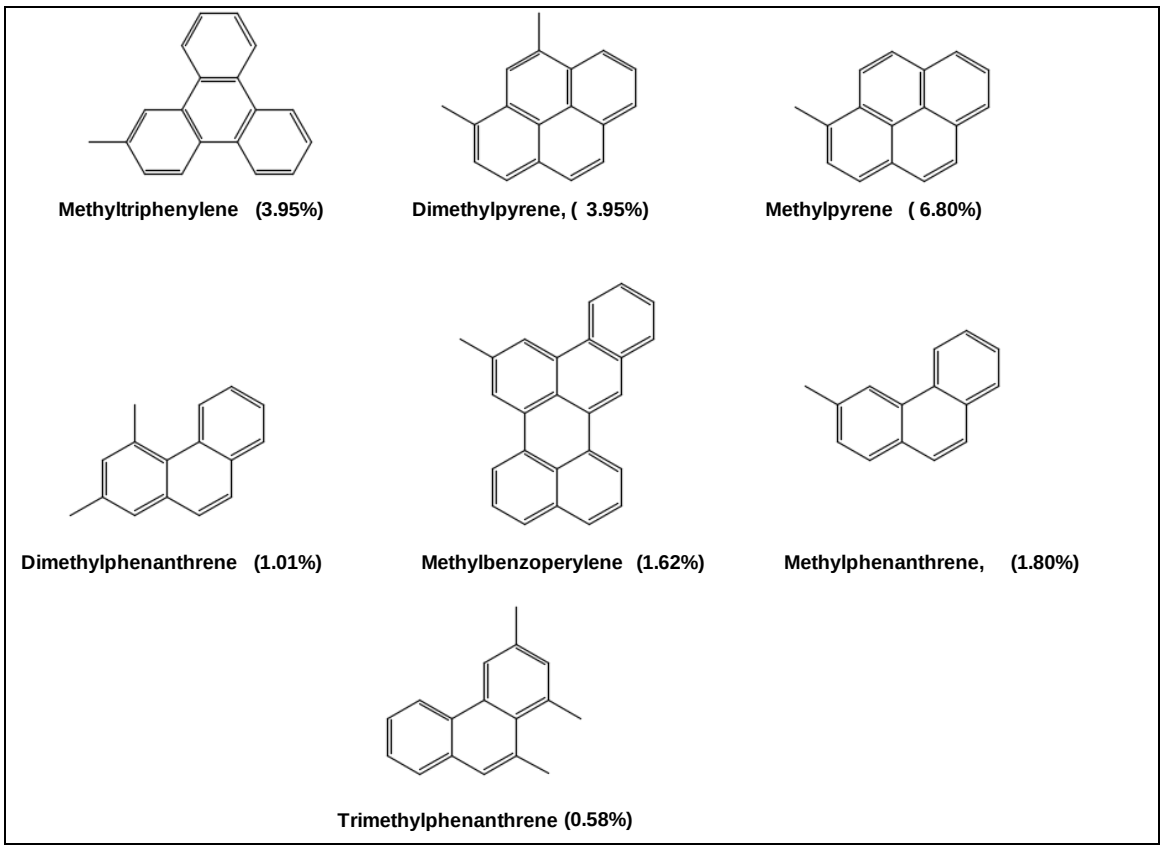

Figure 9-9 Typical alkylated aromatic reaction intermediates in Sample C4

Sample C4 was chosen to study typical alkyl aromatic molecules as they are highly concentrated in this sample. The alkyl aromatics are based on three to five rings with methyl or dimethyl alkyl substituents. These structures are not dissimilar to those found in needle coke feedstock based on petroleum FCCDO, as determined by Wang and Eser (2007). The one- and two-ring compounds are notably absent in quantitative comparison with the three- to five-ring structures. Benzene-type structures may distil during the reaction and it is highly likely that naphthalenes may dimerise forming higher molecular weight species, e.g. alkylated perylene.

9.8.3 Formation of aromatic pre-mesogens

A compilation of typical pure aromatics found in the NMP-soluble fraction of Sample C6 is shown in Figure 9-10.

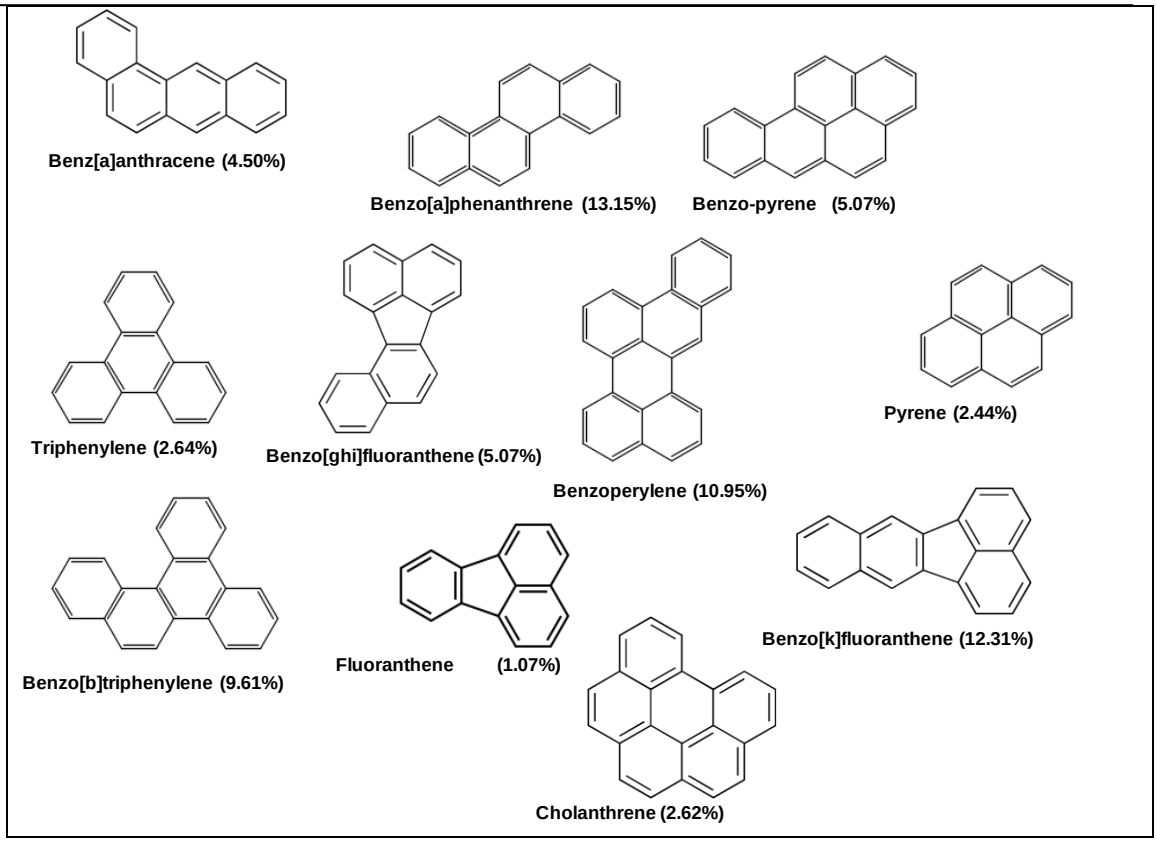

Figure 9-10 Typical pure reaction intermediates in Sample C6

The aromatic species found in Sample C6 are not very dissimilar to those shown in Figure 9-9, apart from the fact that they are dealkylated and do not include three-ring compounds. The molecules shown above are similar to those found by Guillen *et al.* (1998) when studying the composition of coal-tar pitch.

The greater concentration of pure aromatics and the predominance of pyrene/perylene-type molecules (as opposed to phenanthrene molecules) also contribute to the higher degree of mesophase development, discussed in Section 9.4. This was previously determined by Wang and Eser (2007) when studying the composition of petroleum decant oil and by Lewis (1987) when discussing the activating effect of alkyl substituents compared with pure aromatics.

9.9 Quantification of one-to six-ring alkylated aromatic and aromatic compounds

While particular samples were chosen in the previous section to show typical structures, in this section an overall analysis of GC-amenable alkylated and pure aromatics is given for the NMP-soluble fractions of all the samples, shown in Table 9-5.

Table 9-5 Distribution of one- to six-ring alkylated and pure aromatics in the NMP-soluble fractions of Samples C1 to C6

Aromatic type	Sample C1 (10 min)	Sample C2 (20 min)	Sample C3 (40 min)	Sample C4 (60 min)	Sample C6 (120 min)
1-ring alkylated aromatic	1.04	2.14	7.09	1.55	1.56
1-ring pure aromatic	0.00	0.00	0.00	0.00	0.00
2-ring alkylated aromatic	0.75	6.04	6.33	3.86	0.00
2-ring pure aromatic	1.34	0.00	0.00	0.00	2.64
3-ring alkylated aromatic	0.48	6.14	3.32	7.80	0.00
3-ring pure aromatic	0.00	0.14	0.54	4.56	0.00
4-ring alkylated aromatic	6.06	14.15	21.68	25.36	8.94
4-ring pure aromatic	2.28	5.41	17.86	13.32	26.52
5-ring alkylated aromatic	0.35	1.44	7.17	3.35	11.17
5-ring pure aromatic	0.30	1.76	7.28	7.87	44.56
6-ring alkylated aromatic	0.00	0.00	0.99	5.28	0.00
6-ring pure aromatic	0.00	0.00	0.50	6.13	0.00

One-ring alkylated and pure aromatic molecules

The composition of alkylated benzene molecules is low in all the samples for a variety of reasons. The carbonisation producing Samples C1 and C2 does not in all likelihood possess the activation energy to produce many aromatics and if they are produced, they either report to the distillate fraction or polycondense to form heavier polyaromatic hydrocarbons.

Two-ring alkylated and pure aromatic molecules

The highest percentile of two-ring alkylated aromatics is found in Samples C2 and C3 after which there is a high probability of the formation of naphthalene and the subsequent dimerisation thereof to four- to five-ring pre-mesogens. Lewis (1987) previously showed the potential for methyl naphthalene in forming alkyl bridges between aromatics during carbonisation, so dealkylation to form pure aromatics may not be the preferred reaction route.

Three-ring alkylated and pure aromatic molecules

As previously shown in Figures 9-9 and 9-10, the composition of three-ring alkylated phenanthrenes is far more frequent than that of pure phenanthrenes. This is especially evident in Samples C2, C3, and C4. However, as the duration of the reaction increases, there is an increase in the concentration of pure phenanthrenes. The absence of either alkylated or pure phenanthrene in Sample C6 is predictable, but it is surprising that it is completely absent from the product spectrum. There is also a possibility that alkylated naphthalenes may react with phenanthrenes to form five-ring compounds, e.g. benzotriphenylenes.

Four-ring alkylated and pure aromatic molecules

It is clear from Table 9-5 that the greatest percentile of both alkylated and pure aromatics is concentrated as four-ring compounds. There is an increase in the percentage of four-ring

alkylated aromatics from Sample C1 to Sample C4. There is also a percentile increase in four-ring pure aromatics from Sample C1 to C3. In Sample C6 the number of pure four-ring aromatics far exceeds that of the alkylated homologues. This is not unexpected as the four-ring pure aromatics form the basis for the majority of stable pre-mesogens.

Five-and six-ring alkylated and pure aromatic molecules

The absence of six-ring aromatic structures in Samples C1 and C2 is not unexpected given the reasons discussed above. There is a substantial concentration of six-ring alkylated and pure aromatic structures in Sample C5 and a total absence thereof in Sample C6. The formation of five- and six-ring aromatics is the product of either cyclo addition reactions or the reaction between alkylated naphthalenes with alkylated phenanthrenes which condense and dehydrogenate. These types of reaction will be enhanced with increasing carbonisation time, so it is understandable that there is a substantial increase in their presence from Sample C1 to C6.

9.10 Mesophase development

The study of mesophase development has historically been conducted using hot-stage microscopy. As the author did not have access to this equipment, optical micrographs were taken of the solid carbon mass/mesophase formed during carbonisation.

Various authors have argued that mesophase development is dependent on the unhindered inclusion of mesogens into incipient spheres, coalescence and maintaining maximum fluidity of the system to allow the production of anisotropic coke.

The study of mesophase development during the low-temperature carbonisation of Waxy Oil is reported on the basis of the following three themes:

- Observation of mesophase spheres from approximately 1 to 50 µm in diameter
- Coalescence of larger spheres with each other and absorption thereof into the semi-coke
- The effect of mesophase development on the microstructure of the coke

A montage of micrographs showing the development of the mesophase from incipient spheres of less than 1 µm to approximately 50 µm is shown in Figure 9-11.

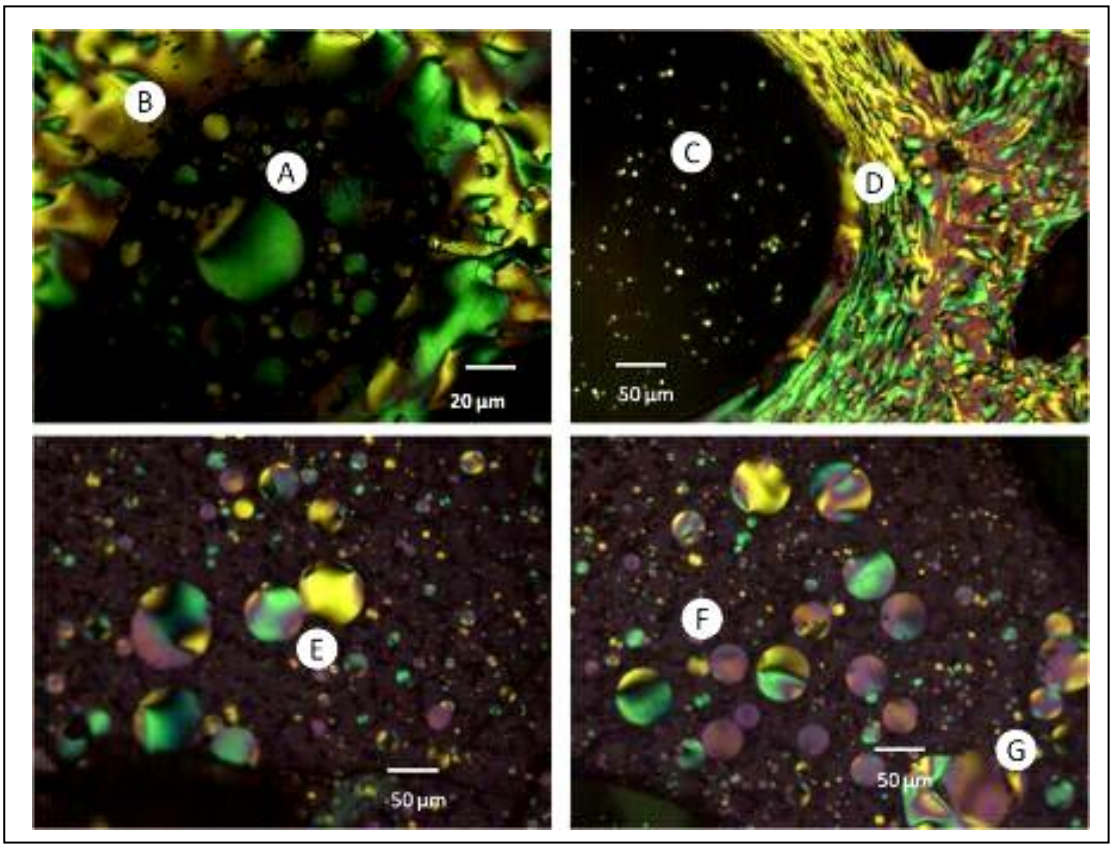

Figure 9-11 Cross-polarised optical microscopy (with the Lambda plate in) of the development of mesophase spherules (approximately 1–50 µm) during low-temperature carbonisation of thermally treated Waxy Oil (Sample C3)

Position C shows incipient mesospheres with diameters of approximately 1–5 µm nucleated from within the isotropic matrix. These are surrounded by the carbon microstructure (Position D). Marsh *et al.* (1999) suggested that incipient mesosphere morphology is not always spherical but may adopt other shapes, including ovoids or cylindrical shapes, which can be seen in the area surrounding Position C. The advantage of studying multi-phase systems (e.g. those composed of an isotropic matrix, semi-coke and solid carbon) is the ability to examine mesophase growth within the isotropic matrix. This is shown in Position A which is surrounded by coalesced mesophase as it forms an isolated reaction system. Observable within this matrix are variants of mesosphere sizes.

Positions E and F show coalescing spherical mesospheres. However, immediately after coalescence the new meso/macrosphere deforms temporarily (as shown in Position G) before returning to a sphere.

Optical microscopy of macrospheres (mostly over 50 µm) produced from carbonisation is shown in Figure 9-12.

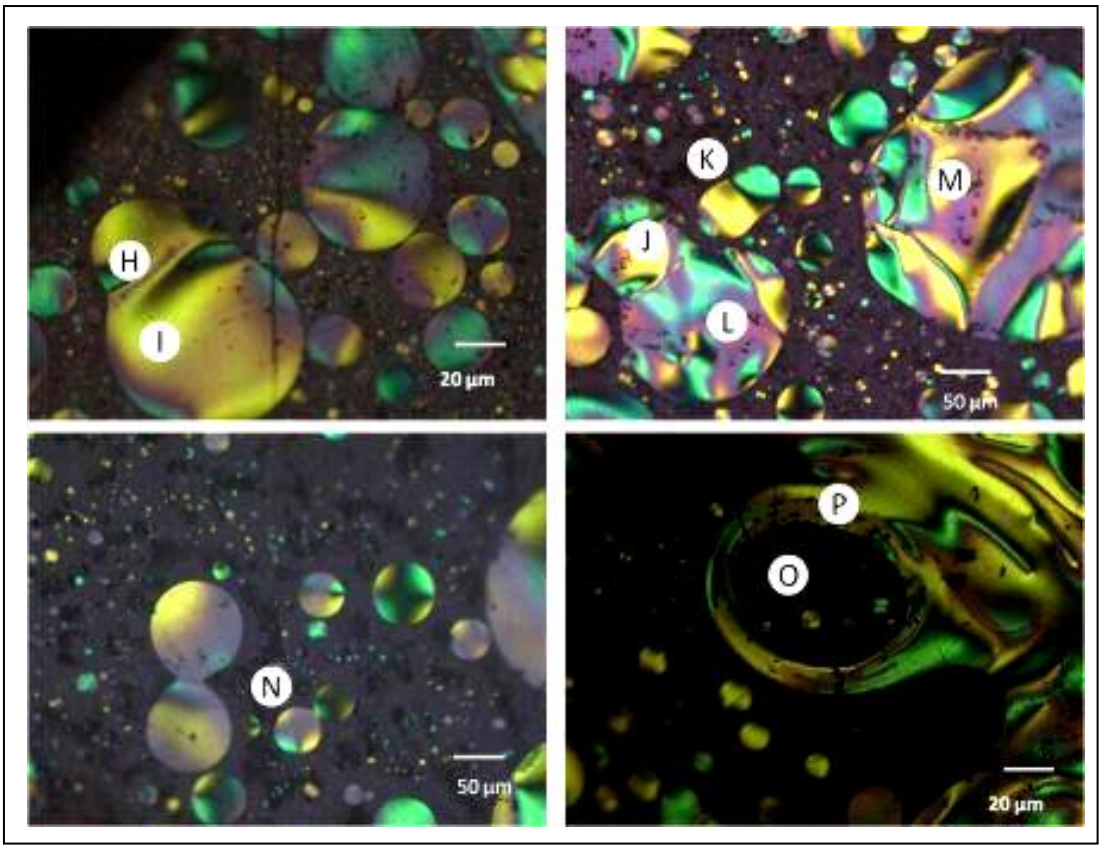

Figure 9-12 Cross-polarised optical microscopy (with the Lambda plate in) of macrospheres (over 50 µm) produced from thermally treated Waxy Oil (Sample C3)

With regard to the size of the mesospheres and the link with the anisotropy of the carbon microstructure, it is seen that the Waxy Oil mesospheres not only reach diameters of 100 µm (as seen in Positions L and M), but remain in the liquid crystal state, forming macrospheres of well over 200 µm as shown in Position M. Lewis *et al.* (1987) established a method for describing the weighted average mean diameter of mesospheres for a variety of heavy residues using hot-stage microscopy. The more reactive of the residues attained smaller weighted mean averages of mesosphere diameters, e.g. vacuum residues (10 µm) and ethylene tar (30 µm), and the less reactive residues attained large weighted mean averages, e.g. coal-tar pitch (190 µm). Although the diameter of the Waxy Oil mesospheres cannot be directly correlated with this work, it is evident that they would trend towards the lower reactivity of needle coke feedstocks. Position O shows development of mesospheres within a ring of semicoke (Position P).

The mechanism of coalescence is demonstrated as one smaller mesosphere (Position H) is seen to envelop a larger mesosphere (Position I). Another interesting feature of mesosphere coalescence is demonstrated by the mesospheres at Position N. Although there is certainly an argument for random collision between mesospheres, as they move into immediate proximity of one another it appears that they attract each other, probably due to Van der Waals forces, as they are individually di-polar. Positions J and K show smaller mesospheres simultaneously coalescing with a larger mesosphere at Position L.

A micrograph of a Waxy Oil macrosphere coalescing with semi-coke is shown in Figure 9-13.

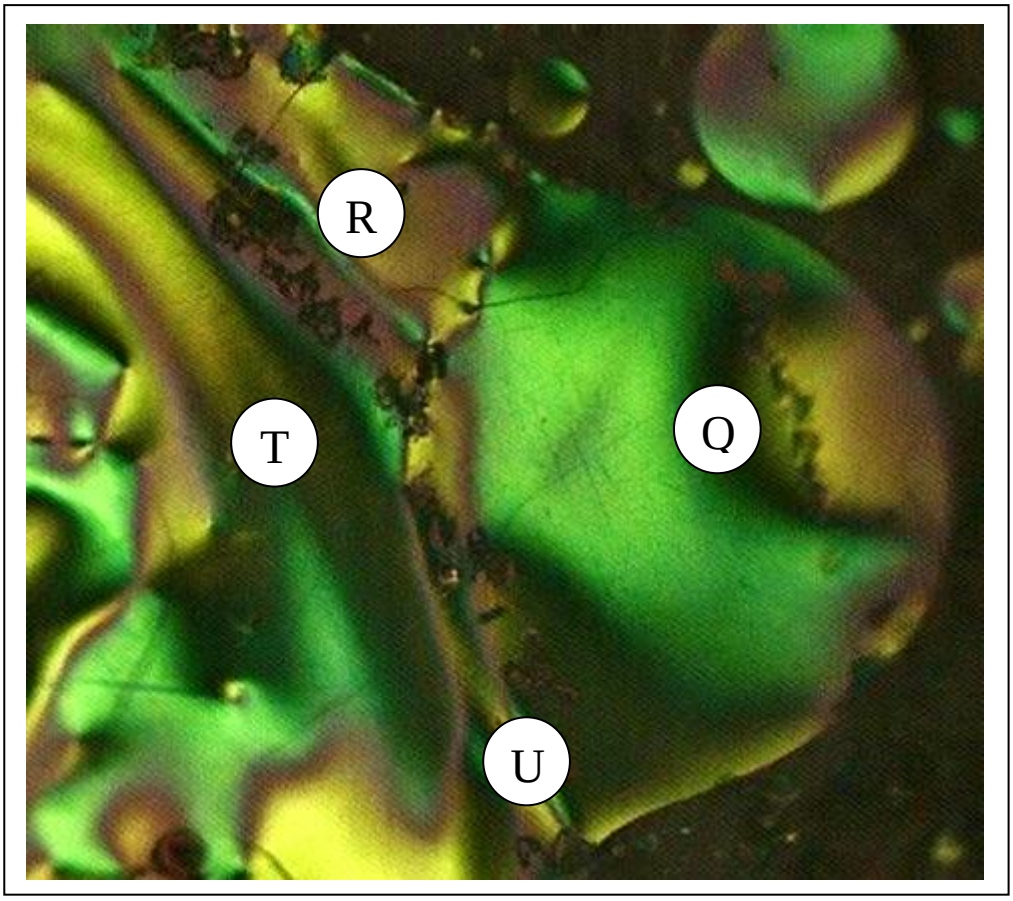

Figure 9-13 Cross-polarised optical microscopy (with the Lambda plate in) of coalescing macrosphere during low-temperature carbonisation of thermally treated Waxy Oil (Sample C3)

In Figure 9-13 a macrosphere (Position Q) approaches the contour of semi-coke (Positions R and T) and starts to deform to a more elliptical shape, as shown by Position U. Thus it is understandable that given the size of the Waxy Oil macrosphere, the length of the deformed sphere increases, thereby providing evidence for the long flow domains seen in the anisotropic microstructures of Waxy Oil coke shown in Figure 9-14.

A montage of micrographs showing the carbon microstructure of Waxy Oil coke is shown in Figure 9-14.

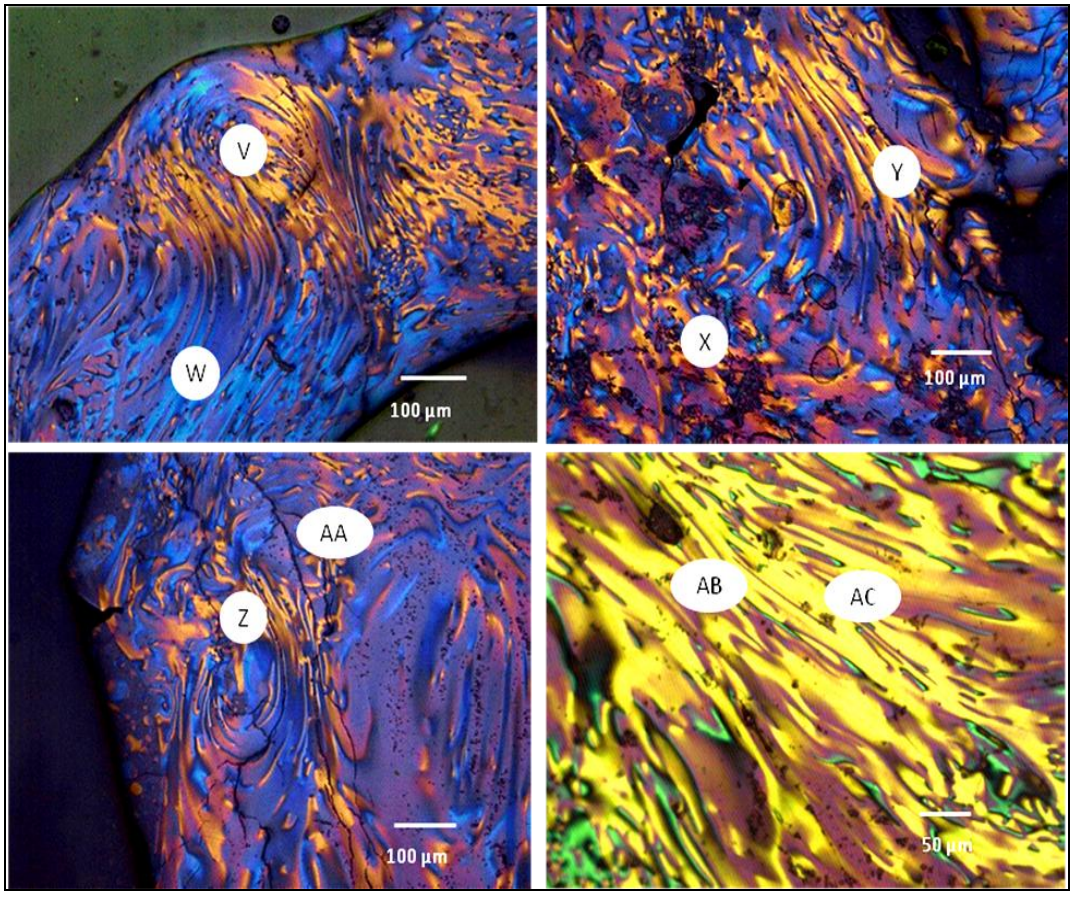

Figure 9-14 Montage of micrographs showing the carbon microstructure of Waxy Oil coke (Sample C6)

As shown in the micrographs, the flow domains of the Waxy Oil coke are laminar and extend well over 50 µm, which has been described by Marsh *et al.* (1999) as being typical of needle cokes. Although many of the flow domains are linear as shown by Positions AB and AC, they may also be curved as shown in Positions V, W, Z and AA. Positions X and Y show microdomains that are not axially orientated with one another. This is due to the lower shear forces in a test tube experiment compared with those in a delayed coker, as previously discussed by Mochida *et al.* (1998) and Mochida *et al.* (1999).

9.11 Conclusions – Carbonisation mechanism of Waxy Oil

This chapter examines the mechanism of pre-mesogen production from Waxy Oil normal alkanes, as well as mesophase development.

The conclusions drawn are as follows:

- The mechanism of pre-mesogen production from normal alkanes involves breakdown to smaller alkanes, cyclation, dehydrogenation, dealkylation and finally the production of a short molecular range distribution of four- to six-ring aromatic compounds.
- The isolation of cyclo-alkanes or hydro-aromatics is difficult due to rapid dehydrogenation.

- The smaller molecular range of four- to six-ring stable pre-mesogens promotes maximum fluidity of the liquid crystal and allows the production of large macrospheres.
- When coalescing with semi-coke, these large macrospheres deform and extend to form large anisotropic flow domains, the length of which is dependent on the volume and plasticity of the macrosphere.
- This is the first research (to the best of the author's knowledge) that has provided a reasonable mechanism for the carbonisation of a multi-component aliphatic residue.

10 CONCLUSIONS

10.1 Introduction

The results of this chapter naturally lend themselves to conclusions based on two main themes: firstly, the effect of the iron oxide catalyst and secondly, the effect of molecular modification on the characteristics of Waxy Oil coke.

10.2 The role of iron oxide in the carbonisation of Waxy Oil

The catalyst concentration of Waxy Oil pre-carbonisation feedstock is naturally variable and at least an order of magnitude higher than is required for needle coke production in terms of the ash content. However, although Waxy Oil could merely be discounted as a needle coke feed based on its catalyst concentration, it was found to be detrimental to many other characteristics of the coke.

The particle size distribution of the catalyst (<100 µm) both provides a physical barrier to mesophase domain flow and actively participates in the chemical reaction, impeding mesophase growth (especially with respect to the smaller catalyst particle sizes). As the catalyst is primarily iron-based, it catalyses the dehydrogenation of organic molecules, thus producing mosaic microstructures in their immediate vicinity.

Increasing the catalyst concentration in Waxy Oil green coke influenced the graphitisation mechanism. When the green coke was thermally treated to 1 400 °C, the graphitisation mechanism of the calcined coke was found to be dominated by iron catalysis. Thermally treating the coke to higher temperatures (2 000 °C) saturated catalytic graphitisation, and the dominant driver for graphitisation was then thermal. It is not possible to compare Waxy Oil calcined coke with calcined needle coke as crystal development is determined by a different mechanism. The iron catalyst in the calcined coke was found to be composed of a variety of oxides and elemental iron, whereas the pre-graphites showed the presence of only elemental iron.

Increasing the catalyst concentration was found to increase substantially the carboxy reactivity of calcined coke samples due to iron catalysis of the oxidation reaction. As ASTM method D2008 prescribes a maximum air reactivity loss of 1.2%.100 min^{-1} (Sien & McGinley, 1983), the influence of the catalyst was determined using TGA which showed an initial increase in air reactivity with increasing catalyst concentration.

The real density of the green and calcined coke increased with increasing catalyst content as the catalyst is predominantly sized below 100 µm and the test is conducted with a –75 µm coke size fraction.

Two potential processes were investigated to reduce the catalyst concentration of the Waxy Oil coke, namely graphitisation of the green coke and removal of catalyst from the Waxy Oil feed.

Green coke graphitisation is not a viable option for the removal of the catalyst to needle coke ash specifications. Apart from the fact that a maximum of 26% ash removal was achieved at

graphitisation temperatures of 3 000 °C, the amount and particle size distribution of the catalyst are limiting factors. Sublimation was also shown to be more effective where the catalyst was in the vicinity of a macropore as opposed to being embedded in the carbon microstructure. Even if graphitisation could reduce the catalyst concentration to required levels (as measured by the ash content), this option would not be able to address the detrimental effect on the microstructure during carbonisation.

Given the large particle size distribution of the catalyst, only filtration through a 0.5 µm sintered plate produces coke with appropriate ash content in terms of the needle coke specification. However, filtering Waxy Oil takes a long time due to its relatively high viscosity. It is concluded that filtering the Synthol Decant Oil (SDO), which has a lower viscosity, may be more appropriate in future studies.

"Static" carbonisation of unfiltered Waxy Oil promotes the formation of a large percentage of mosaic carbon microstructures and increases the carbon yield, compared with the coke from filtered Waxy Oil. The macrostructure of unfiltered Waxy Oil coke resembles a collection of small shot coke particles. This is due to the catalyst particles acting as nuclei for the production of shot coke.

The determination of the air and carboxy reactivity on calcined coke samples from the filtered and unfiltered calcined coke using TGA is problematic due to the build-up of ash at the top of the coke in the crucible. However, the carboxy reactivity shows a sharp mass loss initially due to catalysis, the probable reason being the catalytic effect of the elemental form of the iron.

10.3 The effect of molecular composition on the microstructure of Waxy Oil coke

Waxy Oil is substantially different from better known needle coke feedstocks. Its organic molecular composition includes a range of straight-chain aliphatics (primarily from C_{10}–C_{34}), as well as alkylated homologues thereof. There is also a smaller concentration of one- to two ring aromatics, as well as alkylated homologues thereof. However, perhaps the most surprising discovery is the substantial concentration of oxygenates in Waxy Oil. It is concluded that these oxygenates originate from the use of carbon monoxide as a co-reactant during the Fischer-Tropsch reaction. The thermally unstable organics (oxygenates and iso-alkanes alkanes/aromatics) are reactivity promoters serving to decrease the temperature at which poly-condensation reactions are initiated during carbonisation. It is essential that any modification of the organic molecular composition of Waxy Oil is conducted after filtration as the catalyst participates in reactions at thermal treatment temperatures.

"Static" carbonisation of filtered Waxy Oil produced a substantial concentration of mosaic microstructures. It is concluded that the molecular composition of filtered Waxy Oil (without modification) makes it unsuitable for the production of needle coke due to the reactivity of alkylated molecules and oxygenates which results in a coke with a mixture of mosaic and flow domain microstructures. One of the drawbacks of "static" carbonisation is that it cannot simulate the effect of vertical vector shear forces (seen in dynamic or delayed coking). The shear forces induce flow orientation of the mesophase prior to solidification, increasing the aspect ratio of the carbon microstructure and pores on both a micro- and macroscale.

Distillation is not effective in removing sufficient amounts of lighter hydrocarbons to effect a significant variation in the coke microstructure. Although it may be possible to remove a larger volume of lighter distillates under higher vacuums, distillation does not effectively destroy oxygenates; these remain in the residue and promote the formation of mosaic microstructures. Distillation is further limited as a potential preconditioning process because oxygenates are distributed throughout the molecular weight range of Waxy Oil. A further limitation to increasing the distillation vacuum, while negating cracking (at over 350 °C), is the fact that the molecules that report to the distillate would be too heavy to suit the diesel specification.

Thermal treatment between 400 and 420 °C (at 5 bar pressure) is an optimum conditioning process in that it destroys oxygenates, removes alkyl functions, produces lighter hydrocarbons suitable for the production of a diesel intermediate and stabilises the feed by decreasing the thermal range over which carbonisation occurs.

Thermal treatment at 5 bar pressure does, however, have two notable drawbacks. The first relates to the removal of lighter cracked molecules from the residue during thermal treatment. If these molecules are not removed, they act as reactivity promoters (especially the iso-alkanes and aromatics), having a detrimental effect on the carbon microstructure and producing mosaics towards the bottom of the coke section. The second drawback relates to the stability of long-chain alkanes for longer durations at thermal treatment temperatures. At pre-carbonisation temperatures, the activation energy for aromatisation is insufficient. Stabilised long-chain alkanes may (if the duration is too long) therefore induce dehydrogenation and subsequent polymerisation, forming gum.

It is concluded that thermal treatment at 410 °C followed by distillation is optimum for lowering the amount of Waxy Oil residue, destroying oxygenates, dealkylating organics, increasing the percentage of stable long-chain normal alkanes and removing lighter hydrocarbons from the residue. With the greater percentage of reactivity promoters removed from the residue, “static” carbonisation produces green coke with the highest yield and a microstructure with 100% flow domain. Further to this, inert calcination increases the calcined coke yield from green coke.

The production of lighter hydrocarbons during thermal treatment is of substantial importance to the whole Waxy Oil value chain. The distillates are produced in an approximately 3:1 ratio of petrol to diesel intermediates. This ratio is also dependent on the amount of distillate trapped in the reactor during low-temperature pyrolysis and on the duration of the reaction.

10.4 The mechanism of Waxy Oil carbonisation

The mechanism of pre-mesogen production from normal alkanes involves breakdown to smaller alkanes, cyclation, dealkylation and finally the production of a short molecular range of four- to six-ring aromatic compounds. However, the isolation of cyclo-alkanes or hydro-aromatics is difficult due to rapid dehydrogenation.

The production of a smaller molecular range of four- to six-ring stable pre-mesogens promotes maximum fluidity of the mesophase and allows the production of large spheres. through interation with semi-coke, these large spheres deform and extend to form large anisotropic flow domains, the length of which is dependent on the volume and plasticity of the sphere.

The development of pre-mesogens, large macrospheres and highly anisotropic coke is not dependent on the initial aromaticity of the feed. This is the first research (to the best of the author's knowledge) that has provided a reasonable mechanism for the carbonisation of a multi-component aliphatic residue.

11 CONTRIBUTION TO ORIGINAL KNOWLEDGE

The current study provides a much-needed paradigm shift in defining the feedstock parameters necessary for the production of needle-like coke.

It is the author's opinion that the contribution to original knowledge is justified by providing reasonable answers to the following three questions:

- Does the research address a significant challenge?
- Does the research provide an original solution to this challenge?
- Is the original solution provided significant?

These three questions are discussed below.

11.1 Does the research address a significant challenge?

Historically, needle coke feedstocks have been derived from petroleum or coal-based fossil fuels. Globally, there is evidence that reserves of such residues are in decline. To compound this situation, the characteristics of the feedstocks are also in decline, specifically in terms of sulphur content and environmental restrictions, which leads to the need for a greater degree of pre-carbonisation processing. However, in addressing these concerns, the theory that needle coke feedstock is dependent on **inherent** aromaticity needs to be challenged. Indeed, the lack of academic literature on the production of highly anisotropic coke from aliphatic residues is testament to this. The current research does not negate the value of aromaticity or a self assembling carbonisation system, but suggests that is possible to **create** optimal aromaticity for the production of needle-like coke from a totally aliphatic residue.

Of equal importance is addressing the challenge of the nitrogen and sulphur contents in needle coke and the resultant detrimental effects on the coke due to the puffing process during graphitisation of the electrode. Unfortunately, the great majority of needle coke precursors originate as fossil fuels which contain these stable heteroatoms.

11.2 Does the research provide an original solution to this challenge?

As the synthetic residue of a gas-phase reaction between carbon monoxide and hydrogen, Waxy Oil, unlike other heavy residues originating from coal tar or petroleum, contains considerably less stable nitrogen or sulphur bound as heterocyclic compounds. On the contrary, based on the results of this study, it is also evident that carbonisation of Waxy Oil without pre-processing will not produce an appropriate needle coke. As this study is the first to attempt to produce needle-like coke from Waxy Oil, the solution required an inherent understanding of the composition and carbonisation chemistry of this residue. Thus the following are claimed:

- It is possible to produce a needle-like coke with long-range anisotropic microstructural domains from Waxy Oil by means of filtration and thermal treatment prior to carbonisation.

- It is possible to describe the effect of iron oxide in worsening the characteristics of Waxy Oil coke.
- The molecular composition of Waxy Oil can be determined, as well as the effects of thermal treatment, which does not induce aromatisation.
- This study identifies organic reactivity promoters within filtered Waxy Oil and shows how thermal treatment is able to destroy them, allowing the production of optimal four- to six-ring aromatics during the initial phase of carbonisation.
- Apart from studies on pure alkanes, this study is the first to describe the carbonisation mechanism of a system of multi-component alkanes.

11.3 Is the solution provided significant?

This study has laid the groundwork for further research aimed at producing needle coke from not only Waxy Oil, but also other aliphatic feedstocks with similar molecular compositions. Historically, two key themes have been central to needle coke research, namely the heteroatom content and the aromaticity of the feedstock. Use of a synthetic heavy residue for such research largely negates the hindrance of both nitrogen and sulphur. Further preconditioning of the long-chain normal alkanes allows the production of optimum pre-mesogens for the production of needle-like coke.

11.4 Epitaph

This study would not have been possible were it not for the efforts of past and present researchers in this field. It does not aim to revolutionise needle coke research but if readers at least consider its potential contribution, it will have served its purpose.

---FIN---

12 REFERENCES AND BIBLIOGRAPHY

12.1 References

Akrami, H, Yardim, M & Ekinici, E. 1997. FT-ir characterization of pitches derived from Avgamasya asphaltite and Raman-Dincer heavy crude. *Fuel*, 76(14/15): 1389–1394.

Alcaniz-Monge, J; Cazorla-Amoros, D & Linares-Solano, A. 2001. Characterisation of coal tar pitches by thermal analysis, infrared spectroscopy and solvent fractionation. *Fuel*, 80: 41–48.

Ali, M & Abbas, S. 2006. A review of methods for demetalization of residual fuel oils. *Fuel Processing Technology*, 87: 573–584.

Baraniecki, C; Pinchbeck, P & Pickering, F. 1969. Some aspects of graphitization induced by iron and ferro-silicon additions. *Carbon*, 7: 213–224.

Beuther, H; McKinney, J & Swift, H. 1979. Process for the conversion of gas oil to ethylene and needle coke. United States Patent 4,138,325, http://www.patft.gov.netacgi/4,128,325 [Accessed 13 December 2009].

Beyssac, O; Goffé, B; Petitet, J-P; Froigneux, E; Moreau, M & Rouzaud, J-N. 2003. On the characterization of disordered and heterogeneous carbonaceous materials by Raman spectroscopy. *Spectrochimica Acta A*, 59: 2267–2276.

Blanco, C; Santamaria, R; Bermejo, J & Menendez, R. 2000a. Separation and characterization of the isotropic and co-existing mesophase in thermally treated coal-tar pitches. *Carbon*, 38: 1169–1176.

Blanco, C; Santamaria, R; Bermejo, J & Menendez, R. 2000b. A comparative study of air-blown and thermally treated coal-tar pitches. *Carbon*, 38: 517–523.

Bonilla, J & Elliot, J. 1987. Asphalt coking method. United States Patent 4,686,027, http://www.patft.gov.netacgi/4,686,027 [Accessed 3 October 2003].

Boudou, J; Begin, D; Alain, E; Furdin, G; Mareche, J & Albiniak, A. 1998. 'Effects of $FeCl_3$ (intercalated or not) on the pyrolysis of coal or coal tar pitch. *Fuel*, 77(6): 601–606.

Bounaceur, R; Warth, V; Marquaire, P-M; Scacchi, G; Domine, F; Dessort, D; Pradier, B & Brevart, O. 2002. Modeling of hydrocarbons pyrolysis at low temperature. Automatic generation of free radicals mechanisms. *Journal of Analytical and Applied Pyrolysis*, 64: 103–122.

Calemma, V & Rausa, R. 1997. Thermal decomposition behaviour and structural characteristics of asphaltenes. *Journal of Analytical and Applied Pyrolysis*, 41–42: 569–584.

Clark, J. 2008. Delayed coking of South African petroleum heavy residues for the production of anode grade coke and automotive fuels. MSc (Eng) dissertation, Johannesburg: University of the Witwatersrand Press, pp. 25, 28.

Clark, J; Van Dyk, H; Chang, C; Lewis, I & Orac, T. 2001. Improvement of the quality of delayed coke produced from coal gasification pitch by addition of FCCDO to the feedstock. Proceedings of the ACS Fuel Chemistry Division Conference, Chicago, US.

Clark, J; Van Dyk, H; Chang, C; Lewis, I & Orac, T. 2002. Properties of delayed coke along the coke drum height. Proceedings of the AIChE Spring National Meeting, US.

Crelling, J. 2008. The Petrographic Atlas. http//:www.mccoy.lib.siu.edu/projects/crelling2/atlas. Frame ID: P01, P04, P05, P11, G26, G32 [Accessed 17 October 2010].

Dhakate, S; Mathur, R & Bahl, O. 1997. Catalytic effect of iron oxide on carbon/carbon composites during graphitisation. *Carbon*, 35(12): 1753–1756.

Dickakian, G. 1984. Process for deasphalting cat cracker bottoms and for the production of anisotropic pitch. *United States Patent 4,427,531*, http://www.patft.gov.netacgi/4,427,531 [Accessed 20 September 2009].

Dickakian, G. 1985. Process for preparing an anisotropic aromatic pitch. *United States Patent 4,522,701*, http://www.patft.gov.netacgi/4,522,701 [Accessed 23 September 2009].

Dickinson, E & Moore, A 1988, 'Premium coke from a blend of pyrolysis tar and hydrotreated decant oil', *United States Patent 4,740,293*, http://www.patft.gov.netacgi/4,740,293 [Accessed 17 October 2009].

Didchenko, R & Lewis, I. 1992. Method of forming an electrode from a sulphur containing decant oil feedstock. *United States Patent 5,167,796*, http://www.patft.gov.netacgi/5,167,796 [Accessed 30 October 2009].

Diez, M; Dominguez, A; Barriocanal, C; Alvarez, R; Blanco, C & Canga, C. 1999. Hydrogen donor and acceptor abilities from coal and petroleum evaluated by gas chromatography. *Journal of Chromatography A*, 830: 155–164.

Domine, F; Bounaceur, R; Scacchi, G; Marquaire, PM; Dessort, D; Pradier, B & Brevart, O. 2002. Up to what temperature is petroleum stable? New insights from 5200 free radical reactions. *Organic Geochemistry*, 33: 1487–1499.

Dominguez, A; Blanco, C; Santamaria, R; Granda, M; Blanco, CG & Menendez, R. 2004. Monitoring coal-tar pitch composition changes during air-blowing by gas chromatography. *Journal of Chromatography*, 1026: 231–238.

Driscol, K. 2007. CRU analysis. PowerPoint Presentation, Commodities Research University (CRU) International Limited, London, Slides 1–12.

Dumont, M; Dourges, M; Bourrat, X; Pailler, R; Naslain, R; Babot, O; Birot, M & Pillot, JP. 2005. Carbonization behaviour of modified synthetic mesophase pitches. *Carbon*, 43: 2277–2284.

Eguchi, J; Miyasaka, H; Kinouchi, M; Ohashi, Y; Hori, T & Yamamuru, Y. 1997. Process for producing petroleum needle coke. *United States Patent 5,695,631*, http://www.patft.gov.netacgi/5,695,631 [Accessed 14 October 2010].

Eser, S & Hou, L. 1996. 3-D ^{1}H imaging of porosity in calcined needle cokes. *Carbon*, 34(6): 805–831.

Eser, S & Jenkins, R. 1989. Carbonization of petroleum feedstocks I: Relationships between chemical constitution of the feedstocks and mesophase development. *Carbon*, 27(6): 877–882.

Eser, S; Derbyshire, F & Karsner, G. 1989. Development of coke texture by thermal pretreatment of petroleum residua. *Fuel*, 68: 1146–1151.

Fanjul, F; Granda, M; Santamaria, R & Menendez, R. 2002. On the chemistry of oxidative stabilization and carbonization of carbonaceous mesophase. *Fuel*, 81: 2061–2070.

Frohs, W; Adams, R; Jager, H & Roussel, K. 2007. Graphite electrode and needle coke development. Proceedings of *Carbon 2007 Conference*, 15–20 July 2007, Seattle, Washington, US.

Fu, T & Newman, B. 1989. Method for improving properties of premium coke. *United States Patent 4,822,479*, http://www.patft.gov.netacgi/4,822,479 [Accessed 3 February 2009].

Gentzis, T; Rahami, P; Malhotra, R & Hirschon, A. 2001. The effect of carbon additives on the mesophase induction period of Athabasca bitumen. *Fuel Processing Technology*, 69(3): 191–203.

Goyal, S; Kolstad, J; Hauschildt, F; Venados, G & Joval, C. 1994. Process for producing needle coke. *United States Patent 5,286,371*, http://www.patft.gov.netacgi/5,286,371 [Accessed 30 September 2009].

Griffin, R; Rousell, K & Fu, T. 1991. Method for making graphite electrode nipple. *United States Patent 4,998,709*, http://www.patft.gov.netacgi/4,998,709 [Accessed 16 October 2009].

Guillen, M; Dominguez, A; Iglesias, M; Fuente, E & Blanco, CB. 1996. Analysis of coal-tar pitch: Relations between thermal behaviour and composition. *Fuel*, 75(9): 1101–1107.

Guo, A; Zhang, X; Zhang, H; Wang, Z & Wang, Z. 2010. Aromatisation of naphthenic ring structures and relationships between feed composition and coke formation during heavy oil carbonization. *Energy Fuels*, 24: 525–532.

Gullien, M; Diaz, C & Blanco, C. 1998. Characterization of coal tar pitches with different softening points by ^{1}H NMR. Role of the different kind of protons in the thermal process. *Fuel Processing Technology*, 58: 1–15.

Hippo, E & Walker, P. 1975. Reactivity of heat-treated coals in carbon dioxide at 900 °C. *Fuel*, 54: 245–248.

Hishiyama, Y; Yoshida, A; Kaburagi, Y & Sanada, Y. 1983. Graphitization behaviour of hydrogenated ethylene tar pitch. *Carbon*, 21(3): 197–200.

Hoover, D. 1988. Process for the production of premium grade needle coke from a hydrotreated SRC material. *United States Patent 4,737,261*, http://www.patft.gov.netacgi/4,737,261 [Accessed 25 June 2009].

Hossain, T & Podder, J. 1989. The role of heteroatoms in the carbonisation of graphitization of polynuclear aromatic compounds. *Thermochimica Acta*, 137(2): 225–232.

Hsu, H 1982. Non-puffing petroleum coke. *United States Patent 4,334,980*, http://www.patft.gov.netacgi/4,334,980 [Accessed 14 October 2009].

Hulse, KL. 2000. *Anode Manufacture*, 1st ed. Sierre, Switzerland: R&D Carbon Ltd, pp. 90, 94–95.

Hume, S; Fischer, W; Perruchoud, R & Welch, B. 1993. A model for petroleum coke reactivity. In SK Das (Ed.) *Light Metals*, Warrendale, US: AIME, pp 525–531.

Inagaki, M. 2000. *New Carbons: Control of Structure and Functions*. Oxford: Elsevier Science, Ch. 1, pp. 6–13.

Jenkins, R; Nandi, S & Walker, P. 1973. Reactivity of heat-treated coals in air at 500 °C. *Fuel*, 52: 288–293.

Karacan, C & Badger, M. 2003. Effect of steam injection on pore structure and distribution in coke samples produced by delayed coking. *Fuel*, 82(8): 909–917.

Kawano, Y; Fukuda; T; Kawarada, T; Mochida, I & Korai, Y. 1999a. Suppression of puffing during the graphitization of pitch needle coke by boric acid. *Carbon*, 37: 555–560.

Kawano, Y; Tsutomu, S & Nishihata, T. 1999b. Needle coke for graphite electrodes and process for producing same. *United States Patent 5,900,189* http://www.patft.gov.netacgi/5,900,189 [Accessed 10 October 2009].

Kawano, Y; Fukuda; T; Kawarada, T; Mochida, I & Korai, Y. 2000. Puffing behavior during the graphitization of coal-tar-based needle coke impregnated with iron(II) sulfate and boric acid. *Carbon*, 38: 759–765.

Kegler, W. 1977. Control of feedstock for delayed coking. *United States Patent 4,043,898*, http://www.patft.gov.netacgi/4,043,898 [Accessed 27 March 2010].

Keshun, S; Chengfang, W & Jifu, L. 1985. Influence of microstructure on thermal expansion and graphitisation of oil cokes. *Fuel*, 64(2): 174–177.

Lang, R & Neavel, R. 1982. Behaviour of calcium as a steam gasification catalyst. *Fuel*, 61: 620–626.

Legin-Kolar, M; Radenovic, A & Ugarkovic, D. 1999. Changes in structural parameters of different cokes during heat treatment to 2400 ºC. *Fuel*, 78(13): 1599–1605.

Lewis, I. 1987. Chemistry of pitch carbonization. *Fuel*, 66: 1527–1531.

Lewis, R; Lewis, I; Greinke, R & Strong, S. 1987. Quantitative determination of anisotropic domain size in mesophase pitch. *Carbon*, 25(2): 289–294.

Li, ZQ; Lu, CJ; Xia, ZP; Zhou, Y & Luo, Z. 2007. X-ray diffraction patterns of graphite and turbostatic carbon. *Carbon*, 45: 1686.

Lionetti, T & Schrader, C. 1983. Hydrocarbon conversion processes. *United States Patent 4,388,175*, http://www.patft.gov.netacgi/4,388,175 [Accessed 4 November 2009].

Lutz, I & Wilson, T. 1986. Process for upgrading residuum's by combined donor visbreaking and coking. *United States Patent 4,604,186*, http://www.patft.gov.netacgi/4,604,186 [Accessed 29 September 2009].

Ma, X; Sakanishi, K; Isoda, T & Mochida, I. 1997. Determination of sulphur compounds in non-polar fraction of vacuum gas oil. *Fuel*, 76(4): 329–339.

Machnikowski, J; Kaczmarska, H; Leszcznska, A; Rutkowski, P; Diez, M; Alvarez, R & Garcia, R. 2001. Hydrogen transfer ability of exographic fractions of coal-tar pitch. *Fuel Processing Technology*, 69: 107–126.

Machnikowski, J; Machnikowski, H; Brzozowska, T & Zielinski, J. 2002. Mesophase development in coal-tar pitch modified with various polymers. *Journal of Analytical & Applied Pyrolysis*, 65: 147–160.

Marsh, H; Foster, J; Hermon, G; Iley, M & Melvin, J. 1973. Carbonization and liquid-crystal (mesophase) development. Part 3. Co-carbonisation of aromatic and heterocyclic compounds containing oxygen, nitrogen and sulphur. *Fuel*, 52: 243–252.

Marsh, H; de Lopez, H & Qian, Z. 1984. Co-carbonization of Ashland A240 petroleum pitch with alkali metal carbonates and hydroxides. *Fuel*, 63: 1594–1599.

Marsh, H; Heinz, EA & Rodriguez-Reinoso, F. (Eds). 1997. *Introduction to Carbon Technologies.* Alicante, Spain: Secretariado de Publicaciones.

Marsh, H; Martinez-Escandell, M & Rodriguez-Reinoso, F. 1999. Semicokes from pitch pyrolysis: Mechanisms and kinetics. *Carbon*, 37: 363–390.

Martinez-Escandell, M; Torregrosa, P; Marsh, M; Rodriguez-Reinoso, F; Santamaria-Ramirez, R; Gomez-De-Salazar, C & Romero-Palazon, E. 1999. Pyrolysis of petroleum residues. I: Yields and product analyses. *Carbon*, 37: 1567–1582.

McConaghy, J; Poynor, P & Friday, J. 1979. Process for producing premium coke from vacuum residuum. *United States Patent 4,178,229,* http://www.patft.gov.netacgi/4,178,229 [Accessed 28 December 2009].

Menendez, R; Granda, M; Bermejo, J & Marsh, H. 1993. The development of mesophase in coal tar and petroleum pitches characterised by extrography. *Fuel*, 73(1): 25–34.

Menendez, R; Granda, M & Bermejo, J. 1997. Relationships between pitch composition and the optical texture of cokes. *Carbon*, 35(4): 555–562.

Mizutani, H; Korai, Y & Mochida, I. 2007. Behavior of sulphur species present in atmospheric residue in fluid catalytic cracking. *Fuel*, 86: 2898–2905.

Mochida, I; Maeda, K & Takeshita, K. 1977. Structure of anisotropic spheres obtained in the course of needle coke formation. *Carbon*, 15: 17–23.

Mochida, I; Ohtsubo, R & Takeshita, K. 1980. Catalytic graphitization of non-graphitizable carbon by chromium and manganese oxides. *Carbon*, 18: 117–123.

Mochida, I; Koria, Y; Fujitsu, H; Oyama, T & Nesumi, Y. 1987. Evaluation of several petroleum residues as the needle coke feedstock using a tube bomb. *Carbon*, 25(2): 259–264.

Mochida, I; Oyama, T & Korai, Y. 1988. Formation scheme of needle coke from FCC-decant oil. *Carbon*, 26(1): 49–55.

Mochida, I; Korai, Y; Oyama, T; Nesumi, Y & Todo, Y. 1989. Carbonisation in a tube bomb leading to needle coke. I. Cocarbonisation of a petroleum vacuum residue and a FCC-decant oil into better needle coke. *Carbon*, 27(3): 359–365.

Mochida, I; Fei, YQ & Korai, Y. 1990. A study of the carbonisation of ethylene tar pitch and needle coke formation. *Fuel*, 69: 667–671.

Mochida, I; Fujimoto, K & Oyama, T. 1994. Chemistry in the production of and utilization of needle coke. In PA Thrower (Ed.), *Chemistry and Physics of Carbon*, Vol. 24, Chap. 3, New York: Marcel Dekker, pp. 118, 125, 133–134, 149 & 175.

Mochida, I; Koria, Y; Ku, C; Watanabe, F & Sakai, Y. 2000. Chemistry of synthesis, structure, preparation and application of aromatic derived mesophase pitch. *Carbon*, 38: 305–328.

Murakami, T; Nakaniwa, M & Nakayama, Y. 1989. Process for the preparation of super needle coke. *United States Patent 4,814,063,* http://www.patft.gov.netacgi/4,814,063 [Accessed 22 October 2010].

Murthy, N; Dantas, S; Iqbal, Z & Baughman, R. 2001. X-ray diffraction evidence for the formation of a discotic phase during graphitization. *Carbon*, 30: 809–813.

Murti, S; Choi, K; Sakanishi, K; Okuma, O; Korai, Y & Mochida, I. 2005. Analysis and removal of heteroatom containing species in coal liquid distillate over NiMo catalysts. *Fuel*, 84: 135–142.

Newman, B & Fu, T. 1988. Premium coking process. *United States Patent 4,758,329*, http://www.patft.gov.netacgi/4,758,329 [Accessed 15 October 2009].

Nylen, U; Delgado, J; Jaras, S & Boutonnet, M. 2004. Characterization of alkylated sulphur compounds in light cycle oil from hydrotreated vacuum gas oil using GC-SCD. *Fuel Processing Technology*, 86(2): 223–234.

Obara, T; Yokono, T; Miyazawa, K & Sanada, Y. 1981. Carbonization behaviour of hydrogenated ethylene tar pitch. *Carbon*, 19(4): 263–267.

Obara, T; Yokono, T; Sanada, Y & Marsh, H. 1985. Carbonization behaviour of pitch in the presence of inert material. *Fuel*, 64(7): 995–998.

Oi, S & Onishi, N. 1978. Influence of organic sulphur compounds and metals on mesophase formation. *Carbon*, 16(6): 445–452.

Orac, T; Quandt, H & Ball, D. 1992. Treatment of petroleum cokes to inhibit coke puffing. *United States Patent 5,110,359*, http://www.patft.gov.netacgi/5,110,359 [Accessed 15 October 2009].

Oya, A; Fukatsu, T; Otani, S & Marsh, H. 1983. Catalytic graphitization of cokes by indigenous mineral matter. *Fuel*, 62: 502–507.

Oya, A; Akuzawa, K & Otani, S. 1984. Mineral matter effects on air-oxidation of cokes from a coking coal. *Fuel*, 63: 1547–1551.

Patrick, J & Shaw, F. 1972. Influence of sodium carbonate on coke reactivity. *Fuel*, 51: 69–76.

Perez, M; Granda, M; Garcia, R; Santamaria, R; Romero, E & Menendez, R. 2002. Pyrolysis behaviour of petroleum pitches prepared at different conditions. *Journal of Analytical & Applied Pyrolysis*, 63: 251–239.

Ramos-Fernandez, J; Martinez-Escandell, M & Rodriguez Reinoso, F. 2007. Preparation of mesophase doped with TiO_2 or TIC particles. *Journal of Analytical & Applied Pyrolysis*, 80: 447–484.

Rey Boero, J. 1987. The reaction of petroleum cokes with air. *Carbon*, 25(4): 477–483.

Rodriguez-Reinoso, F; Santana, P; Romero Palazon, E; Diez, M & Marsh, H. 1998. Delayed coking: Industrial and laboratory aspects. *Carbon*, 36(1): 105–116.

Rodriguez-Reinoso, F; Martinez-Escandell, M; Torregrosa, P; Marsh, H; Gomez de Salazar, C & Romero-Palazon, E. 2001. Pyrolysis of petroleum residues. III. Kinetics of pyrolysis. *Carbon*, 39: 61–71.

Sadezky, A; Muckenhuber, H; Grothe, H; Niessner, R & Pöschl, U. 2005. Raman microspectroscopy of soot and related carbonaceous materials: Spectral analysis and structural information. *Carbon*, 43: 1731–1742.

Sakanishi, K; Saito, I; Ishom, F; Watanabe, I; Mochida, I; Okuyama, N; Deguchi, T & Simazaki, K. 2002. Characterization and elution behaviors of organically associated minerals in coals during acid treatment and solvent extraction. *Fuel*, 81: 1471–1475.

Saunders, N. 2003. Alkenes: Thermal cracking. Available at: http://www.creativechemistry.org.uk [Accessed 5 January 2011].

Seshardi, K; Albaugh, E & Bacha, J. 1982. Characterization of needle coke feedstocks by magnetic resonance spectroscopy. *Fuel*, 61: 336–340.

Shuangyou Carbon. 2008. Sichuan Shuangyou Carbon Industry Co Ltd. Available at: http://en.shuangyoucarbon.com [Accessed 17 October 2009].

Sien, H & McGinley, T. 1983. Coker feedstock analysis method. *United States Patent 4,388,408*, http://www.patft.gov.netacgi/4,388,408.htm [Accessed 20 October 2009].

Sima, L; Blanco, C; Santamaria, R; Granda, M; Slaghuis, H & Menendez, R. 2003. Relationship between chemical composition and pyrolysis behaviour of a medium temperature pitch (or Lurgi-gasifier pitch). *Fuel Processing Technology*, 84: 63–77.

Song, H; Chen, X; Chen, X; Zhang, S & Li, H. 2003. Influence of ferrocene addition on the morphology and structure of carbon from petroleum residue. *Carbon*, 41: 3037–3046.

Stecker, G. 1984. Production of premium grade petroleum coke. *United States Patent 4,490,244*, http://www.patft.gov.netacgi/4.490,244.htm [Accessed 28 September 2009].

Torregroso-Rodriguez, P; Martinez-Escandell, M; Rodriguez-Reinnoso, F; Marsh, H; Gomez de Salazar, C & Romero Palazon, E. 2000. Pyrolysis of petroleum residues. II. Chemistry of pyrolysis. *Carbon*, 38: 535–546.

Tsuzuki, N; Takeda, N; Suzuki, M & Yokoi, K. 1999. The kinetic modeling of oil cracking by hydrothermal pyrolysis experiments. *International Journal of Coal Geology*, 39: 227-250.

Ugarkovic, D & Legin, M. 1986. Alteration of metallic microconstituents in petroleum coke by high temperature treatment. *Carbon*, 24: 195–201.

Walker, P; Matsumoto, S; Hanzawa, T; Muira, T & Ismail, M. 1983. Catalysis of gasification of coal-derived cokes and chars. *Fuel*, 62: 140–149.

Wang, G & Eser, S. 2007. Molecular composition of the high boiling components of needle coke feedstocks and mesophase development. *Energy and Fuels*, 21: 3563–3572.

Wang, W; Thomas, K; Poultney, R & Willmers, B. 1995. Iron catalysed graphitisation in the blast furnace. *Carbon*, 33(11): 1525–1535.

Wang, Y; Korai, Y; Mochida, I; Nagayama, K; Hatano, H & Fukuda, F. 2001. Modification of synthetic mesophase pitch with iron oxide, Fe_2O_3. *Carbon*, 39: 1627–1634.

Weinberg, V; Sadeghi, M & Yen, F. 1988. Method of optimizing mesophase formation in graphite and coke precursors. *United States Patent 4,773,985*, http://www.patft.gov.netacgi/4,773,985.htm [Accessed 15 October 2009].

Wolters, F & Van der Walt, TJ. 2007. Upgrading coal tar pitch by delayed coking at Sasol. Proceedings of the *24th Annual International Pittsburgh Coal Conference*, Johannesburg, Session 5, Paper 5-1.

Yokono, T & Marsh, H. 1979. ^{1}H n.m.r study of the co-carbonization of hydrogenated anthracene oil with coal-tar pitch and coal. *Fuel*, 59: 362–364.

12.2 Bibliography

Britannica Student Encyclopedia. 2008. *Iron and Steel Industry*. Available at: http://www.student.britanica.com/comptons/article-202992.htm [Accessed 23 October 2009].

Clark, J. 2008. *Delayed coking of South African petroleum heavy residues for the production of anode grade coke and automotive fuels.* MSc (Eng) dissertation, Johannesburg, University of the Witwatersrand.

Gray, RJ & Krupinski, KC. 1997. Pitch production: Supply, coking, optical microscopy and applications. In M. Inagaki (Ed) 2000, *New Carbons: Control of Structure and Functions*, Oxford: Elsevier Science.

Menendez, R; Granda, M & Bermejo, J. 1997. Pitch pyrolysis chemistry, mesophase chemistry and coking. In H Marsh; EA Heinz & F Rodriguez-Reinoso (Eds), *Introduction to Carbon Technologies*, Alicante, Spain: Secretariado de Publicaciones.

Mochida, I; Fujimoto & Oyama, T. 1994. Chemistry in the production of and utilization of needle coke. In PA Thrower (Ed.), *Chemistry and Physics of Carbon*, New York: Marcel Dekker.

Newman, KL & Newman JW. 1997. A history of pitch technologies. In H Marsh; EA Heinz & F Rodriguez-Reinoso (Eds), *Introduction to Carbon Technologies*, Alicante, Spain: Secretariado de Publicaciones.

Stansberry, PG; Zondlo, JW & Stiller, AH. 1999. Coal-derived carbons. In T Burchell (Ed.), *Carbon Materials for Advanced Technologies*. Oxford: Pergamon/Elsevier Science.

Wikipedia. 2008. *Electric Arc Furnace.* Available at: http://en.wikipedia.org/wiki/Electric_arc_furnace [Accessed 23 October 2009].

Zander M. 1997. Pitch characterisation for industrial applications. In H Marsh; EA Heinz & F Rodriguez-Reinoso (Eds), *Introduction to Carbon Technologies*, Alicante, Spain: Secretariado de Publicaciones.